UNIVERSITY OF SOUTHAMPTON

Probing molecular interactions of a phospholipid surfactant

Christopher John Pynn

A thesis submitted to the University of Southampton for the degree of Doctor of Philosophy

Faculty of Medicine, Health and Life Sciences

School of Medicine

March 2006

University of Southampton

Abstract

FACULTY OF MEDICINE, HEALTH AND LIFE SCIENCES

SCHOOL OF MEDICINE

Doctor of Philosophy

Probing molecular interactions of a phospholipid surfactant

Christopher John Pynn

Lung surfactant is a lipid protein complex which lines the air-liquid interface in the lung. Its primary function is in the maintenance of alveolar patency, although it is also thought to play a major role in modulating immune and inflammatory responses. Although the significance of inadequate surfactant function in neonatal respiratory distress syndrome (NRDS) is well understood, the contribution of surfactant dysfunction in the pathogenesis of other lung diseases is less clear. A synthetic phospholipid-based dry powder surfactant 'PUMACTANT' was found to obliterate the early phase asthmatic response when administered to mild asthmatics prior to bronchial provocation. This discovery prompted the biophysical and immunological analysis of the surfactant/pumactant interaction using a range of physical techniques. A lipid electrospray tandem mass spectrometry (ESI-MS/MS) method was developed, which permitted analysis of pumactant turnover using deuteriated phospholipids. This was used to study the synthesis and turnover of surfactant phosphatidylcholine (PtdCho) substrate in healthy volunteers. Linear incorporation into PtdCho was observed over 30 hours peaking at 0.61% ± 0.04% between 30 and 48 hours. Incorporation decreased to 0.3 ± 0.02% within 7 days. The successful application of this technique to humans *in vivo* has paved the way for the study of exogenous surfactant lipid turnover in future clinical trials. Instrumentation was designed and manufactured to allow controlled dispensation of the very hygroscopic dry pumactant powder in order to study pumactant/surfactant interactions at air/liquid interfaces. The resulting custom built delivery device was capable of dispensing from microgram quantities to 87 ± 3 mg pumactant from a 100 mg vial. This device was used to dose pumactant onto aqueous subphases comprising endogenous surfactant combined with well known surfactant inhibitors under physiological conditions (37°C, 100% RH). Although the effects of pumactant powder on the surfactant inhibitors has yet to be clearly defined, this work led to the discovery that humidity plays a major part in the chemistry of phospholipids at the air-liquid interface. The immunomodulatory properties of pumactant were screened using LacZ inducible antigen/MHC-specific T cell hybrids (B3Z cells). Pumactant inhibited cellular activation in a dose dependant manner both when pre-incubated with cells for 2 hours and when cells were incubated upon stimulation. Incubation of cells with deuteriated [*methyl-d_9*]DPPC followed by ESI-MS/MS revealed a 37% metabolism of exogenous DPPC after 24 hours. Cells maintained tight regulation of membrane composition despite a 65 fold excess of exogenous DPPC to membrane PtdCho, suggesting that any effect of the exogenous lipid on membrane composition was localised, possibly to the outer leaflet of the plasma membrane.

To endure is greater than to dare; to tire out hostel fortune; to be daunted by no difficulty; to keep heart when all have lost it; to go through intrigue spotless; to forgo even ambition when the end is gained – who can say this is not greatness?

William Makepeace Thackeray

The research reported in this thesis is my own original work, except where otherwise stated, and has not been submitted for any other degree.

Acknowledgements

First of all I would like to thank my sponsors Britannia Pharmaceuticals Ltd for supporting the work carried out in this thesis. Particular thanks go to Derek Woodcock for his input and enthusiasm, Jim Thompson for all his invaluable advice on dry powder delivery systems (and for taking me out for many a free lunch!) and also to Tedd Fuel and Isla Irvine for all their support, banter and helpful emails particularly in the latter stages of the project.

A very special thanks goes to my supervisor Dr Tony Postle, for helping me to expand my mind (you are right Tony, it hurts!) and for his belief in me even when I didn't. To the rest of my extended 'Lipid Group' family (Anne George, Lisa Shaw, Grielof Koster and Alan Hunt as well as my friends on the 'dark side') a huge thanks for all your support, encouragement and 'advice' regarding every aspect of my life, work related or otherwise! A particular thanks goes to Dr Neil Henderson for always being there to unstick me when I got stuck and for finding a way to do anything!

To the students over the years, it's been an education. I'd particularly like to acknowledge my project student Dr Eleanor Beecraft who helped establish methods required to generate the results given in Chapter 5. If I end up in education I know who to blame!

To my friends, you know who you are, and that you're appreciated. I'd especially like to thank Dr Rowland Spencer-Smith who proof read the original drafts of my thesis without any complaining! A special thanks also to Linnsey Haswell for sound advice and for putting a roof over my head during the final stages of my PhD. To my house mates over the years, thanks for all the good food and the good times! in particular Dr David Hughes, Dr Justin Hayward and Robin Bell.

Last but certainly not least, a huge and heartfelt thanks to my family, without whom I would never have come this far neither emotionally, nor financially. This ones for you!

Material from this thesis has been published in:

Postle AD; Pynn CJ, Henderson NG, Koster G, Jaworski A and Bernhard W, (2005). Differentielle Synthese von Plasmaphospholipiden via Cholineinbau und N-Methylienrung beim Menschen in vivo. Oral presentation at the 31st Annual Conference of the Society for Neonatology and Paediatruc Intensive Medicine. Magdeburg, Germany. 16th – 18th June 2005.

Pynn CJ, Koster G and Postle AD. (2005) Mechanisms of lymphocyte inhibition by surfactant phospholipid. Poster presentation at the American Thoracic Society Annual Conference, San Diego, California. 20^{th}-25^{th} May 2005.

Pynn CJ, Henderson NG, Bernhard W, Koster G and Postle AD (2005). Lipid dynamics of human plasma phosphatidylcholine synthesis by the CDP:choline and N-methyltransferase pathways *in vivo.* Poster presentation at Bioactive lipids, lipidomics and their targets (Keystone Symposium), Whistler, Canada. 12^{th} – 17^{th} April 2005.

Koster G; **Pynn CJ**, and Postle AD (2005). Molecular species compositions of Phosphatidylinositol phosphates in cultured cells:practice and pitfalls. Poster presentation at Bioactive lipids, lipidomics and their targets (Keystone Symposium), Whistler, Canada. 12^{th} – 17^{th} April 2005.

Bernhard W., **Pynn CJ**, Jaworski A, Rau, GA, Hohlfeld, JM, Freihorst J, Poets CF, Stoll D and Postle AD *Mass Spectrometric Analysis of Surfactant Metabolism in Human Volunteers using Deuterated Choline.* Am. J. Respir. Crit. Care. Med., ***170***, 54-58, 2004.

Postle AD, Dombrowsky H, Clarke H, **Pynn CJ**, Koster G and Hunt AN. Mass spectroscopic analysis of phosphatidylinositol synthesis using 6-deuteriated-myo-inositol: comparison of the molecular specificities and acyl remodelling mechanisms in mouse tissues and cultured cells. Biochem. Soc. Trans. **32**, 1057-1059 2004.

Table of Contents

List of Figures

List of Tables

Abbreviations

γ_{min}	Minimum surface tension
AdoMet	S-adenosylmethionine
AFS	Amniotic fluid surfactant
ALEC®	Artificial lung expanding compound
APC	Antigen presenting cell
APES	3-Aminopropyltriethoxysilane
API	Active pharmaceutical ingredients
ARDS	Acute respiratory distress syndrome
BADH	Betaine aldehyde dehydrogenase
BALF	Bronchoalveolar lavage fluid
BHMT	Betaine:homocysteine methyl transferase
BODIPYPtdCho	2-(4,4-difluoro-5-methyl-4-bora-3a,4a-diaza-s-indacene-3-dodecanoyl)-1-hexadecanoyl-sn-glycero-3-phosphocholine (β-bodipy®500/510 C_{12}- HPC)
BSA	Bovine serum albumin
CDH	Choline dehydrogenase
CDP	Cytidine diphosphocholine
CF	Cystic fibrosis
CFC	Chlorofluorocarbon
CFTR	Cystic fibrosis transductance regulator
CID	Collision induced dissociation
CK	Choline kinase
CMC	Critical micelle concentration
CPRG	Chlorophenol reg beta-galactoside
CS	Capillary surfactometer
CT	Cholinephosphate transferase
CCT	CTP:phosphocholine cytidylyltransferase
DAG	1,2-diacylglycerol
DHA	Docosahexanoic acid
DMPA	Dimyristyl phosphatidylcholine
DMPC	Dimyristyl phosphatidylcholine
DPI	Dry powder inhaler
DPPC	Dipalmitoyl phosphatidyl choline

DPPI	Dipalmitoyl phosphatidyl inositol
EAR	Early asthmatic response
EDTA	Ethylene diamine tetraacetic acid
EI	Electron ionisation
ELISA	Enzyme linked immunosorbent assay
ESI	Electrospray ionisation
ESI-MS/MS	Tandem electrospray ionisation mass spectrometry
ETT	Endotracheal tube
FAB-MS	Fast atom bombardment mass spectrometry
FCS	Fetal calf serum
FEV_1	Forced expiratory volume in 1 second
FPD	Fine particle dose
FPF	Fine particle fraction
HFA	Hydrofluoroalkane
HPLC	High performance liquid chromatography
HRT	Hormone replacement therapy
IgE	Immunoglobulin E
IgG	Immunoglobulin G
IL-2	Interleukin 2
IP_3	1,4,5-*tris*phosphate
LA	Large aggregate
LAR	Late asthmatic response
LDL	Low density lipoprotein
LSA	Large surfactant aggregates
LS	Lung surfactant
LTC_4	Leukotriene C_4
MACS	Magnetic assisted cell sorter
MALDI	Matrix assisted laser desorption ionisation
MHC	Major histocompatibility complex
MRI	Magnetic resonance imaging
MRM	Multiple reaction monitorring
m/z	mass/charge ratio
MS	Mass spectrometry
NRDS	Neonatal respiratory distress syndrome
OVA	Ovalbumin

PADD	Pressurised aerosol dry powder device
PBS	Pulsating bubble surfactometer
PGD_2	Prostaglandin D_2
PEMT	Phosphatidylethanolamine methyltransferase (PEMT)
PHA	Phytohemagglutinin
PMA	Phorbol myristate acetate
pMDI	Pressurised metered dose inhaler
PIP_2	Phosphatidylinositol 4,5-*bis*phosphate
PKC	Protein kinase C
PLC-γ1	Phospholipase Cγ1
POPC	Palmitoyloleoyl phosphatidyl choline
pMDI	Pressurised metered dose inhaler
PtdCho	Phosphatidylcholine
PtdEtn	Phosphatidylethanolamine
PtdGly	Phosphatidylglycerol
PtdIns	Phosphatidylinositol
PtdOH	Phosphatydic acid
PtdSer	Phosphatidylserine
RH	Relative humidity
RDS	Respiratory distress syndrome
RPMI	Rosewell park medical institute
SA	Small aggregate
SP	Surfactant protein
TBAS	Tetrabutylammonium sulphate
TCR	T cell receptor
T_H cells	T-helper cells
TLC	Thin layer chromatography
TMB	Tetramethyl benzidine
VLDL	Very low density lipids
WB	Wilhelmy surface tension balance

Chapter 1

Introduction

1.1 General Introduction

Pulmonary surfactant is a highly surface active material composed of proteins and lipids that lines the lungs at the air-liquid interface. Surfactant prevents alveolar collapse at low lung volume and preserves bronchiolar patency during respiration. A pathophysiological role for surfactant was first determined in preterm infants suffering from neonatal respiratory distress syndrome (NRDS), caused by lung immaturity and the absence of effective surfactant[1]. NRDS is now routinely and successfully treated with exogenous surfactant replacement. Surfactant is also involved in the protection of the lungs from injuries and infections caused by inhaled particles and micro-organisms. Biochemical surfactant abnormalities of varying degrees have been described in a range of lung diseases. These include obstructive lung diseases such as asthma[2], bronchiolitis[3] and chronic obstructive pulmonary disease[4], infectious and suppurative lung diseases, such as cystic fibrosis[5] and pneumonia[6], as well as adult respiratory distress syndrome[7] and pulmonary oedema[8].

While surfactant therapy has proved invaluable in NRDS, where primary surfactant deficiency has been unequivocally demonstrated, clinical benefit of surfactant administration in other lung diseases has been less easily demonstrated. In contrast to the surfactant-deficient lungs of preterm infants, lung diseases of the mature lungs are characterised by inflammation and surfactant dysfunction to a greater or lesser extent. Surfactant therapy in such diseases would involve administering exogenous surfactant to an environment containing a complex mixture of compromised surfactant. Consequently, for the development of effective surfactant therapy tailored to specific diseases, study is required of both the pathophysiological role of the surfactant abnormalities and the way in which exogenous surfactant interacts with the complex mixture of compromised endogenous surfactant in different disease states.

A synthetic phospholipid-based dry powder surfactant (Pumactant – commercially known as ZoFac™) abolished the early phase asthmatic response when administered prophylactically to mild asthmatics prior to exposure to inhaled antigen[9]. However, very little is known about the nature of the interaction of Pumactant with endogenous surfactant, or its mode of therapeutic intervention. The aim of this project was to explore the interactions of Pumactant both with endogenous pulmonary surfactant and with components of the immune system.

1.2 Phospholipids

Phospholipids are lipid molecules in which phosphate ester groups feature as the common component. There are two main classes of phospholipid, glycerophospholipids containing glycerol, a three-carbon alcohol and sphingophospholipids containing sphingosine, a complex alcohol. The general structure of a glycerophospholipid is that of a three carbon sugar molecule with a fatty acyl or alkyl group at the *sn*-1 position and fatty acyl group at the *sn*-2 position (Figure 1.1).

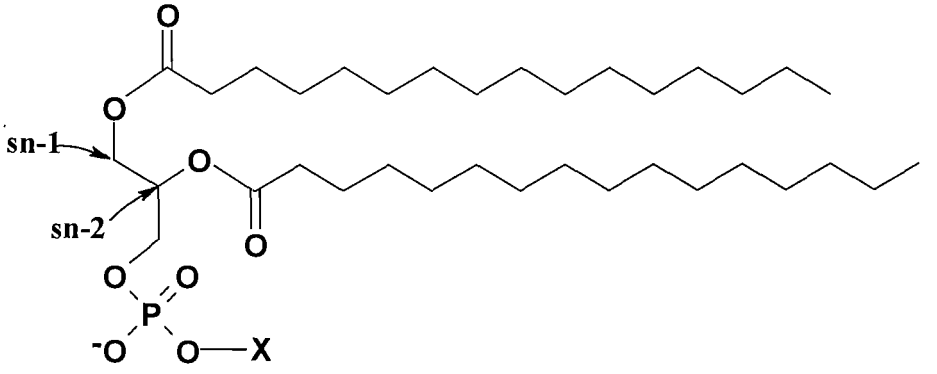

Phospholipid	Headgroup(X)
Phosphatidylcholine (PtdCho)	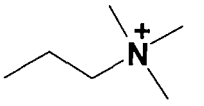
Phosphatidylglycerol (PtdGly)	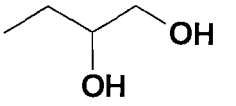
Phosphatidylinositol (PtdIns)	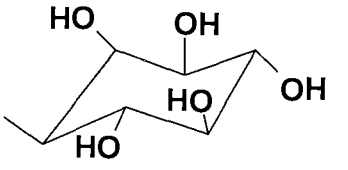

Figure 1.1: Molecular structures of glycerophospholipids. The class of phospholipid is defined by the nature of the polar head group esterified to the phosphate group (X). The species distribution within any phospholipid class is determined by the fatty acyl substitutes at the sn-1 and sn-2 positions of the glycerol backbone. The dipalmitoyl species above would be designated PC16:0/16:0 if X was choline. If arachidonic acid was esterified at sn-2, the molecule would be designated PC16:0/20:4

Glycerophospholipids are structures based on phosphatidic acid (PtdOH); the polar headgroup attached to the phosphate defines the class of glycerophospholipid, of which there are six main classes. These are: phosphatidylcholine (PtdCho), phosphatidylethanolamine (PtdEtn), phsophatidylserine (PtdSer), phosphotidylinositol (PtdIns) phosphatidyglycerol (PtdGly) and phosphatidic acid. The molecular species composition within each phospholipid class is determined by the combination of fatty acids attached to the glycerophosphate backbone. The fatty acids usually contain an even number of carbon atoms, and may be saturated or unsaturated. In eukaryotes, the fatty acids are linked to the glycerophosphate backbone at the *sn*-1 position by either an ester, vinyl ether (plasmalogen or alkenyl phospholipid) or an alkyl ether (ether or alkyl phospholipid). The fatty acid at the *sn*-2 position is usually linked by an ester bond. Only glycerophospholipids comprising fatty acid chains linked by either an ester, or alkyl ether at the *sn*-1 position and ester at the *sn*-2 position will be considered in this thesis. The systematic name for a phospholipid with a choline headgroup and palmitic acid attached at the *sn*-1 position with oleic acid attached at the *sn*-2 position would be *sn*-1palmitoyl *sn*-2oleoylphosphatidylcholine (abbreviated as POPC). For simplicity and clarity, phospholipid molecular species will be designated PXA:n/B:n where X is the headgroup, A and B are the number of carbon atoms of the fatty acyl groups esterfied at the *sn*-1 and *sn*-2 positions and n is the number of unsaturated double bonds in each fatty acid and (see figure 1). Hence, the example POPC given above would be designated PC16:0/18:1. For alkylacyl ether molecular species (comprising an alkyl ether linkage at the *sn*-1 position and acyl linkage at the *sn*-2 position) an 'a' will added following the *sn*-1 fatty acid assignment. For example *sn*-1palmityl *sn*-2palmitoylphosphatidylcholine will be designated PC16:0a/16:0.

1.3 Mass spectrometry (MS)

A mass spectrometer is an analytical tool that determines the molecular weight of chemical compounds by separating molecular ions according to their mass to charge ratio (m/z) [10]. In order to analyse a sample by mass spectrometry, a sample at atmospheric pressure must be introduced into the instrument such that the vacuum within remains largely unchanged. This can be achieved in many ways, the most common being with a direct insertion probe or by infusion through a capillary column.

In order for a molecule to be detectable by mass spectrometry it must carry a charge. Molecular ions are generated by inducing either the loss or gain of a proton in the ionisation source. Charged molecules are then separated according to their mass/ charge ratio by the mass filter/ analyser and subsequently detected by the ion detector. The result of ionisation, ion separation and detection is a mass spectrum that can provide molecular weight and structural information. The fundamental components of a mass spectrometer are shown in figure 1.2.

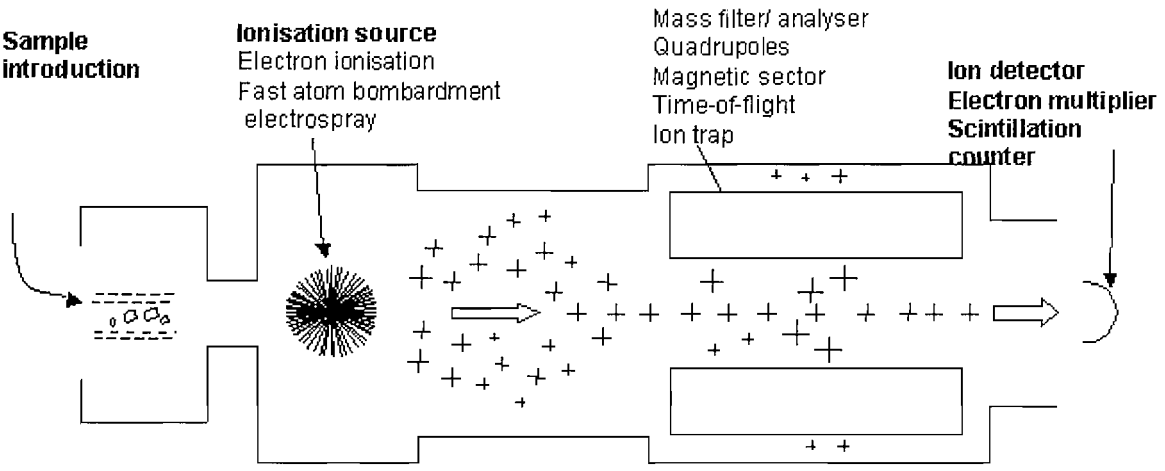

Figure 1.2: Fundamental components of a mass spectrometer. The ion source does not necessarily have to be within the vacuum of the mass spectrometer. External ion sources are known as atmospheric pressure ionisation (API) sources.

1.3.1 Electron ionisation

Electron ionisation (EI) was the primary ionisation source for mass analysis up until the 1980s. This method requires that the sample is delivered as a gas, a process accomplished by thermal desorption or 'boiling off' the sample from the probe. This is achieved by heating the sample within the high vacuum of the mass spectrometer. Once in the gas phase, the compound passes into an electron beam. Fast moving electrons impact on the gaseous sample molecules and cause an electron to be 'ejected' from the sample resulting in production of molecular ions.

EI is a highly sensitive technique, enabling the detection of sub picomole to picomole quantities. However, the requirement that the sample be heated often leads to

decomposition prior to vaporisation. This, combined with the involatility and excessive fragmentation of large molecules, renders this technique ineffective in the analysis of molecules of molecular mass greater than 400 Da.

This limitation motivated scientists to develop the techniques for biomolecule analysis such as fast atom/ion bombardment (FAB), matrix assisted laser desorption/ionisation (MALDI) and electrospray ionisation (ESI).

1.3.2 Electrospray ionisation mass spectrometry (ESI-MS)

ESI is a technique used to generate gaseous ionised molecules from a liquid. The sample of interest is sprayed out of a fine capillary, across which a high voltage is applied (typically 1.5 – 4 kVolts). This produces charged droplets which are electrostatically attracted to the mass spectrometer inlet. Dry heated gas is applied to the droplets before they enter the vacuum of the mass spectrometer causing the solvent to evaporate from the droplet surface. As the droplets decrease in size, the electric field density on its surface increases. The repulsion between like charges on the droplet surface become so great that they eventually exceed the force of surface tension and ions begin to leave the droplet through a 'Taylor cone' (figure 1.3). This 'soft' ionisation technique is capable of producing unfragmented molecular ions.

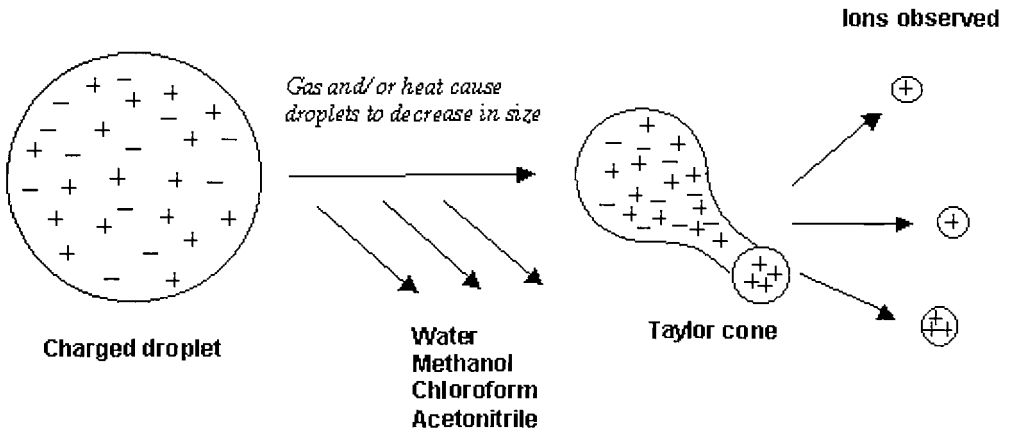

Figure 1.3: Ion formation resulting from charged droplets produced by an electrospray ion source.

1.3.3 Phospholipid analysis by ESI-MS

Conventional methods for the characterisation of phospholipids involved laborious multi-step procedures (see section 3.1.1). Mass spectrometry offers fast universal analysis of complex mixtures with unequalled levels of detection and sensitivity. Phospholipids gain a single charge through the loss or gain of a proton (which has a mass of 1 a.m.u.). The resulting m/z for the lipid is therefore detected either one mass unit below or one mass unit above the molecular mass respectively, providing relatively simple analysis.

1.3.4 Tandem electrospray ionisation mass spectrometry (ESI-MS/MS)

Tandem MS/MS is a facility only available on mass spectrometers which possess two mass analysers which are linked in series and separated by a collision cell. Molecular ions which enter the first mass analyser are then fragmented in the collision cell by bombardment with an inert gas (typically argon) and the fragments separated in the second mass analyser prior to detection. Tandem MS/MS aids in identifying the structural conformation of compounds as well as providing a way to confirm the identity of molecular ions.

1.3.5 Product ion scanning

Product ion analysis can be used both for the structural elucidation of various mass ions as well as in the determination of fragments specific to certain classes of molecules such as the phospholipids. In this analysis mode, a specific ion of interest is selected in MS 1, all other molecular ions are ignored. The selected molecular ion is then fragmented in the collision cell through 'collision induced dissociation' (CID). The fragment or 'product' ions originating from the selected precursor molecule are then separated in the second mass analyser and detected (figure 1.4).

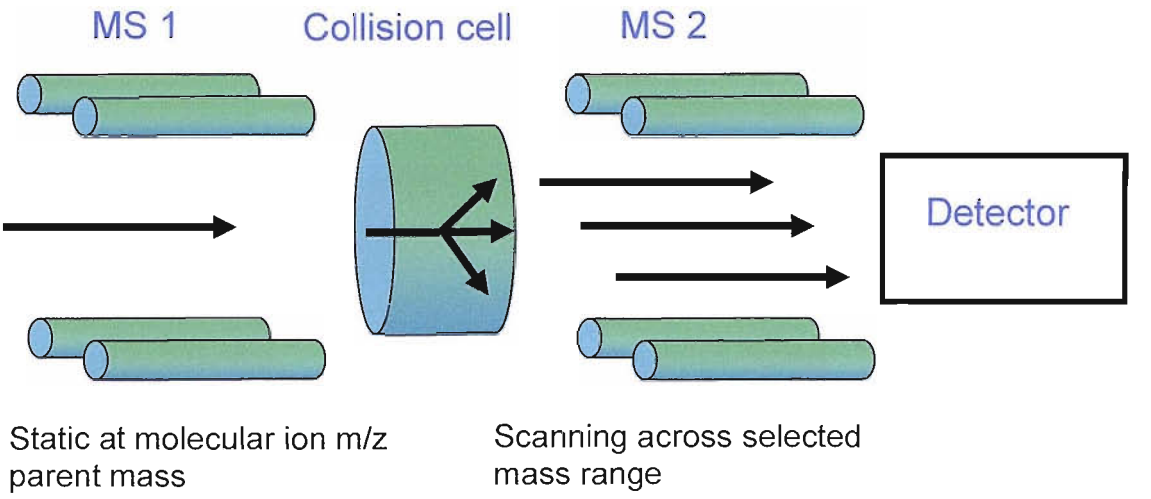

Figure 1.4: Diagrammatic representation of a product ion scan. The ion of interest is selected by MS 1 and fragmented in the collision cell. The resulting molecular fragments are resolved in MS 2.

1.3.6 Precursor ion scanning

In this acquisition mode, MS 1 is set to scan across a selected mass range allowing any molecular ion within that selected range to pass through the first mass analyser. These molecular ions all undergo CID in the collision cell. The resulting fragments then pass through into MS 2. However, MS 2 is set to monitor only one specific fragment ion of interest, therefore only fragments of the selected m/z ratio will pass through the second mass analyser to the detector. Because the two mass analysers are connected, the mass spectrometer is able to determine which molecular ions originated from the selected product ion. Precursor ion analyses can be used to identify and confirm known groups of compounds that produce a common product ion upon fragmentation (figure 1.5).

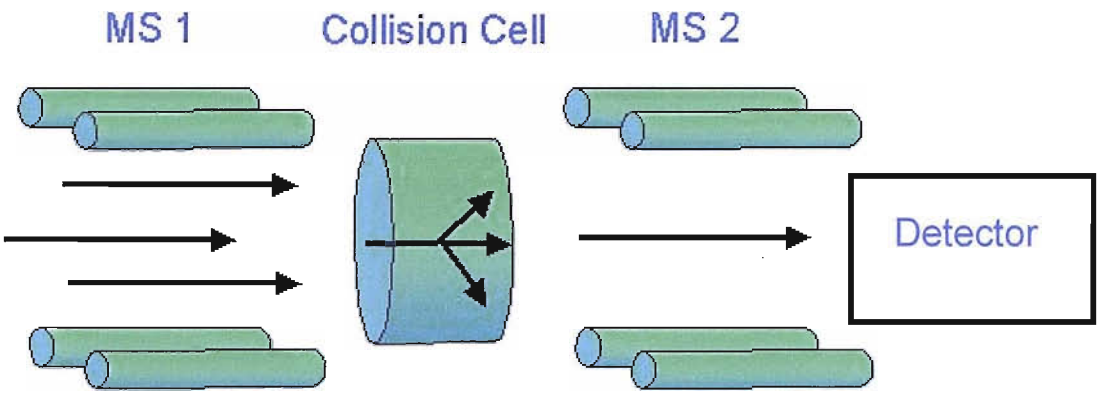

Figure 1.5: Diagrammatic representation of a precursor ion scan. All molecular ions pass through MS 1 and are fragmented in the collision cell. MS 2 only allows fragment ions of a specific pre-selected mass to pass through to the detector.

1.3.7 Multiple reaction monitoring (MRM)

MRM acquisitions only allow transitions from selected precursor ions to selected product ions to be monitored. Because both mass analysers are static, this enables greater 'dwell time' on the ions of interest which in turn enhances the sensitivity (~100 fold). Only ions which satisfy the transition criteria are detected by the ion detector. This acquisition method is only used for screening samples for known analytes and is particularly useful in situations were high sensitivity is required. A schematic of the principles of MRM is given in figure 1.6.

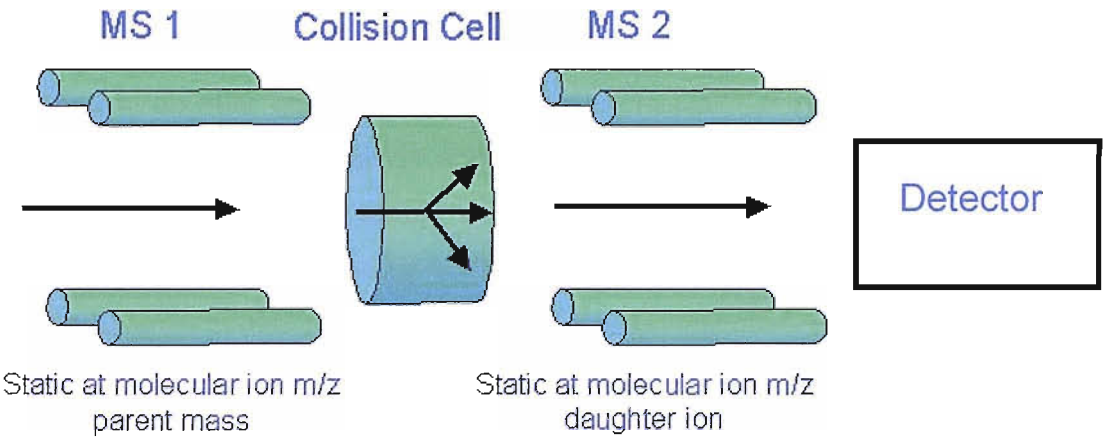

Figure 1.6: Diagrammatic representation of MRM scanning. This allows only specific transitions from pre-designated molecular ions in MS 1 to pre-designated fragment ions in MS 2.

1.4 Lung surfactant

1.4.1 Composition

Lipid is the major component of human surfactant by weight, making up approximately 90% of isolated surfactant[11,12] with protein contributing the remaining 10%. Phospholipids account for 90% of the lipid fraction, the remaining 10% being neutral lipid, mainly cholesterol.

Approximately 80% of the protein component in healthy lungs is derived from transudates of plasma protein. The remaining 20% comprise of four surfactant associated proteins, surfactant proteins (SP), namely, SP-A, SP-B, SP-C and SP-D. Surfactant proteins A and D are hydrophilic with major roles in innate immune responses in the lungs, whilst surfactant proteins B and C are hydrophobic and promote the surface active functions of surfactant.

1.4.2 Synthesis, secretion and turnover

Surfactant is continually being made throughout the lives of air breathing animals. It is synthesised in alveolar type II cells and packaged in lamellar bodies as an anhydrous mixture of selected phospholipids and proteins[13]. Lamellar bodies are secreted by exocytosis in response to a variety of stimuli including β-adrenergic agonists and alveolar stretch. Released lamellar bodies are secreted into the thin liquid layer that covers the alveolar epithelium where they are hydrated and converted into large vesicles which are highly surface active. During the ventilatory cycle, surfactant is adsorbed to the air-liquid interface. How surfactant arranges itself at the air liquid interface is still the subject of some debate. As the surface pressure increases (upon exhalation), the unsaturated phospholipids are thought to be squeezed out of the interface leaving a refined (single or multi) layer enriched in PC16:0/16:0.

1.5 Surfactant at the air/liquid interface

The key physical characteristics of endogenous surfactant are its ability to transfer to, and spread very rapidly at the air/liquid interface in order to achieve stability on initial opening of the lungs, to sustain very high surface pressure over fairly long time periods and to differentially vary surface tension with change in size of the alveolus during the breathing cycle.

1.5.1 Alveolar surface tension

The alveoli form the final branching of a system of tubes in the mammalian lung. They are sac like structures closely surrounded by a network of capillaries that enable gas exchange. Alveoli change in size during the breathing cycle, expanding and contracting upon inhalation and exhalation. The idea that alveoli are subject to surface tension forces was first suggested by Kurt Von Neergard.[14] He came to this conclusion after he discovered that when lungs were isolated and inflated, less pressure was required to inflate lungs filled with saline than with air. As alveoli normally have a wet lining, he assumed that the force of surface tension must be adding to elastic recoil in the air filled lungs. When the lungs are filled with saline, there is no air water interface and consequently no surface tension.

Surface tension is the skin-like property of a liquid and is caused by the attraction between the molecules of the liquid due to various intermolecular forces. In the bulk of the liquid each molecule is pulled equally in all directions by neighbouring liquid molecules resulting in a net force of zero. At the surface, the molecules are pulled inwards by molecules within the liquid, however as there are no liquid molecules on the external surface to balance the forces, all of the molecules at the surface are subject to an inward force of molecular attraction which can only be balanced by the resistance of the liquid to compression[15]. Thus, the liquid squeezes itself together until it has the smallest possible surface area. Surface tension is typically measured in $mN.m^{-1}$. In the alveolus, surface tension is the force around the circumference resisting expansion and therefore contributing to its collapsing pressure. The relationship between alveolar collapsing pressure and surface tension is given by LaPlace's law:

$$P=2\gamma/r$$

Where P= the collapsing pressure, γ= surface tension and r = radius.

Upon exhalation, the alveoli get smaller and the collapsing pressure increases. Von Neergard predicted the presence of an agent in the lungs necessary to maintain constant alveolar pressure and prevent alveolar collapse.[14] This material was finally isolated by Clements from oedema fluid and lung extracts 25 years later.[16] The material, consisting of a mixture of phospholipids and proteins, was termed surfactant (surface active agent).

1.5.2 Surfactant spreading

Lung surfactant has a high percentage of dipalmitoyl phosphatidylcholine (DPPC) compared to other biological membrane preparations[17] and the rigid, disaturated nature of this phospholipid is widely considered responsible for the surface tension-lowering properties of the material. DPPC, and phospholipids in general, are amphipathic molecules with a polar hydrophilic head group and a non-polar hydrophobic tail. DPPC adsorbs to the pulmonary air/liquid interface with the hydrophobic fatty chains oriented towards the gas phase and the hydrophilic head group towards the aqueous phase. Spreading of DPPC from an aqueous suspension is greatly enhanced by the presence of other phospholipid components of surfactant, especially unsaturated PtdGly, but

absorption rates of phospholipid-based surfactants are still well below those of the natural material.[18]

1.5.3 Role of the hydrophobic surfactant proteins SPB and SPC

Dispersed bilayers reconstituted from material extracted from surfactant by organic solvents, presumed initially to contain only lipid species, adsorbed quite well to form interfacial films. These observations led to the discovery of the presence of the hydrophobic surfactant associated proteins SP-B and SP-C.[19,20]

The pulmonary surfactant proteins play a key role in modulating the interfacial properties of the surfactant phospholipids. SP-B and C are essential for rapid adsorption of surfactant into the air-liquid interface and respreading of surfactant from the collapse phases during expansion. Although there is currently no known direct role for SP-A in the surface tension reducing properties of surfactant, SP-A is essential for the formation of tubular myelin, a unique surfactant structure in the hypophase that is believed to be an immediate precursor of the surface film.[21] The biological significance of tubular myelin has been questioned however by the lack of any pulmonary dysfunction in the $SP\text{-}A^{-/-}$ mouse[22].

1.5.4 Measuring the interfacial properties of surfactant

Administering therapeutic surfactants to preterm infants at birth as an aqueous suspension is well established and relatively straightforward (see section 1.7.1). In contrast, attempts to treat diseases of the mature lung with exogenous surfactant are complicated by the presence of many disease related components, including dysfunctional endogenous surfactant. Very little is known about the interactions of exogenous and endogenous surfactants at the air/liquid interface and nothing at all about those interactions in the diseased lung.

Key interfacial properties need to be characterised in order to understand the mechanism of action of therapeutic surfactants. For example, does the exogenous material form discrete domains at the interface? Do the lipids in the interface exchange with endogenous material? Does the nature of the exogenous/ endogenous interaction

change when the exogenous surfactant is impaired? Some of these questions can be answered using the physical techniques described below (section 1.5.4.1 and 1.5.4.2).

1.5.4.1 The Wilhelmy surface tension balance

Measuring surface tension properties of surfactant films using the Wilhelmy-Langmuir method was introduced by Clements in his pioneering study about the surface tension of lung extracts.[16] The device consists of a hydrophobic Teflon trough containing saline, together with a varying composition of other electrolytes. The surfactant film is spread at the air-liquid interface and this surface film is then cyclically compressed by a moving Teflon barrier. Surface tension is measured by a platinum dipping plate which penetrates the aqueous phase and is attached to a force transducer. Typically the Wilhelmy dipping plate is arranged to hang vertically in the air-liquid interface, supported by an electromechanical balance. A chemically cleaned roughened platinum plate provides two very high energy surfaces as metals have surface energies in the region of 500 – 1000 mJm^2m^{-2} compared, for instance, to paraffin wax with a surface energy of $30mJm^2m^{-2}$. The molecules of a liquid, such as water, experience a grossly unequal pull and are attracted up the sides of the metal plate. At equilibrium with gravitational forces, the profile of the meniscus developing around the perimeter of the high-energy surface is therefore reporting on the equilibrium tension of the surface layer of liquid.[23]

Baseline surface tension is measured first on a pure aqueous phase to calibrate the instrument. Surfactant is then added to generate a surface film. This film is 'refined' by the oscillating barrier, and changes in surface tension are measured by changes in the attractive force between the aqueous phase and the dipping plate, which are detected by the force transducer.[24] The key components of the Wilhelmy balance (trough, barrier and plate) are given in figure 1.7.

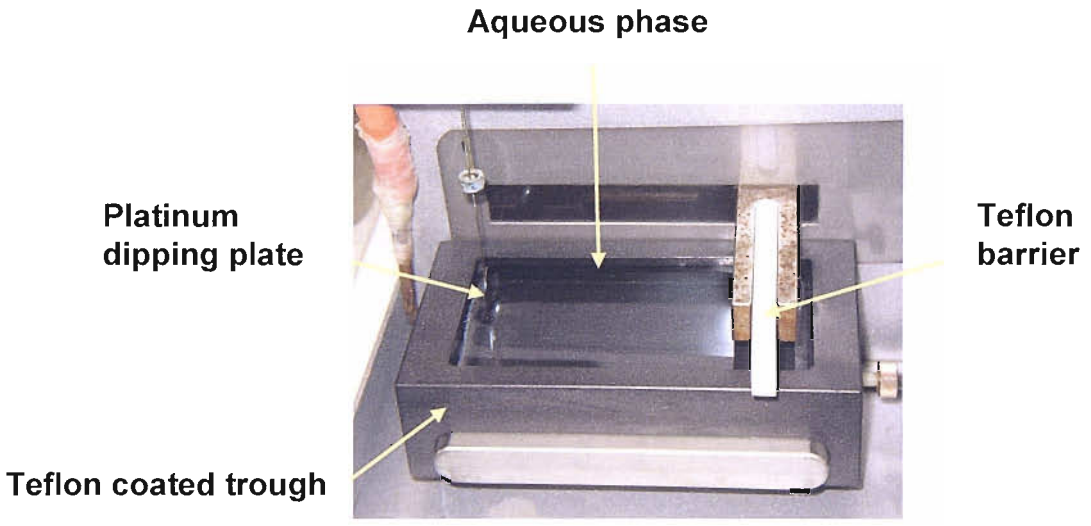

Figure 1.7: The principle components of the Wilhelmy surfactometer

The Wilhelmy-Langmuir method is easy to understand and provides an immediate analogue output, however the method has several disadvantages. It requires large liquid volumes (typically 50-80ml) and hence large amounts of sample, and the barrier cannot be cycled sufficiently quickly to mimic breathing, as this creates waves (a typical operating rate is 1.5 cycles per minute). All the components are prone to surface contamination, and rigorous, time consuming cleaning is required between sample measurements. Another problem with the Wilhelmy-Langmuir balance is the contact angle on the Wilhelmy plate. The meniscus decreases at low surface tension, often leaving behind a film of lipid material. Upon re-expansion of the surface layer, the liquid meniscus must re-spread and advance upward to attract the Wilhelmy plate. This problem can be a major source of error with this technique. A description of the application of the Wilhelmy balance to the assessment of lung surfactant surface activity is given in section 5.1.1.

1.5.4.2 The capillary surfactometer

It is well recognised that surfactant is crucial in maintaining patency of pulmonary alveoli. The concept that surfactant might also be important for keeping the narrow conducting airways open was first suggested by Macklem and colleagues. They concluded this after discovering that the pressure required to open terminal airways closed by liquid could be reduced by the detergent Tween[25]. Subsequent experiments carried out by Enhorning et al,[26] demonstrated the capability of a surfactant suspension

to maintain free airflow through a narrow glass tube and how this ability was lost in the presence of surfactant inhibitors.

A variety of alternative techniques have been developed to mimic alveolar function by cycling small volumes of surfactant at physiologically relevant rates. These include the pulsating and captive bubble surfactometers. Recently the capillary surfactometer has been introduced to model the function of airway surfactant.

The capillary surfactometer measures surfactants ability to maintain patency (or openness) of narrow terminal airways of the lung. The sample to be evaluated (0.5 ul) is introduced into the narrow section of a glass capillary, the internal diameter of which, is comparable to that of a terminal airway (0.3 mm). The capillary is connected to a bellows and a pressure transducer at one end and incubated at 37°C in a water bath.

As the bellows are compressed, pressure is raised. Increasing pressure causes the sample to be extruded from the narrow section of the capillary. As air gets through, pressure is abruptly lowered. If the capillary contains well functioning surfactant, the capillary will remain unblocked and the pressure recorded will be zero. However, if the sample does not contain well functioning pulmonary surfactant, the sample will return to the narrow section of the capillary, blocking it repeatedly (figure 1.8).

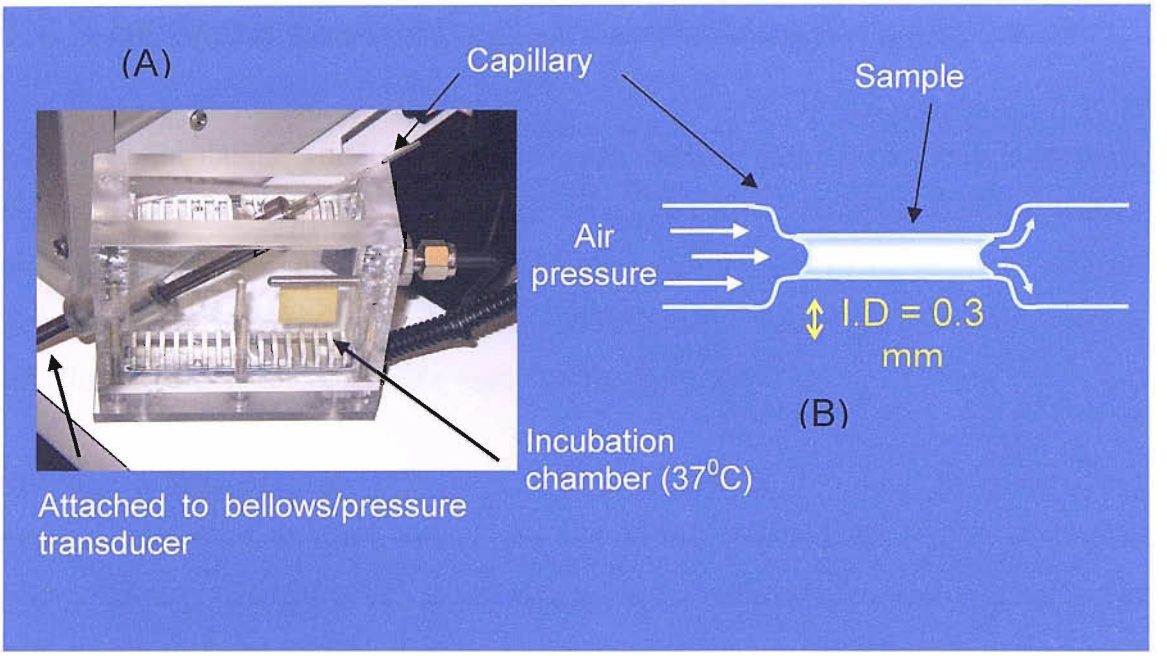

Figure 1.8: The principle components of a capillary surfactometer. A)The capillary attached to the bellows feed pipe and pressure transducer incubated in water bath B) Schematic enlargement of the capillary containing sample (0.5µl) to be evaluated.

The capillary surfactometer offers several advantages over the Wilhelmy surface tension balance. Firstly, it gives a direct and quantitative indication of a surfactant's ability to maintain an open terminal airway in a very short space of time on extremely small sample volumes. Operation of the instrument is very straightforward. All components exposed to the sample in question are discarded after use making the possibility of cross contamination unlikely, and the results produced are not influenced by changes in ambient temperature and humidity because the capillary is incubated at constant temperature in a water bath.

Capillary surfactometry studies on patients suffering from mild asthma have shown that bronchoalveolar lavage fluid (BALF) obtained after segmental allergen challenge with an antigen had a disturbed surfactant function, accompanied by a leakage of serum proteins[27] and lipoproteins[2]. The evaluation of surfactant function from sputum samples by capillary surfactometry has permitted assessment of the surfactant status of asthma patients over time and enables the determination of the effects of various types of treatment.[28] The application of capillary surfactometry to the study of surfactant function is discussed in greater detail in section 5.1.2.

1.6 The Immunological properties of surfactant

With each inhalation, small particles, viruses, bacteria and antigens are potentially deposited onto the epithelial lining of the lung. This lining provides a critical barrier between inspired gas and pulmonary blood flow. Due to its large surface area, delicate membranes and anatomic location, it is potentially easily susceptible to damage through infection, inflammation or any of a wide variety of insults.

Although a host defence response is crucial to protect the lung, an uncontrolled response may result in disruption of the thin epithelial-endothelial barrier leading to leakage of serum components into the air spaces and ultimately to severe, if not lethal impairment of gas exchange. Because the lung epithelium is in such close contact with the environment and because disruption of that epithelium can have such dire consequences, an appropriate balance between pro and anti-inflammatory responses in the lung is critical.

Lung surfactant has long been recognised as playing a crucial role in regulating inflammatory cell function within the lung, although the precise mechanisms of its action are still unclear. The function of four major groups of inflammatory cell in the lung is described below, together with literature examples of how surfactant has been shown to alter their function where appropriate.

1.6.1 Surfactant and the inflammatory cells of the lung

1.6.1.1 Alveolar Macrophages

Macrophages are derived from mononuclear phagocytic cells called monocytes and are dispersed throughout the body. Some take up residence in particular tissues, becoming fixed macrophages, where-as others remain motile. Macrophages are activated by a variety of stimuli in the course of an immune response exhibiting greater levels of phagocytic activity, an increased ability to kill ingested microbes, increased secretion of inflammatory mediators and an increased ability to activate T cells.

Alveolar macrophages in the lower respiratory tract protect the lungs from inhaled micro-organisms, primarily by phagocytosis of invading antigens. Alveolar

macrophages have been shown to be less active than other tissue macrophages. They express lower levels of complement receptors, are less effective at binding immunoglobulin-G (IgG) coated particles and show reduced antigen presentation.[29,30] Lung surfactant is thought to be responsible for the differences observed between the macrophage populations, [31] however the effects of surfactant are somewhat controversial. For example, immune suppression is thought to be catalysed by the lipid portion of surfactant, however, studies by Coonrod et al. describe the lysophosphoplipids and free fatty acids present in surfactant as facilitating the enhanced killing observed in the presence of surfactant.[32]

1.6.1.2 Neutrophils

Neutrophils are phagocytic cells produced in the bone marrow and subsequently released into the blood. They are recruited to a site of inflammation in response to chemotactic factors such as complement components, components of the blood clotting system and cytokines excreted by T-helper cells (T_H cells), where they ingest invading micro-organisms and destroy them by the respiratory burst oxidase response.

Fewer investigations have been performed on the effects of surfactant on neutrophil function, however lung surfactant has been shown to regulate the respiratory burst of neutrophils in a concentration dependant manner.[33] Significantly for the studies described in this thesis, this phospholipid-mediated neutrophils inhibition was achieved after only a brief 15 minute pre-incubation before cell stimulation (see chapter 6).

1.6.1.3 Eosinophils

Eosinophils, like neutrophils, are motile phagocytic cells that can migrate from the blood into the tissue spaces. Their phagocytic role is significantly less important than that of neutrophils and it is thought that their major role is in defence against parasitic organisms. Eosinophils play an important role in chronic airway inflammation in asthma. It has been shown by Cheng et al [34] that SP-A suppresses the production and release of interleukin-8 (IL-8) by ionomycin stimulated eosinophils. The SP-A effect was concentration dependant and reversed by addition of an SP-A antibody. Hohlfeld et al[35] have also demonstrated that IL-5 stimulated expression of activation markers on eosinophils was reduced in the presence of natural bovine lipid extract in a

concentration dependant fashion, hence the effect must have been mediated by the lipid components of surfactant. In addition, work by Okumura et al[36] showed stimulation of PtdCho secretion from cultured type II pneumocytes by activated eosinophils. Taken together these results suggest a possible feedback loop between surfactant release and eosinophil activation.

1.6.1.4 Lymphocytes and antigen presenting cells

Lymphocytes are the central cells of the immune system, responsible for acquired immunity and the immunologic attributes of diversity, specificity, memory and self / non-self recognition. Lymphocytes constitute 20 – 40 % of the body's white blood cells and can be divided up into two major subpopulations B lymphocytes, which confer humoral (antibody mediated) immunity and T lymphocytes which confer cell mediated immunity. The humoral response is best suited to the elimination of exogenous antigens and the cell-mediated response for the elimination of endogenous antigens.

1.6.1.4.1 B-lymphocytes

B-lymphocytes mature within the bone marrow; each possessing a unique antigen-binding receptor on the plasma membrane. When a naïve B cell first encounters its cognate antigen, it binds leading to rapid cell division into memory B cells and effector B cells called plasma cells. Antigens which are generally very large and complex are not usually recognised in their entirety by lymphocytes and both B and T-lymphocytes recognise discrete antigen epitopes. B cells recognise a large array of epitopes, including: those displayed on the surfaces of bacteria or viral particles, as well as those displayed on soluble proteins, glycoproteins, polysaccharides or lipopolysaccharides that have been released from invading pathogens.

1.6.1.4.2 T-lymphocytes

T-lymphocytes occupy a pivotal role in immune cell regulation by virtue of their ability to promote B cell maturation, drive antibody production and influence the growth and proliferation of macrophages, neutrophils, mast cells, eosinophils and other T cells. T cells are non-phagocytic cells produced in the bone marrow which then migrate to the thymus to mature. During maturation, the T cell comes to express a unique antigen binding molecule called the T cell receptor. Unlike membrane-bound antibodies on B

cells, which can recognise antigen alone, T cell receptors can only recognise antigen bound to major histocompatibility complex (MHC) molecules. There are two major types of MHC molecule, class I MHC expressed by most nucleated cells and class II MHC expressed only by antigen presenting cells (see section 1.6.1.4.3).

T-lymphocytes can be subdivided into two main classes, the T-helper cells (T_H) and the cytotoxic T-cells (T_c). After a T_H cell recognises and interacts with an antigen-MHC class II molecule complex, the cell is activated and becomes an effector cell that secretes various growth factors known collectively as cytokines. These cytokines play an important role in activating B cells, T_c cells, macrophages and various other cells that participate in the immune response. Under the influence of T_H derived cytokines, a T_c cell that recognises an antigen-MHC class I molecule complex proliferates and differentiates into an effector cell called a cytotoxic T lymphocyte.

Two main subpopulations of T_H cells have been identified. The T_H1 subpopulation, and the T_H2 sub-population. T_H1 cells are responsible for a number of cell mediated functions, for delayed-type hypersensitivity and are also associated with the promotion of excessive inflammation and tissue injury. The T_H2 subset is able to stimulate eosinophil activation and differentiation.

T-Lymphocytes obtained from lung lavage have long been known to be less responsive to mitogens than peripheral lymphocytes.[37] Wilsher et al [38] reported that pure phospholipids inhibited lymphocyte proliferation stimulated by phytohemagglutinin and that the purified phospholipids seemed to cause more inhibition than whole surfactant. These findings, in conjuction with those of Kremlev and Phelps [39], that SP-A stimulates and surfactant lipids inhibit lymphocyte proliferation, suggest that the lipids and proteins may be counter-regulatory and may therefore explain the ability of surfactant to regulate the immune response. This ability to regulate lymphocyte proliferation may be altered in disease [40].

1.6.1.4.3 Antigen presenting cells

Activation of both the humoral and cell-mediated branches of the immune system requires cytokines produced by T_H cells. T_H cells themselves have to be carefully regulated because an inappropriate T_H-cell response to self-components can have fatal autoimmune consequences. As a result T_H can only respond to antigen that is displayed

together with MHC class II molecules on the surface of antigen presenting cells (APC's). APC's, which include macrophages, B lymphcytes and dendritic cells are distinguished by two properties: they express class II MHC molecules on their membranes and they are able to deliver a co-stimulatory signal which is also necessary for T_H- cell activation. APC's firstly internalise antigen, either by phagocytosis or endocytosis and then display part of the antigen bound to a class II MHC molecule on their membrane. The T_H cell recognises and interacts with the antigen-class II MHC molecule complex on the membrane of the APC. An additional co-stimulatory signal is then produced by the APC, leading to T_H cell activation.

The role of the APC is crucial in initiating the immune cascade through the activation of T cells. Their role along with T cells in the context of airways disease and subsequently as a target for surfactant therapy is discussed in further detail in chapter 6.

1.7 Surfactant and airways disease

1.7.1 Neonatal respiratory distress syndrome

Respiratory distress syndrome (RDS) occurs in very low birth weight babies. It is caused by surfactant deficiency in the under-developed lungs of preterm infants [1]. Fujiwara and co. were the first to use natural surfactant extract to successfully treat premature infants with RDS [41]. This work lead to the wide spread study of natural and synthetic surfactants that are now available. The use of artificial surfactant for the treatment of RDS in pre-term babies has reduced the mortality rates of this disease significantly over the past 15 years (see section 1.9.1.3).

1.7.2 Adult respiratory distress syndrome

In 1967, Ashbaugh et al. [42] described the development of acute respiratory failure in 12 patients with progressive dyspnoea (difficulty in breathing) and hypoxemia (insufficient oxygenation of the blood). The clinical and pathological features observed resembled those seen in neonates suffering from NRDS, hence the disease was coined "adult respiratory distress syndrome" (ARDS). It was renamed the "acute respiratory distress syndrome" by an American-European consensus conference on ARDS[43]. ARDS is a non specific reaction of the lungs to a wide variety of insults; e.g. septic shock, sepsis,

fat embolism, trauma, burns, pancreatitis, cardiopulmonary bypass, lung contusion, pneumonia, and near drowning [44].

Because of the observed similarities between NRDS and ARDS, Petty and Ashbaugh postulated that the surface active material of the lung is abnormal in ARDS and that this defective surfactant may contribute to the pathophysiology of respiratory failure[42]. Although in contrast to NRDS, the deficiency of surfactant material is not the initiating problem in ARDS, a broad range of biophysical and biochemical abnormalities of the lung surfactant system have been observed.

The biophysical and biochemical alterations of the surfactant system in ARDS include: increased surface tension to more than 15-20 mNm^{-1} compared to near zero in healthy controls[45,46]; alteration of the phospholipid profile with reduction in the relative percentages of phosphatidylcholine and phosphatidylglycerol and an increase in the relative percentages of phosphatidylinositol, phosphatidylethanolamine and sphingomyelin[45,46,47,48]; alteration of the fatty acid composition with a marked reduction of the relative content of the saturated phospholipid fraction, especially palmitic acid[6,47]; decreased levels of surfactant apoproteins as shown for SP-A[45,46] and SP-B[45,46]; reduced content of large surfactant aggregates that are more surface active[49,50]; inhibition of surfactant by plasma proteins[45,51]; inhibition of surfactant by inflammatory mediators, in particular proteases[52] and oxygen radicals released by inflammatory cells which may attack surfactant proteins[53] and exert phospholipolytic activity that degrades surfactant lipids[47].

1.7.3 Cystic fibrosis

Cystic fibrosis (CF) is a lethal recessive genetic disorder that is expressed when the protein, Cystic fibrosis transmembrane conductance regulator (CFTR) is defective or absent. CFTR facilitates the transport of chloride ions across the exterior cell membranes in epithelial cells. In CF, defective CFTR function causes alterations to the dynamic balance of salt and water content at epithelial surfaces, leading to wide ranging clinical manifestations. These include gastrointestinal, reproductive and respiratory disorders [54].

The development of pulmonary complications as a consequence of chronic bacterial infection is responsible for 95-97% of the morbidity and mortality in individuals who suffer from CF. CF is characterised by an excessive immune response, which is accompanied by a massive infiltration of activated neutrophils into the lungs.

Improvements in the management of cystic fibrosis over the last two decades have led to significant increases in the life expectancy of CF patients. However, for the majority of patients, the combined effects of chronic pulmonary infections and the associated excessive immune responses lead ultimately to respiratory failure. In the current absence of a successful means of correcting the fundamental CFTR defect, strategies to delay or reduce the onset and development of pulmonary disease are the main focus of therapeutic intervention [54].

In CF there are no absolute deficiencies in surfactant quantity, and no major abnormalities in phospholipid composition. Surfactant therapy would therefore be targeted at suppressing the inflammatory response and enhancing bacterial clearance in the lungs.

1.7.4 Asthma

Asthma is a chronic disease caused by swollen and inflamed airways that are prone to constrict suddenly and violently [55]. Asthma affects 3 million people in the UK with 110,000 admissions to hospital excluding those dealt with in accident and emergency. Over the past 20 years, the prevalence of asthma has increased in both developed and developing countries that are adopting a westernised life style [56].

Bronchial asthma is recognised as a chronic inflammatory disorder of the airways with increased bronchial responsiveness and reversible airway narrowing in response to a wide range of stimuli. Asthma is a highly complex disease and although the causes are not yet fully understood, the resulting symptom of airway inflammation is the same. The allergic airway inflammation is triggered by exposure to inhaled allergens, which cause an immediate hypersensitivity reaction by prompting mast cells to release histamine and other mediators (discussed in detail in section 6.1.2) . These mediators sustain the reaction by activating T-lymphocytes to generate cytokines such as IL-4, IL-5 and tumour necrosis factor-α TNF-α[57]. IL-4 and TNF-α-induced leukocyte

recruitment, through up-regulation of adhesion molecules, may aggravate bronchial inflammation, thereby leading to oedema and leakage of plasma proteins into the airway spaces[58] (see section 6.1.3).

It is possible that surfactant dysfunction is involved in the accumulation of liquid in the airways, since normal functioning surfactant prevents liquid filling. Data on surfactant composition and function in asthma have been derived both in asthmatic patients and from animal asthma models. Guinea pigs sensitised with ovalbumin and then challenged with aerosolised antigen reacted with leakage of plasma proteins into the airways, a markedly increased airway resistance and altered surfactant performance indicating dysfunction[59]. In mite allergen-induced airway inflammation, decreased levels of SP-A and SP-D from sensitised mice have been reported.[60] In contrast, in various strains of sensitised mice, allergen challenge induced an increase in SP-A and SP-D immunostaining in nonciliated airway epithelial cells whereas SP-B immunostaining was unchanged.[61]

Data from patients with asthma are slowly accumulating. Kurashima et al[62] reported poor surface activity in sputum samples from patients with asthma. In addition, when asthmatics were compared with healthy controls, the percentage of DPPC decreased in sputum but not in BALF whilst SP-A levels were found to be unchanged.[63] In BALF, mole percent 16:0/16:0PC correlated with lung function (forced expiratory volume in 1 second). A study by Hohlfeld et al[64] investigated the inflammatory changes of BALF and the performance of BALF surfactant in healthy controls and patients with mild allergic asthma before and after segmental allergen challenge. Allergen challenge of asthmatics significantly increased eosinophils, proteins, the ratio of small to large surfactant aggregates (SA/LA) and decreased surface activity measured with the pulsating bubble and capillary surfactometers compared to controls. Interestingly, removal of the water soluble inhibitors by washing the surfactant fraction *in vitro* resulted in a substantial restoration of surfactant function.[64]

Analysis of phospholipid molecular species from BALF and plasma suggested that changes in PtdCho composition in BALF in asthmatic subjects following allergen challenge were due to infiltration of plasma lipoproteins and not phospholipid catabolism.[2] Therefore, the most likely reason for impaired surfactant function was that proteins had invaded the airways as they reached a ten-fold increase in concentration.

Surfactant inhibition by proteins has been well documented[65,66]. As inhaled allergens are initially suspended into the airway lining fluid before they come into contact with immune cells, an initial contact between allergens and surfactant components will occur soon after inhalation and deposition into the airway lining fluid. Consequently, surfactant involvement in immuno-modulation has attracted increasing interest in asthma.

1.8 Mechanisms of surfactant inactivation in disease

Various mechanisms have been proposed to explain how surfactant becomes inactivated, based on an interactions between surfactant and substances with increased concentration in the airways during inflammation.[7]

1.8.1 Incorporation of surfactant into hyaline membranes

A common finding in interstitial lung diseases is the presence of fibrin-rich hyaline membrane material.[67] In inflammation there is a shift towards pro-coagulation and hence a decrease in fibrinolytic activity. Seeger et al[68] showed that surfactant phospholipids and proteins B and C become incorporated into the fibrin strands losing their solubility and thus their surface tension lowering properties. This surfactant inhibition appears to be reversible, given that the addition of fibrinolytics resulted in regeneration of surfactant.[7]

1.8.2 Surfactant inhibition by inflammatory mediators

The inflammatory response involves a wide range of cellular and humoral mediators that can be generated by local neutrophils, macrophages, lung epithelial cells and fibroblasts. A number of species isolated from BALF samples have been implicated in surfactant inhibition. Oxygen free radicals generated by neutrophils have been shown to enhance lipid peroxidation.[69,70] The presence of protease and phospholipase enzymes can also lead to surfactant degradation and inactivation.

1.8.3 Plasma protein leakage

During lung injury, the capillary and alveolar endothelium become more permeable allowing the extravasation of plasma components into the alveolar space.[7] This has been confirmed by the presence of plasma proteins in BALF.[66,71,72] Albumin, haemoglobin and fibrinogen have been identified as potential inhibitors of surfactant. *In vitro* experiments have demonstrated their ability to inhibit surfactants surface tension lowering properties.

1.8.3.1 Lipoproteins

Whilst several plasma proteins have been investigated for their effects on surfactant function, lipoproteins have not been considered. Lipoproteins transport hydrophobic cholesterol, triacylglyceride and phospholipid molecules in the blood. They consist of a hydrophobic core composed of triacylglycerol molecules and cholesterol esters. This is surrounded by an outer layer of protein, free cholesterol and phospholipids.[73] The proportion of the various constituents varies altering their density, which is inversely related to their lipid content. Low density lipoprotein (LDL) has a density of between 1.019-1.063 $g.ml^{-1}$, it is 20 nm in size, composed of 20% apoprotein B-100, 21% phospholipids and 46% cholesterol. LDL provides cholesterol to the tissues and is the most common lipoprotein in blood. BALF samples from mild asthmatics following antigen challenge contained a phospholipid molecular fingerprint characteristic of plasma lipoprotein PtdCho, with enrichment of $PC16:0/18:2^2$, following plasma exudation into the airways. The impact of lipoprotein on surfactant function has not been studied.

1.9 Surfactant therapy

1.9.1 Natural, synthetic and recombinant surfactants

1.9.1.1 Composition of exogenous surfactants

Exogenous surfactant therapy has been part of the regular therapeutic arsenal of the neonatologist since the early 1990s. Surfactant preparations can be grouped into

different categories, natural animal-derived surfactant products, synthetic products and recombinant products. Animal-derived surfactants have different compositions to synthetic ones and both differ from naturally occurring mature human surfactant (table 1.1). The natural surfactants include bovine lipid extract surfactant (BLES Biochem, Canada), Infrasurf (Forest laboratories, USA), Alveofact (Boehringer Ingelheim, Germany) and Curosurf (Chiesi Pharmaceuticals, Italy) are all superior to the synthetic products that contain no surfactant associated proteins (Exosurf neonatal [Glaxo Smith Kline]), and Artificial Lung Expanding Compound (ALEC®) [Britannia Pharmaceuticals, UK]). Newer recombinant products include Venticute, which is based on a recombinant SP-C protein and Surfaxin (Discovery Laboratories, USA) which is based on an SP-B like peptide.

Source	Animal	Generic name	Trade name	% DPPC	Proteins
Amniotic fluid	Human[a]			54	ABCD
Minced lung	Bovine	Surfactant TA	Surfacten	50	BC
Minced lung	Bovine	Beractant	Survanta	50	BC
Minced lung	Porcine	Poractant alfa	Curosurf	35	BC
Lung lavage	Bovine	SF-RI-1	Alveofact		BC
Lung lavage	Bovine(calf)	CLSE	Infasurf	50	BC
Lung lavage	Bovine(calf)	CLSE	bLES	53	BC
Synthetic		Pumactant	ALEC	70	None
Synthetic		Colfosceril	Exosurf	84.5	None
Synthetic			Turfsurf[b]	91	Lipoprotein
Synthetic			Aposurf[b]	70	Apoprotein
Synthetic		Lucinactant	Surfaxin	70	KL_4 polypeptide
Synthetic		rSP-C	Venticute	67	Recombinant SP-C

Table 1.1: Composition of exogenous surfactants

[a] Human surfactant (from amniotic fluid) is no longer in use
[b] Turfsurf and Aposurf have been used in small studies but are not available for clinical use

1.9.1.2 Biophysical attributes

Animal-derived surfactants are more effective at lowering surface tension in vitro than synthetic ones, probably due largely to the presence of the hydrophobic proteins SP-B and SP-C[74,75]. Surfactant obtained by lung lavage (bovine or calf lung surfactant

extracts) are more resistant to inhibition in vitro by serum proteins than either synthetic surfactant with added SP-B and SP-C or minced lung surfactant extracts[66]. The new synthetic peptide or recombinant surfactants show better resistance to inactivation than any of the surfactants currently available for clinical use[76].

1.9.1.3 Clinical studies on exogenous surfactant formulations used to treat NRDS

Of all the therapies during the neonatal period, none have been tested as extensively as surfactant replacement therapy. More than 400 clinical trials have evaluated the overall efficacy of surfactant therapy, as well as aspects such as the relative efficacy of different surfactant preparations, the optimal timing of administration and the optimal dosage. Although both synthetic and animal-derived surfactants are effective in clinical trials, improvements in lung mechanics and oxygenation occur more rapidly after animal derived than synthetic surfactants.[77] A systematic review[78] of the 10 randomised trials that studied the effects of animal-derived versus synthetic surfactant for the treatment of RDS supports the use of animal derived surfactants. In a meta-analysis carried out by Murdoch[79], there was a significant reduction in air leak in favour of animal-derived surfactants but only trends towards reductions in mortality and combined mortality/chronic lung disease. Two studies have been published since Murdoch's review. Ainsworth et al found that infants given poractant had less than half the mortality of those given Pumactant[80]. Mortality was not a primary outcome in this trial and the trial had been stopped early. Kukkonen et al[81] found no difference in duration of ventilation or supplemental oxygen or mortality between poractant and colfosceril, but infection was more common after treatment with poractant. Future trials will evaluate third-generation surfactant products, clarify product differences and further refine what constitutes optimal use of surfactant in conjunction with other respiratory interventions.

1.9.1.4 Surfactant therapy and lung disease

There has been growing insight into the functional role of surfactant components and the mechanisms by which exogenous surfactant exerts its therapeutic effects on lung mechanics, gas exchange and host defence over the last 15 years.

1.9.1.4.1 ARDS

ARDS is a multi-factorial disease in which surfactant alteration is one of the factors. Initial trials to treat ARDS with surfactant replacement therapy were disappointing [82,83]. This may be due to low dose used, the phospholipid and protein composition and the severity of ARDS at the time of administration. One large randomised multi-centre study has investigated the efficacy of aerosolised Exosurf a synthetic surfactant preparation however no improvement on clinical outcome was observed. In one study, repetitive intratracheal application of the bovine preparation Survanta was given to adults suffering from acute respiratory failure with cumulative doses between 300 and 800 $mgkg^{-1}$ body weight. An improvement in gas exchange and a trend towards an increase in survival were noted[84]. Similar positive effects were seen with the porcine preparation Curosurf.[82] A recombinant SP-C based surfactant (Venticute) has been found to have favourable results in preclinical studies[85] and a phase I/II clinical study showed a trend towards benefit[86]. However in a recent two multi-centre randomised trial comparing standard therapy with standard therapy plus four intratracheal doses of a recombinant surfactant protein C based surfactant, the use of the exogenous surfactant did not improve survival[87]. However, patients receiving surfactant treatment did show a greater improvement in gas exchange during the treatment period suggesting potential benefits of a longer treatment course[87].

1.9.1.4.2 Asthma

Published literature data support the concept that a poor function of surfactant contributes to the pathophysiologic scenario in asthma (see section 1.7.4). There are two different ways to improve surfactant balance in the airways. Various drugs commonly used in asthma therapy such as corticosteroids, β-adrenergic agents and theophylline, have been shown to stimulate surfactant synthesis and secretion.[88,89,90] However it remains to be seen whether pharmacological stimuli can augment surfactant secretion to clinically significant levels. Secondly, treatment with exogenous surfactant has been shown to improve allergic airway obstruction in animal models of asthma. Prophylactic treatment of sensitised animals with intra-tracheal instillation of surfactant reduces the deteriorating function that would otherwise have developed.[91] This effect was also shown in guinea pigs which were administered inhaled surfactant.[92]

The therapeutic potential of the lung collectins SP-A and D have also specifically been tested in murine asthma models[93,94]. Here, treatment of aspergillus-sensitised mice with a recombinant SP-D fragment was effective in reducing eosinophilic inflammation and specific IgE production. Furthermore, bronchial hyper-responsiveness was alleviated in SP-D treated animals along with a shift in cytokine profile from T_H2 to T_H1 with increases in IL-12 and IFN-γ and decreases in IL-4 and IL-5.

Human data are restricted to the use of commercially available natural or synthetic surfactant preparations. Results from a controlled pilot study in Japan [95], showed that inhalation of surfactant during acute asthmatic attacks led to improvement of lung function in the surfactant treated subjects. However, in another study on asthmatic children with mild airflow limitation, nebulization of surfactant did not alter airflow, airflow obstruction and bronchial responsiveness to histamine[96]. A randomised controlled trial of aerosolised synthetic surfactant (Exosurf) in patients with stable bronchitis revealed a significant improvement of forced expiratory volume in one second (FeV_1) of 11%, a decrease in thoracic gas trapping by 6% and an improvement in sputum transportability[97]. Exogenous surfactant therapy has also been shown to improve disease course in infants with respiratory syncytial virus bronchiolitis.[98] A small randomised controlled trial demonstrated a significant improvement of pulmonary function data following prophylactic inhalation of a synthetic surfactant preparation artificial lung expanding compound (ALEC) as a dry powder, prior to allergen challenge in patients suffering from mild atopic asthma[9] (see section 1.9.3). All these results together demonstrate beneficial effects of exogenous surfactant therapy in the treatment of asthma and obstructive airways disease. Future laboratory and clinical investigations will help to determine the surfactant components with the most pronounced anti-obstructive effects and the most potent anti-inflammatory capabilities.

1.9.2 From ALEC® to PUMACTANT

1.9.2.1 ALEC® and NRDS

A synthetic phospholipid mixture for the treatment of NRDS consisting of DPPC and Egg PtdGly in a ratio of 7:3 w/w was developed initially by Bangham & Morley [99] given the trade name ALEC® (Artificial Lung Expanding Compound) for reconstitution with saline for intra-tracheal administration to newborn infants of less than 30 weeks

gestation. ALEC® was licensed and marketed by Britannia Pharmaceuticals in the UK in 1994.

It was manufactured by dissolving the DPPC and Egg PtdGly in chloroform to enable sterilisation by filtration. In an aseptic room, the chloroform was evaporated off, and the resultant material rehydrated with sterile water. Aliquots were subsequently placed in vials from which the product was freeze dried. The resulting lipid plug was then agitated to de-aggregate to a lose powder which was the marketed product. Although ALEC® was a cheap and reasonably effective substitute for natural lung surfactant in very premature babies, it was not as potent as other phospholipid mixes and animal extracts available on the market e.g. KL4, Survanta, Curosurf and Alveofact. ALEC® was withdrawn from the market in May 2000[100], following results published from a clinical trial comparing it with porcine exogenous surfactant (poractant alfa) for treatment of NRDS. The trial showed that infants treated with ALEC® had a lower survival rate that of poractant alfa.[80]

1.9.2.2 Formulation of a dry powder surfactant (Pumactant)

The concept that surfactant could be successfully administered as a dry powder was first realised in the treatment of NRDS by Bangham and Morley[101]. By 1999, Britannia had already considered the use of their synthetic phospholipid product for the treatment of adult respiratory conditions. Britannia re-formulated ALEC® as a dry powder in preparation for the Southampton trial to evaluate the effect of Pumactant on the development of early and late phase bronchoconstriction in allergen induced asthma[9]. This new formulation became known as Pumactant which is the original British approved name for the DPPC/egg PtdGly mix regardless of the manufacturing process. As a fine powder, Pumactant can theoretically penetrate deeper into the lung where, once in contact with the lower airways energy of hydration will aid spreading [102].

Since powders for inhalation do not have to be sterile but do require particle size control, it was suggested by the active pharmaceutical ingredients manufacturers Lipoid, that the DPPC and egg PtdGly could be dissolved in ethanol, vacuum dried in bulk and then micronised to generate the required respirable particle size. The resulting powder was subsequently hand filled into the vials for clinical trial (see section 1.9.3).

1.9.3 Prophylactic administration of Pumactant to mild asthmatics

Pumactant was employed in a small scale clinical trial in which mild asthmatics were pre-treated with the inhaled dry powder preparation and then challenged with allergen[9]. Surprisingly, pumactant abolished the early asthmatic response (EAR) in all seven subjects, but had no effect on the late asthmatic response (LAR). Demonstration of the inhibition of the EAR by exogenous surfactant provided the first evidence of a contribution of pulmonary surfactant dysfunction to the early asthmatic response to allergen. Exogenous surfactant administration could therefore serve as a useful addition in controlling the symptoms of patients with allergic asthma. Despite this profound discovery, the mechanism of action of the exogenous material on the allergic response is completely unknown. This product is now being exclusively developed by airPharma under the trade name of ZoFac™.

1.9.4 Development of the PADDS (Pressurised Aerosol Dry-Powder Device)

As part of an ongoing development programme, a novel hand-held "active" dry-powder inhalation device (pressurised aerosol dry-powder delivery) has been developed for the delivery of high dose (25-250 mg) cohesive powders to the respiratory tract.[103] This prototype was tested using Pumactant as a model drug. The PADD device is a 'stand alone' hand-held high-energy aerosolisation system utilising a pressurised gas to supply a positive pressure through a series of venturi tubes into a carrier-free powder bed. The aerosolised powder is entrained and inhaled through a conventional mouthpiece. The powder bed is contained in a sealed disposable vial which can be filled under aseptic and controlled environmental conditions. A schematic diagram of the PADD device is shown in figure 1.9.

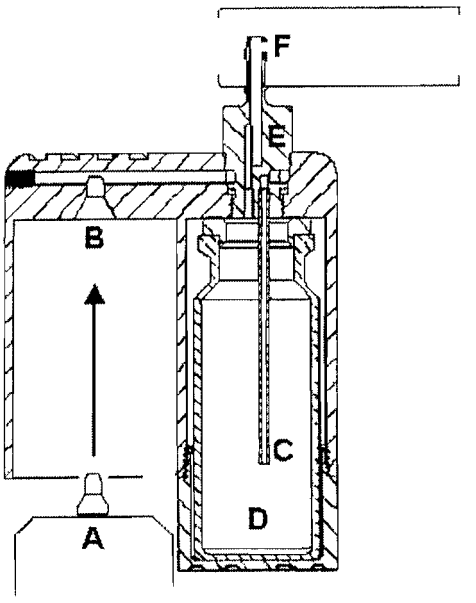

Figure 1.9: Schematic of the PADD dry powder aerosolisation device. (A) 28-ml aluminium gas canister. (B) Connection duct. (C) Aerosolisation pipe. (D) Vial containing drug material, (E) Exit channel. (F) PADD orfice and patient mouthpiece. Reproduced from Young et al [103].

1.10 Aims

The aims of this project were to investigate structural and functional interactions between Pumactant and pulmonary surfactant by modelling and measuring physical interactions at air/liquid interfaces *in vitro* and to probe how Pumactant alters immune cell responses. The project also required development of mass spectrometric techniques in order to assess the turnover of this artificial surfactant in the lung.

Chapter 2

Materials and Methods

2.0 Materials and methods

2.1 Materials

Amniotic fluid surfactant was a gift from Samantha Williams, Southampton General Hospital.

Jurkat cells were a gift from Samantha Williams, Southampton General Hospital.

All solvents were HPLC grade, obtained from VWR international (Lutterworth), or Fischer Scientific (Leicestershire). All other reagents were obtained from Sigma-Alrich (Poole, UK).

Roswell Park Medical Institute (RPMI) (x1) with HEPES, Fetal Calf Serum (FCS), heat inactivated and antibiotic/antimyotic solution (x100) (penicillin and streptomycin) were obtained from PAA laboratories, Austria.

Pumactant sterile freeze dried powder was obtained from Britannia Pharmaceuticals, Redhill, Surrey.

β-mercaptoethanol (50 mM) was obtained from Gibco BRL.

MACS anti-hapten microbeads and the LS^{+} separating columns were obtained from Miltenybiotec.

Phospholipid standards DMPC DMPA etc were obtained from Avanti Polar Lipids, Canada.

DuoSet ELISA development system (human IL-2) was obtained from R&D systems, Abingdon, Oxon.

Tetramethylbenzidine (TMB) and Hydrogen peroxide (H_2O_2) (ELISA reagents) were obtained from Pharmingen, (Cambridge Bioscience).

2.2 Mass spectrometry of phospholipids

2.2.1 Phospholipid analysis by ESI-MS

All mass spectrometry was performed using a triple quadrupole electrospray mass spectrometer. (Quattro Ultima, Micromass UK) equipped with an electrospray ionisation interface. All samples were analysed by direct infusion unless otherwise stated ($5\mu l min^{-1}$) using $MeOH/CHCl_3/H_2O/NH_3$ (in the ratio of 70:20:7:3) as the solvent. Spectra were acquired in both positive and negative ionisation mode typically between 450 *m/z* and 900 *m/z* with a scan time of 12 seconds and a resolution of 0.1 mass units. The mass spectrometer tune parameters were varied to optimise ion current for the lipid class being analysed. Typical tune page settings for ESI-MS/MS are given in table 2.1.

Settings	**Positive ionisation mode (ES+ve)**	**Negative ionisation mode (ES-ve)**
Capillary (KV)	2.5	2.5
Cone (V)	90	90
Hexapole 1 (V)	1	0.2
Apperture 1 (V)	0.9	0.2
Hexapole 2 (V)	0	0.3
Source temperature (^oC)	80	80
Collision energy (eV)	34	35

Table 2.1: Typical tune page settings used for electrospray tandem mass spectrometry

2.2.2 Processing mass spectrum data

Data generated by the mass spectrometer is visualised as a spectrum with the mass/charge ratio (m/z) plotted against intensity. Individual molecular species were identified according to their m/z ratio or molecular weight as phospholipids are singularly charged (z=1). Spectral data were typically averaged for 10 scans, background noise was subtracted and the data was smoothed using MassLynx NT software. The mass spectrometer collects about 10 intensity values per Dalton. In order

to analyse the data a numerical value must be assigned to each mass ion. The mass spectrum is centred to obtain one single numerical value for each mass. The height of this single peak is proportional to the sum of the individual intensities for that particular mass. These numerical values were then transferred to excel spreadsheets. An excel macro programmed in visual basic has been developed within the laboratory which enables the extraction and isolation of ion intensities corresponding to specific phospholipid molecular species of interest. The corresponding selected intensities are combined in a results spreadsheet where they are corrected for ^{13}C isotope effects and reduced response with increasing m/z values. Results are reported as a percentage of the total present in the sample unless otherwise stated.

2.3 Determination of surfactant phospholipid turnover *in vivo*

2.3.1 Collection of samples for the determination of surfactant phospholipid turnover in vivo

Sample collection and extraction carried out by Dr Wolfgang Bernhard, Eberhard-Karls-University, Tübingen

[D-9 methyl] choline chloride (3.6 mg per kg body weight) was intravenously infused into the forearm of healthy volunteers over 3 hours.

2.3.1.1 Collection of plasma samples

Blood samples (2ml EDTA-tubes) were collected from a vein on the other forearm, at 0, 6, 24, 48, and 72hours after the start of [methyl-D_9]choline chloride infusion. EDTA blood was centrifuged at 1000 x g at 4°C for 15 minutes and plasma aspirated for PtdCho analysis.

2.3.1.2 Collection of sputum samples

Induced sputa were collected prior to the start of [D-9 methyl] choline chloride infusion (t = 0 hours) and at time points 12, 24, 30, 36, 48, 72, 96 and 168 hours after the start of the infusion. Fifteen minutes before sputum induction, two doses of 100μg salbutamol

(Sultanol® MDI, GlaxoSmith Kline, Munich, Germany) were inhaled using a Volumatic® spacer device (GlaxoSmith Kline, Munich, Germany). Volunteers then inhaled 5.85% sterile sodium chloride solution with a pressure driven nebulization device (Pariboy master®, Pari GmbH, Starnberg, Germany) in 4 intervals of five minutes. Following each interval, the mouth and larynx were cleaned four times with 200-300ml tap water and sputum (1 to 4ml) was expectorated into a plastic beaker over a 1.5 minute period. Sputum samples were immediately cooled (0 – 4°C) in an ice-water mixture, diluted with ice cold sterile phosphate buffered saline (pH7.2) to a final volume of 15ml and suctioned through disposable filters (FALCON® Cell strainer, 100µm Nylon, Becton Dickinson Labware, Franklin Lakes, NJ, USA) into a 50ml plastic vial to remove viscous material. Cells were removed by centrifugation (10mins, 4°C, 400xg). Supernatants were frozen (-20°C) in 5ml fractions for storage. Prior to total phospholipid extraction, the diluted filtrated material (5ml), was thawed and PC14:0/14:0 (25 nmol), PG14:0/14:0 (10 nmol) and PE14:0/14:0 (10 nmol) internal standards were added. Samples were extracted using an acidified phospholipid extraction (Downes and Wustemann, 1983), and concentrated to dryness under N_2 gas. Vials were closed, packed on dry ice and shipped to Southampton for ESI-MS/MS analysis.

2.3.2 Plasma phospholipid extraction and analysis by ESI-MS/MS

0.9% saline (750µl) was added to plasma (50µl) from which phospholipids were extracted according to the method of Bligh and Dyer.[104] All lipid extracts were dried under a stream of nitrogen and stored in the freezer (-20°C) until analysis. Samples were injected into a Micromass Quattro ultima electrospray ionisation mass spectrometer (see section 2.2.1) and analysed by ESI-MS/MS. Collision gas-induced dissociation produced protonated head group fragments with m/z = +184 for endogenous PtdCho[105] and m/z = +193 for newly synthesised PtdCho from the CDP-choline pathway corresponding to their respective protonated headgroups. Analysis of the intermediates with m/z = +187 and +190 (i.e. containing one or two recycled and labelled methyl groups) revealed indirect incorporation of deuterium into choline headgroups via the PtdEtn N-methylation pathway.[106] The 13 most abundant plasma PtdCho molecular species were chosen to represent plasma PtdCho. These are given in table 2.2, along

with their corresponding precursor and production ion masses. Acquired mass spectrometry data was processed as described in section 2.2.2.

PtdCho molecular species	Endogenous fragmentation (m/z)	N-methylation synthesised fragmentation (m/z)	CDP-choline synthesised fragmentation (m/z)
PC16:0/16:1	732.7 – 184.1	735.7 – 187.1	741.7 – 193.1
PC16:0/18:2	758.7 – 184.1	761.7 – 187.1	767.7 – 193.1
PC16:0/18:1	760.7 – 184.1	763.7 – 187.1	769.7 – 193.1
PC16:0/20:4	782.7 – 184.1	785.7 – 187.1	791.7 – 193.1
PC18:1/18:2	784.7 – 184.1	787.7 – 187.1	793.7 – 193.1
PC18:0/18:2	786.7 – 184.1	789.7 – 187.1	795.7 – 193.1
PC18:0/18:1	788.7 – 184.1	791.7 – 187.1	797.7 – 193.1
PC16:0/22:6	806.7 – 184.1	809.7 – 187.1	815.7 – 193.1
PC18:1/20:4	808.7 – 184.1	811.7 – 187.1	817.7 – 193.1
PC18:0/20:4	810.7 – 184.1	813.7 – 187.1	819.7 – 193.1
PC18:1/22:6	832.7 – 184.1	835.7 – 187.1	841.7 – 193.1
PC18:0/22:6	834.7 – 184.1	837.7 – 187.1	843.7 – 193.1
PC18:0/22:5	836.7 – 184.1	839.7 – 187.1	845.7 – 193.1

Table 2.2: Mass spectrometry assignments for the 13 major plasma PtdCho molecular species.

2.3.3 MRM analysis of surfactant phospholipids extracted from patients

Sputum samples were dissolved in MeOH/$CHCl_3$/H_2O (7:2:1) (15µl per sample) and injected into the mass spectrometer by auto sampler (Hewlett Packard 1100 series). An MRM method was set up to monitor the transition of 8 PtdCho molecular species (given in table 2.3) to their diagnostic product ion fragments corresponding to the protonated phosphocholine headgroup.

In positive ionisation mode, fragmentation of endogenous PtdCho with argon gas, produces a fragment at *m/z* = 184. Newly synthesised PtdCho which contains 9 deuterium atoms produced an analogous fragment at *m/z* = 193 (see table 2.3). Dwell time was 0.1 seconds. The mass spectrometer produces two time response curves corresponding to the endogenous and labelled PtdCho fractions respectively. These will be referred to as MRM chromatograms throughout this thesis (see figure 3.14). The area under each chromatogram corresponds to the sum of all the individual transitions monitored. The fractional incorporation of [methyl-D_9]choline into sputum PtdCho was calculated by dividing the area under the D_9 labelled chromatogram by the sum of the areas of labelled and endogenous chromatograms and is expressed as a percentage.

PC molecular species	Endogenous transition upon fragmentation *m/z*	Newly synthesised transition upon fragmentation *m/z*
PC 16:0/ 14:0	706.7 – 184.1	715.7 – 193.1
PC 16:0a/16:0	720.7 – 184.1	729.7 – 193.1
PC 16:0/ 16:1	732.7 – 184.1	741.7 – 193.1
PC 16:0/ 16:0	734.7 – 184.1	743.7 – 193.1
PC 16:0a/ 18:0	748.7 – 184.1	757.7 – 193.1
PC 16:0/ 18:2	758.7 – 184.1	767.7 – 193.1
PC 16:0/ 18:1	760.7 – 184.1	769.7 – 193.1
PC 16:0/ 20:4	782.7 – 184.1	791.7 – 193.1

Table 2.3: MRM transitions for the 8 major sputum PC species for endogenous and newly synthesised material. (key: a= alkyl group)

2.4 Dry powder phospholipid administration

2.4.1 Pumactant administration by air/CO_2 filled syringe

To a plastic syringe (Terumo, 10ml) was attached a piece of plastic tubing (internal diameter (I.D) 2mm approx), which was in turn pierced through a suba seal into a vial containing dry amorphous pumactant (100mg). A second piece of plastic tubing pierced through the same suba seal, was used as an 'outlet'. Pumactant was dispensed with either air (2ml) or CO_2 (3ml) into glass screw top tissue culture tubes. Pumactant was resuspended in $CHCl_3$ (1ml), diluted (1 in 100), spiked with DMPC internal standard (0.59μmol) and quantified for PC16:0/16:0 content (m/z = +734.7) by ESI-MS/MS relative to DMPC internal standard.

2.4.2 Pumactant administration using the initial actuation device

The device consisted of two inverted syringes, placed one on top of the other, plunger to plunger. The air tight seal on the upper most syringe was removed and replaced with a spring. This spring loaded syringe was used to depress the plunger of the lower syringe,

which was filled with CO_2 (4ml), when the catch on the spring loaded syringe was released.

The CO_2 filled syringe was connected to a CO_2 inlet and an HPLC tube outlet via a three way tap. The HPLC tube outlet, fed directly into the Pumactant vial. A second piece of HPLC tubing, leading out of the vial, was used to dispense Pumactant to the atmosphere (see figure 4.1).

The 'actuation hood' (figure 4.1) was constructed from a plastic container lid (dimensions 143 x 74 x 31 mm).

2.4.3 Pumactant administration using the automated actuation device

This automated actuation device was one of two identical administration units, commissioned by Britannia Pharmaceuticals, as part of a clinical trial, involving pre-dosing mild asthmatics with Pumactant. The device was supplied by PA consulting group (London) and was equipped with an electronically controlled timer switch which controlled the actuation duration (0.1 – 10 seconds) and a needle valve enabling adjustment of the output CO_2 pressure (figure 4.2, section 4.2.3). HPLC tubing was used to interface the automated actuation device with the Pumactant vial and the Pumactant vial with the atmosphere as described in section 2.4.2. The actuation hood (section 2.4.2) was employed for the duration of each actuation

Pumactant vials were housed on a vortexer (Corning, 4010 multi-tube vortexer). The vial was agitated as the powder was dispensed (speed setting 4).

2.4.4 The Vibrating Powder Aerosol Generator (VPAG)

2.4.4.1 The VPAG control unit

A digitally controlled dry powder actuation device was commissioned from SMC Pneumatics Ltd (Milton Keynes, UK) according to my design specifications. The device incorporated 'ultra clean' components and was fitted with a precision adjustable pressure valve and a digital display reporting the CO_2 output pressure (figure 4.3a and 4.3b, section 4.2.1.4.1).

2.4.4.2 The vibration table

A pneumatically driven vibrator was commissioned alongside the actuation device, to agitate and hence 'fluidise' the Pumactant powder, whilst it was being dispensed. The table was custom built by Vibratechniques Ltd (Brighton, uk). It was constructed from stainless steel (140 x 100mm) and fitted with rubber anti-vibration mounts. Two white 'delrin' vial holders were attached to the top plate of the table, each with a nitrile 'O' ring to clamp the vials. The vibration table was powered by a GT4 pneumatic turbine vibrator (Findever, Switzerland) and supplied complete with airline filter, regulator, gauge, on/off valve and 8mm O/D hose (see figure 4.4). The device was equipped with an on/off valve and a combined pressure gauge and regulator which reported the pressure being used to drive the vibration turbine.

Agitation speed was determined by the pressure of the compressed air propelling the device. The vibrator was typically operated at a pressure of 1.5 bar (section 4.2.1.4.2).

2.4.5 VPAG vibration table characterisation using accelerometers

Vibration characteristics of the vibration table were carried out in the dynamics laboratory (Institute of Sound Vibration Research, University of Southampton). Two accelerometers (Brűel and Kjaer) were attached to the upper and lower plates of the vibration table using bees wax. The accelerometers were attached to a charge amplifier (Brűel and Kjaer type 2135) which interfaced with a PC. To replicate the device when in use, a Pumactant filled vial was placed in one of the vial holders.

The threshold of vibration frequencies for the device was determined by measuring vibration with the vibration table set at 0 bar (stationary) and 2 bar output pressure. Acceleration measurements were then carried out at 0.5, 1, 2, 3 and 4 bar output pressures. The accelerometer measured the acceleration across a frequency spectrum (0-1500Hz). One acceleration measurement was prepared by averaging 20 x 1 second spectra.

2.4.6 Delivered dose studies using the VPAG

All experiments were carried out in ambient laboratory conditions (23-25°C, 60% RH) using amorphous Pumactant (Britannia Pharmaceuticals Ltd). Delivered dose was assessed gravimetrically by weighing the vial before and after actuation.

2.4.6.1 Delivered dose vs. vial vibration frequency

Pumactant was actuated for 5 seconds using 1 bar Powder delivery pressure from the VPAG control unit. Delivered dose was assessed at 0, 0.5, 1, 2, 3 and 4 bar vial excitation pressure (corresponding to 0-404 Hz excitation frequency and 0 – 375m.s^{-2} acceleration amplitude).

2.4.6.2 Delivered dose for micronised Pumactant

Microionised Pumactant was actuated for 10 seconds at 2 bar delivery pressure. Delivery dose was assessed for 100, 125, and 150mg samples.

2.4.7 Aerosolisation efficiency studies using the VPAG

2.4.7.1 Characterisation of amorphous Pumactant

The particle size distribution of amorphous pumactant was determined using laser light scattering (Mastersizer X, Malvern, UK) using a 100 mm lens and small volume stirring circulation cell. The amorphous pumactant was dispersed in cyclohexane and ultrasonicated for 5 minutes prior to analysis (determined as sufficient to fully de-aggregate the powder).

2.4.7.2 Aerosolisation efficiency studies of dry amorphous Pumactant using the VPAG

Particle size distribution of amorphous dry powder Pumactant dry was carried out by laser light scattering (Mastersizer X, Malvern, UK) using a 100 mm lens and a dry flow cell attached to a suction device. Pumactant was either actuated into the dry flow cell using the VPAG (vibration table pressure 2 bar, actuation pressure 1 bar, actuation duration 30 seconds) or introduced into the flow cell by spatula.

2.5 Collection and processing of lung surfactant from amniotic fluid

In order to assess the physical interactions between Pumactant and lung surfactant, a source of endogenous lung surfactant was required. Lung surfactant is typically obtained from BALF.[107] However, due to the invasive nature of the procedure and the large quantities of material that would be required for the experiments, obtaining lung surfactant from BALF was not ethically feasible. In the early 1980's, lung surfactant isolated from amniotic fluid collected at full term elective Caesarean sections was used in a clinical trial to treat NRDS in premature babies resulting in a positive clinical outcome.[108] This material was found to have good in vitro surface active properties consistent with reference surfactant preparations derived from animal extracts.[109] As amniotic fluid is typically collected and discarded during elective section, it is a source of surfactant that can be harvested by 'non-invasive' means and as such was the method of choice.

2.5.1 Amniotic fluid collection

Amniotic fluid was collected from full term Caesarean section deliveries at the Princess Anne Maternity Hospital, Southampton and was stored in 1 litre bottles containing EDTA, (5mM), sodium azide (NaN_3, 0.2%) and sodium chlroride (NaCl, 0.9%) at 4°C.

2.5.2 Amniotic fluid processing

The amniotic fluid was filtered through glass wool into 50 ml universal containers. Tubes were centrifuged (100xg, 10 mins, 4°C). The pellet was discarded and the supernatant transferred to 500ml bottles and stored at –20°C.

2.5.3 Isolation of Surfactant from Amniotic fluid

Surfactant was purified from amniotic fluid surfactant according to the method of Hallman et al.[109] Ice-cold amniotic fluid was added to 6 x 80ml polyallomer ultracentrifuge tubes. Tubes were centrifuged (60,000xg, 1 hour, 4°C in an angle rotor). The supernatant was discarded and the pellets re-suspended in ice cold NaCl solution (0.9%, 20 ml). Concentrated amniotic fluid was homogenised using a hand held

homogeniser and layered at a ratio of 1:2.6 over sucrose solution (0.75M), in 6 x 38ml polyallomer ultracentrifuge tubes. Tubes were centrifuged (60,000xg, 1 hour, 4°C) in a swing-out rotor. Surfactant was removed from the NaCl/sucrose interface and transferred to 6 x 80ml polyallomer ultracentrifuge tubes. Each tube was made up with ice-cold NaCl solution (0.9%, up to 70ml).

Tubes were centrifuged (100,000xg, 1hour, 4°C) in an angle rotor. Supernatant was discarded and the pellets were re-suspended in ice-cold NaCl solution (0.9%, 10ml) and isolated surfactant was stored at –20°C.

2.5.4 Total lipid extraction (Bligh and Dyer method)

Samples to be extracted (800µl) were added to screw top glass culture tubes, to which $CHCl_3$ (1ml) and MeOH (2ml) was added. Tubes were vortexed (single phase formed). Distilled water was then added (1ml), to form a biphasic solution. Tubes were centrifuged (1000xg, 10 mins, 4°C), the lower chloroform rich layer was transferred into open top pyrex disposable culture tubes and concentrated to dryness under nitrogen gas, 40°C [104]. Samples were stored in the freezer (-20°C) until required.

2.5.5 Phospholipid phosphorous determination

Phospholipid phosphorus was determined according to the method described by Bartlett in 1959[110]. DMPC standard in $CHCl_3$ ((1mM), 0, 5, 10, 20, 30, 40 and 60 µl (0.- 60 nmol)) was added to open top tissue culture tubes. Standards and Bligh and Dyer extracted samples (section 2.5.4) were concentrated to dryness under nitrogen (40°C). Distilled water (60 µl) was added to samples and standards. Perchloric acid (70%, 100 µl) was then added, samples mixed and heated on a dry block (180°C, 40 mins). Samples and standards were cooled, after which hydrogen peroxide (30%, 5 µl) was added.

Samples and standards were heated (180°C, 30 mins), cooled and distilled water added (760µl). Ammonium molybdate (5%w/v in 2M HCl, 40 µl) was added, samples and standards were agitated after which Fiske and Subbarow reducer (0.25% 1-amino-2-napthol-4-sulphonic acid, 7.5% $Na_2S_2O_5$, 0.5% $Na_2S_2O_3$ w/v) was added (150 µl). Tubes were mixed again and heated (100°C, 10 mins). Samples and standards were

transferred to $1cm^3$ cuvettes and absorbance (830 nm) measured against a phosphate free blank standard. The concentration of each sample was calculated against the DMPC standard curve.

2.5.6 ESI-MS/MS characteristion of amniotic fluid surfactant (AFS)

AFS (3 x 800µl) was total phospholipid extracted as described in section 2.5.4. Dried samples were dissolved in MeOH/$CHCl_3$/H_2O/NH_3 (70/20/7/3, 500µl) and analysed by ESI-MS/MS as described in section 2.2.1. PtdCho composition was determined by precursor ion scanning of fragment = + 184 m/z (the phosphocholine head group). A representative mass spectrum is given in figure 2.1.

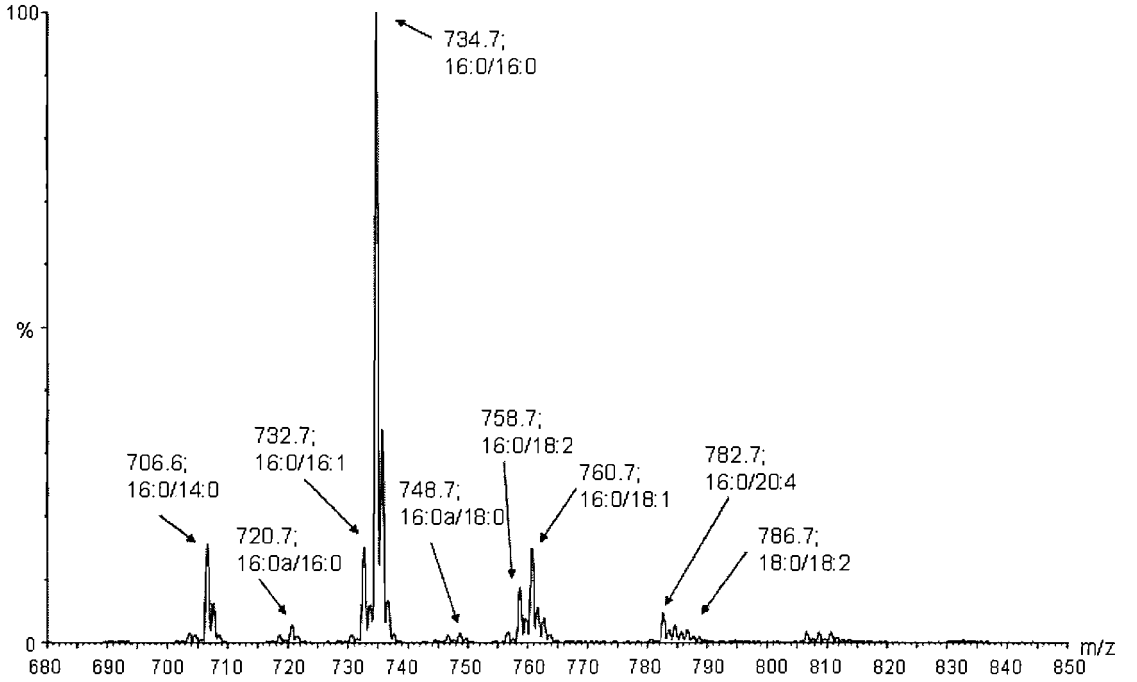

Figure 2.1: A representative mass spectrum of AFS PtdCho (precursors of m/z = + 184).

Mass spectrometry data was processed as described in section 2.2.2 and the relative proportions of the principle PtdCho molecular species present (identified in figure 2.1) determined as percentages. AFS comprised 55.3 ± 3.5 % PC16:0/16:0, 6.9 ± 1.3% PC 16:0/14:0, 8.8 ± 0.9% PC16:0/16:1 and 11.6 ± 2.5% PC16:0/18:1 as principle

components. This is consistent with PtdCho compositions report for lung surfactant isolated from BALF and sputum from healthy individuals.[63,111]

2.5.7 Sterilisation of surfactant phospholipid

In the case of endogenous surfactant material, a total lipid extraction (section 2.5.4) was carried out on samples prior to sterilisation. Pumactant phospholipid was sterilised directly from the vial. Dried down surfactant phospholipid extract was dissolved in ethanol (70% v/v) (volume depended on the quantity of surfactant), transferred to a 25cm^2 filter top culture flask and lyophilised over night. Dried phospholipid was re-suspended in sterile culture medium and stored at 4°C.

Sterilised Pumactant was reconstituted in cell medium and assayed for phospholipid phosphorous prior to use.

2.6 Pumactant evaluation using a Wilhelmy balance

2.6.1 Measuring Surface tension on the Wilhelmy Surface Tension balance

Before any measurements were carried out, all components of the balance which are exposed to the liquid sub phase had to be carefully cleaned to ensure they were free from any surface active materials. The Wilhelmy trough, barrier and the platinum plate where cleaned by rinsing in $CHCl_3$, then MeOH, then H_2O. The platinum plate was also heated with a flame torch. Saline (0.9% w/v) was prepared in 500 ml aliquots in glassware which had been rinsed in acid washed (0.1M HCl) to ensure it was free from all surface active contaminants. Saline (80ml) was added to the sub phase and the Wilhelmy balance calibrated to read a baseline surface tension of 72 mMm^{-1}.

2.6.1.1 Characterisation of dry powder Pumactant

The Wilhelmy balance was calibrated and baseline surface tension recorded on a saline sub phase as described in section 2.6.1. The automated actuation device (VPAG) described in section 2.4.4 was used to deposit aerosolised pumactant onto the warmed (37°C) saline sub phase (80ml) of a Biegler Electronic Wilhelmy Surface Tension

Balance. Pumactant was actuated for 2 seconds using an actuation pressure of 2 bar and a vial vibration pressure of 1 bar unless stated otherwise. Surface area cycling (1.5 cycles min^{-1}) was carried out until equilibrium surface tension profiles were obtained at which point the Surface Tension vs. Surface Area profile was printed. The concentration of phospholipid present in the sub phase was used as a surrogate marker for the quantity of lipid present at the interface. 3 x 800µl aliquots were isolated from the sub phase following acquisition of an equilibrium surface tension/ surface area profile. These samples were spiked with DMPC internal standard (1 nmol), total phospholipid extracted (section 2.5.4) and assayed for DPPC content relative to DMPC internal standard (section 2.2).

2.6.1.2 Characterisation of Pumactant a suspension

Baseline surface tension was recorded on a saline sub phase as described in section 2.6.1. Saline, (10.5 ml) was subsequently removed by pipette and replaced with Pumactant suspension (1 $mg.ml^{-1}$, 10.5 ml). Surface area cycling was recommenced and equilibrium surface tension recorded.

2.6.2 Measuring ST at ambient and saturated humidity

2.6.2.1 Environmental control using a purpose built incubation chamber

The Wilhelmy balance was placed inside a Stuart Scientific S160D incubator (37°C). Air was pumped into the incubator, using a KNF Neuberger VP series pump, through a scrubber filled with water, which was heated on a Voss heater stirrer (water temperature ≈ 60°C). Humidity inside the incubator was measured using a thermo-hygro humidity detector.

2.6.2.2 ST characteristics of Pumactant powder and suspension at ambient and saturated humidity

Baseline ST measurements were determined as described previously (section 2.6.1) at both ambient and saturated humidity. Pumactant was then either administered as a dry powder using the VPAG (see section 2.6.1.1 for actuation parameters) or prepared as suspension as previously described (section 2.6.1.2). Surface tension profiles were obtained at both ambient and saturated humidity (37°C) on each preparation.

2.6.3 Surface tension measurements at ambient and saturated humidity using a filter paper dipping plate

A filter paper dipping plate (11mm by 18 mm) was constructed from Whatmann Number 1 filter paper and attached to the Wilhelmy balance. The filter paper was allowed to saturate before baseline calibration was carried out. A base line Surface tension measurement was carried out as described in section 2.6.1. Pumactant was subsequently actuated onto the sub phase using the VPAG (see section 2.6.1.1 for actuation parameters). A ST profile was subsequently recorded at ambient laboratory humidity. A second ST profile was then acquired under conditions of saturated humidity using the humidity device (section 2.6.2). Humidification was then halted and a third ST profile recorded once ambient laboratory humidity was reached.

2.6.4 Surface tension measurements of amniotic fluid surfactant (AFS), in the presence and absence of Surfactant inhibitors

Surface tension measurements were made at 37°C in a humid environment ($\geq$ 92% R.H)

2.6.4.1 AFS plus Bovine Serum Albumin (BSA, 20mgml^{-1})

To the trough on the Wilhelmy balance, was added saline sub phase (0.9%, 80 ml). A background surface tension measurement was made, after which saline (8ml), was removed from the trough and replaced with a BSA solution in saline (200mgml^{-1}, 8 ml). Again, a surface tension measurement was made. Saline containing BSA (4ml) was removed from the sub phase and replaced with amniotic fluid surfactant (2.77 μmolml^{-1} total phospholipid in 0.9% saline, 4ml). A surface tension measurement was again made.

Pumactant was subsequently actuated onto the sub phase using the VPAG as described in section 2.6.1.1. CO_2 actuation pressure 1 bar, actuation duration, 2 seconds, vial vibration pressure 2 bar. Surface area cycling was recommenced and equilibrium surface tension measured. A second pumactant actuation was made using the same actuation parameters and equilibrium ST again measured.

2.6.4.2 AFS plus plasma

Background Surface tension was measured as in section 2.6.1. Saline (1.6ml) was removed and replaced with AFS (1.6ml, 2.77μmolml^{-1} total phospholipid) and equilibrium surface tension measured. Sub phase, containing AFS was removed (8ml) and replaced with plasma (8ml). Equilibrium surface tension was again measured. Amorphous pumactant was subsequently actuated onto the balance, using the VPAG described in section 2.6.4.2 equilibrium ST was measured, after which a second dose of Pumactant was applied using the VPAG. Equilibrium ST was again measured.

2.7 The isolation and purification of low density lipoproteins (LDL)

2.7.1 Preparation of LDL

2.7.1.1 Fractionation of human plasma lipoproteins

Blood collected in an EDTA tubes was centrifuged for 15 minutes at 2000rpm. Plasma was isolated and mixed with KBr (1.15g) to generate a KBr density of 1.21gml^{-1}. This was transferred to a 13.5ml ultracentrifuge tube and overlaid with KBr (density 1.063gml^{-1},3ml) using a hypodermic needle connected to a syringe, followed by 1.019gml^{-1} KBr (3ml) and 1.006gml^{-1} KBr (3ml). Tubes were heat sealed and ultracentrifuged using a Beckmann NVT 65, near vertical rotor for 6 hours (50,000rpm). LDL appeared as a band near the bottom of the tube. The LDL band was isolated using a needle connected to a syringe which was inserted into the tube at this point. LDL was aliquotted into eppindorfs and stored at 4°C.

2.7.1.2 Purification of LDL

A filtration column containing Sepharose CL-6B was washed by running PBS through it over night. LDL (1ml) was loaded onto the top of the column and allowed to drop through at 6 drops per minute. As the yellow band (denoting LDL) reached the bottom, the liquid was harvested in 400μl aliquots using a fraction collector.

2.7.1.3 Gel electrophoresis

The purity of LDL aliquots was confirmed by Gel electrophoresis. Barbitone buffer (10.6g sodium barbitone, 0.7g NaEDTA and 1 litre of water) was prepared and poured into the electrophoresis tank. The gel was prepared by heating 0.4-0.5g of agarose with 40-50ml Barbitone buffer using a microwave, until the agarose was fully dissolved. When it had cooled, 0.5ml BSA was added and the gel poured onto a glass plate. Combs were placed on it to make wells. A marker consisting of 40µl of lipoprotein and a drop of bromphenol blue was prepared. Once the gel had set, the plate was placed on a flat bed and 8µl of sample or marker was inserted into the wells. Filter paper soaked in buffer was placed on the edges of the plate to ensure good conductance. The power pack was set at 200V and left for 20 minutes. After half an hour the gel was placed into 5% trichloroacetic acid for 15 minutes causing the bands to bleach yellow. The gel was subsequently pressed between filter paper for 15 minutes and then dried for an hour (50°C) until the gel was invisible. A solution of Sudan black and 60% ethanol was poured over the plate and after 20 minutes rinsed with 40% ethanol. The plate was then photographed. Sharply defined bands could be seen in the samples that contained LDL.

2.7.1.4 Determination of LDL protein concentration

LDL protein concentration was determined using a Bicinchoninic Acid (BCA) Kit for Protein Determination (Sigma, Dorset UK). BSA standards were prepared at concentrations of 1,000-0µl.ml^{-1}. 50µl of standard/ sample was added to a well on a 96 well plate. To this, 200µl of BCA reagent (1 volume of $CuSO_4$ to 49 volumes of BCA) was added. The plate was covered and incubated for 15 minutes. Optical density was measured at 540nm on a plate reader. From this a standard curve was created, which was used to determine the protein concentration of the LDL samples. All assays were performed in duplicate and the mean calculated.

2.8 Pumactant evaluation by Capillary Surfactometry

2.8.1 Sample evaluation by Capillary Surfactometry

All samples were thawed and vortexed prior to evaluation. A 0.5µl aliquot of the sample to be evaluated was drawn up into a micro-pipette and then inserted into the narrow part

of the capillary tube. The capillary was connected to the capillary surfactometer in at 37 °C water bath. A flow of air at 0.3ml.min^{-1} was passed through the capillary for 2 minutes. The pressure in the tube over this period was recorded and, from this the percentage, opening of the tube can be calculated. All samples were run twice.

2.8.2 Dry powder Pumactant actuation into a capillary

Amorphous Pumactant was actuated into four separate CS capillaries from a single Pumactant vial using the VPAG. A piece of neonatal tubing was used to interface the VPAG with the capillaries. The four sequential actuations were carried out using an actuation pressure of 0.8 bar and a vibration table pressure of 1.5 bar. The actuation duration was 1 second. Follow the actuations, saline (0.5µl), was added to each capillary, the sample was then evaluated using the capillary surfactometer (see section 1.5.4.2). Pumactant was subsequently isolated from the narrow section of the capillary by instilling saline (5 x 0.5µl aliquots) using the CS micropipette (see section 2.8.3.2). The saline aliquots relating to each capillary were pooled into 12ml screwtop tissue culture tubes, spiked with DMPC internal standard (1 nmol), total phospholipid extracted (section 2.5.4) and assayed for DPPC content relative to DMPC internal standard (section 2.2).

2.8.3 Assessing Pumactants ability to maintain an open capillary in the presence of surfactant inhibitors by Capillary Surfactometry

2.8.3.1 Sample isolation from capillaries

Following capillary patency measurements, phospholipid from the narrow section of the capillary was isolated by instilling a 0.5µl aliquot of fresh saline into the narrow capillary section and drawing out the contents using the CS micropipette. This process was repeated a further 4 times.

2.8.3.2 'Micro' phospholipid extraction of lipids isolated from the narrow section of the capillary

As the sample volumes undergoing phospholipid extraction were so small (2.5 µl), the following micro-extraction technique was devised which required far smaller quantities of solvents. Pooled saline sample extracts (2.5µl, 2.8.3.1) were placed in 1.5 ml brown auto sampler vials (Jones Chromatography) to which saline (197.5µl) was added, along with DMPC internal standard (0.002nmol.µl^{-1}, 10µl). Methanol (500µl), chloroform (480µl) and water (250µl) were subsequently added to the vials. The samples were centrifuged (1000xg, 10 mins, 4°C) and the lipid layer isolated and dried under N_2 gas. Samples were assayed by ESI-MS/MS as previously described (section 2.2).

2.8.3.3 Titration of Pumactant against LDL and subsequent evaluation by Capillary surfactometry

A Pumactant stock suspension (30mg.ml^{-1}) was prepared by suspending 100mg of Pumactant powder in 3.3ml of saline. Doubling dilutions of the stock were prepared from 30mg.ml^{-1} to 0.9375mg.ml^{-1}. The top (30mg/ml) and bottom (0.9375mg/ml) concentrations of Pumactant were assessed by Capillary Surfactometry as described in section 2.8.1.

To LDL, (2.75mg.ml^{-1}, 12µl), was added either 30mg.ml^{-1}, 7.5mg.ml^{-1} or 0.9375mg.ml^{-1} Pumactant suspension (3µl) in a 1.5ml eppindorf. Samples were vortexed and 3x0.5µl aliquots evaluated by Capillary Surfactometry in triplicate. The remainder of each sample was incubated for 1 hour (37°C). Following the incubation, samples were re-evaluated using the Capillary Surfactometer.

2.8.3.4 Titration of LDL against Pumactant and subsequent evaluation by Capillary Surfactometry

Doubling dilutions of a stock LDL solution (2.75mg.ml^{-1}) were prepared at 1.375mg.ml^{-1}, 0.6875mg.ml^{-1}, 0.34375mg.ml^{-1}, 0.1719mg.ml^{-1} and 0.0859mg.ml^{-1} respectively with PBS. A Pumactant suspension was prepared at 30mg.ml^{-1} in saline. To Pumactant (30mg.ml^{-1}, 12µl) was added LDL (3µl) at either 0.34375mg.ml^{-1}, 0.1719mg.ml^{-1} or 0.0859mg.ml^{-1} in a 1.5 ml eppindorf. Samples were vortexed and evaluated by Capillary

Surfactometry (3x0.5µl aliquots). The remainder of each sample was incubated for two hours (37°C) and re-evaluated by Capillary Surfactometry (3x0.5µl aliquots).

2.8.3.5 Evaluation of Amniotic Fluid Surfactant (AFS) by Capillary Surfactometry

AFS (2,43mg.ml^{-1}, 6mg.ml^{-1} and 7mg.ml^{-1} total phospholipid) was vortexed and evaluated by Capillary Surfactometry (3x0.5µl aliquots).

2.8.4 Assessing Survantas ability to maintain an open capillary in the presence of LDL by Capillary Surfactometry

Survanta (supplied at a concentration of 25mg.ml^{-1}) was diluted to 5mg.ml^{-1}, 1.76mg.ml^{-1} and 0.586mg.ml^{-1} with saline and evaluated by Capillary Surfactometry (3x0.5µl aliquots). To each survanta dilution (5mg.ml^{-1} – 0.586mg.ml^{-1}, 5µl) was added LDL 1.76mg.ml^{-1} (5µl) in a 500 µl eppindorf. Samples were vortexed and evaluated by Capillary Surfactometry in triplicate.

2.9 Cell culture

2.9.1 Cell thawing

2.9.1.1 Jurkat cells

1 x 10^7 frozen Jurkat cells (1ml), were defrosted in a water bath (37°C) for 1-2 minutes. Defrosted Jurkat cells were added to warm Jurkat cell medium (RPMI 1640, 10% Fetal calf serum (FCS), 1% penicillin and streptomycin (antibiotics), 1% L-glutamine) centrifuged (300xg, 10 mins, 4°C with the brake). The supernatant was discarded and the pellet re-suspended in warmed Jurkat cell medium (10ml). Jurkat cells were subsequently transferred to a 25cm^2 tissue culture flask and placed in the incubator (37°C).

2.9.1.2 B3Z cells

1 x 10^7 frozen B3Z cells (1ml), were defrosted in a water bath (37°C) for 1-2 minutes. Defrosted cells were transferred to a 25cm^2 tissue culture flask containing B3Z cell medium (RPMI 1640, 10% FCS, 1% penicillin and streptomycin, 1% L-glutamine, 50 μM 2-mercaptoethanol, 1mM Sodium Pyruvate) (10ml) and placed in the incubator (37°C).

2.9.2 Cell passage

2.9.2.1 Jurkat cells

At a density of approximately 1 x 10^6 cells ml^{-1}, Jurkat cells were sub-cultured with warmed Jurkat cell medium to produce a density of 5 x 10^5 cells ml^{-1}.

2.9.2.2 B3Z cells

At a density of 1 x 10^6 cells ml^{-1} (i.e. when cells were just making contact with one another), adherent B3Z cells were scraped from the bottom of the flask using a cell scraper and sub-cultured with warmed B3Z cell medium to produce a density of approximately 3 x 10^5 cells ml^{-1}. Cells were placed back into the incubator (37°C).

2.9.3 Cell counts

Cells were diluted (1:1) with trypan blue stain and left to stand for approximately 5 minutes. The stained cell suspension was visualised with an Improved Neubauer manual haemocytometer, dead cells were identified by the blue stain. The concentrations of live cells was determined by multiplying the number of cells by 2 (to account for the dilution with trypan blue). This value was then multiplied by 10^4. Cell concentration expressed in cells ml^{-1}.

2.9.4 Isolation of CD3$^+$ T-lymphocytes from Jurkat cells

CD3$^+$ Jurkat cells were isolated from mixed Jurkat cells by positive selection using magnetic microbeads. 1 x 10^8 Jurkat cells were centrifuged (300xg, 10 mins, 4°C), the supernatant was discarded and the cell pellet resuspended (800μl/10^8 cells) in ice cold

PBS-BSA (0.5% w/v) EDTA (2mM) buffer. 50µl/10^8 cells of OKT3 antibody (anti-CD3) was added to the cell suspension which was mixed and incubated for 30 mins (6-12°C). The suspension was maded up to 15ml with ice cold PBS-BSA (0.5% w/v) EDTA (2mM) buffer and the cells pelleted (300xg, 10mins, 4°C). The supernatant was discarded and the cells washed by resuspending in ice cold PBS-BSA (0.5% w/v) EDTA (2mM) buffer (15ml). Cells were again pelleted (300xg). The wash step was repeated a further two times. The cell pellet was resuspended (800µl/10^8 cells) in ice cold PBS-BSA(0.5% w/v) EDTA (2mM) buffer. MACS goat anti-mouse IgG microbeads (MACS GAM) (200µl/10^8 cells), was added to the cell suspension, which was mixed and incubated for 15 mins (6 – 12 °C). The cell microbead mixture was made up to 50 ml with ice cold PBS-BSA (0.5% w/v) buffer and centrifuged (300xg, 10 mins, 4°C). This wash step was repeated a further two times and the Jurkat cell pellet resuspended in ice cold PBS-BSA buffer (0.5% w/v, 500µl) and kept on ice until required.

The MACS cell separator magnets were set up and an LS^+/VS^+ column attached. The separating column was washed with ice cold PBS-BSA buffer (0.5% w/v, 3ml), the Jurkat cells were added (500µl) and the elutant was collected beneath the column. Ice cold PBS-BSA (0.5% w/v, 3x3ml) was washed through the column and collected underneath. The column was removed from the magnet and suspended above a 50 ml universal. Ice cold PBS-BSA (0.5% w/v, 5ml) was then added to the column and the plunger used to remove the positive fraction of $CD3^+$ Jurkat cells.

The cells were washed (PBS, 50ml), centrifuged (300xg, 10 mins, 4°C), the supernatant discarded and the cell pellet re-suspended in warmed Jurkat cell medium (10ml) and transferred to a 25cm^2 tissue culture flask which was agitated and placed in the incubator (37°C).

2.9.5 Cell stimulation

2.9.5.1 Addition of agonists to Jurkat cells

OKT3 (100µgml^{-1}, 1ml) in PBS, was added to the appropriate concentration of Jurkat cells on a 24 well plate. Cells were placed in the incubator (37°C, 24 hours).

PMA (20ngml^{-1}, 1ml) in PBS was prepared from a stock solution (1μgml^{-1} in dimethyl Sulphoxide (DMSO)) and added to Jurkat cells (1 x 10^6 in 1 ml). Cells were placed in the incubator (37°C, 24 hours). PMA was also added to cells in combination with OKT3, however the method for treating cells with PMA did not alter.

2.9.5.2 Stimulation of B3Z cells with OVA peptide in the presence and absence of Pumactant

To B3Z cells (1x10^5 per 90μl), was added Ova peptide (200μM, 10μl)) in triplicate on a 96 well round bottomed plate. Sterile pumactant (total phospholipid concentration = 575.4 nmolml^{-1} in B3Z cell medium, 100μl), was added to cells in triplicate. To control cells, was added B3Z medium (100μl). Blank wells contained cells (1x10^5) prepared in B3Z medium (100μl) plus Jurkat cell medium (100μl).

The plate was agitated (650rpm, 5mins) and placed in the incubator over night. The plate removed from the incubator and centrifuged (300xg, 22°C, 3 mins). Supernatant was decanted, cells washed with PBS (200μl) and centrifuged (300xg, 22°C, 3 mins). Chlorophenol Red beta-Galactoside ((CPRG), 0.15mM in PBS/ 0.5% Nonidet P-40) was added to wells (100μl oer well). Plate placed in the incubator (37°C, 2.5 hours). The optical densities of the wells were determined using a microplate reader set at 570nm.

2.10 Human IL-2 Enzyme Linked Immunosorbent Assay (ELISA)

The concentration of IL-2 present in Jurkat cell supernatants was established using a direct human IL-2 ELISA. The ELISA capture antibody (mouse antihuman IL-2) was diluted to its working concentration with PBS (4μgml^{-1}). Antibody (100μl) was then added to each of the appropriate wells on a 96 well plate, which was covered and incubated overnight at room temperature.

Excess capture antibody was washed from the wells three times with ELISA wash buffer (0.05% Tween 20 in PBS, pH 7.2 – 7.4, 200μl per well). Blocking buffer (1% bovine serum albumin (BSA), Sucrose (5%) in PBS, with sodium azide (NaN_3, 0.05%), 300μl) was then added to the wells. The plate was covered and incubated at room

temperature (1 hour) and washed three times with wash buffer (200µl per well). Recombinant human IL-2 standards were prepared (1000 pg ml^{-1} – 15.625 pg ml^{-1}, doubling dilutions). Standards and samples (100µl per well,) were added to the plate in duplicate which was subsequently covered and incubated for 2 hours (room temperature).

The plate was again washed three times with wash buffer (200µl per well). Detection antibody (biotinylated goat anti-human IL-2) was prepared in reagent diluent (0.1% BSA, 0.05% Tween-20 in tris-buffered saline, pH 7.2 – 7.4) at its working concentration (50 $mgml^{-1}$) and was added to the plate (100µl per well). The plate was covered and incubated at room temperature (2 hours). The plate was again washed (200µl per well). A 1 in 200 dilution of streptavidin-horse radish peroxidase (HRP) (100µl) was added to the wells. The plate was again covered and incubated in the dark (room temperature, 20 minutes).

The plate was again washed three times (200µl per well) and substrate solution (1:1 mixture of colour reagent A, hydrogen peroxide and colour reagent B, tetramethyl Benzidine (TMB)), was added to the wells (100µl per well). The plate was covered and incubated in the dark (20 minutes, room temperature). The substrate/ horse radish peroxidase reaction was stopped by adding stop solution (2M sulphuric acid (H_2SO_4) (50µl) to each of the wells. The optical densities of the wells were determined using a microplate reader set at 450nm, with a correction wavelength of 540nm. A standard curve was drawn and the concentration of IL-2 in each of the samples was determined.

2.11 Effects of Pumactant on Jurkat cell PtdCho composition

2.11.1 Preparation of [methyl-D_9]DPPC containing bodipyPtdCho

Deuterium labelled Pumactant containing bodipy® ((2-(4,4-difluoro-5-methyl-4-bora-3a,4a-diaza-s-indacene-3-dodecanoyl)-1-hexadecanoyl-*sn*-glycero-3-phosphocholine)β-bodipy500/510 C_{12}-HPC) labelled PtdCho was prepared by mixing [*Methyl*-D_9]DPPC

with egg PG, and endogenous DPPC in a 7/30/63 ratio and freeze dried in 100 mg aliquots (prepared by Gerald Adams, Salisbury Consultancy, Salisbury UK).

[*Methyl*-D_9]DPPC enriched Pumactant was resuspended in 70% EtOH (approx 70ml) with sonication and aliquotted equally into 4x 25cm^2 sterile tissue culture flasks. To a single flask was added 0.134mM bodipy PtdCho (21μ) in $CHCl_3$. The resulting solution was sonicated and freezedried over night. The resulting dry sterile pumactant was resuspended in Jurkat cell medium (5ml) and stored in the fridge (4°C).

Two aliquots of the resulting suspension underwent phospholipid extraction by the Bligh and Dyer method (section 2.2.4). One was then used to determine total phospholipid phosphorus (section 2.2.5) the second was charcterised by ESI-MS/MS.

2.11.2 Addition of labelled Pumactant to Jurkat cells

Sterile deuterium labelled pumactant (section 2.2.6) was re-dissolved in Jurkat cell medium (final total phospholipid concentration = 15800 $nmol^{-1}$), diluted to a final concentration of 300 $nmolml^{-1}$ in Jurkat cell medium and then added (5ml) to a 25cm^2 tissue culture flasks containing 1 x 10^6 cells for 2, 24 and 48 hours in triplicate. The flasks were agitated and placed in an incubator (37°C/ 5%CO_2) for the duration of the incubation period.

2.11.2.1 Removal of Pumactant from Jurkat cells

Following incubation with pumactant, cells were washed prior to mass spectroscopic analysis. To remove pumactant, Jurkat cells were centrifuged (300xg, 10 minutes, 4°C). The supernatant was discarded and the cell pellet was resuspended in sterile PBS. Cells were washed three times, resuspended in 0.9% NaCl (800μl) and extracted according to the method of Bligh and Dyer (see section 2.2.4).

2.11.3 Mass spectrometry analysis

The concentrated lipid extracts were re-suspended in MeOH/$CHCl_3$/H_2O/NH_3 (7/2/0.3/0.7) (200μl) for analysis by ESI-MS/MS. Samples were either analysed by nano-flow or direct injection (5 μl per minute) in positive ionisation mode by ESI-

MS/MS. Precursor ion scans of diagnostic fragment ions m/z 184 and 193 were collected.

2.11.4 Processing Jurkat cell PtdCho mass spectrometry data

Mass spectrometry data was smoothed, subtracted, centred and copied and pasted into excel spread sheets. Data was processed using a macro written by Dr Grielof Koster (University Child Health, Southampton General Hospital). The 24 major Jurkat cell PtdCho molecular species were chosen to represent Jurkat cell PC as a whole (see table 2.4):

PC molecular species	Endogenous fragmentation transition	Newly-synthesised fragmentation transition
14:0a/16:1	690.7 – 184.1	699.7 – 193.1
14:0a/16:0	692.7 – 184.1	701.7 – 193.1
14:0/16:1	704.7 – 184.1	713.7 - 193.1
14:0/16:0	706.7 – 184.1	805.7 – 193.1
14:0a/18:2	716.7 -184.1	815.7 – 193.1
16:0a/16:1	718.7 – 184.1	727.7 – 193.1
16:0a:16:0	720.7 – 184.1	729.7 – 193.1
14:0/18:2	730.7 – 184.1	739.7 – 193.1
16:0/16:1	732.7 – 184.1	741.7 – 193.1
16:0/16:0	734.7 – 184.1	743.7 – 193.1
16:0a/18:1	746.7– 184.1	755.7 – 193.1
16:0/18:2	758.7 – 184.1	767.7 – 193.1
16:0/18:1	760.7 – 184.1	769.7 – 193.1
18:0a/18:2	772.7– 184.1	781.7 – 193.1
18:0a/18:1	774.7 – 184.1	783.7 – 193.1
16:0/20:4	782.7 – 184.1	791.7 – 193.1
18:1/18:1	786.7– 184.1	795.7– 193.1
18:0/18:1	788.7– 184.1	797.7– 193.1
18:0/20:4	810.7 – 184.1	819.7 – 193.1
18:0/20:3	812.7– 184.1	821.7 – 193.1
18:0/20:2	814.7– 184.1	823.7– 193.1
18:0/22:6	834.7 – 184.1	843.7 – 193.1
18:0/22:5	836.7 – 184.1	845.7 – 193.1
18:0/22:4	838.7 – 184.1	847.7 – 193.1
Bodipy PC	882.7 – 184.1	891.7 – 193.1

Table 2.4: The major Jurkat cell PtdCho molecular species. Transitions from endogenous(m/z = + 184) and deuterium labelled (m/z = +193) species were detected.

The macro selected intensities corresponding to the assigned PC peaks of interest and carried out intensity corrections to account for ^{13}C contribution and differential ionisation.

2.12 Fluorescence microscopy of B3Z and Jurkat cells following incubation with bodipy labelled Pumactant

2.12.1 Preparation of cells for confocal analysis

B3Z cells and Jurkat cells (1x10e6 per ml, 1ml) were incubated with 300nmol labelled Pumactant containing bodipy PtdCho (β-Bodipy®500/510 C_{12}-HPC, molecular probes, invitrogen Ltd, Paisley) (section 2.10.1). Cells were washed three times in PBS (15ml) and pelleted (300xg, 10mins, 4°C). Cells were fixed with formaldehyde solution, (1 ml of 4% solution in PBS) and gently pelleted (100xg, 10 mins, 4°C). Cell pellets were either resuspended in TO-PRO-3® iodide (molecular probes, invitrogen ltd, Paisley) 200µl (1µM in PBS) nuclear counter stain for 5 minutes or Propidium iodide (PI) (25µgml^{-1}, 200µl) . Washed with PBS (3 x 15 ml), pelleted (300xg, 10mins, 4°C) and then mounted on 3-aminopropyltriethoxysilane (APES) coated slides using MOWIOL® fluorescent mounting medium (Calbiochem, Nottingham, UK).

2.12.2 Fluorescence microscopy of labelled cells

Fluorescence microscopy was performed using a Leica SP-2 confocal laser scanning microscope (Leica Microsystems GmbH, Wetzlar, Germany) equipped with argon and Helium/Neon lasers. Bodipy and TO-PRO-3 fluorphores were excited at 488nm and 650nm respectively.

2.13 Extraction and quantitation of the phosphatidyl inositides

2.13.1 Silination of glassware

To disposable screw top extraction tubes, was added dichloro-dimethyl silane solution in toluene (3%, 500ml). Tubes were soaked (1 hr), rinsed with MeOH (twice), H_2O (twice), soaked in H_2O (1 hr) and sonicated in MeOH (1 hr).

2.13.2 Acid extraction of Phosphoinositides

To samples in saline (800µl) in a glass screw top tissue culture extraction tube, was added ice cold MeOH (2ml), conc HCl (25µl). Samples were then mixed after which ice cold $CHCl_3$ (1ml) was added. Samples were then vortexed and incubated on ice (4°C, 15 mins). Ice cold $CHCl_3$ (1ml) and ice cold H_2O (1ml) were then added.

Tubes were then centrifuged (1000 x g, 10 mins, 4°C). The lower layer was isolated using a glass pateur pipette and concentrated to dryness on a pre-cooled heating block (-20°C) under Nitrogen.

2.13.3 Tetrabutylammonium Sulphate (TBAS) extraction of Phosphoinositides

To samples, was added $CHCl_3$ (1ml), MeOH (500µl) and Tetrabutylammonium Sulphate (TBAS, 5mM) in HCl (1M) (375µl). Tubes were then vortexed and left to stand (10 mins), after which tubes were spun (1000 x g, 10 mins, 4°C). The lower (chloroform rich) layer was transferred to silanated glass autosampler vials and concentrated to dryness on a pre-cooled heating block (-20°C) under Nitrogen.

2.13.4 Mass spectrometry of Phosphoinositides

Samples were re-suspended in $CHCl_3$/ MeOH/ H_2O/ $C_5H_{11}N$ (450:450:100:3), (typically 1ml) and analysed by ESI-MS/MS. Samples were introduced by direct injection (5µl per min)

2.13.5 Phosphatidyl Inositol – basal compostion and synthesis in Jurkat cells

2.13.5.1 Incubating cells with *myo*-d_6-Inositol

Jurkat cells at a concentration of 5 x 10^6 cellsml^{-1}, were incubated with D-6 Inositol (100 µgml^{-1}, 0.5 mg), for 1.5, 3, 4.5, 6 and 24 hours at 37°C. Excess D-6 Inositol was washed from cells using sterile PBS. The supernatant was discarded and the Jurkat cell pellet was re-suspended in saline (800µl) and stored in the freezer (-20°C).

2.13.5.2 Extracting cells following incubation with *myo*-d_6-Inositol.

Cell pellets were thawed, spiked with 0.25μg $DPPIP_2$ and 2.25μg DPPI and acid extracted according to the method described in section 2.9.1.2.

2.13.5.3 Processing Jurkat cell PtdIns mass spectrometry data

Mass spectrometry data was smoothed, subtracted, centred and copied and pasted into excel spread sheets. Data was processed using the macro written by Dr Grielof Koster. The 19 major Jurkat phosphatidyl Inositol molecular species were chosen to represent Jurkat cell PI as a whole (see table 2.5).

PI molecular species	Endogenous fragmentation transition	Newly-synthesised fragmentation transition
PI16:1/18:1	833.5 – 241.5	839.5 – 247.5
PI16:0/18:1	835.5 – 241.5	841.5 – 247.5
PI16:0/20:4	857.5 – 241.5	863.5 – 247.5
PI16:0/20:3	859.5 – 241.5	865.5 – 247.5
PI18:1/18:1	861.5 – 241.5	867.5 – 247.5
PI18:0/18:1	863.5 – 241.5	869.5 – 247.5
PI18:1a/20:4	869.5 – 241.5	875.5 – 247.5
PI18:0a/20:4	871.5 – 241.5	877.5 – 247.5
PI18:0a/20:3	873.5 – 241.5	879.5 – 247.5
PI18:0a/20:2	875.5 – 241.5	881.5 – 247.5
PI18:1/20:4	883.5 – 241.5	889.5 – 247.5
PI18:0/20:4	885.5 – 241.5	891.5 – 247.5
PI18:0/20:3	887.5 – 241.5	893.5 – 247.5
PI20:0a/20:4	899.5 – 241.5	905.5 – 247.5
PI20:0a/20:3	901.5 – 241.5	907.5 – 247.5
PI20:2/20:4	909.5 – 241.5	915.5 – 247.5
PI20:1/20:4	911.5 – 241.5	917.5 – 247.5
PI20:0/20:4	913.5 – 241.5	919.5 – 247.5
PI20:0/20:3	915.5 – 241.5	921.5 – 247.5

Table 2.5: Jurkat cell PI molecular species assigned to determine basal flux in cells

Chapter 3

Phosphatidylcholine synthesis and metabolism by electrospray ionisation mass spectrometry

3.1 Introduction

3.1.1 Characterisation and quantification of phospholipids

From the time of discovery of the major biological membrane phospholipid PtdCho in 1847[112] until the 1980's, phospholipid analysis remained largely unchanged. Methods of analysis employed were highly complex multi-step procedures often involving hydrolysis or derivatisation prior to resolution by either TLC or HPLC[113,114,115] (Figure 3.1). Unfortunately these methods are time consuming and require large quantities of phospholipid which are not always available.

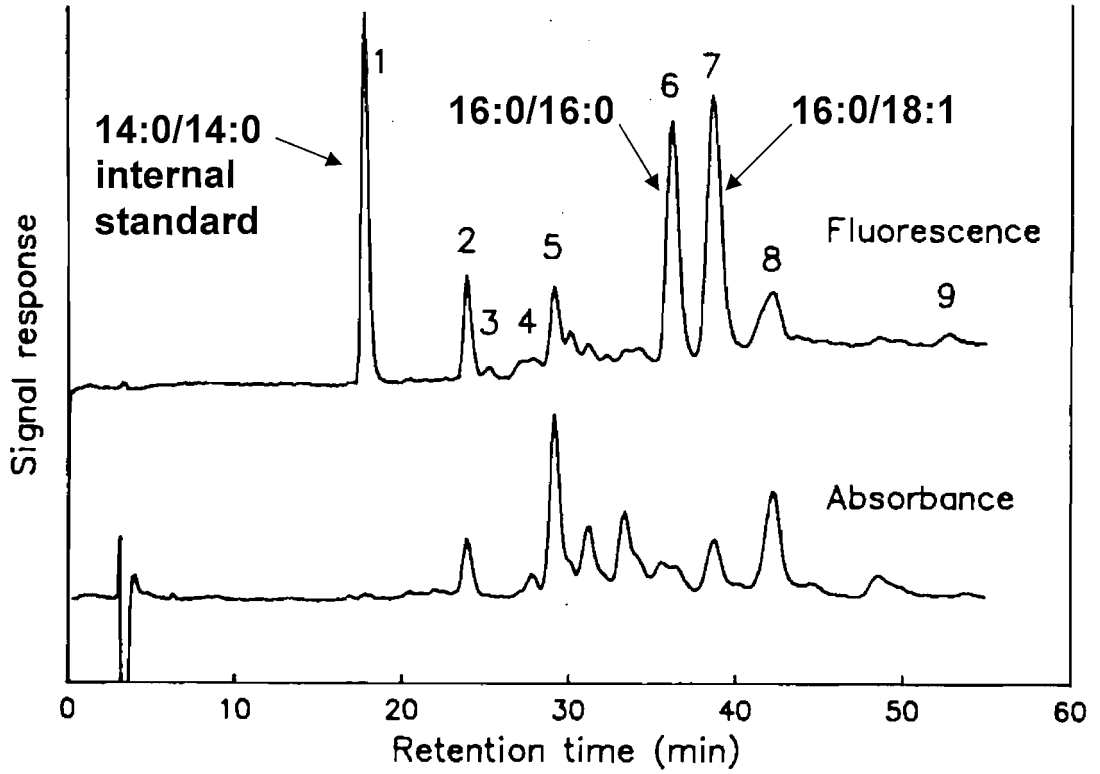

Figure 3.1: The resolution of PtdCho molecular species by reversed-phase HPLC. Column: 25cm x 4.6 mm Apex ODS 2, 5µm at 50°C. Mobile phase: 40 mmol l^{-1} choline chloride in methanol-water (92.5:7.5) at 1 ml min^{-1} (reproduced from J Chromatogr (1987) 415, 241-251).

The development of fast atom bombardment mass spectrometry (FAB-MS) completely changed this situation. FAB-MS involved mixing the phospholipids into a matrix and bombarding it with high energy atoms (e.g. Xe or Cs^+).[116] Using this technique, it

became possible to directly analyse phospholipids as intact molecules and to preserve the information inherent in their chemical structure[117]. It was also possible to carry out very detailed studies on the esterification site at *sn-1* vs *sn-2,* and also to define the position of double bonds present within the fatty-acyl chain.[118] Although FAB-MS was useful for providing structural information on phospholipids, it was less applicable to quantitative analysis. This is because the very high energy required to ionise lipids also causes differential fragmentation of different phospholipid classes and molecular species.

The application of electrospray ionisation mass spectrometry (ESI-MS) (see section 1.8.2) to the analysis of lipids represented a major breakthrough in biological MS. It exploits low energy (soft) ionisation which generates whole phospholipid molecular ions without fragmentation in an event that is largely independent of the surface properties of individual phospholipid classes and molecular species.[119] ESI-MS offers several advantages over FAB-MS, including lower background signals because of the absence of matrix ions, longer lasting and stable ion currents, ease of sampling, compatibility with liquid chromatographs and quantitative analysis of phospholipids.

Early work mainly involved method development using phospholipid standards.[120] The first study in which electrospray ionisation was validated for structural identification and quantitative analysis of synthetic and naturally derived phospholipids was carried out by Gross et al in 1994.[119] This was followed by further investigation of other biological membrane phospholipids.[121,122,123,124] The application of precursor ion mass spectrometery (see section 1.3.6) to the analysis of phospholipids made it possible to identify specific classes of lipid from crude extracts without the need for chromatographic separation. This was made possible by generating fragment ions through collision induced dissociation of whole molecular ions which are specific and therefore diagnostic for each lipid class.[121]

The role of lipids in cellular biochemistry is only partly understood, however our knowledge is rapidly expanding. Detailed analysis of lipid structure and molecular species composition has emerged as an active area of research in cellular biochemistry, an area important for understanding cellular metabolism, signalling and membrane trafficking. 'Lipidomics' as it has begun to be known, is focused on identifying lipid metabolism and lipid-mediated signalling processes which regulate cellular homeostasis

during health and disease. Much of this type of analysis has been conducted by making 'static' measurements of lipid molecular species composition at specific time points. As important as this is, it does not yield information regarding underlying mechanisms affecting the kinetics of synthesis and turnover in specific metabolic pathways, nor how this may be affected in different disease states.

Radioactively labelled precursors were the method of choice for tracing biomolecules through molecular transformations. [^{3}H] and [^{14}C] have both been used to follow labelled choline headgroups through PtdCho molecular species post HPLC using a flowthrough radiochemical detection system.[125,126] However, this was not ideal as it was expensive and detection was limited by small incorporations, poor resolution of molecular species by HPLC and low efficiency of counting. Coupled with the toxic nature of radioactive labels, these limitations precluded the application of such experimental protocols to clinical studies in human volunteers and patients.

Labelling of glucose and fatty acids with the stable isotope ^{13}C, combined with combustion interface isotope ratio mass spectrometry has been applied to the investigation of surfactant metabolism in preterm infants[127,128,129]. Exogenous surfactant has also been used to monitor surfactant kinetics in infants,[128] however, this required the use of large quantities of labelled precursors, for instance, 245 mg kg^{-1} of ^{13}C-labelled glucose have been used. Subsequent analyses were time consuming and did not reveal metabolism of individual PtdCho molecular species.[127,128,129]

The combination of ESI-MS/MS and stable isotope labelling using deuterium have provided a powerful alternative tool which is more sensitive, more specific, cheaper than radio labelling and importantly, also non-toxic thus applicable to the study of humans. The availability of stable isotope labelled choline headgroups, most notably choline-d_9, choline-d_{13} and [^{13}C]-labelled alternatives, combined with precursor ion scanning mass spectrometry have enabled analysis of PtdCho metabolism in subcellular organelles.[130]

For any analyte to be detectable by ESI-MS it needs to acquire either a positive or negative charge. In the case of PtdCho, the quaternary nitrogen atom on the head group readily forms an abundant $[M+H]^+$ ion following protonation of the phosphate anion. ESI is two to three orders of magnitude more efficient than FAB ionisation[119]. The non-fragmented molecular ions then pass through the first quadrupole of the mass

spectrometer into the collision cell where they are fragmented with inert argon gas to form predominantly the phosphocholine headgroup (m/z +184) which is diagnostic for PtdCho (figure 3.2A).

Labelling PtdCho molecules with deuterium makes them readily distinguishable from endogenous PtdCho by mass spectrometry. For example, substitution of the nine protons on the phosphocholine headgroup with nine deuterons increases the molecular mass of the molecule by nine mass units. Breakdown of these labelled lipid molecules in the collision cell of the tandem mass spectrometer generate a diagnostic labelled fragment nine mass units higher than the endogenous fragment (figure 3.2B). Besides the minor increase in mass, these labelled molecules are to all intensive purposes physiologically identical to their non-labelled counterparts and are thus expected to behave accordingly.

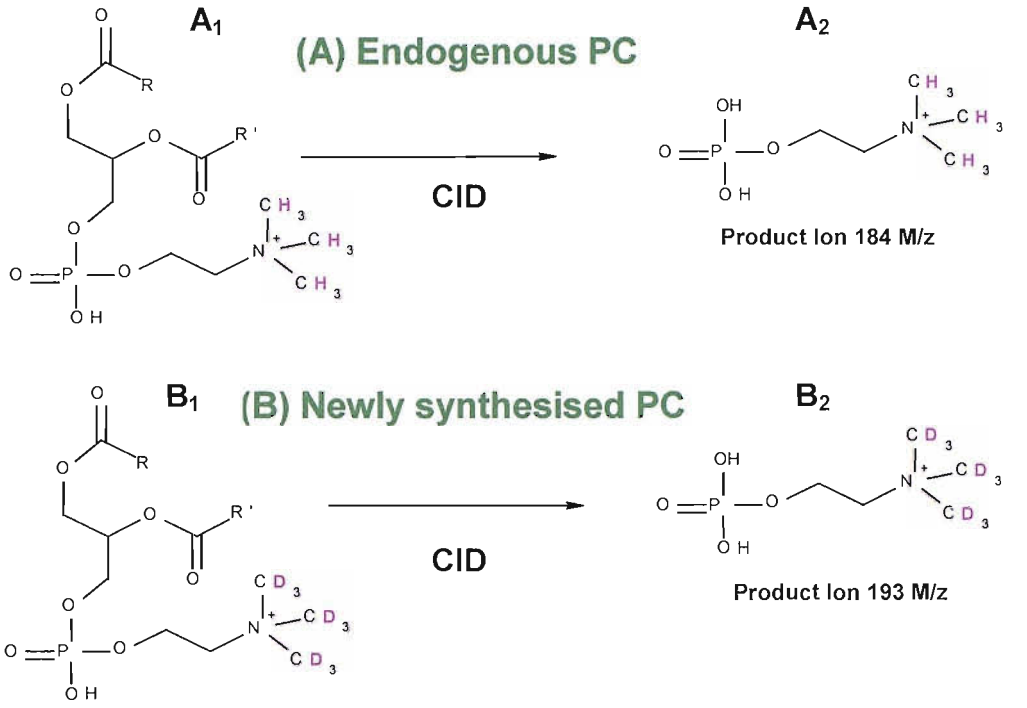

Figure 3.2 Fragmentation of endogenous and newly synthesised PtdCho by tandem MS/MS. Collision induced dissociation (CID) of endogenous PtdCho (A_1) yields the diagnostic choline phosphate headgroup (A_2) at m/z 184. CID of deuteriated PtdCho (B_1) yields the corresponding deuteriated headgroup (B_2) 9 mass units higher.

ESI-MS/MS of PtdCho species labelled with specific deuteriated precursors make it possible to distinguish between newly synthesised and endogenous PtdCho. A graphic illustration of the application and power of the technique is shown in figure 3.3. This depicts the positive electrospray ion mass spectrum analysis (ESI-MS) derived from a total lipid extract containing both endogenous and deuterium labelled PtdCho. The stable isotope labelled fraction (figure 3.3C) effectively represents newly synthesised PtdCho when the label is at saturation.

The x axis on each spectrum denotes mass to charge ratio (m/z). In the case of PtdCho, the charge on the ions is plus one, hence the x-axis depicts the 'molecular mass plus one peak' (M+1). The y axis denotes peak intensity (%) relative to the largest peak in the spectrum. Positive ionisation mass spectrometry analysis of a lipid extract (figure 3.3A) will contain both PtdCho and any non-PtdCho molecules soluble in the carrier solvent which are capable of carrying a positive charge. In this example, the major peak corresponds to PC16:0/18:1 (m/z 760). Any newly synthesised PC16:0/18:1 containing the deuterium labelled phosphocholine headgroup will appear nine mass units higher in

the spectrum (m/z 769) together with other positively charged ions which occur at 769 m/z, e.g. the ^{13}C isotope of PC16:0a/20:4.

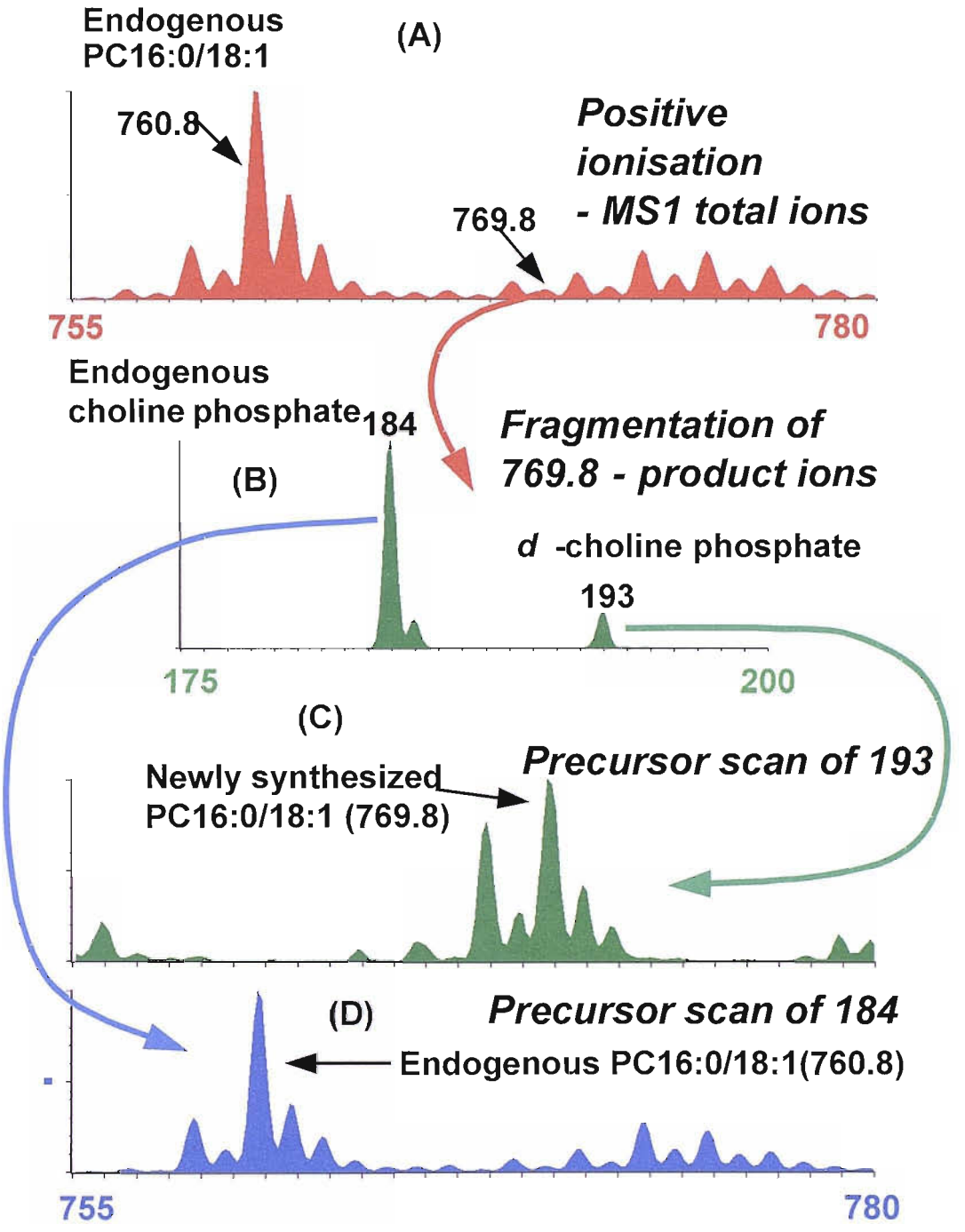

Figure 3.3: Characterisation of endogenous and newly synthesised PtdCho from a lipid extract. Positive ionisation (A) yields all analytes capable of positive ionisation. Fragmentation of m/z 769.8 yields both endogenous (m/z = +184) and deuteriated (m/z = +193) phosphocholine headgroups (B). Precursor scanning of m/z = + 193 yields exclusively newly synthesised PtdCho incorporating the deuterium label (C) whilst precursor scanning for m/z = +184 yields only endogenous PtdCho.

Collision induced dissociation of the peak at m/z 769 (product ion scanning, see section 1.8.5) confirms the presence of both endogenous and deuterated phosphocholine (figure 3.3B). The relative abundances of the m/z +184 and +193 peaks are directly indicative of the relative proportions of deuterated and endogenous PtdCho comprising the peak at m/z 769. Precursor ion scanning of m/z 193 identifies all of the newly synthesised PtdCho molecular species in the sample incorporating the deuterium labelled phosphocholine headgroup (Figure 3.3C) whilst precursor ion scanning of m/z 184 identifies all of the endogenous species (Figure 3.3D).

The first reported use of choline-d_9 to characterise PtdCho synthesis in whole cells came from Delong et al in 1999[131]. They combined the use of this stable isotope with ethanolamine-d_4 to investigate the two PtdCho synthesis pathways in hepatocytes (see section 3.1.2). As well as demonstrating proof of concept, this study confirmed the power of this technique in establishing molecular species data attributable to the two synthesis pathways.

Phospholipids are the major components of surfactant, of which 80-85% are PtdCho molecular species.[12,111] Lung surfactant function becomes impaired following pulmonary injury and alterations in composition are observed.[132] Although BALF is a common source for studying surfactant composition, harvesting samples is very invasive and therefore not always practical, particularly when the collection of sequential samples is required. Whereas collection of BALF requires direct administration of saline into the bronchus[64], sputum can be expectorated spontaneously following inhalation of saline administered via ultrasonic nebuliser.[133] Several studies have demonstrated that in healthy lungs, airway phospholipids isolated from sputum samples are representative of those in the alveoli, as the airways do not secrete significant quantities of phospholipid.[63,111] With the advent of deuterium isotope labelling of PtdCho precursors combined with surfactant phospholipid analysis of total lipid extracts from induced sputa, it is possible to probe surfactant PtdCho metabolism in humans.

3.1.2 PtdCho synthesis

Phosphatidylcholine (PtdCho) is a major phospholipid present in all mammalian cells[134]. The molecular diversity of PtdCho and other phospholipids is dictated by the

combination of different chain lengths, number of double bonds and type of linkage; acyl, alkyl or alkenyl. Each mammalian cell contains at least one thousand phospholipid molecular species.

3.1.2.1 CDP-Choline pathway

In most mammalian cells, PtdCho is synthesised via the CDP-choline (or kennedy) pathway. This pathway uses choline as an initial substrate and is catalysed by three enzymes: choline kinase (CK), CTP:phosphocholine cytidylyltransferase (CCT) and cholinephosphate transferase (CPT) with CCT as the rate limiting enzyme (figure 3.4). The CDP-choline pathway uses exogenous choline as the initial substrate and generates PtdCho molecular species containing mainly short chain (16:18 and 18:18) fatty acids. In the liver however, the CDP-choline pathway only accounts for approximately 80% of PtdCho. Hepatocytes are unique because they contain enzymes capable of converting phosphatidylethanolamine (PtdEtn) to PtdCho.[135]

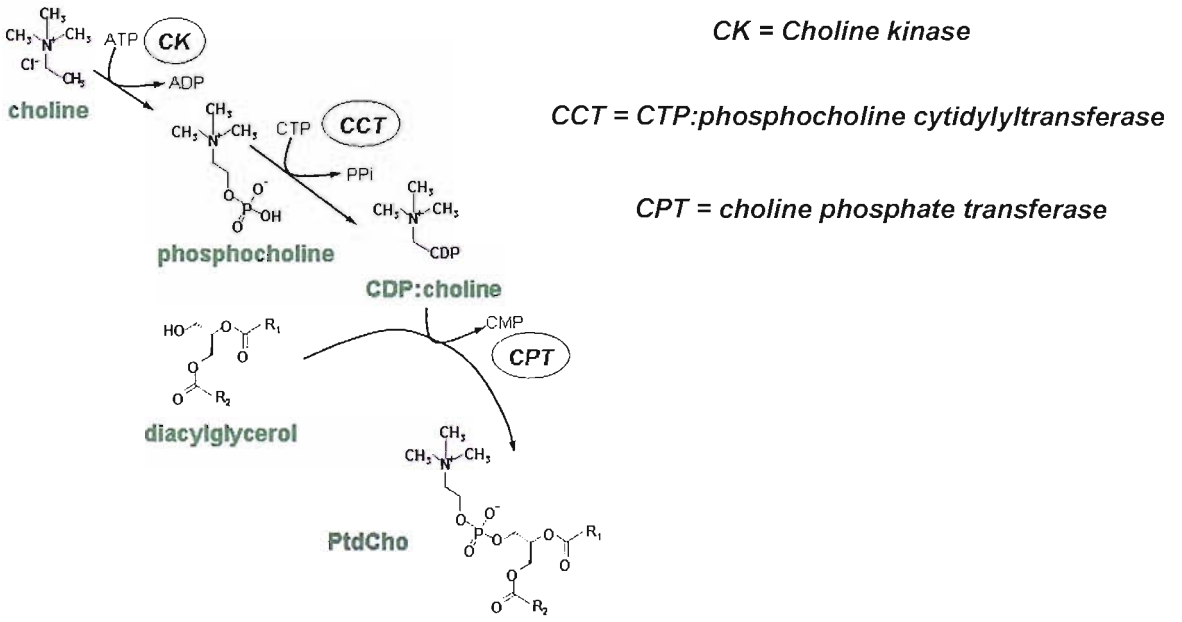

Figure 3.4: PtdCho synthesis via the CDP-choline (Kennedy) pathway. This pathway uses choline as the initial substrate and is catalysed by 3 enzymes: choline kinase (CK), CTP:phosphocholine cytidylyltransferase (CCT) and cholinephosphate transferase (CPT) with CCT as the rate limiting enzyme.

3.1.2.2 PtdEtn N-methylation pathway

Hepatocytes possess a high activity of phosphatidylethanolamine methyltransferase (PEMT), an enzyme which catalyses the conversion of PtdEtn to PtdCho,[135] using the general methyl donor S-adenosylmethionine (AdoMet) as a substrate.[136] AdoMet is derived from methionine that can be obtained either from extracellular sources or intracellular methylation of homocysteine. Choline, as a precursor to betaine, is a methyl source for the methylation of homocysteine. In the liver, choline is converted to betaine via oxidation steps in the mitochondria by choline dehydrogenase (CDH)[137] and betaine aldehyde dehydrogenase (BADH)[138]. A methyl group of betaine is transferred to homocysteine by betaine:homocysteine methyltransferase (BHMT) to generate methionine. Methionine is subsequently converted to AdoMet by methionine adenosyltransferase.

PEMT catalyses the stepwise transfer of three methyl groups from AdoMet to the amino headgroup of PtdEtn (figure 3.5). Methylation of PtdEtn in the liver is highly responsive to the dietary content of components that may have metabolic consequences on methylation reactions.[106]

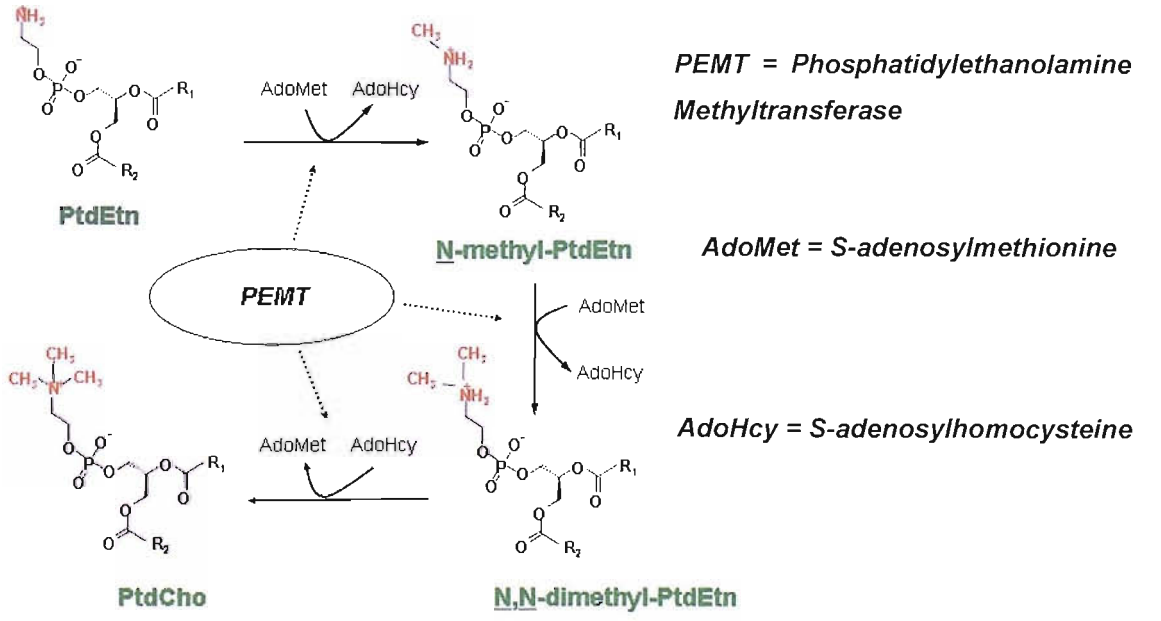

Figure 3.5: PtdCho synthesis by the PtdEtn methylation pathway. PtdEtn N-methyltransferase catalyses the synthesis of PtdCho by the stepwise transfer of 3 methyl groups from S-adenosyl-L-methionine (AdoMet) to the amino headgroup of PtdEtn.

The biological significance of the PEMT pathway in hepatocytes is of great interest because the CDP-choline pathway is already present in all mammalian cells and is sufficient for PtdCho synthesis. As a result the PEMT pathway was traditionally considered as a backup for PtdCho synthesis in hepatocytes.[139] Indeed, the survival of rats fed diets deficient in choline resulted in a 5 fold upregulation of PEMT activity suggesting that *N*-methylation may compensate at least in part, for CDP choline synthesis[139].

Recent *in vitro* investigation of primary hepatocytes[131] and rat hepatocarcinoma[106] cell lines by ESI-MS/MS and deuterium labelling allowed for accurate and sensitive evaluation of PtdCho molecular species synthesised by the two pathways. PtdCho produced by the CDP-choline pathway is comprised mainly of medium-chain, saturated and mono-unsaturated species (16:0/18:0, 16:0/18:1) whereas PtdCho species produced via PEMT activity were comprised of longer chain polyunsaturated fatty acid species (e.g. 16:0/20:4, 18:0/22:6). Additionally, $PEMT^{-/-}$ mice have substantially diminished plasma concentrations of docosahexanoic acid (DHA) (22:6) and arachidonic acid (20:4) containing species independent of nutritional choline intake.[140] As yet there has been little or no investigation of these phenomena in humans as the appropriate safe technologies have only just been developed.

3.2 Methods

The protocol for measuring deuterium incorporated PtdCho was developed using induced sputum and plasma samples in collaboration with Dr Wolfgang Bernhard at Hannover Medical School, Germany. Three female and one male healthy volunteer participated in the study following approval by the local ethics committee at Hannover Medical School, written consent and clinical examination by an independent physician. In this study, healthy patients were given deuterium-labelled [*methyl*-D_9]choline chloride by direct intravenous infusion over three hours (see section 2.3.1). Sputa were induced at specific time points before and following the infusion (from12 to 168 hours) and collected at four 5 minute intervals at each time point. Sputum lipids were extracted using an acidified extraction protocol (see section 2.3.1.2.)

EDTA blood was also collected from 1 to 72 hours after the start of the infusion and plasma aspirated (see section 2.3.1.1) in order to compare the kinetics of choline

incorporation into plasma PtdCho with that observed in the lungs. Plasma lipids were extracted according to the method of Bligh and Dyer (see section 2.3.2).

Endogenous choline and [*methyl*-D_9]choline were extracted from blood plasma and analysed by liquid chromatography followed by mass spectrometry [141] by Dr Wolfgang Bernhard at Hannover Medical School.

Plasma PtdCho composition was quantified by positive electrospray ionisation mass spectrometry (ESI+ MS) using precursor ion scanning (see section 2.3.2). Collision gas-induced dissociation produced protonated headgroup fragments with m/z = + 184 [105] for endogenous PtdCho and m/z = +193 [130] for newly synthesised PtdCho produced via the CDP-choline pathway. Analysis of the intermediates at m/z = +187 (containing one labelled methyl group) produced PtdCho molecular species synthesised via the PtdEtn-*N*-methylation pathway [106] (see table 2.2).

Sputum PtdCho was also quantified by ESI+ MS. Endogenous and newly synthesised PtdCho were quantified by multiple reaction monitoring (MRM) transitions from 8 pre-selected diagnostic PtdCho precursor ions to either the m/z +184 (endogenous) or m/z +193 (newly synthesised) phosphocholine headgroup (see section 2.3.3 and table 2.3).

3.3 Results

There are two parts to this chapter and they will be considered separately. Firstly the composition of endogenous and newly synthesised PtdCho in plasma will be discussed, followed by the synthesis and composition of surfactant PtdCho from induced sputa.

3.3.1 Plasma PtdCho synthesis and turnover

3.3.1.1 Incorporation of [Methyl-D_9]choline into human plasma PtdCho

3.3.1.1.1 Fractional incorporation of deuterium label into human plasma PtdCho

The fractional incorporation of deuteriated label in plasma PtdCho at a given time point is the proportion of plasma PtdCho which contains the deuteriated label. Fractional incorporations were calculated to determine both the extent of uptake of label by the CDP-choline and N-methylation pathways and the kinetics of labelled choline incorporation by each pathway. Fractional incorporations were calculated by dividing the sum of the intensity of all the labelled PtdCho molecular species ([precursors of m/z = +193 for CDP-choline and precursors of m/z = +187 for N-methylation respectively) by the sum of all the PtdCho molecular species (endogenous and labelled, see table 2.2). Fractional incorporations are expressed as percentages. Incorporation of [*methyl*-D_9] label into plasma PtdCho through the CDP-choline pathway (figure 3.6) was detectable after 6 hours, reached a maximum level of incorporation at 24 hours (0.78% ± 0.14%) (N=4) and was still approximately 70% of its maximum value after 72 hours. Linear regression of CDP-choline derived labelled PtdCho relative to native PtdCho revealed an increase of 0.035% per hour between 6 and 24 hours.

Fractional incorporation of recycled [*methyl*-D_3] label into plasma PtdCho through the PtdEtn N-methylation pathway was barely detectable at 6 hours and increased at a slower rate compared to [*methyl*-D_9] incorporation, (0.16 % per hour between 6 and 24 hours) from where the incorporation rate dropped to one tenth of the rate (to 0.016% per hour) between 24 and 48 hours, peaking at 48 hours (0.35% ± 0.055%) and maintaining a plateau up to 72 hours (0.32% ± 0.036%). Fractional incorporation of [*methyl*-D_3] was maintained for longer than the [*methyl*-D_9] label. At 72 hours, fractional incorporation of the plasma pool from the N-methylation pathway was still 95% compared to 70% incorporation of [*methyl*-D_9] though the CDP-choline pathway. The long term stability of [methyl-D_3] incorporation probably arises due to continued recycling of [methyl-D_3] groups through the system.

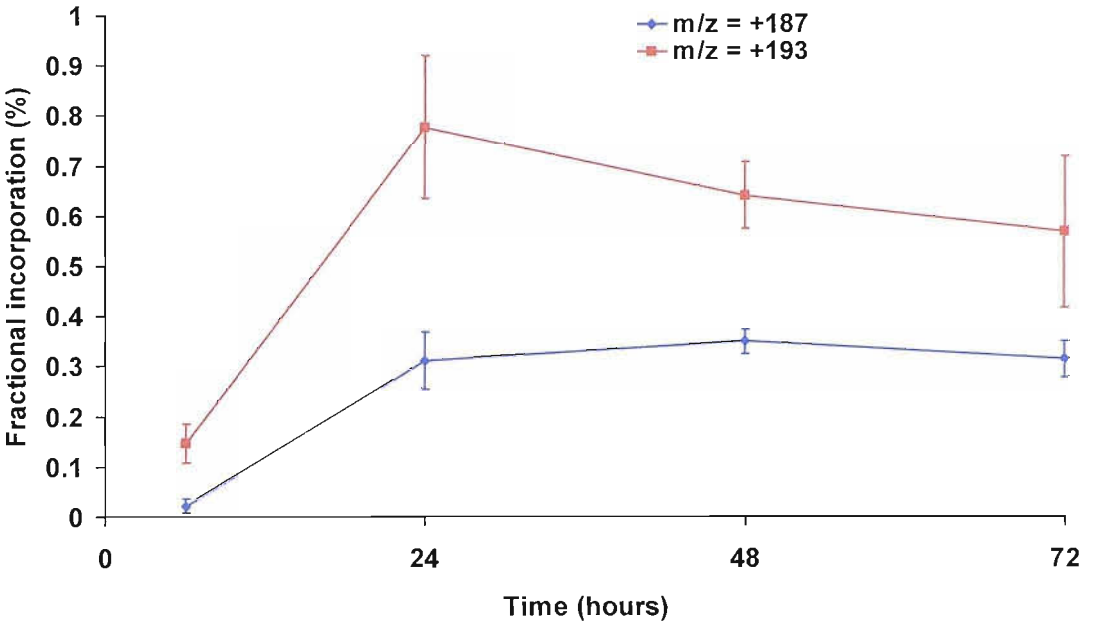

Figure 3.6: Time course for the incorporation of deuterium label into plasma PtdCho via the N-methyl (m/z = +187) and CDP choline (m/z = +193) pathways. Data indicate the fraction of deuterium labelled PtdCho. ([methyl-D_3] for N-methyl synthesised and [methyl-D_9] for CDP choline synthesised PtdCho) relative to native PtdCho. Results = mean (N=4) ± S.D at each time point.

3.3.1.1.2 Differentiation and molecular specificity of PtdCho synthesis by the CDP-choline and N-methyalation pathways in human plasma

Plasma PtdCho molecular species differentiation was determined by ESI-MS/MS. Figure 3.6 shows example mass spectrometry traces of PtdCho molecular species from human plasma measured 48 hours after [methyl-D_9]choline chloride infusion. All three traces were acquired simultaneously and demonstrate how PtdCho synthesised through the CDP-choline and N-methylation pathways can be differentiated and compared to endogenous PtdCho composition. The endogenous material (figure 3.7C: precursor m/z = +184) is comprised of a mixture of short chain saturated and monounsaturated species (e.g. 16:0/18:2) as well as long chain polyunsaturated molecular species (e.g. 16:0/22:6). A precursor scan for m/z = +193 (comprising PtdCho molecular species containing the D_9 labelled head group), identifies molecular species synthesised through the CDP-choline pathway (figure 3.7A) and is composed predominantly of the shorter chain monounsaturated species (16:0/18:2,16:0/18:1). In comparison a precursor scan for m/z = +187 (containing one salvaged methyl group) identifies PtdCho synthesised

through the N-methylation pathway (figure 3.7B) and comprises predominantly longer chain polyunsaturated PtdCho species (e.g. 16:0/22:6, 18:0/20:4 and 18:0/22:6).

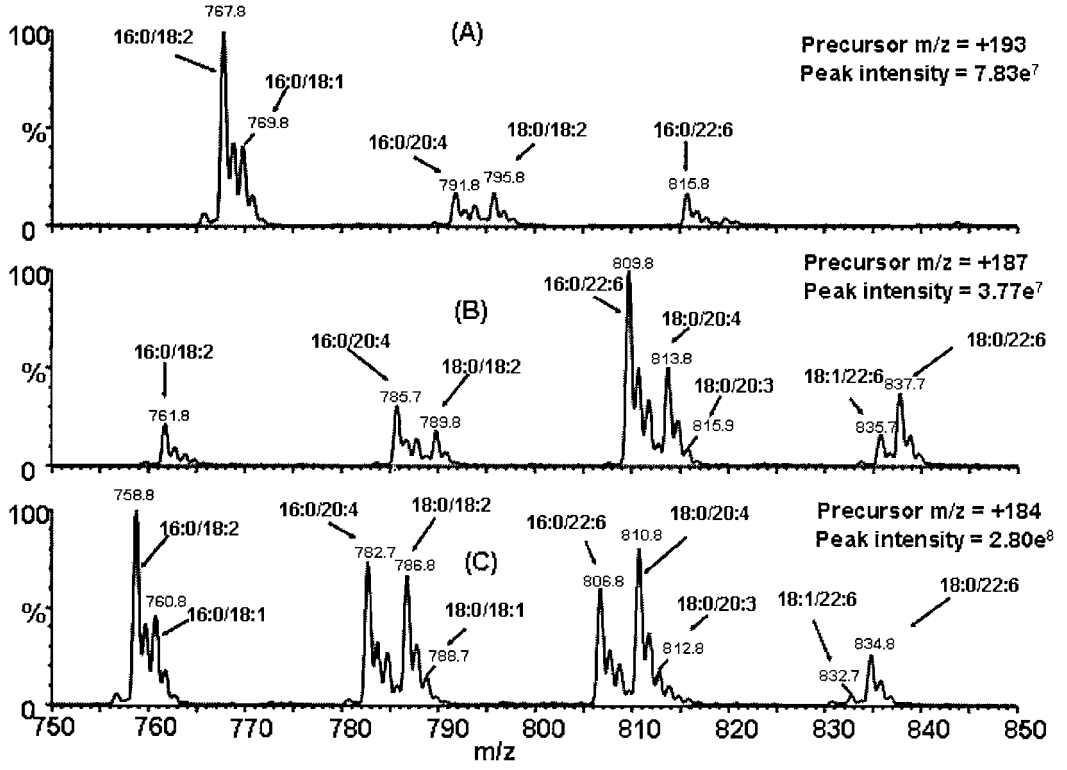

Figure 3.7: Precursor ion scans of product m/z 187 and m/z 193 for Plasma PtdCho 48 hours after administration of deuterium label (A and B) vs endogenous PtdCho (C)

3.3.1.2.3 CDP-choline and N-methylation PtdCho molecular specificity in human plasma

The molecular species composition of PtdCho in human plasma is shown in figures 3.8 and 3.9. PtdCho molecular species have been separated into three groups: The first group contains shorter chain saturated, monounsaturated and diunsaturated species; the second group, arachidonoyl (20:4) containing species and the third group docosahexaenoyl (22:6) containing species. The *N*-methylation (+187) pathway (figure 3.8) demonstrates a preference for synthesis of longer chain polyunsaturated species over short chain highly saturated species at 6 hours compared to endogenous composition. However, the composition tends towards equilibrium over time, presumably as a result of acyl remodelling and is largely comparable to endogenous PtdCho by 72 hours.

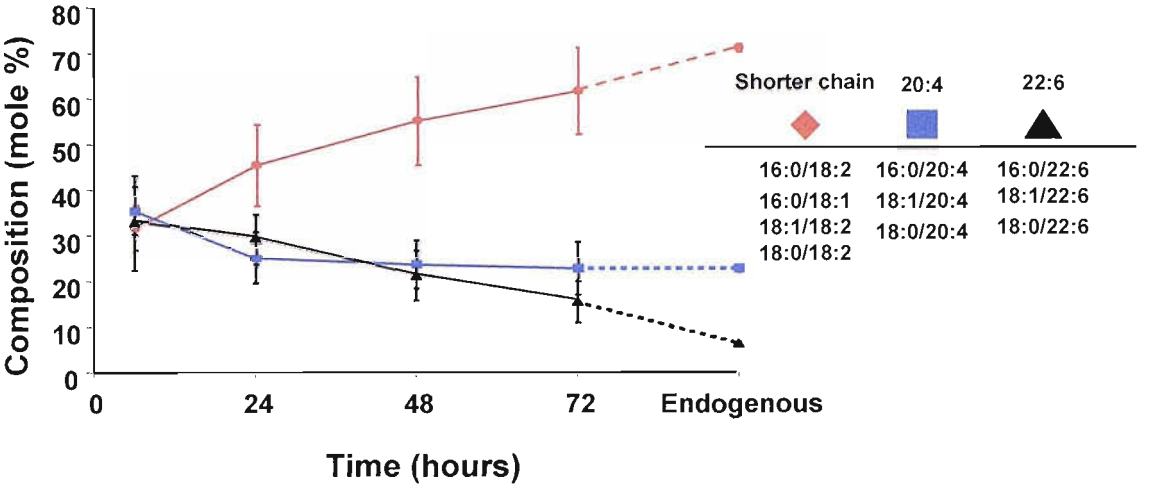

Figure 3.8: Time course showing the molecular specificity of plasma PtdCho synthesised via the N-methylation pathway in human volunteers. Data indicate the proportion of [methyl-D_3] containing shorter chain, 20:4 containing and 22:6 containing PtdCho molecular species at each time point. Results = mean (N=4) ± S.D.

In contrast, there is very little distinction between newly CDP-choline synthesised PtdCho composition (m/z = +193) and final equilibrium composition, with only a slight preference for the synthesis of short chain highly saturated species by the CDP-choline pathway (see figure 3.9). This suggests that the molecular species composition of the diacylglycerol (DAG) pool (the fatty acid precursor for CDP-choline synthesised PtdCho, section 3.1.2.1) largely reflects that of the PtdCho pool. This would imply little requirement for molecular species refinement by acyl remodelling for PtdCho synthesised by the CDP-choline pathway.

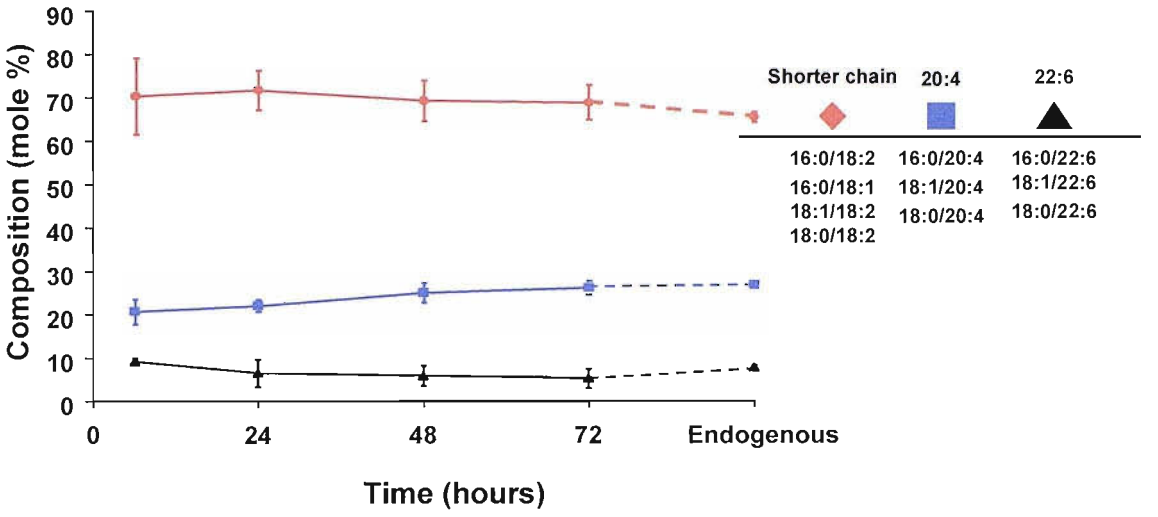

Figure 3.9: Time course showing the molecular specificity of plasma PtdCho synthesised via the CDP-choline pathway in human volunteers. Data indicate the proportion of [methyl-D_9] containing shorter chain, 20:4 containing and 22:6 containing PtdCho molecular species at each time point. Results = mean (N=4) ± S.D.

3.3.2 Surfactant PtdCho synthesis and turnover in humans by tandem ESI-MS/MS

The second part of this chapter concerns the synthesis and composition of sputum PtdCho. Because PtdCho synthesis does not occur by N-methylation in the lung, only deuterium labelled with nine deuterons need be considered as a marker for newly synthesised PtdCho.

3.3.2.1 Sputum PtdCho analysis by precursor ion scanning

Initially, ESI-MS/MS was used to determine the molecular species distribution of endogenous and newly synthesised PtdCho in sputum samples by scanning for precursors of m/z = +184 (endogenous PtdCho) and m/z = +193 (newly synthesised PtdCho) respectively. Representative ESI-MS/MS spectra of endogenous and [*methyl*-D_9]choline labelled PtdCho from an induced sputum samples collected 24 hours after the start of the infusion of [methyl-D_9]choline label are given in figure 3.10A and 3.10B). Incorporation of the deuteriated phosphocholine headgroup into the newly synthesised PtdCho species generated molecular species 9 mass units higher (see figure 3.10B).

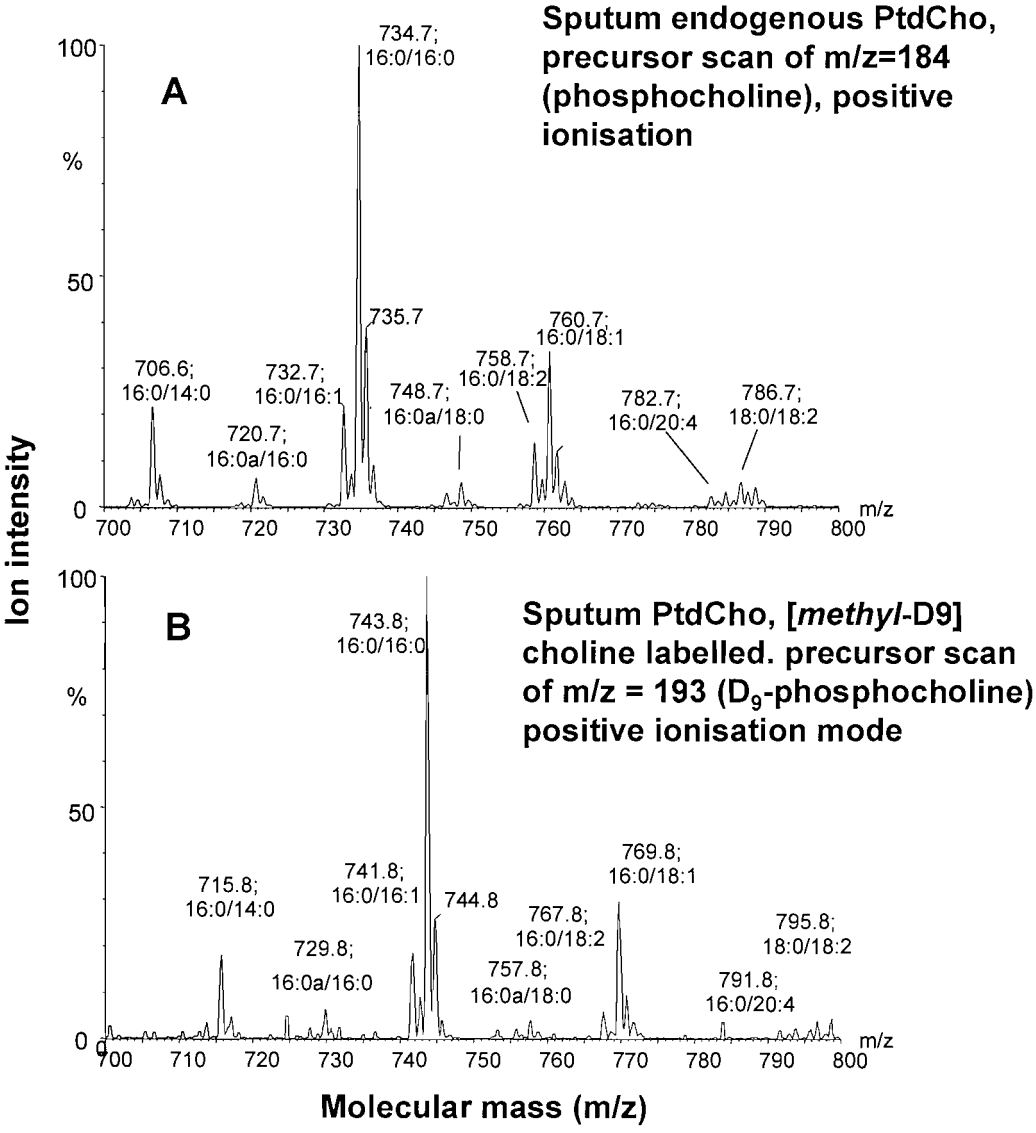

Figure 3.10: Representative ESI-MS/MS analyses of endogenous and D_9-choline labelled PtdCho from induced sputa. Figure shows precursor scans of (A) endogenous PtdCho (m/z = +184) and (B) newly synthesised ([*methyl*-D_9] labelled) PtdCho (m/z = +193) from an induced sputum sample collected 24 hours after the start of the infusion. Masses of individual PtdCho species are indicated with molecular species designation.

Endogenous sputum PtdCho molecular species composition was determined by ratio of the ion intensity corresponding to each individual PtdCho species, divided by the sum of the intensities of all PtdCho molecular species present in the spectrum. Endogenous sputum PtdCho consisted of 54 ± 1.5 % PC16:0/16:0, 9.7 ± 0.7 % PC16:0/14:0, 10 ± 1% PC16:0/16:1 and 13.1 ± 0.3% PC16:0/18:1 as principle components comprising more than 85% of total PtdCho. Less abundant PtdCho components detected were the alkylacylether species PC16:0a/16:0 and PC16:0a/18:0 (3.2 ± 0.3% and 1.8 ± 0.1% respectively) and the polyunsaturated species PC16:0/18:2 and PC16:0/20:4.

Analysis of endogenous PtdCho molecular species in individual sputum samples revealed that molecular species composition differed between fractions 1 and subsequent fractions of the 20 minute induction course (see table 4.1). Concentrations of PC16:0/18:1, PC16:0/18:2 and PC16:0/20:4 were increased at the expense of PC16:0/16:0 and PC16:0/14:0. However, these decreases in PC16:0/16:0 and PC16:0/14:0 in fraction 1 compared to fractions 2 to 4 were small (51.5±1.1% vs 54 to 55% and 8.8% ±0.4 vs. 9.7 to 10.1% respectively) as were the increases of mono-, di- and polyunsaturated PtdCho species.

PtdCho species	1st fraction %	2nd fraction %	3rd fraction %	4th fraction %
16:0/14:0	8.8±0.4 II,††	9.7±0.3	10.1±0.3	10.1±0.3
16:0alk/16:0	3.4±0.2	3.1±0.1	3.1±0.1	3.1±0.1
16:0/16:1	9.4±0.4	10.1±0.4	10.5±0.4	10.5±0.4
16:0/16:0	51.5±1.1 †,§	55.1±0.7	54.7±0.7	54.1±0.6
16:0alk/18:0	1.8±0.1	1.8±0.1	1.8±0.1	1.7±0.1
16:0/18:2	8.4±0.5 ‡,¶,‡‡	6.3±0.2	6.2±0.2	6.6±0.2
16:0/18:1	14.8±0.6 ‡,¶,‡‡	12.7±0.3	12.5±0.3	12.5±0.3
16:0/20:4	2.0±0.2 ‡,¶,‡‡	1.2±0.1	1.2±0.1	1.3±0.1

Table 3.1: Comparing the endogenous PtdCho composition of sequential sputum fractions. Data represent means ± S.E. of mean sputum PtdCho compositions from fractions 1 through to 4 collected at the 9 time points (from 0 to 168 hours see methods section 2.3.1.2) from 4 volunteers. Abbreviations: †:P<0.01, ‡:P<0.001 versus fraction2; §:P<0.05, II:P<0.01, ¶:P<0.001 versus fraction 3; ††:P<0.01, ‡‡:P<0.001 versus fraction 4.

Unfortunately, routine quantification of PtdCho molecular species was not possible by precursor ion scanning due to the very small quantities of newly synthesised [*methyl*-D_9] labelled PtdCho present in the sputum samples collected at the earlier time points. The problems encountered are highlighted in figure 3.11. At 12 hours, for example, there is evidence of newly synthesised PtdCho as indicated by the characteristic PC16:0/16:0 (m/z = 743), however due to the poor signal response, its authenticity cannot be determined due to the lack of discernible associated ^{13}C peak which would distinguish it from a 'spike' in the spectrum. Similarly, a peak at m/z = +769 at the 6 hour time point, would suggest the presence of newly synthesised PC16:0/18:1, but the

surprising lack of associated PC16:0/16:0, which is the dominant species at the 48 hour time point again brings the reliability of this data into question.

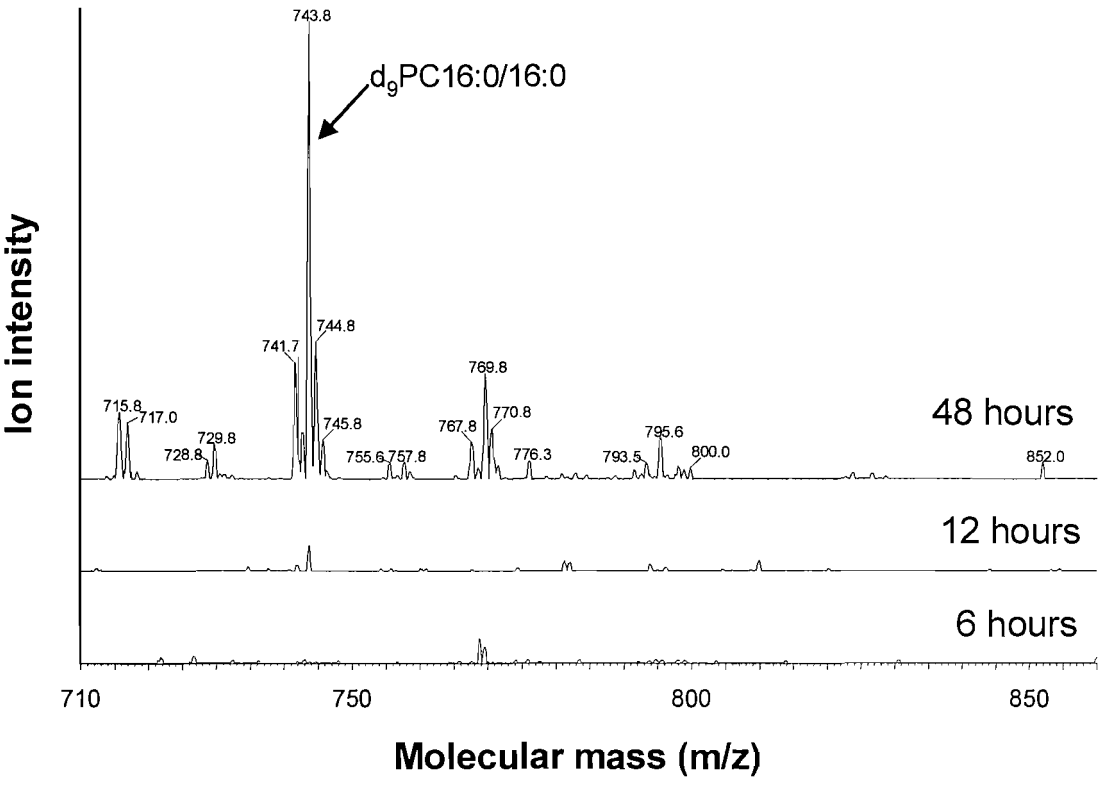

Figure 3.11: Example precursor ion scans of [methyl-D_9] labelled newly synthesised PtdCho (m/z = +193) in induced sputum samples collected at 6 hours, 12 hours and 48 hours.

3.3.2.2 Surfactant PtdCho analysis of induced sputum samples by multiple reaction monitoring (MRM)

3.3.2.2.1 Synthesis and turnover of sputum PtdCho in healthy volunteers

To meet the demands of high sensitivity and requirement for quantitative results for baseline (*methyl*-D_9)choline incorporation into sputum PtdCho, multiple reaction monitoring (MRM) was employed (see section 1.3.7). This was the method of choice because of the greater sensitivity of detection afforded by the greater dwell time available for selected ion transitions. The 8 major PtdCho species in sputum were identified from previous precursor ion scans (figure 3.10). To determine endogenous sputum PtdCho composition, MRM transitions from these 8 molecular species to the

breakdown to the diagnostic fragment ion m/z = +184 was monitored. To determine the composition of newly synthesised sputum PtdCho, the transition from their corresponding methyl-D_9 labelled counterparts, to the diagnostic deuterium labelled fragment m/z=+193 was monitored (see tables 2.3 and 3.2).

Assignment	Endogenous molecular ion (m/z)	Deuteriated molecular ion (m/z)
16:0/14:0	706.6	715.6
16:0a/16:0	720.6	729.6
16:0/16:1	732.6	741.6
16:0/16:0	734.6	743.6
16:0a/18:0	748.6	757.6
16:0/18:2	758.6	767.6
16:0/18:1	760.6	769.6
16:0/20:4	782.6	791.6

Table 3.2: MRM assignments for the 8 major endogenous and PtdCho molecular species in sputum

The increase in sensitivity afforded by MRM comes as a result of the highly selective nature of the technique. Hence all information regarding other species in the sample is lost. MRM analysis produces a time response curve which resembles a chromatogram, although technically no chromatography has taken place (see section 2.3.3). The area under the MRM chromatogram corresponds to the sum of all the individual transitions detected (see figure 3.12).

Due to the small quantities of surfactant PtdCho present in sputa, samples were re-suspended in the minimum quantity of sample buffer possible for auto sampler injection (15 µl). 10 µl of sample was injected into $CHCl_3$/ MeOH/ H_2O mobile phase. The flow rate was optimised to 100 µl per minute. For flow rates greater than 100µl per minute, the sample was eluted too quickly to allow sufficient time for the mass spectrometer to detect trace amounts of PtdCho. For flow rates less than 100 µl per minute, the sample adhered to the silica tubing and internal components of the auto sampler, and was therefore not eluted in one discrete peak.

Two MRM analyses were carried out simultaneously on each extracted sputum sample, resulting in the production of two chromatograms, one corresponding to breakdown to the m/z 184 fragment (endogenous phosphocholine) and the other corresponding to breakdown to the m/z 193 fragment (deuteriated phosphocholine). Example chromatograms are given in figure 3.12.

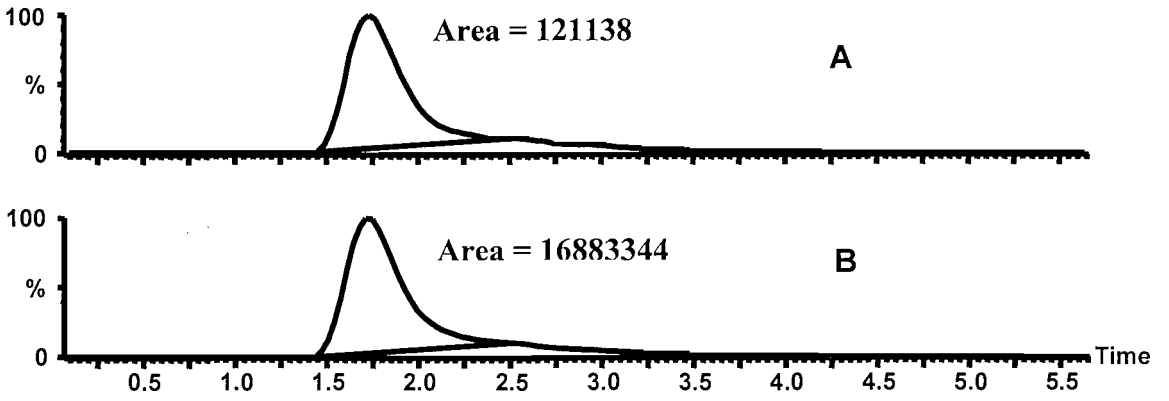

Figure 3.12: Example MRM chromatograms for endogenous (B) and newly synthesised PtdCho (A) using MRM assignments given in table 4.2.

Chromatograms were integrated using Mass Lynx NT software and the ratio of the endogenous to deuteriated peak areas were used to determine D_9-choline incorporation (see figure 3.13). [*Methyl*-D_9]choline incorporation increased linearly from 12 to 30 hours after the start of the infusion. The mean rate of PtdCho synthesis during this time as determined by linear regression was 0.0251% per hour relative to endogenous PtdCho and extrapolation of the regression line to the x axis intercept suggested a lag phase of 5.7 hours before labelled PtdCho appeared in sputa. [*Methyl*-D_9]choline incorporation reached a plateau between 30 and 48 hours (mean fractional label = 0.61%) and only reduced by 50% after one week.

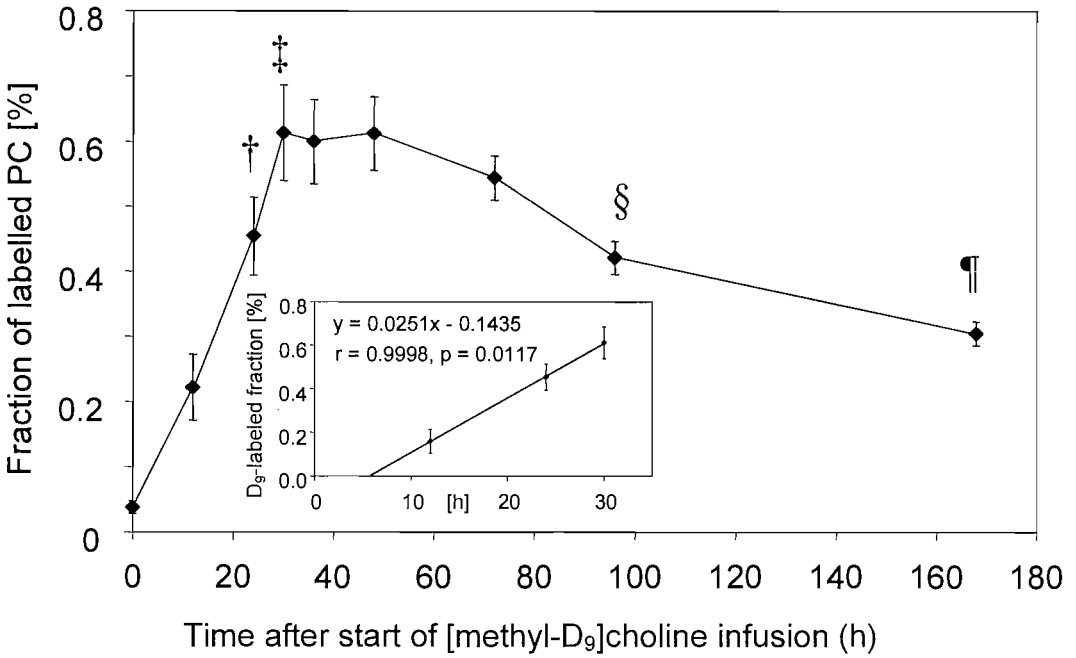

Figure 3.13: Time course for [methyl-D_9]choline incorporation into total PtdCho from induced sputa for four healthy patients. Data represent the fraction of D_9-labelled PtdCho relative to endogenous PtdCho and are represented as means ± SE of 4 sequential sputum samples from 4 volunteers at each time point. †, P<0.01 vs t = 12 hours; ‡, P<0.01 vs. t = 12 hours; §, P<0.05 vs t = 48 hours; ¶, P<0.001 vs t = 48 hours

3.3.2.2.2 Analysis of [methyl-D_9] labelled PtdCho composition in individual sputum fractions

Analysis of [*methyl*-D_9]choline incorporation into individual sputum samples revealed a degree of variation in composition between fractions 1 to 4 of the 20 minute sputum induction courses (see figure 3.14). Until reaching the incorporation plateau, [*methyl*-D_9]choline labels tended to increase from fractions 1 to 4. However, these differences did not reach significance ($p>0.05$) and after 48 hours no such differences among the D_9-label in the PtdCho of sputum fractions 1 to 4 could be demonstrated.

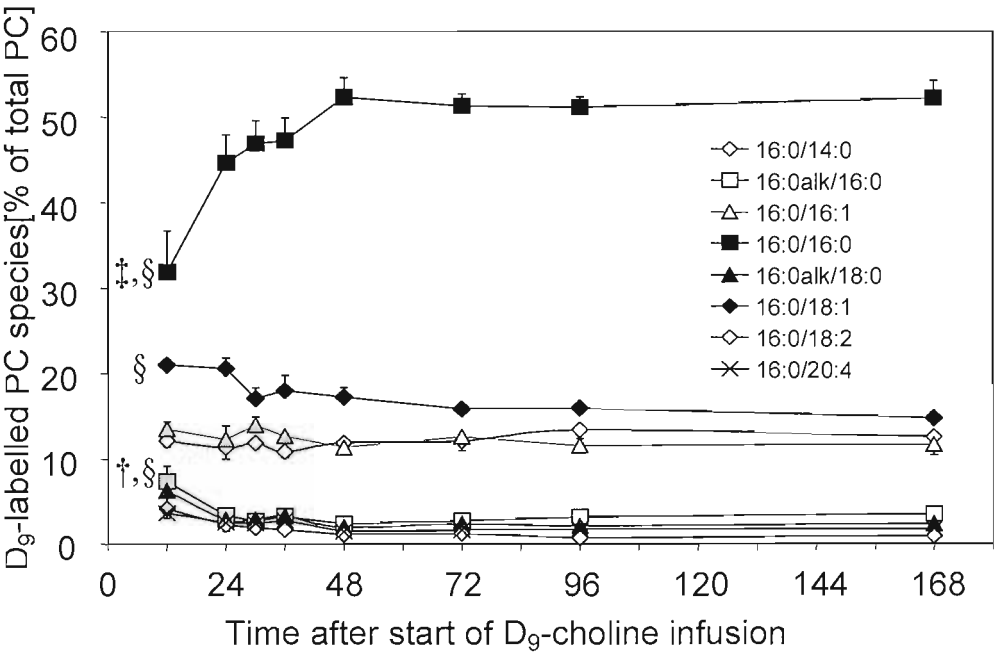

Figure 3.14: Time course of [methyl-D_9]choline fractional incorporation into total PtdCho from individual sputum fractions. Fractional label of individual PtdCho species in relation to total PtdCho label was calculated from total parents of m/z = +193 at the given time points Data indicate means ± SE of 4 sputa from 4 volunteers at each time point. Abbreviations †, P<0.01; ‡, P<0.001 vs. t = 24 hours; §, P<0.001 vs. equilibrium (48 to 168 hours).

3.4 Discussion

The work presented in this chapter contributes towards an emerging group of studies which have been termed "dynamic lipidomics"[142] and which comprise a technology that is likely to dominate phospholipid metabolism in the coming years. With the current strategy of stable isotope labelling and ESI-MS/MS detection, all PtdCho molecular species can be cleanly resolved and readily quantified.

Using the combination of [methyl-D_9]choline chloride incorporation together with ESI-MS/MS described here, analysis of plasma and sputum PtdCho metabolism has been feasible using as little as 3.6 mg of [methyl-D_9]choline chloride per kg body weight, generating results in terms of individual PtdCho molecular species. Additionally, in contrast to the extensive derivatisation steps required for combustion interface isotope ratio mass spectrometry or HPLC based approaches[127,143] phospholipid extracts did not have to be fractionated or derivatised prior to ESI-MS/MS analysis.[144]

The kinetics of both plasma PtdCho and alveolar surfactant PtdCho metabolism analysed from induced sputa are influenced by the uptake of choline from the circulation, kinetics of precursor processing amd secretion of PtdCho into the circulation and alveolar spaces respectively. Quantification of endogenous and [methyl-D_9]choline in blood plasma was determined by Dr Wolfgang Bernhard, University of Tuebingen, Germany. The concentrations of endogenous choline in blood plasma did not change during or after infusion of [*methyl*-D_9]choline chloride (8.4 ± 0.3μM) (N=52). During infusion (1-3 hours), mean values of [*methyl*-D_9]choline chloride were 8.2±0.9 μM (N=12) but dropped to near zero values within 3 hours after the end of the infusion. By nine hours after the end of the infusion [*methyl*-D_9]choline was virtually absent from blood plasma (figure 3.15)

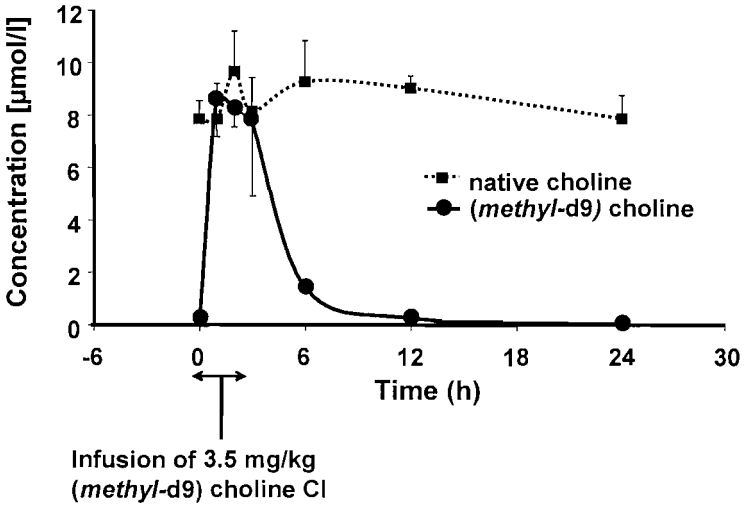

Figure 3.15: Kinetics of endogenous and [methyl-D_9]choline in plasma (Reproduced courtesy of Dr Wolfgang Bernhard, University of Tuebingen).

It is known that at choline dosages of up to 0.2 mmol.kg^{-1} (as a pose to 24 μmol.kg^{-1} used in the study described in this chapter), infused choline is rapidly removed from the circulation via uptake into tissues (Haubrich, 1975, Buchman et al, 1994). In mice, maximal label of lung tissue occurs within 1.5 hours following injection of [methyl-^{3}H]choline, followed by a plateau of at least 24 hours.(Bernhard et al, 2001). The data in figure 3.15 showing the rapid removal of [methyl-D_9]choline from the circulation are consistent with these findings. They suggest loading of tissues with [methyl-D_9]choline, during and shortly after the end of the infusion, whereas the time course of PtdCho labelling in lungs and plasma results from subsequent processes of synthesis, intracellular trafficking, secretion and turnover (see sections 3.3.1 and 3.3.2).

PtdCho synthesis in hepatocytes is critical to lipoprotein LDL and VLDL assembly and secretion. LDL provides cholesterol to the tissues, whilst VLDL transports triglycerides from the liver to extra hepatic tissues. In most cells, PtdCho is synthesised exclusively by the CDP-choline pathway which uses choline as an initial substrate.[134] However, PtdCho can also be synthesised by three rounds of PtdEtn methylation which is catalysed by PEMT.[135] Hepatocytes are the only cell type which can synthesise PtdCho through the N-methylation pathway which accounts for approximately 20-30% of total liver PtdCho synthesis.[131] The data presented in this chapter details the molecular specificity of liver PtdCho synthesis, secretion and turnover through unequivocal distinction between the two PtdCho synthesis pathways for the first time in humans *in vivo*. This has been achieved through the analysis of distinctive pre-cursors and by enabling direct comparison between newly synthesised and pre-existing PtdCho molecular species. Compared to equilibrium PtdCho composition, PtdCho synthesised via the N-methylation pathway was found to be comprise significantly more long chain polyunsaturated (20:4 and 22:6 containing) species (figure 3.8) which presumably reflects the molecular species composition of the precursor PtdEtn pool from which it is derived. Over time, N-methylation synthesised PtdCho became refined to reflect endogenous PtdCho composition. In contrast, CDP-choline synthesised PtdCho was synthesised with a distinct preference for short chain saturated and mono and di-saturated PtdCho species in keeping with equilibrium plasma PtdCho composition (figure 3.9). These observations are consistant with recent *in vivo* evidence utilising rat primary hepatocyte[131] and rat hepatocarcinoma[106] cell lines, which also demonstrated molecularly distinct N-methylation and CDP-choline synthesis pathways.

A comparative study was carried out within my research group, in which mice received intraperitoneal injections of [methyl-D_9]choline chloride. Mice were sacrificed at 1.5,3,6 and 24 hours. Liver and plasma phospholipids were subsequently isolated and analysed by tandem ESI-MS/MS. PtdCho synthesised by the N-methylation and CDP-choline pathways was determined in the sameway as for humans. The time course for [methyl-D_9]choline incorporation into liver PtdCho by both the CDP-choline and N-methylation pathways is given in figure 3.16.

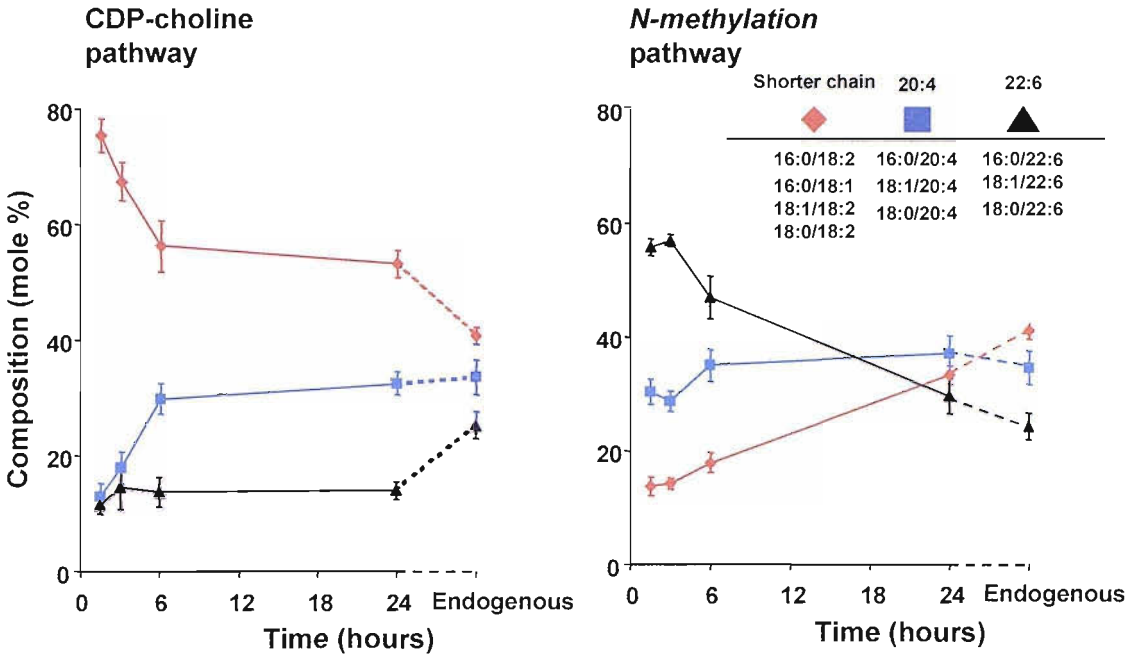

Figure 3.16: Time course showing the molecular specificity of PtdCho synthesised by (A) the CDP-choline and (B) *N*-methylation pathways in mouse liver. Results = mean (N=5) ± S.D (reproduced courtesy of Dr Neil Henderson, University of Southampton).

In contrast to humans, there is clear distinction between CDP-choline synthesised PtdCho molecular species composition and endogenous composition (figure 3.16A cf figure 3.9) implying that the diacylglycerol (DAG) pool in mice is of a significantly different composition to the endogenous PtdCho pool. Nevertheless, the composition of CDP-choline synthesised PtdCho is rapidly refined, presumably through acyl remodelling, to yield a molecular species composition comparable to the endogenous pool by 24 hours. The preference of the N-methylation synthesised PtdCho for long chain polyunsaturated molecular species relative to endogenous PtdCho composition is consistent with the human data (figure 3.16B cf figure 3.8).

Molecular specificities for both N-methylation and CDP-choline synthesis pathways were also measured for mouse plasma. Both time course and composition directly mirrored that observed in the liver pathways(data not shown). Comparable results between mouse and human plasma suggest that the mouse is a good model for the human and suggest that the synthesis and secretion scenario found in mouse liver can be extrapolated to human liver. These observations have major implications on the role of the liver in the regulation of extra-hepatic lipoprotein homeostasis in vivo. The hepatocyte is the only mammalian cell capable of producing PtdCho via methylation of

PtdEtn. Although this could be a back up for choline synthesis in times of dietary deficiency, these results also suggest that the N-methylation pathway provides a means for the direct supply of polyunsaturated fatty acids from the liver to extra hepatic tissues. This hypothesis is support by the substantially diminised plasma concentrations of docosahexanoic acid (DHA, [22:6(n-3)]) and arachidonic acid [20:4(n-6)] observed in $PEMT^{-/-}$ mice irrespective of nutritional choline intake.[140] This capability is particularly important in pregnancy, where the 22:6n-3 containing species are required for the period immediately preceding neurite formation by fetal brain.[145] Furthermore, given the widespread involvement of arachidonic acid in cellular regulation, PtdCho species derived from PEMT in the liver may serve as an important source for generating lipids active in cellular regulation. Taken together these findings underline the importance of the N-methylation pathway in producing the polyunsaturated fatty acids produced by the liver.

Liver growth and liver carcinogenesis have also been associated with activation of the CDP-choline pathyway[146] and inactivation of the PtdEtn methylation pathway[147]. The capacity to scrutinise the synthesis of these two key pathways simultaneously, relatively cheaply and at high throughput without exposing patients to toxic substances could herald lipidomic technology as a key for characterising biomarkers of diseases such as liver carcinogenesis in the future.

Nutrition research and its public health applications have achieved a major impact on the prevention of diseases caused by deficiencies caused by essential nutrients. Technologies for broad scale and parallel analysis of metabolites are required, which once applied to large clinical assessments of populations, can produce databases that are simultaneously annotated according to various aspects of the effective phenotypes of all individuals involved. The information this produces will provide guideposts for each individual based on their own personal metabolic profile. This methodology has already been applied to the cholesterol programme in the US for example.[148] Although this was successful for drug development, it did not go far enough for foods by deciding to focus on a single metabolite. While measuring cholesterol per se can provide a quantitative estimate of disease risk in a population and an individual, the simple measurement of cholesterol does not provide sufficient information to deduce why that individual accumulated the cholesterol, nor does it suggest the appropriate intervention to solve the problem.[149,150] The power of Lipidomic technology to probe multiple components of

metabolic systems simultaneously means it has great potential as a component part of personal metabolomic technology in the future.

Application of lipidomic technology to the study of surfactant synthesis has enabled the study of the synthesis and metabolism of individual molecular species in humans *in vivo* for the first time. Differences in surfactant phospholipid molecular species have been observed in a variety of lung diseases including NRDS, ARDS, pneumonia, cystic fibrosis and asthma, however the extent to which these changes are due to alterations in synthesis or hydrolysis of phospholipids has remained uncertain. Until recently, the required characterisation of phospholipid metabolism in humans has been impossible due to the harmful effects of radioactive substrates a problem which can be overcome with the use of stable isotopes.

Previous approaches to the analysis of surfactant PtdCho metabolism have employed glucose or fatty acid precursors as well as exogenous surfactant labelled with the carbon isotope ^{13}C followed by analysis of ^{13}C enrichment by combustion interface istope ratio mass spectrometry, however these techniques provide little information about metabolism of individual PtdCho molecular species and require extensive derivatisation or HPLC. Lipidomic analysis using as little as 3.6mg per kg deuterated choline per kg body weight made it possible to study the synthesis and metabolism of individual molecular species without the requirement for derivatisation or HPLC.

Radioactive labelling of choline and palmitate have also been used to investigate PtdCho metabolism in animal models. However, analysis of the results *in vivo* is complicated by the fact that palmitate can originate from the circulation as well as from synthesis within the lungs, is incorporated into a number of different lipid classes, metabolised to unsaturated palmitoleic acid and targeted to β oxidation. In contrast choline is essentially derived from the circulation and only small quantities incorporated into other lipids such as sphingomyelin. Initial choline incorporation into PtdCho reflects *de novo* synthesis and any subsequent change is attributable to acyl remodelling.

Although BALF is the ideal source for studying surfactant composition and the kinetics of metabolism, we used induced sputum because of the ethical implications of repetitive harvesting of BALF samples. Other studies have shown that airway phospholipids in healthy lungs are representative of alveolar lipids.[63,111] The data from this study are in agreement and show that induced sputum displays an overall phospholipid composition

identical to that in BALF. Nevertheless, due to mucociliary transit time, sputum samples do not correctly reflect surfactant kinetics of the alveoli. This problem is compounded in the diseased lung where contamination by airway epithelia, inflammatory cells and exuded plasma lipids are likely to have a major impact on surfactant composition.[2] Under these conditions, BALF extraction would be necessary to determine any alterations in alveolar synthesis and metabolism.

Although the composition of native PtdCho species in sputum was representative of alveolar surfactant, this was not the case for [methyl-D_9]choline labelled PtdCho species after 12 hours. Indeed, equilibrium with the endogenous PtdCho pool was not achieved until after 48 hours. Estimates of *de novo* synthesis and acyl remodelling predict that both contribute approximately 50% to the synthesis of PC16:0/16:0. However, the data presented in this chapter indicate an initial fractional label of PtdCho 16:0/16:0 of only 30% instead of more than 50% after reaching equilibrium. These results suggest that a significant quantity of newly synthesised PtdCho is rapidly incorporated into lamellar bodies and secreted before it has time to be remodelled to equilibrium surfactant composition.

One of the original aims of my PhD was to develop a method for measuring Pumactant turnover in the lungs of treated patients. Now that the technique and principles for *in vivo* analysis of surfactant PtdCho has been established and validated, it can be easily adapted to achieve this goal. Pumactant powder has been synthesised containing labelled [methyl-D_9]choline for laboratory experiments. This labelled Pumactant could be employed in future clinical trials involving prophylactic administration of the powder to asthmatics followed by allergen challenge, as well as administration of Pumactant as a rescue therapy post allergen challenge. Sputum and/or BALF samples could then be collected (depending on disease severity) at specific time points. Turnover of the material could then be determined by measuring the loss of D-9 labelled Pumactant over time by ESI-MS/MS. The data produced could also be used to correlate any potential changes in symptoms with metabolism/ turnover or even incorporation of Pumactant into sputum PtdCho.

This type of labelling experiment could also be of use to study the long term implications of exogenous surfactant therapy on surfactant homeostasis in the lung as there are ambiguities concerning the acute effect of exogenous surfactant administration

on endogenous surfactant metabolism.[151] Studies conducted in our laboratory on lung lavage samples isolated from SP-D knockout mice revealed accumulation of surfactant PtdCho in the lavage despite an observed down regulation of PtdCho synthesis in the lung (Dr NG Henderson, personal communication). It is possible that down regulation of synthesis is a result of negative feed back due to accumulation of surfactant in the lung. This could have important implications in the long term dosing of exogenous surfactants on lung surfactant synthesis and secretion. Deuteriated choline could be administered to patients prescribed Pumactant or any lipid based preparations on a prophylactic bases to suppress airways disease as part of a clinical trial, to establish any long whether the long term inhalation of exogenous surfactant has an impact on fraction synthesis rates of endogenous surfactant. If this is indeed the case, the effect of halting treatment on surfactant homeostasis could also be assessed.

Deuterium can also be 'visualised' by magnetic resonance imaging (MRI). It could be possible to combine ESI-MS/MS and MRI technologies in the future, using the same label to determine spatial distribution of exogenous lipids MRI as well as assessing their impact on homeostasis.

Chapter 4

Pumactant delivery

4.1 Introduction

4.1.1 The physiology of the lung

The airways of mammalian lungs form a system of branching tubes (more than 17 bifurcations[152]) whose diameter decreases from the trachea to the periphery. The conducting airways are surrounded by smooth muscle and are innervated. They are also lined with specialised cells, some which produce mucus and others that carry cilia. Together they form an escalator, carrying mucus and deposited inhaled material from the periphery to the trachea to maintain sterility of the lung. The alveoli form the final branching of this system and are small sac like structures closely surrounded by a network of capillaries that enable gas exchange. These capillaries contain a combined volume of approximately 80ml of blood through which oxygen is absorbed. There are approximately 300 million alveoli in the adult lung covering a surface area of approximately $150m^2$.[153,154] The diameter of a fully inflated alveolus of a human adult lung is believed to be between 145 to 250μm depending on age and body size.[155,156] However, within a given lung there is very little variation in fully inflated alveolar size.[157]

4.1.2 Drug delivery to the respiratory tract

The administration of drugs directly into the respiratory tract is widely regarded as the method of choice for treating respiratory disease. The chief advantage of targeting drugs directly into the lungs, lies in the reduction of systemic bioavailability and consequently of unwanted side effects[158]. Efficient delivery of a drug to the periphery of the lung conducting network or to the respiratory regions themselves means overcoming the immense power of the lung to filter particles and rapidly remove them by mucociliary action[158].

4.1.2.1 Commercially available 'non invasive' administration devices

There are currently three types of commercially available device available for drug administration therapies which do not require patient intubation. These are the pressurised metered-dose inhaler (pMDI), the dry powder inhaler (DPI) and nebulisers.

4.1.2.1.1 The pressurised metered-dose inhaler (pMDI)

Since its introduction in 1956, the pMDI has been the method of choice for delivery of inhaled therapies for airway diseases such as asthma[159]. Metered-dose inhalers are compact pressurised aerosol dispensers specially designed for oral inhalation delivery of multiple doses of finely dispersed drug to the lungs. pMDI's consist of five essential components, namely the drug, propellant/ excipient (inactive ingredient added to the drug to dilute it or give it form or consistency) liquid mixture, container, metering valve and actuator. The pMDI discharges up to several hundred accurately metered shots each with a medicament content ranging from less than 50μg to 5mg of drug and generally delivered in a metered liquid volume of between 25 and 100μl.[160] Although the traditional pMDI has a relatively consistent delivered dose, it is very dependant on patient use. Even with correct use, only 10 – 20 % of the dose will enter the lung with approximately 70 - 80% being deposited in the oropharynx and the rest retained in the device.[161] Despite this record of inefficiency combined with an unacceptably high level of drug wastage, the chlorofluorocarbon (CFC)-driven pMDI has retained popularity as a relatively inexpensive, robust and convenient delivery system.[162] The general perception that the pMDI is easy to use probably stems from the efficiency of β_2-agonists such as salbutamol, since the bronchodilator effect can be felt within a matter of minutes by the patient and multiple dosing to achieve a clinical response is very easy. Due to the socio-economic impact of chronic respiratory diseases, environmental concerns over the use of propellant gases have forced the pace of pharmaceutical research into suitable replacements for the CFC propelled pMDI. Improvements in pMDI design and reformulation with 'ozone friendly' propellants such as hydrofluoroalkanes (HFA's), will enable continued use of the pMDI in the short term. However HFAs are also greenhouse gases, although only 33% as potent as CFC's they are still 2000 times greater than carbon dioxide (CO_2). With the growing concern of

global warming, these substances are almost certainly destined to be subject to environmental controls in the 21st century.[163,164]

4.1.2.1.2 The dry powder inhaler (DPI)

Major constraints in the development of replacement administration devices include the need for improved patient compliance and cost-effective treatment[162]. The major alternative to the pMDI is the breath actuated dry powder inhaler (DPI). Inhalant dry powder technology began in earnest with the discovery of sodium cromoglycate in 1967 as a topical, non-steroidal inhibitor of allergic asthma. The need to deliver 20 mg doses of this low potency drug by inhalation far outside the capability of pMDI technology, resulted in the development of a gelatine capsule, single-dose DPI, the Fisons Spinhaler®[165]. The device was particularly useful in the treatment of children and elderly patients as it used the patients own inspiratory flow to provide the energy required to aerosolise particles from a pierced capsule. Consequently it avoided the problem encountered with the pMDI of coordinating device actuation and inspiration. The choice of drug treatment by single-dose DPI was expanded with the introduction of the GlaxoSmithKline Rotahaler®[166] followed by the Boehringer Ingelheim Aerohaler®[167]. However, single dose DPI's require dexterity to load each time with an individual capsule and these capsules are themselves vulnerable to extremes of temperature and humidity. To ensure effective drug delivery to the lungs, the turbulent air stream created in any DPI during inhalation must be sufficient to produce an aerosol of respirable fine particles. Lung delivery from DPI's improves with increasing flow rate, however at best it resembles pMDI performance with lung deposition *in vivo* and respirable fraction *in vitro* ranging from 6 to 14% of the nominal dose[168,169,170]. Competition with pMDI's in terms of convenience, ease of use and portability, heralded the advent of multiple dose DPI's. Sweden was among the first countries to embrace the environmental hazards of CFC-driven aerosols and this concept underlay development of the first reservoir multiple dose DPI, the AstraZeneca Turbuhaler® in 1987[171].

Powder inhalation products consist of two elements: an inhalation device to deliver unit doses of powder formulation into the inspired air stream and a reservoir of the powder formulation containing the drug substance. This reservoir can take two forms: either a bulk load, from which aliquots of the formulation are dispensed as required for each administration, or a series of pre-packaged unit doses which are inserted into the device

for inhalation as required. Patient driven propellant free multiple dose DPI's are likely to emerge as one of the major devices of the future for the control and management of asthmatic disease[172].

All currently marketed DPI's rely on the patients inspiratory effort to withdraw the powder from the metering system, entrain the powder in the air-stream and to 'aerosolise' any aggregated drug particles such that they are small enough to penetrate and deposit in the deep airways of the lung. There are a number of new developments that are aimed at providing additional energy to either pre-aerosolise the drug or enhance the aerosolisation process during inhalation. The Spiros DPI from Dura Pharmaceuticals is equipped with motor and impeller to create a high shear zone, through which the drug formulation must pass to exit the device.[162]

Inhale therapeutics are developing a DPI delivery system that uses a small volume of compressed air to pre-aerosolise the drug into a holding chamber prior to inhalation[173]. The prohaler from Valois also uses a small volume of compressed air but in this case it is released during the inspiratory cycle to facilitate drug particle dispersion[173]. A new technology is also being developed by Microdose technologies that combines the use of a piezo-electric de-aggregation system and electrostatic particle charging to facilitate the aerosolisation process.[173]

4.1.2.1.3 Nebulisers

Nebulisation is widely regarded as 'old' technology, however recent developments in liquid spray delivery systems have revitalised interest in this highly innovative inhalation route.[174] Nebulisers fall into two catergories, Jet and Ultrasonic. Traditional air driven (jet) nebulisers use a flow of compressed gas to aerosolise an aqueous solution or suspension of drug contained in a chamber equipped with a capillary feed system for the liquid. Liquid is drawn from a fluid reservoir through a feed tube, fragmented into droplets and is accelerated to a velocity sufficient for more than 99% of the droplet mass to impact on baffles on the nebuliser wall where the drops coalesce and drain back into the fluid reservoir. Only 1% of the aerosol mass leaves the nebuliser directly. The outgoing air becomes saturated with water derived from liquid retained in the nebuliser.

Therapeutic aerosols are also produced by ultrasonic nebulisers in which the mechanical energy needed to produce the spray is derived from a piezoelectric transducer, vibrating at a frequency in the 1-3 MHz range.

The advantages and disadvantages of each type of Aerosol-Generating device or system clinically available are given in the table 4.1.

Type	Advantages	Disadvantages
Pressurised MDI	Portable and compact Treatment time is short No drug preparation required No contamination of contents Dose-dose reproducibility high Some can be used with breath-actuated mouth piece	Coordination of breathing and actuation needed Device actuation required High pharyngeal deposition Upper limit to unit dose content Remaining doses difficult to determine Potential for abuse Not all medications available Many use CDC propellants in the US
DPI	Breath actuated Less patient coordination required Propellant not required Small and portable Short treatment time Dose counters in most new designs	Requires moderate to high inspiratory flow Some units are single dose Can result in high pharyngeal deposition Not all medications available
Small-volume jet nebuliser	Patient coordination not required High dose possible Dose modification possible No CFC release Can be used with supplemental oxygen Can deliver combination therapies if compatible	Lack of portability Pressurised gas source required Lengthy treatment time Device cleaning required Contamination possible Not all medication available in solution form Does not aerosolise suspensions well Device preparation required Performance variability Expensive when compressor added in
Ultrasonic nebuliser	Patient coordination not required High dose possible Dose modification possible No CFC release Small dead volume Quiet Newer designs small and portable Faster delivery than jet nebuliser No drug loss during exhalation (breath actuated devices)	Expensive Need for electrical power source Contamination possible Not all medication available in solution form Device preparation required before treatment Does not nebulise suspensions well Possible drug degradation

Table 4.1: The advantages and disadvantages of aerosol-generating devices or systems clinically available

4.1.3 Surfactant administration

Lung surfactant is mostly administered in the form of intratracheal instillations of liquid boluses directly into the lungs through an endotracheal tube, as well as administration via bronchoscopic lavage. Although these methods allow delivery of a known amount of surfactant directly into the lungs whilst avoiding losses in the upper airways, neither technique is suitable for airways diseases which do not require the patient to be intubated. Tracheal instillation has also been shown to cause a heterogeneous distribution of surfactant in the alveoli, however this problem is overcome with intratracheal inhalation[175].

The use of dry powder inhalation (DPI) devices for respiratory therapy has become increasingly popular in recent years, however delivered doses from these devices is usually limited to microgram quantities[162] (6μ to 500μg for Oxis® and Bricanyl® Turbohaler® devices respectively. The highest quantity commercially available dry-powder device is the Intal® spincap at 20 mg, produced by Rhone-Poulenc Rorer.[103] However, there are several high-dose medicaments that could potentially be delivered as dry powders via a pulmonary route. The treatment of lung infections using antibiotics could have increased efficacy if delivered in this way.[176] In a clinical trial involving prophylactic administration of Pumactant powder to mild asthmatic patients, treatment with two separate doses of 400 mg Pumactant prior to allergen challenge resulted in abolishment of the early phase asthmatic response.[9]

In order to model the behaviour of dry powder Pumactant *in vitro,* a high delivery dry powder device capable of consistently dosing in excess of 50mg was required which was not possible with any commercial device. Recently, a novel handheld pressurised aerosol dry-powder device (PADD, see section 1.9.4) was developed specifically for the delivery of high dose (25 – 250mg) cohesive powders to the respiratory tract.[103] Although capable of delivering the high doses of Pumactant necessary, powder delivery was limited to single doses, the duration of which was pre-determined by the fixed volume of the gas canister used to aerosolise the powder. Moreover, without the required facilities for filling the gas canisters, the pressure of gas used to deliver the powder was limited to what was available from the suppliers. The goal of the work presented in this chapter was therefore to develop and characterise a dry powder administration device capable of delivering large reproducible quantities of Pumactant, but where the variables affecting the powder delivery could be tailored to suit specific experimental requirements.

4.2 Results and Discussion

The worked described in this chapter is separated into three parts. The first part (section 4.2.1) describes dry powder Pumactant dosing, discusses the problems encountered and explains how the results obtained from a series of laboratory built delivery devices was used to develop a prototype automated dry powder dispensing device. The second part (section 4.2.2) details experiments carried out to characterise this delivery device and the final part deals with the characterisation of the powder it dispensed (section 4.2.3).

4.2.1 Pumactant delivery

4.2.1.1 Pumactant delivery using a gas filled syringe

Pumactant was supplied as an amorphous white powder (100 mg quantities) in glass vials sealed with rubber stoppers. Initial experiments were aimed at expelling powder from the vial using a syringe (section 2.4.1). The dispensed powder was collected in disposable glass screw top tubes and quantified by ESI-MS/MS (table 4.2). The powder appeared to coagulate upon repeated exposure to the air and as a result became progressively hard to dispense upon repeated actuations. This was also evident from the quantity of assayed material, which decreased upon successive actuations.

This aggregation of the powder was thought to be due to its hygroscopic nature. The same experiment was therefore repeated using dry CO_2 to dispense the powder (Table 4.2). Variation in delivered dose was significantly less for the dry gas and the powder no longer agglomerated with successive actuations.

Actuation No.	**Mass delivered/ µg**	
	2 ml Air	**3 ml CO_2**
1	157	314
2	29	200
3	43	300
4	86	329
5	14	357
Mean	66 ± 58	305 ± 55

Table 4.2: Pumactant administration using air and dry CO_2. Results shown are delivered doses (µg) from 5 successive actuations using air (2ml) or CO_2 (3ml) from which the mean dose (N=5) ± S.D. has been calculated.

These observations were supported by the Bath pharmaceutics laboratory where dynamic vapour sorption profiles showed very rapid uptake of water (<30 minutes) before stabilisation.[103] An increase in mass of 14% was observed as humidity was increased from 0 to 90% relative humidity (RH).

4.2.1.2 The initial Pumactant delivery device

Using a hand held syringe, it was impossible to reproducibly depress the plunger with uniform pressure. This problem was addressed by fabricating a spring loaded device to depress the plunger on the CO_2 filled syringe. This device was prepared by inserting a spring into the barrel of a syringe beneath the plunger. The spring was compressed and the plunger held in place by a pin which acted as a catch. This spring loaded syringe was then inverted and butted against the syringe attached to the vial of Pumactant. Removing the pin released the spring loaded plunger which then depressed the CO_2 filled syringe with a constant and reproducible force (figure 4.1).

The CO_2 filled syringe was connected to a CO_2 inlet and an HPLC tube outlet via a three way tap so that the syringe could be charged with CO_2 and used to actuate pumactant without the need to dismantle the apparatus. The HPLC tube outlet fed directly into the pumactant vial. A second piece of HPLC tubing was then used as the outlet. Expelling (actuating) Pumactant generated a widely dispersed plume of hygroscopic lipid. To direct the plume away from the apparatus and thus prevent contamination, an 'actuation hood' was created to shield the dispensing apparatus (see section 2.4.2).

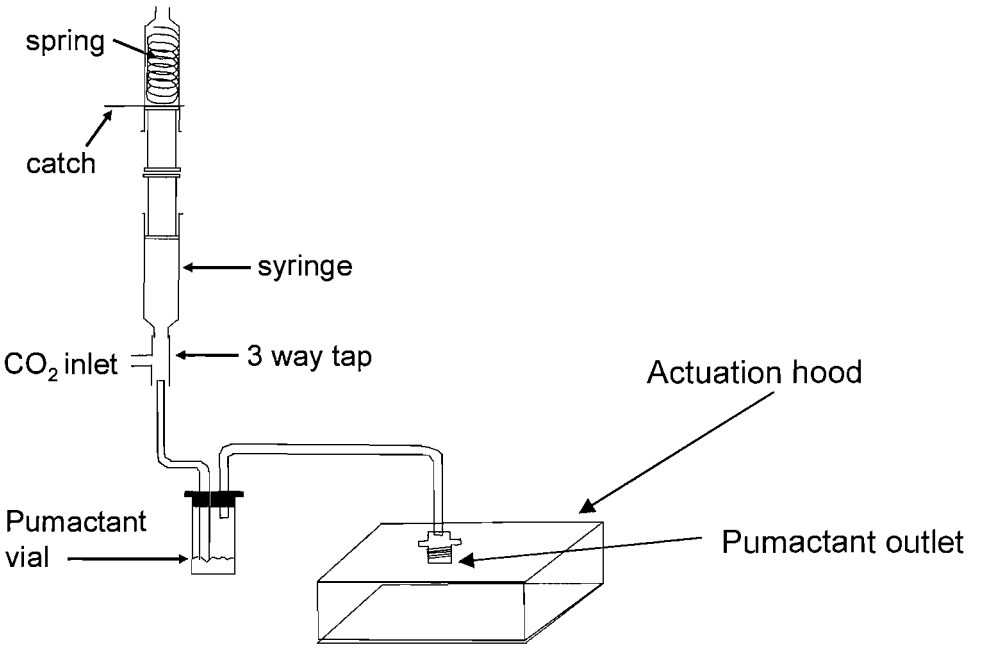

Figure 4.1: Schematic of the initial actuation device used for dispensing Pumactant.

Using this device, Pumactant was actuated using 5ml CO_2. Four sequential actuations were used to dose Pumactant into borosilicate extraction tubes from two Pumactant vials. The quantity of Pumactant actuated was then assayed by ESI-MS/MS.

Actuation No.	Mass delivered/ µg	
	Vial 1	Vial 2
1	171	86
2	429	171
3	414	100
4	71	29
Mean	271 ± 178	96 ± 58

Table 4.3: 4 sequential actuations of Pumactant using the initial actuation device. Results shown are delivered doses (µg) from 4 successive actuations using CO_2 (5ml) from which the mean dose (N=4) ± S.D. has been calculated.

Although this initial device was able to supply uniform pressure with a constant pulse of CO_2 gas, the variability in the quantity of material produced upon each actuation was large (table 4.3). More importantly, the maximum delivered dose upon each actuation

(quantity of material actuated from the device) was two orders of magnitude below the target dose required (section 4.1.3). This limitation was imposed both by the limited capacity of the CO_2 syringe and the limited force that could be applied using the spring loaded firing syringe.

4.2.1.3 An automated actuation device

To overcome the problems described in section 4.2.1.2 above, an 'automated actuation device' was obtained from Britannia pharmaceuticals. This was one of two identical actuation devices commissioned for use in a clinical trial, in which mild asthmatics were administered pumactant prophylactically prior to allergen challenge and had been custom built for this purpose.[9]

The automated actuation device was equipped with an electronically controlled switch that enabled control of the duration of the CO_2 output. The device was also fitted with a needle valve, enabling adjustment of the output CO_2 pressure. A schematic of the principle components of the actuation device are given in figure 4.2:

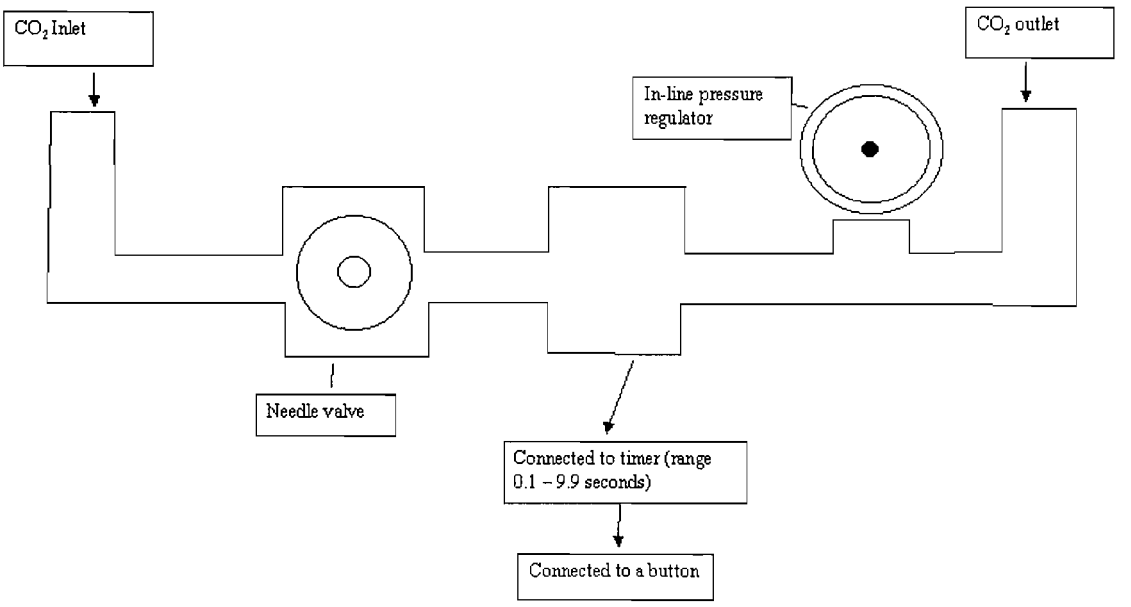

Figure 4.2: Schematic of the automated actuation device. This device is electronically operated and has the capacity for altering both the duration and pressure of the output gas.

With the introduction of the new device, it was possible to actuate the powder for longer periods of time. Whilst experimenting with longer actuation times, it became clear how inconsistent the flow of powder was and that more consistent powder flow could be achieved by manually agitating the Pumactant vial. The problem was caused by the redistribution of the Pumactant powder bed away from the CO_2 inlet pipe making the powder hard to dispense. Agitation of the vial as automated by placing it onto a Corning 4010 multi-tube vortexer (section 2.4.3).

4.2.1.4 The Vibration Powder Aerosol Generator (VPAG)

4.2.1.4.1 Design of the control unit

Although the automated device described above (section 4.2.1.3) functioned well, there was no way of determining the output CO_2 pressure used to expel Pumactant. Furthermore, once the needle valve position had been altered, it was impossible to replicate CO_2 pressures used for previous experiments. Also, the needle valve only enabled crude control of the output pressure.

To resolve these problems and refine the existing device, a new device was conceived following consultation with my industrial supervisor Jim Thompson (Britannia Pharmaceuticals) and was built by SMC pneumatics Ltd (SMC pneumatics Ltd, Milton Keynes, UK) to our design specifications. The device was the first of its kind, incorporating high purity fluoropolymer fittings and tubing. These are ultra-clean grease free components, selected to maintain gas purity to point of use. The device was fitted with a precision adjustable pressure valve and digital display readout to report the output CO_2 pressure (figure 4.3a and 4.3b).

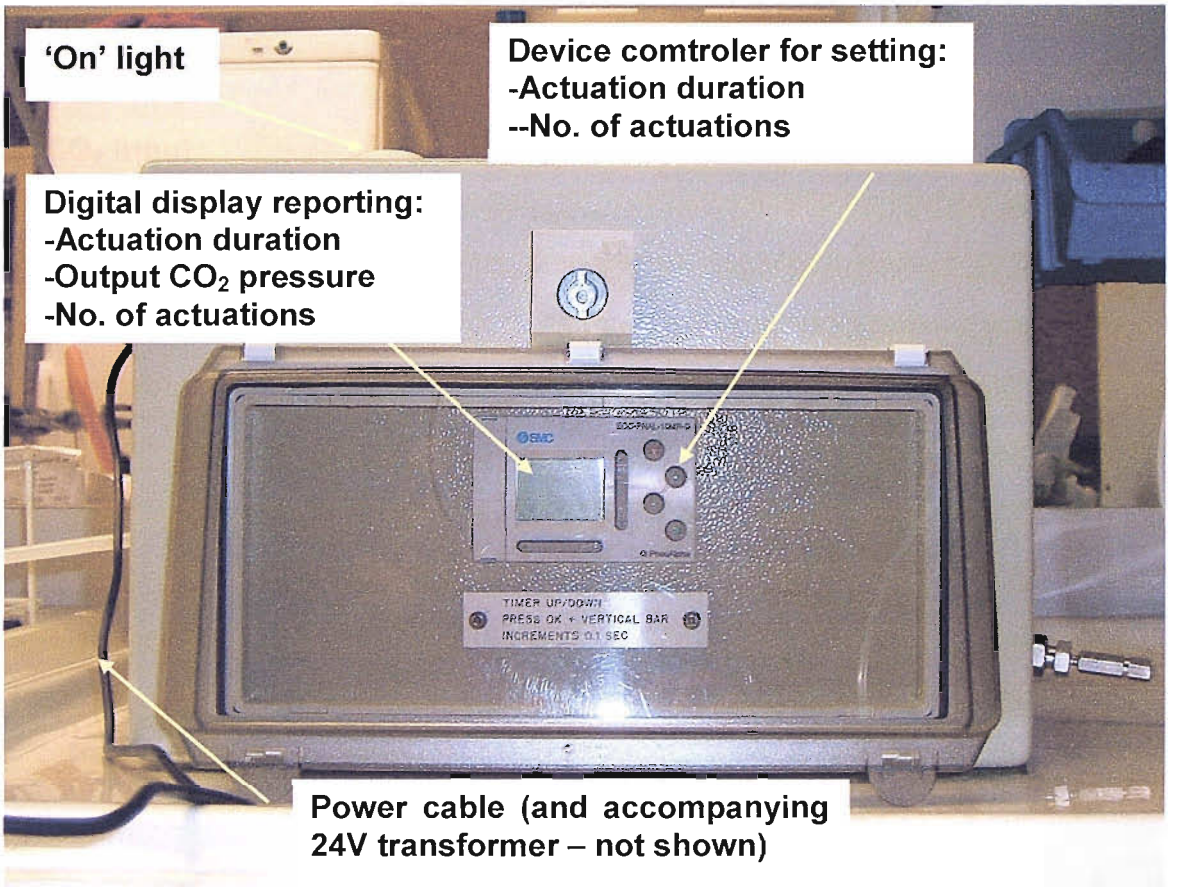

Figure 4.3a: The external workings of the custom built actuation control unit.

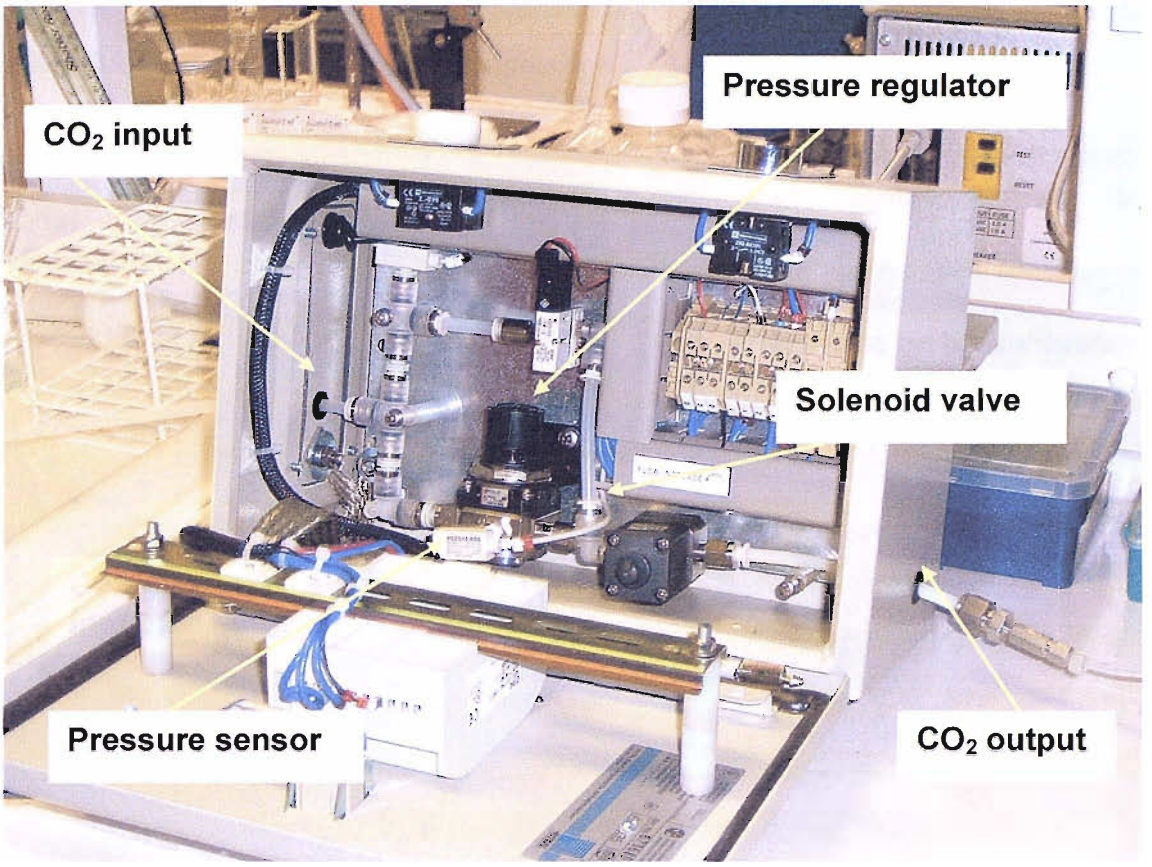

Figure 4.3b: The internal workings of the actuation control unit. Compressed CO_2 (> 3 bar pressure) is fed into the device through the CO_2 input. The output pressure is adjusted using the pressure regulator and pressure recorded by the pressure sensor. The duration of the CO_2 output and number of pulses is controlled by the compressed gas powered solenoid valve.

The device components have a 10 bar burst pressure threshold, however the device is fitted with an internal regulator that limits flow through to 4 bar. The output pressure measured from the device is managed by a manual pressure regulator value fitted with a digital piezoelectric measuring device capable of reading output pressures between 0 and 2 bar in 0.02 bar increments.

4.2.1.4.2 Design of the compress gas powered vibration table

Alongside the actuation control device, a pneumatically driven vibration table was constructed to agitate the powder bed whilst the powder was being dispensed. The vibration table was designed and constructed by a company specialising in fluidising powders using vibration (Vibratechniques, Brighton, UK) according to my design requirements (see section 2.4.4.2 and figure 4.4). The pneumatic vibration table is much less cumbersome than the corning multi-tube vortex mixer (section 4.2.1.3) and

fluidises the powder by agitating vertically at small amplitude, and high frequency (14,000 vibrations per minute at 2 bar pressure).

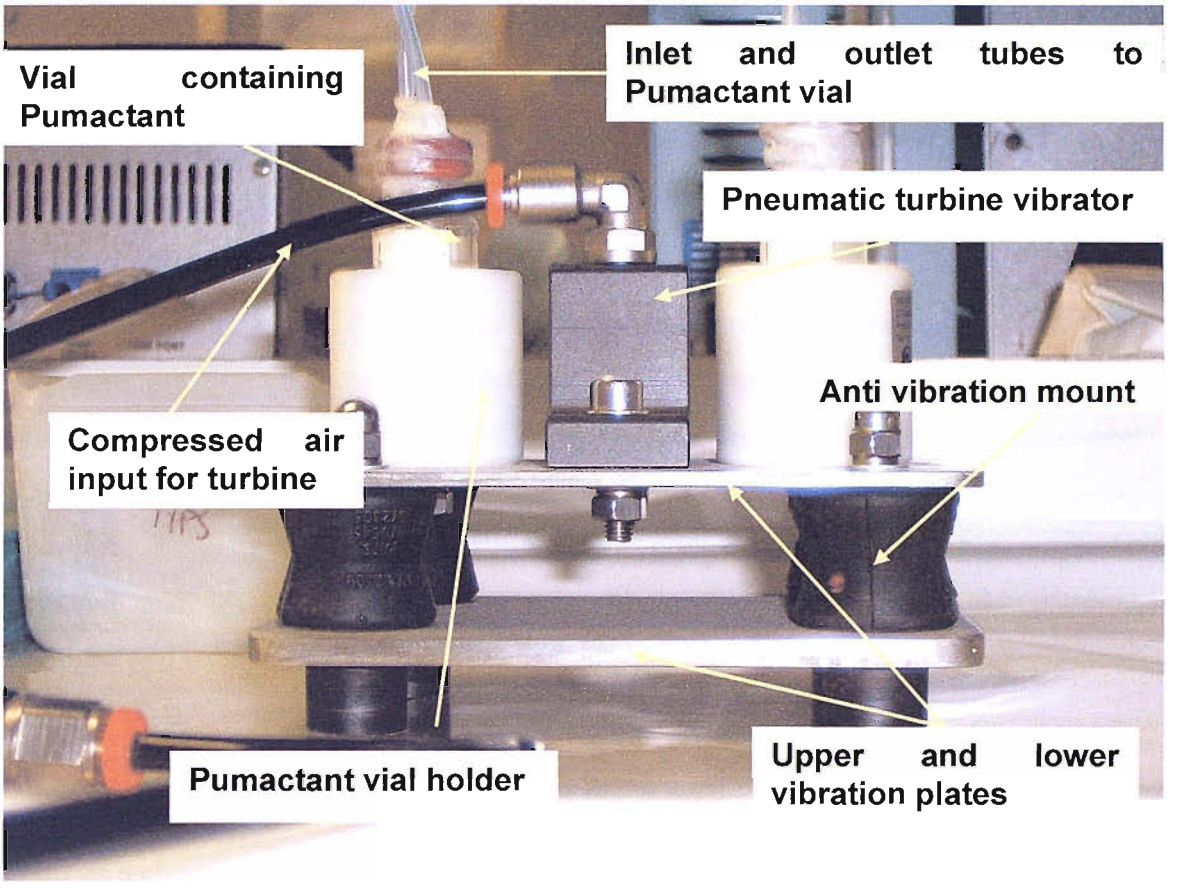

Figure 4.4: The compress gas powered vibration table

The gas propelled vibration table has a number of distinct advantages over the electrical vortex mixer. The vibration table operates by vertical agitation, whereas the Vortexer applies a swirling motion. Agitating the powder particles vertically, gives the particles lift and helps to distribute them evenly in the presence of the gas propellant. In contrast, swirling particles does not aid particle lift as the powder particles do not have much freedom of movement in the horizontal plane. The small amplitude, relatively high motion frequency of the vibration table is also preferable to the vortex mixer, which tended to shake the bench violently. A further advantage of a pneumatically driven vibration unit over an electronically powered device is that the gas powering the vibration table and aerosolising the Pumactant could be derived from the same source. This would be particularly beneficial if the device were to be re-designed as a hand held dispense. The combined actuation unit and vibration table was named the Vibrating

Powder Aerosol Generator (VPAG). A United Kingdom patent application was filed for the VPAG in January 2005 (Patent application no. 0500677.0)[177].

4.2.2 VPAG characterisation

4.2.2.1 VPAG vibration table characterisation using accelerometers

The VPAG is a custom built prototype device, capable of dosing variable quantities of Pumactant powder for a duration ranging from 0.1 seconds upwards, at delivery pressures ranging from 0.02 to 2 bar. The control unit reported the duration and output CO_2 pressures used which could be documented for the reproduction of experimental conditions. Although the pressure of gas used to power the vibration turbine could be measured and therefore documented, the relationship between the gas pressure employed and its significance for Pumactant powder delivery was not known.

The vibration characteristics of the vibration table were determined using two accelerometers (section 2.4.5). An accelerometer is a piezo electric crystal which produces a charge proportional to acceleration. Acceleration, measured in $m.s^{-2}$ provides an indication of the magnitude of the vibration, hence the greater the acceleration, the greater the vibration. The accelerometer was attached to the vibration table using bees wax. Bees wax is used because it is highly adhesive enabling secure but non-permanent fastening of the accelerometer to the device being characterised. The accelerometer needs to be secured as tightly as possible so that it experiences all the vibration characteristics of the device. Similarly, the mass of the accelerometer needs to be small in comparison to the device being measured so that it does not influence the vibration characteristics of the device being assessed.

Initially both accelerometers were attached to the top plate of the vibration table to determine whether the position of the accelerometer affected the vibration response of the table. One accelerometer was placed on top of the GT4 turbine (the vibration source) and the other was placed as close to the vial holder as possible on top of the vibration table. Two acceleration-frequency response curves were generated, one from the accelerometer placed on top of the turbine and one from the accelerometer on the

top plate of the vibration table. The measurement was taken when operating the vibration table using 3 bar driving pressure (see figure 4.5).

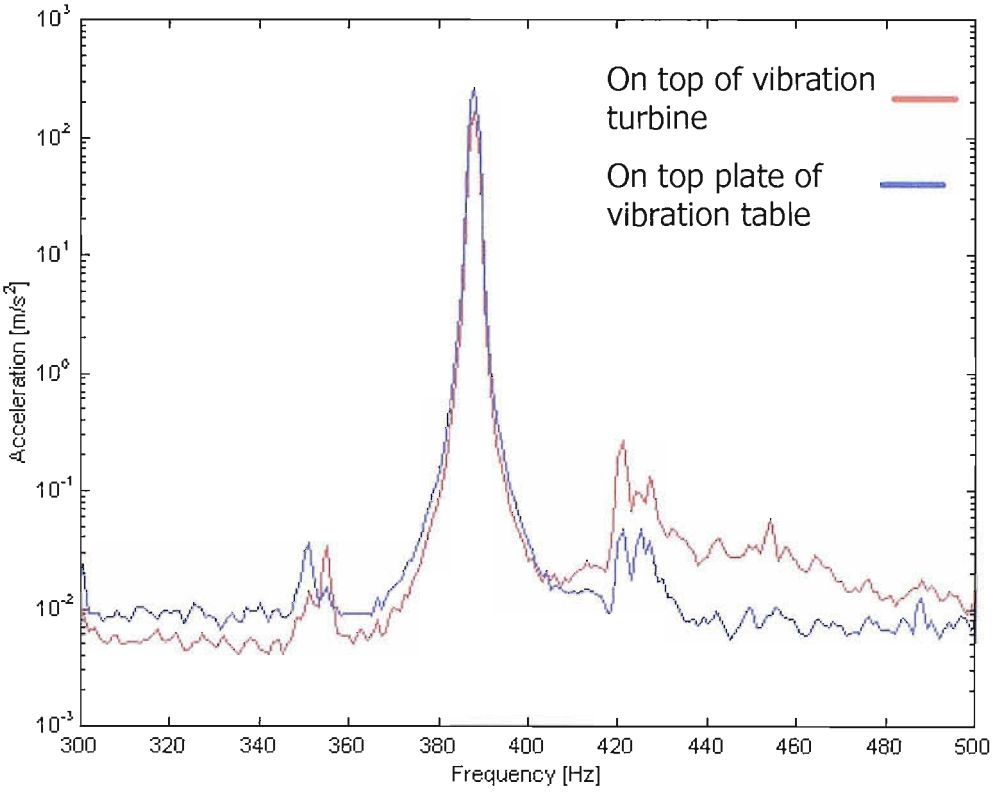

Figure 4.5: Comparative frequency-acceleration responses for an accelerometer attached to the top of the vibration table turbine and one attached to the top plate of the vibration table using 3 bar driving pressure. Results shown are an average of 20 one second measurements.

The frequency spectrum produced a major acceleration peak at 390 Hz. This was labelled the excitation frequency. The excitation frequency for vibration in the proximity of the vial holder was greater than that on top of the vibration unit (275ms^{-2} vs 150ms^{-2} respectively). As it is the vibration characteristics being imposed on the powder which are important, the accelerometer positioned next to the vial was used to determine the vibration characteristics of the top vibration plate of the table. The second accelerometer was placed in the centre of the bottom plate of the table to compare with the upper plate.

Acceleration-frequency spectra were acquired for the top and bottom vibration plates at 0.5, 1, 2, 3 and 4 bar driving pressures. The acceleration-frequency response measured at 1 bar is shown in figure 4.6 as an example.

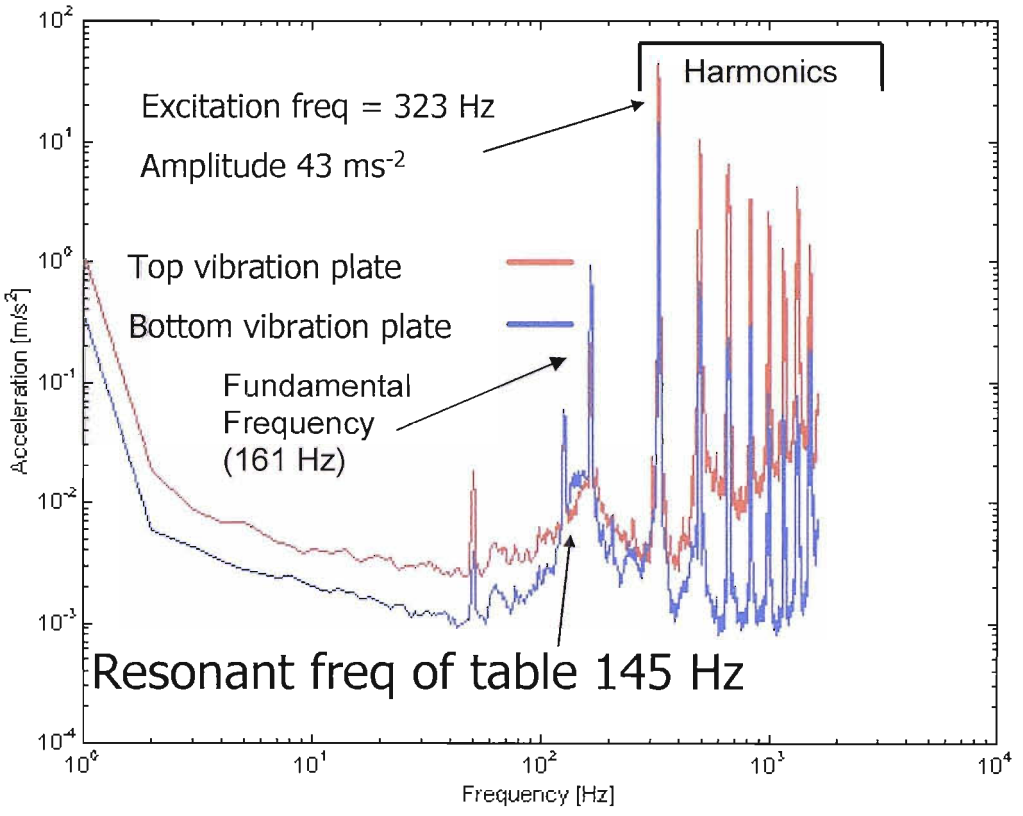

Figure 4.6: Acceleration-vibration spectrum measured at 1 bar driving pressure. Spectrum is an average of 20 x 1 second measurements

The acceleration-frequency response measured at 1 bar pressure revealed a series of vibration harmonics (323Hz, 484Hz, 646Hz etc) of the fundamental frequency at 161Hz and resonant frequency of 145 Hz for the structure.[178] The vibration table produced multiple vibrations across the frequency spectrum. This is not unexpected as the structure consists of multiple component parts. A log linear relationship between excitation frequency and driving gas pressure was observed (figure 4.7).

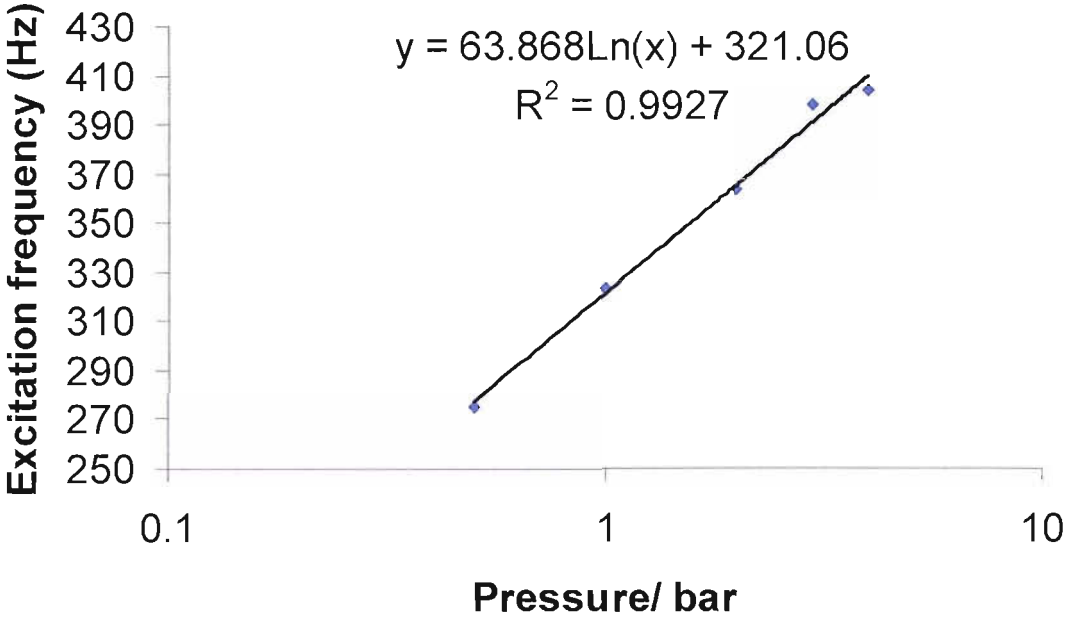

Figure 4.7: VPAG vibration table turbine pressure vs Excitation frequency for vibration pressures of 0.5,1,2,3 and 4 bar. Results = mean excitation frequency from 20 x 1 second measurements.

The maximum excitation frequency of the table exceeded that suggested by the accompanying descriptive literature supplied with the device of 250 Hz at 6 bar pressure.[179] There was also a trend ($r = 0.97$, $P = 0.007$) between the pressure used to drive the turbine and the magnitude of the vibration (figure 4.8).

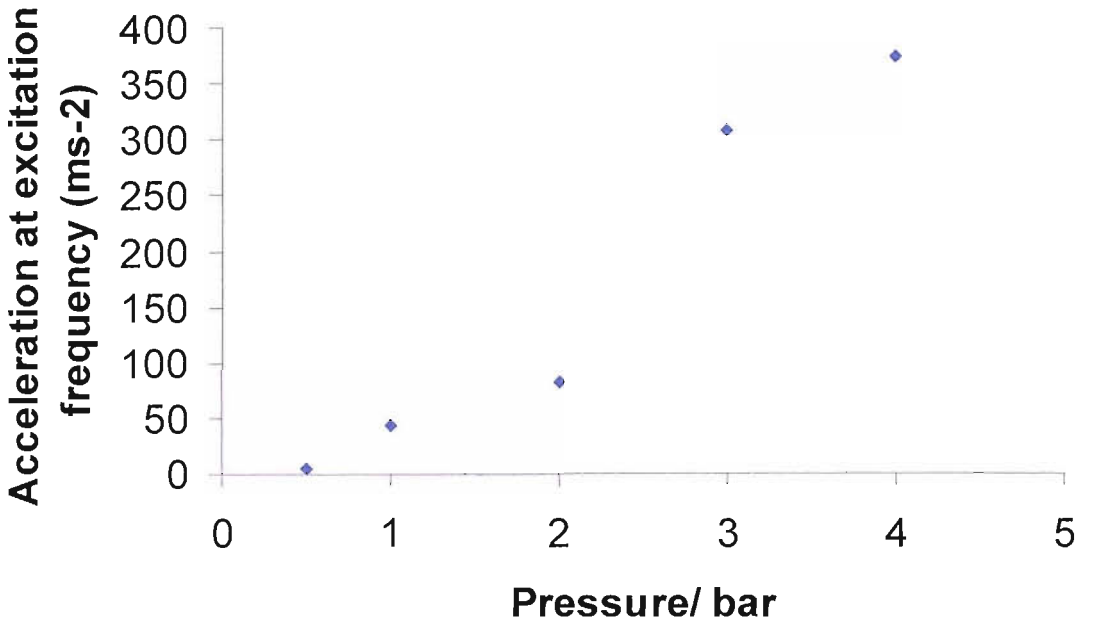

Figure 4.8: Vibration table turbine pressure vs. excitation frequency for vibration pressures at 0.5, 1, 2, 3 and 4 bar. Results = mean acceleration frequency from 20 x 1 second measurements.

Whilst making accelerometer measurements, slight fluctuations in vibration speed were observed. This prolonged acquisition of acceleration measurements because the accelerometer will only measure the steady state. Vibration measurements could not be performed at pressures higher than 4 bar (even though the device components were certified up to 6 bar) because the Pumactant vial would not grip in the vial holder at these vibration speeds. Also, the push-fit connectors used to attach the hosing to the vibration table and regulator had a tendency to leak above 4 bar causing greater fluctuation in the consistency of vibration.

4.2.3 VPAG delivered dose characteristics

Pumactant is prepared as two dry powder formulations. An amorphous powder, (ALEC®), originally designed to be re-suspended in saline and administered to premature intubated babies, and a micronised material. Micronisation involves processing the amorphous powder in a Jet Mill to produce respirable particles (particles of median diameter $\leq$ 5μm.). The aerodynamic size of aerosol particles generated by inhalers is fundamental to drug delivery since only the fine particle fraction (FPF) of approximately $\leq$ 5μm diameter can potentially reach the target surface within the

lung.[168] The therapeutic dose actually available to the patient is therefore only a small proportion of the nominal dose delivered from the device. The delivered dose characteristics of the VPAG were assessed for both the amorphous and the micronised material.

4.2.3.1 Amorphous Pumactant delivered dose characterization

The VPAG is capable of delivering 87 ± 3 mg pumactant from a vial containing 100mg. The majority of the material is dispensed within the first 20 seconds using a delivery gas pressure of 0.8 bar. Non aerosolised material coagulated into a spherical ball at the bottom of the vial. Ideally the VPAG would have been characterised for dosing efficiency according to the different variables (actuation pressure and duration) as well as vial agitation. Unfortunately lack of availability of Pumactant prevented this. The influence of VPAG vial vibration on the delivered dose of Pumactant was investigated as vial agitation exerted the greatest bearing on uniformity of dose as discovered whilst developing the device (section 4.1.2.3). Vials containing amorphous pumactant were accurately weighed then inserted into the VPAG. 5 second actuations were performed using an actuating gas pressure of 1 bar and vibration table driving pressures from 0 to 4 bar (see section 2.4.6.1). Pumactant vials were subsequently re-weighed and delivered dose was calculated by mass difference. Vial excitation frequencies corresponding to each of the vibration table driving pressures section 4.2.2.1 (figure 4.7) were plotted as a function of delivered dose (see figure 4.9).

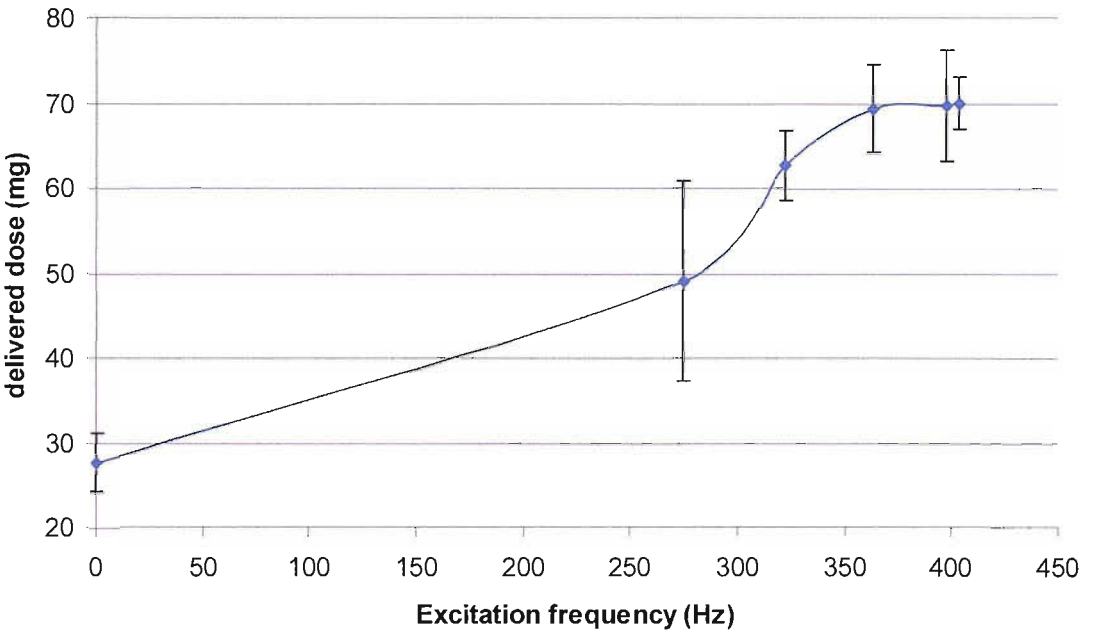

Figure 4.9: Effect of VPAG vial excitation frequency on the amorphous Pumactant delivered dose from 5 second actuations carried out using an actuation pressure of 1 bar. Results = mean (N = 3) ± S.D.

Delivered dose is tending towards a maximum by 364 Hz excitation frequency (corresponding to 2 bar vibration table driving pressure).

The relationship between delivered dose and vial acceleration corresponding to each of the vibration table driving pressures (as determined experimentally, figure 4.8) is shown in figure 4.10.

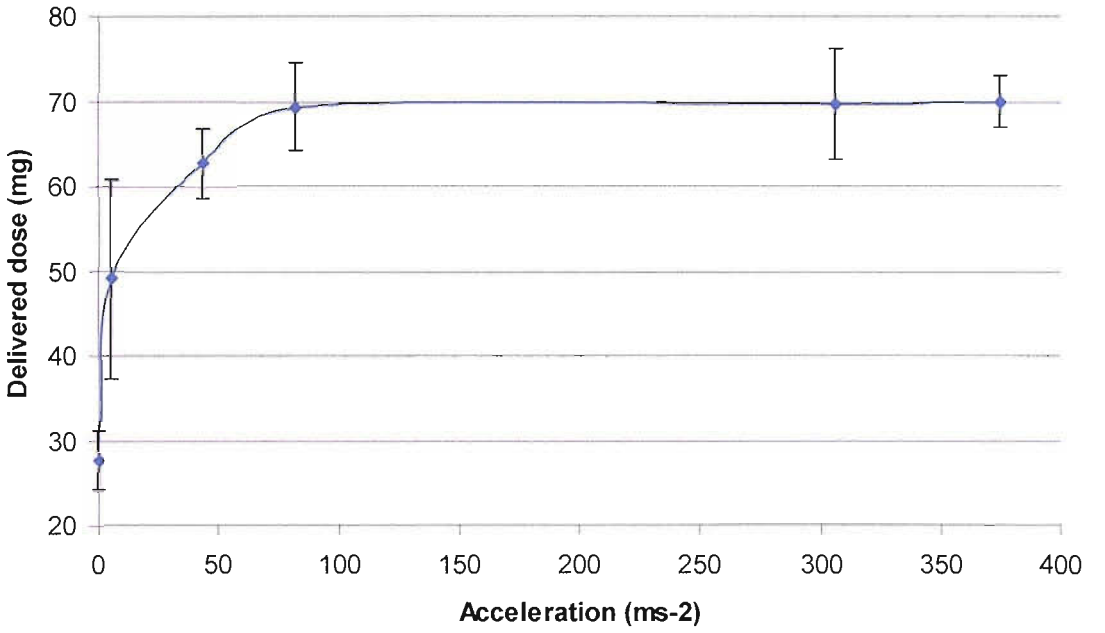

Figure 4.10: Effect of the magnitude of vial vibration on amorphous Pumactant delivered dose for 5 second actuations carried out using an actuation pressure of 1 bar. Results = mean (N = 3) ± S.D.

The maximum delivered dose was reached by the equivalent of 2 bar vial vibration frequency (364 Hz excitation frequency, 82ms^{-2} acceleration).

4.2.3.2 Micronised Pumactant delivered dose characterization

Three vials of freshly prepared micronised Pumactant were supplied (Britannia Pharmaceuticals) (containing 100,125 and 150mg respectively) to test the feasibility of the VPAG for dosing the respirable material. Delivered dose was determined gravimetrically by mass difference before and after a 10 second actuation from each vial (see figure 4.11). The actuation time was chosen so that it could be compared to the duration reported for the handheld PADD device (section 1.9.4) designed for dosing respiratory grade (micronised) Pumactant.[180] Optimal vial vibration pressure (2 bar) and maximum actuation pressure (2 bar), determined from experiments carried out on amorphous Pumactant (section 4.2.3.1) were selected to obtain the highest possible delivery from the device (see section 2.4.6.2).

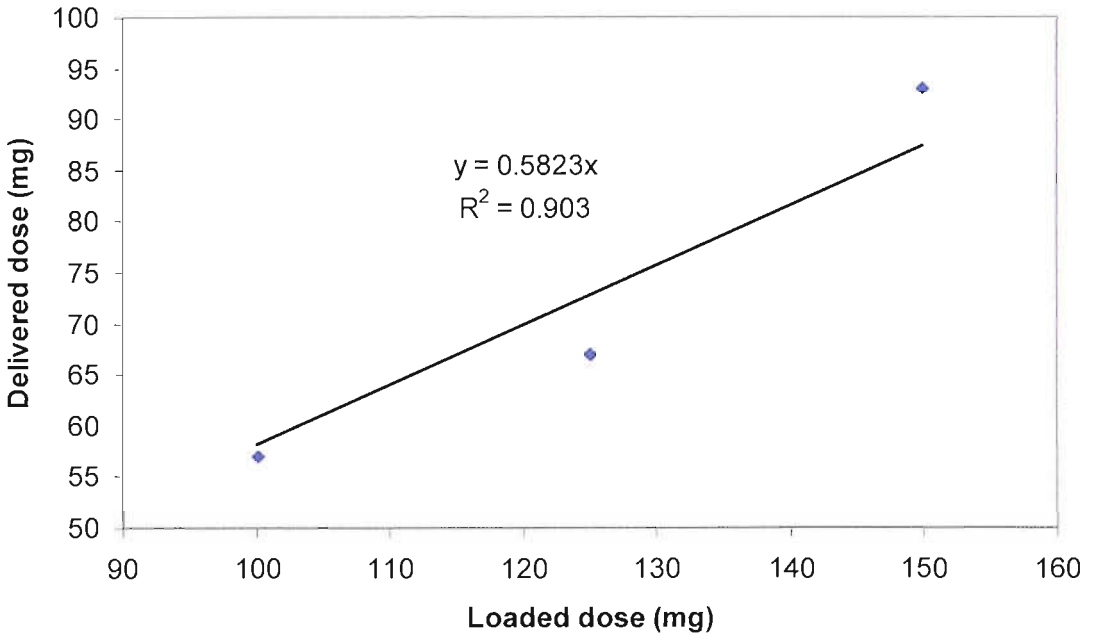

Figure 4.11: Relationship between loaded dose and delivered dose for 3 vials of micronised Pumactant using a 2 bar vial vibration pressure, a 1 bar actuation pressure and a 10 second actuation time. Gradient of the line represents the delivered dose efficiency (58.2%).

The gradient of the line of best fit was calculated to determine the proportion of the loaded dose which was delivered (actuated) by the VPAG. Although this data is preliminary (due to lack of available samples), delivered dose efficiency was observed at approximately 58%. Although dose efficiency for the hand held PADD delivery device, was rated at 70% device it required 10 times the actuation pressure.[103] Experiments on the PADD device were also carried out in a purpose built pharmaceutics laboratory with environmental control (45% RH), where-as the VPAG delivered dose experiments were carried out at higher ambient humidity (60% RH) which could have impaired particle aerosolisation.

4.2.3.3 Aerosolisation characterization of amorphous Pumactant when actuated using the VPAG

In addition to uniformity of delivered dose, the fine particle characteristics of aerosol clouds generated by inhalers must be established in vitro in line with regulatory guidance and pharmacopoeial requirements and procedures.[181] Particle size distribution of the amorphous Pumactant was carried out by laser light scattering (Mastersizer X,

Malvern UK). A suspension of amorphous Pumactant was prepared in cyclohexane which was sonicated to de-aggregate the powder and poured into a liquid flow cell (section 2.4.7.1). The particle size distribution is shown in figure 4.12

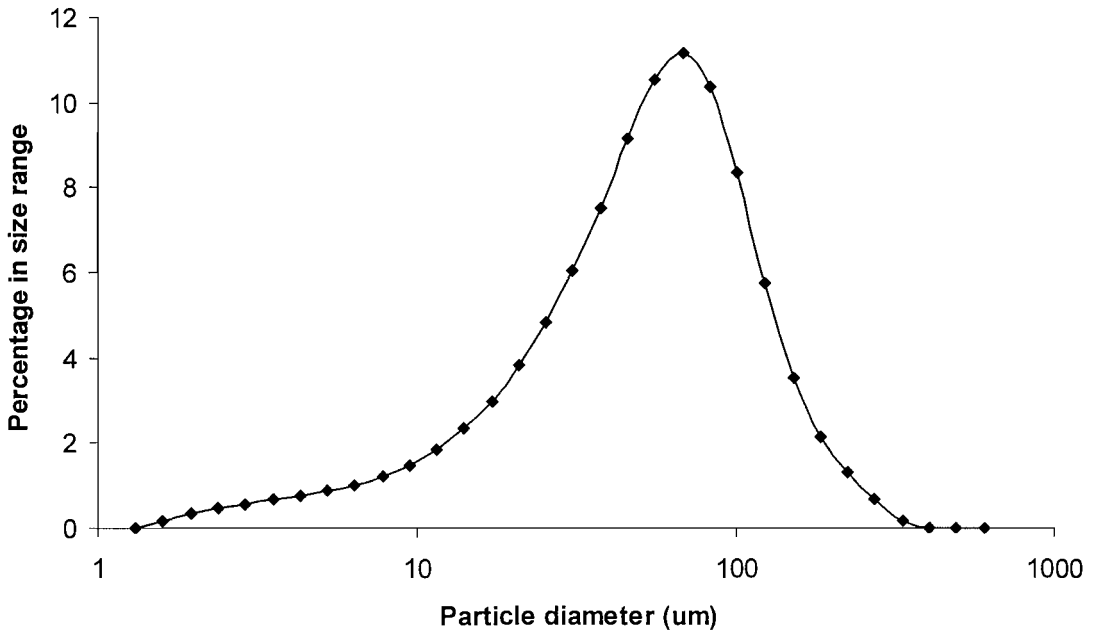

Figure 4.12: Particle size distribution of non micronised 'amorphous' Pumactant suspension in cyclohexane. Median particle size = 49.9 ± 2.9 µm. N=3 ± S.D.

Amorphous Pumactant has a median particle size of approximately 50µm (ten times larger than the size required for respiration). The liquid cell on the Malvern particle sizer was then replaced with a dry flow cell which was attached to a suction device. Pumactant was then actuated into the dry flow cell using the VPAG (section 2.4.7.1 and figure 4.13).

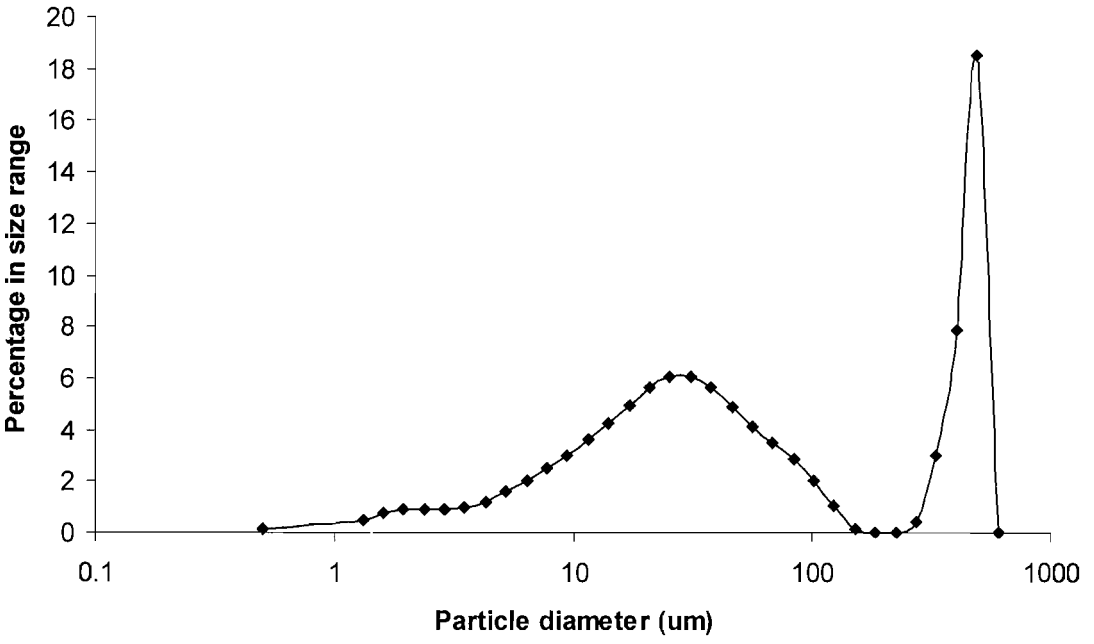

Figure 4.13: Particle size distribution for amorphous Pumactant actuated for 30 seconds, with the VPAG using a 1 bar Actuation pressure and 2 bar vial vibration pressure. Median particle size = 43.3 µm

The median particle size for Pumactant emitted from the VPAG (figure 4.13) resembled that of the pre-sonicated suspension (43.3µm vs. 49.9µm respectively) suggesting that the VPAG successfully de-aggregated the material upon aerosolisation. Some of the aerosolised material was emitted as aggregates (denoted by the dominant peak at particle diameter 492µm). Comparison of the particle size distribution generated by the VPAG (4.13) with that produced by introducing amorphous Pumactant to the flow cell with a spatula (figure 4.14) revealed comparative particle size distributions.

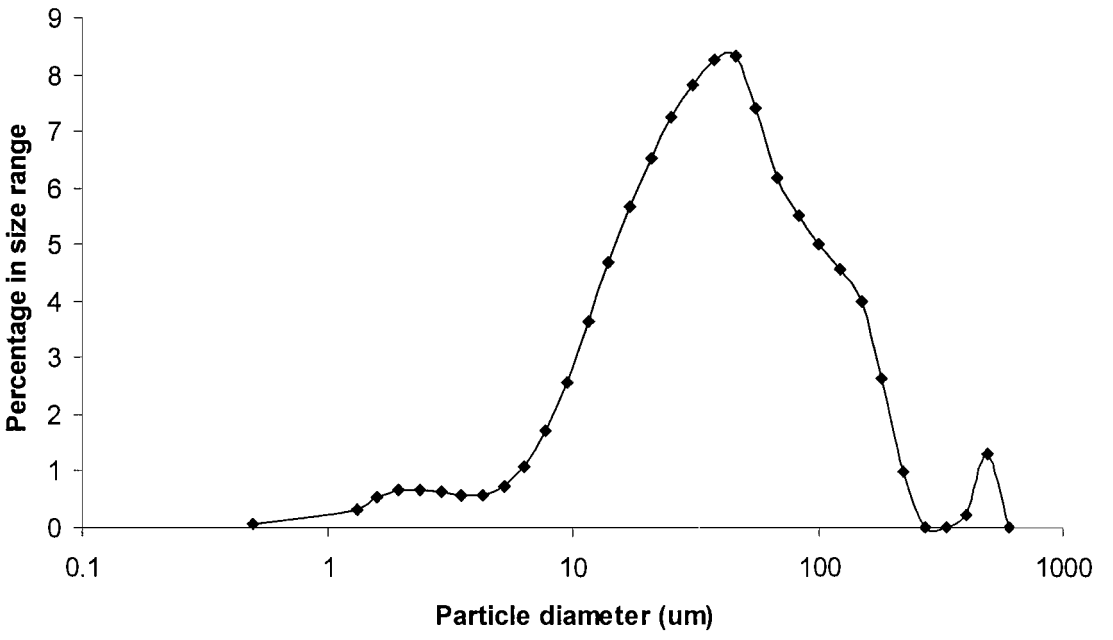

Figure 4.14: Particle size distribution of amorphous Pumactant added by spatula. Median particle size = 41.96 µm

The similarity in particle size distribution revealed that the amorphous Pumactant was being de-aggregated as a result of suction through the flow cell. As a result it is impossible to distinguish any de-aggregation capacity of the VPAG from that already occurring as a result of suction through the flow cell. Particle size characterisation for the VPAG could therefore not be determined using this technique.

4.3 Discussion

The increase in knowledge of the importance of lung surfactant in various diseases will have a more significant impact if surfactant therapy can be delivered in a non invasive manner, both because it will become more widely applicable and also because the method used to deliver surfactant can influence the patient's response to the therapy.

Several studies have shown that the fine particle dose is correlated with the quantity of drug deposited in the lung[182,183]. However, the relationship between clinical efficacy and fine particle dose (FPD) is still in question. Studies by Melchor et al in 1993[184] showed that differences in lung deposition of radiolabelled salbutamol did not result in differences in bronchodilation. Furthermore, studies by Fishwick et al[185] revealed that dose-response curves of 50+50+100+200µg salbutamol did not differ from the

100+100+200+400μg. Since increasing the dose is equivalent to increasing the FPD, these findings also indicate that there is no difference in bronchodilator effect between high and low amounts of salbutamol deposited in the lung. These results were further corroborated by Weda et al[186] that showed no difference in clinical efficacy of salbutamol preparations with a low or high FPD within the doses currently used in practice. These findings could proffer an explanation as to why dry powder lipid administered by Morley et al in 1981[101] to premature neonates via endotracheal tube resulted in a significant clinical improvement relative to control, despite the fact that the material used was of particle size 100μm and the size of neonatal airways significantly smaller than that of an adult. Despite this, it is suggested that the material is able to move down the bronchial tree either as particles or by surface adsorption/ spreading to a great enough extent as to facilitate clinical improvement.

Another consideration of importance regarding dry powder delivery is the affects of humidity on dry powder particles entering the lung. This is of particular significance with regards to Pumactant because it has such high affinity to moisture.[103] Work carried out on the effects of humidity on aerosols delivered by pMDI's to intubated patients, demonstrated a reduction in the fraction of particles reaching the lung[187,188] Reductions of 40 to 50% in lung deposition have been reported with *in vitro* adult models[189,190] where-as reductions of up to 85% have been found in paediatric models[191,192] when normal ventilator conditions (35 to 37°C and 90% RH) were compared with dry ambient conditions (25 to 27°C and ≤ 10% RH). The most common explanation for the drop in dose delivery in heated and humidified ventilator circuits suggests that hygroscopic growth of the pMDI particles occurs in the humid air flow and results in increased deposition by impaction in the spacer and ETT.[191,193] However, this suggestion does not explain why non hygroscopic drugs such as salbutamol used in chlorofluorocarbon (CFC) pMDI's suffer from the same problem of reduced delivery.

The VPAG was originally designed to dose varying quantities of amorphous Pumactant for the purpose of characterising Pumactant interactions at air-liquid interfaces *in vitro*. At the commencement of this project, lack of availability of respirable material meant that there was none available for experimentation in the laboratory. Initial attempts to deliver micronised material using the VPAG were unsuccessful, however this was later discovered to be due to the age of the material used, when freshly prepared micronised material was successful delivered (section 4.2.3.2). The VPAG is one of only three

devices yet to have been reported, capable of high dosing of hygroscopic powders. The first of these was developed for a clinical trial in which mild asthmatics were administered high prophylactic dose of Pumactant prior to bronchial provocation[9] and the second being the PADD[103] (see section 1.9.4). The VPAG possesses unique versatility in being able to produce either single or multiple pumactant doses for any specified duration at low actuation gas pressures. The flexibility of the device combined with the active generation of powder aerosol means that it can be readily adapted to suit individual patient needs.

The reproducible and automated actuation control of the VPAG make it ideally suited to integration with a ventilator circuit, such that actuation of the powder could be timed to coincide with the respirable air generated by the ventilator circuit. Where the VPAG is attached to an ET tube, respirable particles are not required as the material is being delivered directly to the airways. Moreover the capacity of the VPAG to deliver respirable particles, increases its versatility as a dry powder inhalation device.

Chapter 5
The study of Pumactant at air/liquid interfaces

5.1 Introduction

Absence or dysfunction of lung surfactant results in clinically important respiratory complications in both pre-term infants (NRDS)[1] and adults (ARDS)[43]. In the past twenty years administration of human or animal derived surfactants has proven effective in treating NRDS, but the potential of contamination and/or adverse immunological response to natural surfactant has shifted the interest of researchers towards the development of synthetic analogues.[194,195,196]

The rational design of synthetic surfactant therapies requires an understanding of the mechanism of action of natural lung surfactant (LS) as well as some appreciation of the interaction between components of the exogenous and impaired endogenous material.

Because lung surfactant is isolated from the moist surface of the lungs, it was long assumed to be in the form of a suspension. However, in 1978 Morley et al[102] reported that it spread best as an active surface layer when the surfactant source was dry particles added to surface rather than adsorbed from a suspension. It had also been postulated that the surfactant containing lamellar bodies (section 1.4.2) are functionally dry surfactant particles, an idea that was substantiated by Ikegami et al[197], who showed that natural surfactant improves lung compliance when given as a suspension but not when particles are fully equilibrated with water (i.e. destroyed by sonication). Following up on these ideas, Grathwohl et al[198], showed that the lamellar bodies are packages of phospholipids and free protein but lack hydration.

Nevertheless, Fujiwara et al[41] demonstrated a dramatic improvement in symptoms of infants suffering from NRDS using exogenous lung surfactant prepared from a chloroform-methanol extract of bovine lung surfactant (surfactant TA) and administered intratracheally as a suspension. However, Morley and co workers felt that such a preparation was unacceptable due to its foreign protein content and the large volume of fluid that has to be poured into the trachea.[101] They therefore developed a synthetic, protein-free surfactant[199] which consists of a simple mixture of the two major phospholipids normally present in lung surfactant. The formulation, as prescribed for the treatment of NRDS became known as ALEC (Artificial Lung Expanding Compound).

The critical micellar concentration (CMC) of DPPC (the principle LS phospholipid) is low ($\leq 10^{-10}$M).[200] As such, the much preferred environment for a single DPPC molecule in water is in association with other lipid molecules. The aggregates which result were termed liposomes (or smectic mesophases) because of the hydrophobic lipid component of the molecule. A liposome[201] is characterised by alternating bimolecular sheets of lipid separated by aqueous spaces, whereby each lipid sheet forms a closed membrane system and where all the hydrocarbon chains are shielded from water by the polar head-group region. It is unlikely that this material, in a fully hydrated state, could facilitate a rapid extension of an air/fluid interface by donating surface active molecules upon inspiration.

This hypothesis was supported by experiments by Morely et al[102] which demonstrated improved surface tension lowering properties of dry surfactant compared to equivalent amounts of 'hydrated' surfactant extract on a Wilhelmy surface tension balance. In 1981, Morley et al[101] went on to demonstrate that the application of this phospholipid material as a dry powder was effective in the treatment of NRDS.

It was this rationale which prompted efficacy testing of Pumactant dry powder in airways disease following withdrawal of ALEC from the NRDS treatment market as a direct result of damaging clinical trial results[80]. A small scale clinical trial was established, involving prophylactic administration of dry powder ALEC (called Pumactant) to people with mild asthma prior to allergen challenge. Administration of this material lead to abolishment of the early phase asthmatic response.[9] This outcome provided the first evidence in vivo that surfactant may contribute to the early asthmatic response to allergen and demonstrated the use of an exogenous lipid based surfactant, which contains no surfactant proteins, in controlling symptoms in allergen-induced asthma.

Despite this very encouraging outcome,[9] little is known about the mechanisms responsible for this clinical effect, as the interactions between dry powder lipids and endogenous LS in either in health or disease, have rarely been studied. The main aim of the work described in this chapter was therefore to elucidate and evaluate the physical interactions between endogenous and exogenous surfactant components in order to further understand the therapeutic action of this material.

5.1.1 The Wilhelmy Surface Tension Balance

Experiments on the surface activity of Pumactant delivered as a dry powder were initially carried out using a Wilhelmy surface tension balance, the basic principles of which are described in section 1.5.4.1. In the Wilhelmy-Langmuir method, interfacial surface properties of samples being evaluated are determined by preparing liquid suspensions. The surface of the liquid is then refined by repeatedly compressing and expanding the surface from 100% to 20% of its original area using a Teflon barrier. Surface area cycling is continued until equilibrium is achieved. Equilibrium, as determined by the Wilhelmy balance, occurs when two consecutive surface area/ surface tension profiles differ by less than 3 per cent. Throughout this process, changes in surface tension are measured by the change in pull on a platinum plate which is dipped into the liquid. Repeated compression and expansion of surfactant films present at the air-liquid interface on the trough result in the production of a surface area/tension hysteresis curve. Typical examples of such curves, for well and poorly functioning surfactant are shown in figure 5.1. The compression cycle is denoted by the lower curve and the expansion cycle by the upper curve. The fact that there is a difference between them (blue shaded area) is due to hysteresis. Hysteresis maybe defined as a 'retardation in the effect when the forces acting on a body are changed' (as if from viscosity or internal friction).

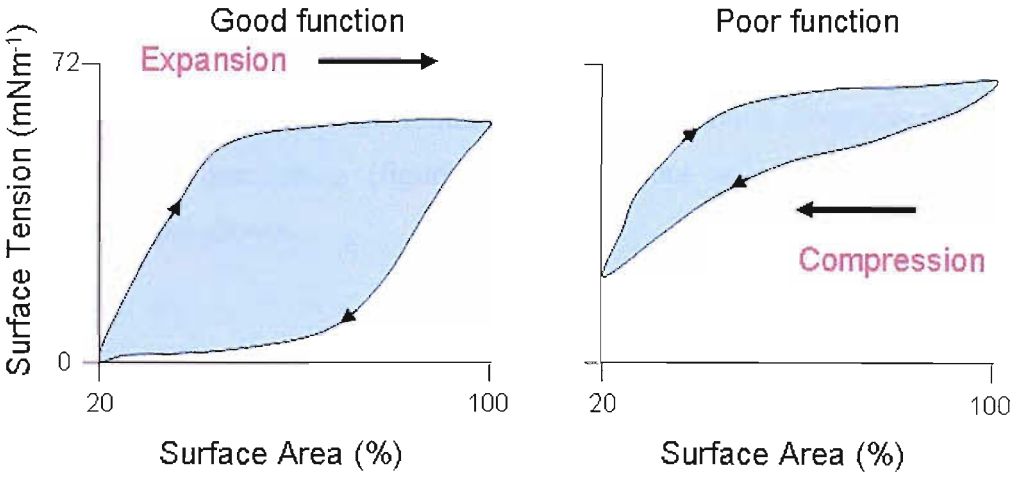

Figure 5.1: Schematic of typical surface tension/ surface area hysteresis curves for both good and poor functioning surfactant

Well functioning surfactant is characterised by a high rate of decrease in surface tension, with decreasing surface area on compression and a low minimum surface tension on maximum compression. Conversely, poorly functioning surfactant is characterised by a low rate of decrease of surface tension with decreasing surface area and a comparatively high minimum surface tension at maximum compression (figure 5.1).

5.1.2 The capillary surfactometer

The second technique used to evaluate the interactions between Pumactant and LS is Capillary Surfactometry. Capillary Surfactometry offers a quantitative, high throughput method for assessing the ability of LS to maintain the patency of terminal airways. A detailed description of the capillary surfactometer components and their function is given in section 1.5.4.2. Briefly, 0.5 µl of material to be analysed is introduced into the narrow section of a capillary which is attached to a bellows and pressure transducer at one end and open to the atmosphere at the other. As soon as the sample is introduced to the capillary, it forms a meniscus blocking the capillary.

Evaluation of the sample is determined by measuring the back pressure recorded by the pressure transducer, caused by the sample meniscus over a two minute time period. For well functioning surfactants, the liquid sample is prevented from returning to the narrow section of the capillary once expelled by the initial pressure. For samples containing poorly functioning surfactant, the liquid meniscus returns blocking the tube and resulting in a recurring pressure build up. This repeats for the duration of the measurement resulting in a 'saw-tooth' pressure time readout. Examples of poor (figure 5.2a) and well functioning (figure 5.2b) surfactant as characterised by capillary surfactometry are shown.

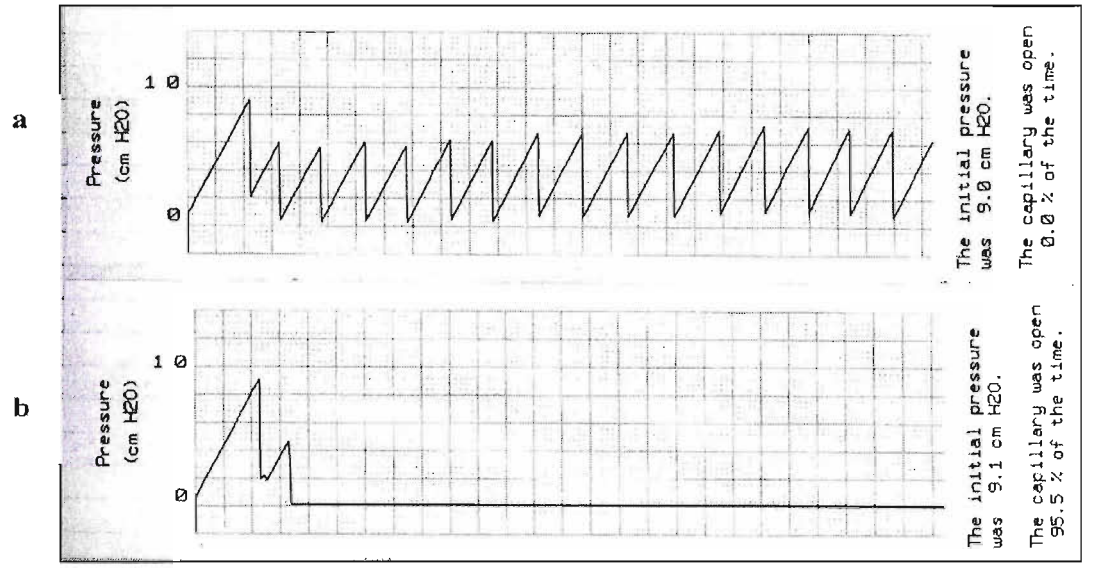

Figure 5.2: Examples of a) poorly functioning and b) well functioning surfactant measured by capillary surfactometry

5.2 Methods

The precise experimental protocols for the experiments carried out on the Wilhelmy balance and CS are described in sections 2.6 and 2.8 respectively. Therefore, only a brief overview of the experiments will be given here along with a rationale for their design.

5.2.1 Wilhelmy balance measurements

Pumactant interactions at the air-liquid interface were initially studied using a Biegler Electronic Wilhelmy-Tensiometer surface tension balance. The VPAG dry powder administration device (see section 4.2.1.4) was used to deposit aerosolised pumactant onto a saline sub phase (80ml, 37°C). The lipid which adsorbed to the sub phase surface was then refined through surface compression and expansion (100-20% of surface area) by the Teflon barrier. Changes in surface tension were measured using a platinum plate and the surface tension vs. surface area profile displayed on an LCD screen. Refinement of the air/liquid interface was continued until an equilibrium ST vs. surface area profile was achieved (i.e. when two consecutive surface tension/area profiles differed by less than 3 percent). Once an equilibrium ST profile was achieved, the Wilhelmy balance produced a printout which reports the equilibrium surface tension profile. The cycle

number at which equilibrium was reached, the area under the hysteresis curve and the surface tensions at both minimum surface compression (100% surface area, γ_{max}) and maximum surface compression (20% surface area, γ_{min}) were also reported numerically on the printout (see figure 5.4). Because it is not feasible to determine the quantity of phospholipid at the air-liquid interface of the trough, the concentration of lipid in the sub phase was used as a surrogate marker of Pumactant present at the interface. Experimentally, this was achieved by performing a Bligh and Dyer total lipid extraction on aliquots of the sub phase and assaying for DPPC by mass spectrometry (see section 2.6.1).

5.2.2 Capillary surfactometer measurements

Capillary patency measurements on the surfactometer require the presence of a liquid meniscus (0.5µl). To determine the surface activity of Pumactant dry powder, Pumactant was first actuated into one end of the capillary. Saline (0.5µl) was then added and capillary patency measured (section 2.8.2). For all other capillary surfactometer measurements, samples to be analysed were already present as liquid suspensions. All measurements were carried out in triplicate.

5.3 Results

The experiments described in this chapter are separated into two parts. The first part details characterisation of Pumactant at the air/liquid interface, measured on a Wilhelmy surface tension balance. The second describes Pumactant characterisation by Capillary Surfactometry.

5.3.1 Evaluation of Pumactant at the air/liquid interface using a Wilhelmy balance

5.3.1.1 Dry powder versus saline suspension

5.3.1.1.1 Characterisation of dry powder pumactant

Before any measurements could be made, the problem of how to direct material from the nozzle of the VPAG onto the sub phase surface of the Wilhelmy trough needed to be addressed. *In vivo*, dry powders and aerosols are channelled into the airways by suction through inhalation. However, emulating this mechanism in *vitro* was considered too complex. Also, applying suction to the system in the vicinity of the actuation nozzle would only serve to draw the powder away from the sub phase surface towards the suction device.

The alternative chosen was to manufacture an 'actuation hood' which would fit onto the Wilhelmy trough, to which the actuating nozzle could be attached. This helped to contain the bulk of the powder once dispersed from the nozzle. The hood also helped to reduce possible lipid contamination of the other components of the balance. Once the balance had been calibrated and background surface tension acquired, the actuation hood was applied and Pumactant actuated, after which the hood was removed and surface area cycling recommenced. The actuation hood alone and attached to the Wilhelmy trough are shown in figure 5.3.

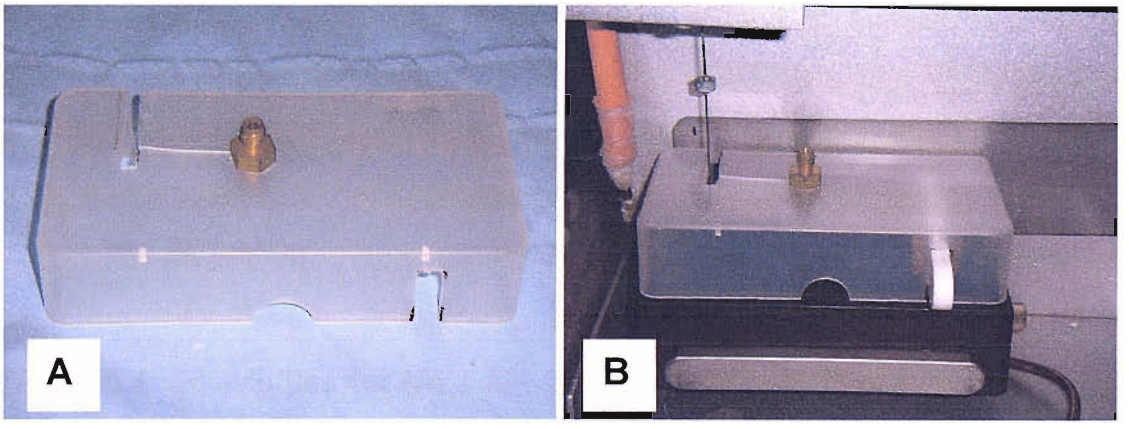

Figure 5.3: The actuation hood (A) and the actuation hood attached to the Wilhelmy trough (B)

The hood was designed so it could be applied and removed quickly and easily, nevertheless much care was needed so as not to disturb the calibrated balance which was very sensitive to any movement. All measurements were carried out using a sub phase temperature of 37°C and ambient laboratory conditions. The balance was calibrated and baseline surface tension measured using a saline sub phase (section 2.6.1). The actuation hood was subsequently attached to the surface of the Wilhelmy trough taking care not to disturn the platinum dipping plate (figure 5.3B). Pumactant was subsequently actuated onto the sub phase using the VPAG for 2 seconds using an actuation pressure of 1 bar and a vial vibration pressure of 2 bar (see section 2.6.1.1). The humidity hood was removed and surface area cycling commenced. Once equilibrium surface tension was achieved, three 800µl aliquots of the sub phase were isolated, lipid extracted and quantified for DPPC content by mass spectrometry. The balance was then cleaned (as described in section 2.6.1) and the experiment repeated. A total of four experiments were carried out. A fresh vial of pumactant was used for each experiment Absolute quantities of Pumactant phospholipid in the sub phase following dry powder application ranged from 3.3 ± 0.5mg to 10.5 ± 3 mg (N=3). Example surface tension profiles are shown for a saline sub phase, and following application of Pumactant dry powder in figure 5.4.

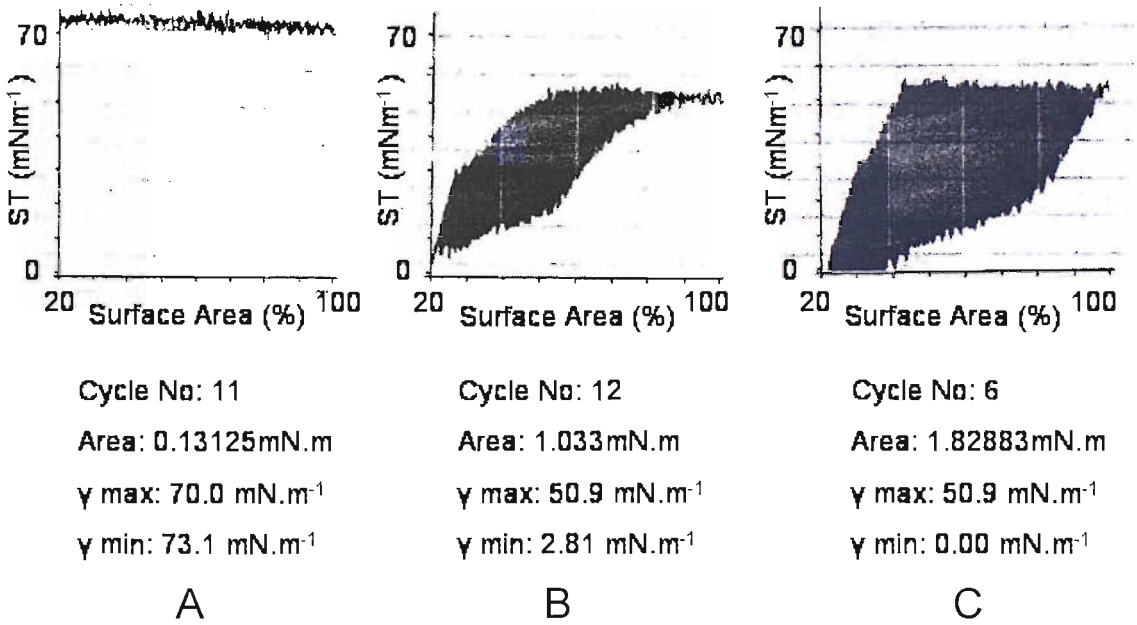

Figure 5.4: ST profiles for (A) a saline sub phase (pumactant free control), and (B & C) following application of dry powder Pumactant to the sub phase surface using the VPAG. Actuations were carried out for 2 seconds using 1 bar actuation pressure and 2 bar vial vibration pressure.

5.3.1.1.2 Characterisation of Pumactant suspensions

To compare the two modes of application, surface tension measurements were carried out on Pumactant suspensions prepared in the saline sub phase containing 10.5mg Pumactant phospholipid (see section 2.6.1.2). Baseline surface tension was recorded on a saline sub phase, after which saline (10.5 ml) was removed by pipette and replaced with 10.5 ml of a stock (1 $mg.ml^{-1}$) suspension. Surface area cycling was then carried out until equilibrium was reached. The experiment was carried out twice. Example equilibrium surface tension profiles for a saline sub phase (pumactant free control) and saline suspensions are shown in figure 5.5.

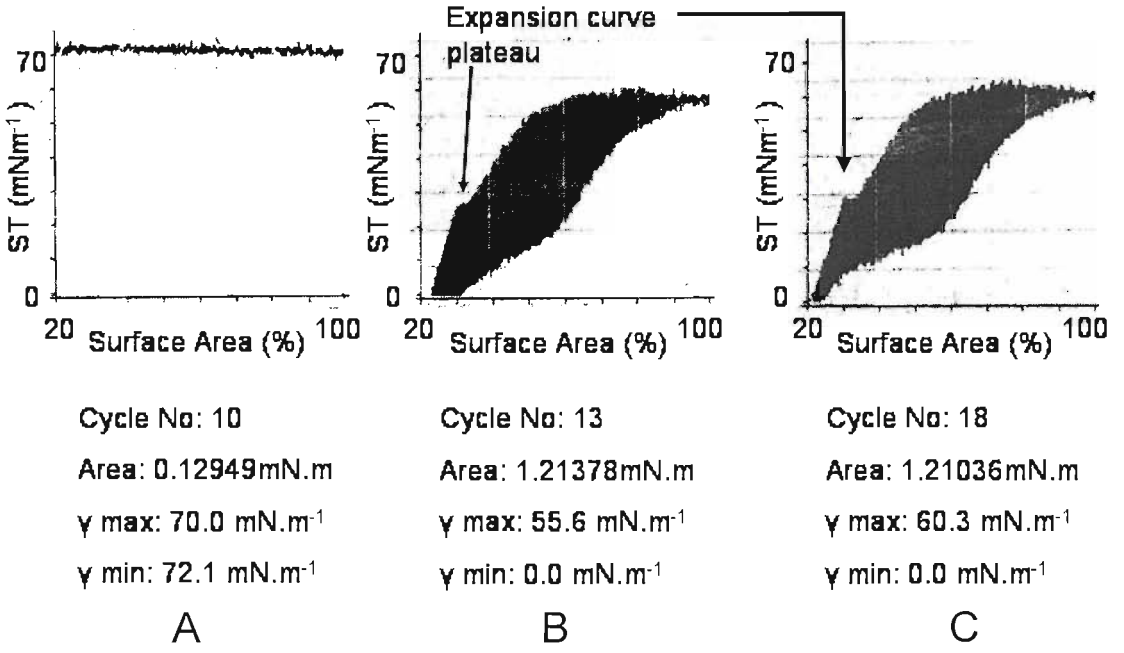

Figure 5.5: ST profiles for (A) a saline sub phase (pumactant free control) and (B and C) Pumactant suspensions (10.5 mg per 80 ml). A plateau is present on the expansion curve which was a common feature of all Pumactant ST profiles.

For each experiment (dry powder and suspension applications), values of maximum (γmax), and minimum (γmin) surface tension were recorded, together with hysteresis area. The results from all the experiments are summarised in table 5.1.

Mode of application	Pumactant sub phase conc^{-n}/ mg per 80ml	γ max/ mNm^{-1}	γ min/ mNm^{-1}	Hysteresis area/ mN.m
Dry	3.3	50.9	2.81	1.03
Dry	5.4	35.6	1.17	1.17
Dry	6.1	36.5	0.82	0.82
Dry	10.5	51.8	1.82	1.82
Suspension	10.5	55.6	0	1.21
Suspension	10.5	60.3	0	1.21

Table 5.1: Surface tension characteristics (γ max, γ min and hysteresis area) for dry powder and saline suspensions of Pumactant acquired using a Wilhelmy Balance

Maximum surface tension (ST) values of 43.7 +/- 8.9 mNm^{-1} and minimal ST values of 2.7 ± 3.7 mNm^{-1} were observed for dry powder administration, compared with 58 ± 3.3 mNm^{-1} and 0 mNm^{-1} for saline suspensions. Hysteresis areas were 1.21 ± 0.43 mNm and 1.21 ± 0 mMm for dry powder and Pumactant suspension respectively. ST profiles for both modes of administration were characterised by a small plateau on the expansion curve (at 25 mNm^{-1}) which appeared to be a characteristic finger print for the material, although these were more apparent for suspension ST profiles than for the dry powder profiles (see figure 5.5). There was a greater degree of variability in terms of both Pumactant sub phase concentration and ST parameters for the dry powder application, as could be expected due this imprecise mode of administration. However, the differences in γ max, γ min and hysteresis area did not correlate with changes in sub phase phospholipid content suggesting that sub phase lipid concentration is not an appropriate marker for interfacial function.

5.3.1.2 Effect of humidity on in vitro ST measurements

One of the problems encountered whilst carrying out surface tension measurements using the Wilhelmy balance, was that the baseline surface tension persistently drifted to off-scale values (>72.9 mNm^{-1}, the surface tension of water). This was caused by evaporation of the sub phase during surface area cycling (rate of loss of sub phase at ambient temperature and humidity was approximately 3.2 ml per hour). This arouse

because the saline evaporation, resulted in a lower level of liquid meniscus surrounding the dipping plate which in turn resulted in a lower 'pull' on the plate as measured by the balance. To alleviate this problem, the surface tension balance was placed in an incubator fitted with a laboratory built humidifying device (see section 2.6.2).

All subsequent experiments were carried out at 37°C and saturated humidity, both in an attempt to prevent or at least slow the rate of sub phase evaporation and also to mimic the normal physiological conditions of the lung. A schematic of the experimental setup is shown in figure 5.6.

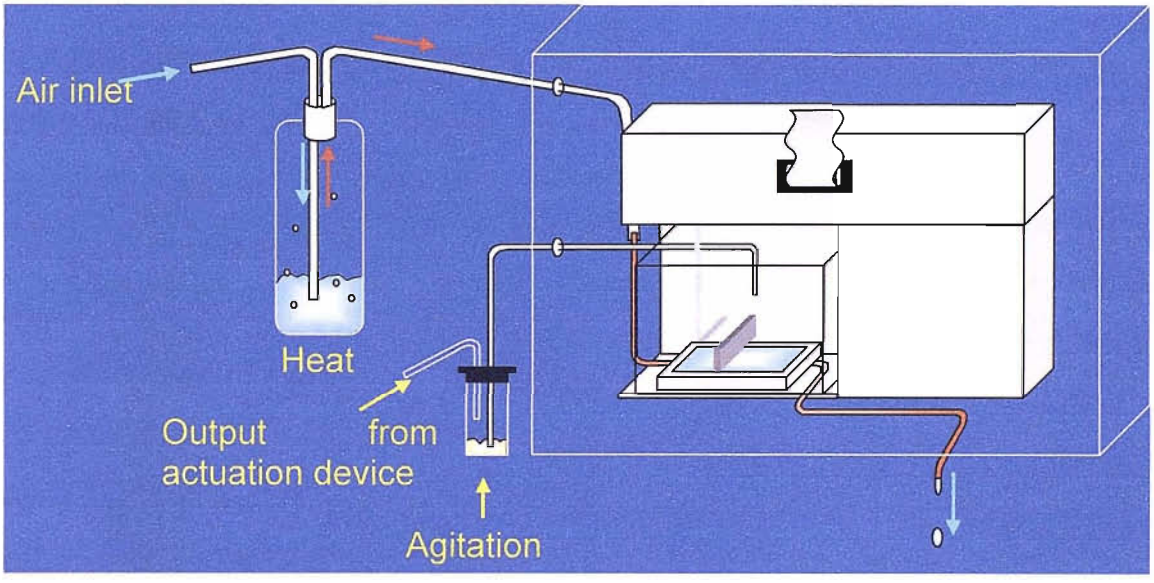

Figure 5.6: Experimental set up for measuring surface tension on the Wilhelmy Balance in controlled atmospheres.

There were concerns about operating the Wilhelmy balance in a saturated atmosphere, both because of the safety implications of running a mains powered device under such conditions and because of the problem of corrosion of the electrical components. In an attempt to minimise this, a 'humidity hood' was manufactured from a plastic container to concentrate the humid air around the trough. Pictures of the trough alone and attached to the Wilhelmy balance are shown in figure 5.7.

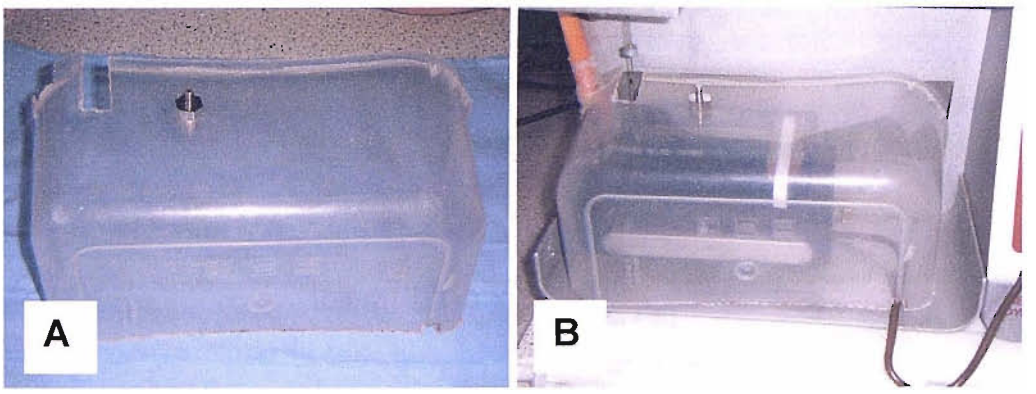

Figure 5.7: (A) the humidity hood (B) the humidity hood attached to the Wilhelmy balance

5.3.1.2.1 ST Measurements at low and high humidity measured using a platinum dipping plate

Pumactant powder was actuated onto saline sub phases following calibration of the Wilhelmy balance and acquisition of baseline surface tension readouts as previously described (section 2.6.1.1). Surface tension measurements were then carried out at ambient laboratory humidity and saturated humidity for comparison. The ST measurements carried out in a saturated atmosphere were found to differ significantly from those obtained at ambient humidity for the same sub phase preparation. High humidity measurements were characterised by an increase in γ min and a reduction in hysteresis area compared to ambient humidity measurements. The effect also appeared reversible, such that reverting from high back to ambient humidity regenerated ST profiles characteristic of the original ambient humidity measurements. Examples of two sequential measurements made on the same Pumactant preparation at both ambient (low) and high humidity are shown in figure 5.8.

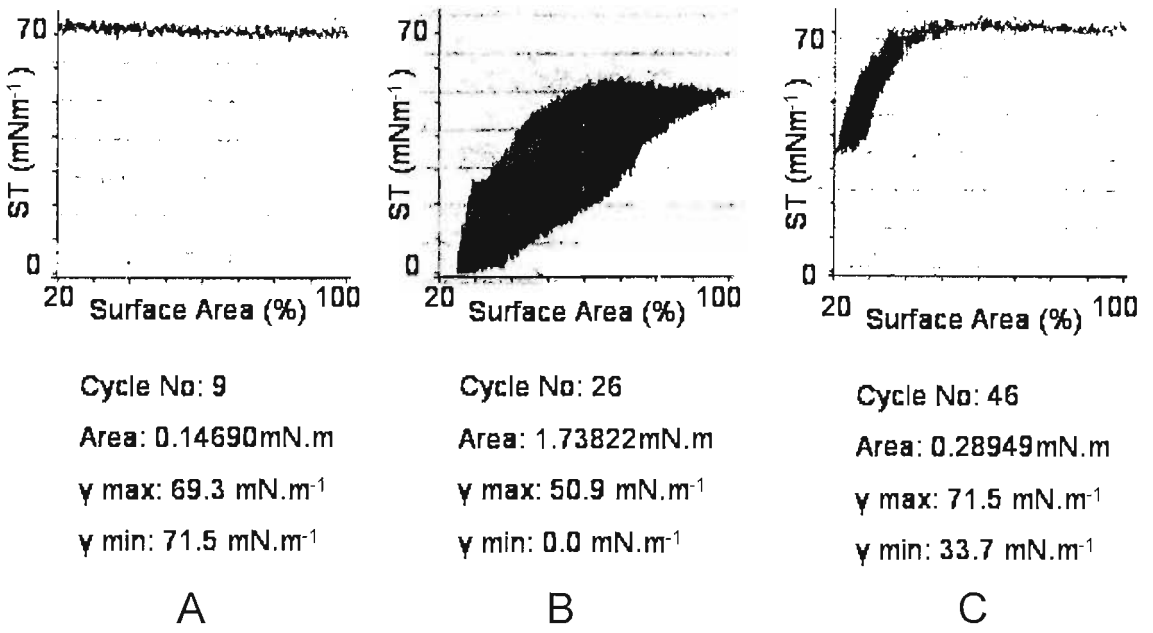

Figure 5.8: ST profiles measured at (B) 35% humidity and (C) >93% humidity on the same dry powder Pumactant sample vs. Pumactant free control (A) which was not affected by humidity changes. Actuations were carried out for 2 seconds using 1 bar actuation pressure and 2 bar vial vibration pressure.

To determine whether this phenomenon was unique to dry powder applications, ST measurements were carried out on pumactant suspensions (10.5 mg per 80ml) at ambient and high humidity. The same differences were observed as for the dry powder with high humidity measurements characterised by an increase in γ min and decrease in hysteresis area. Once again this effect was also reversible (see figure 5.9).

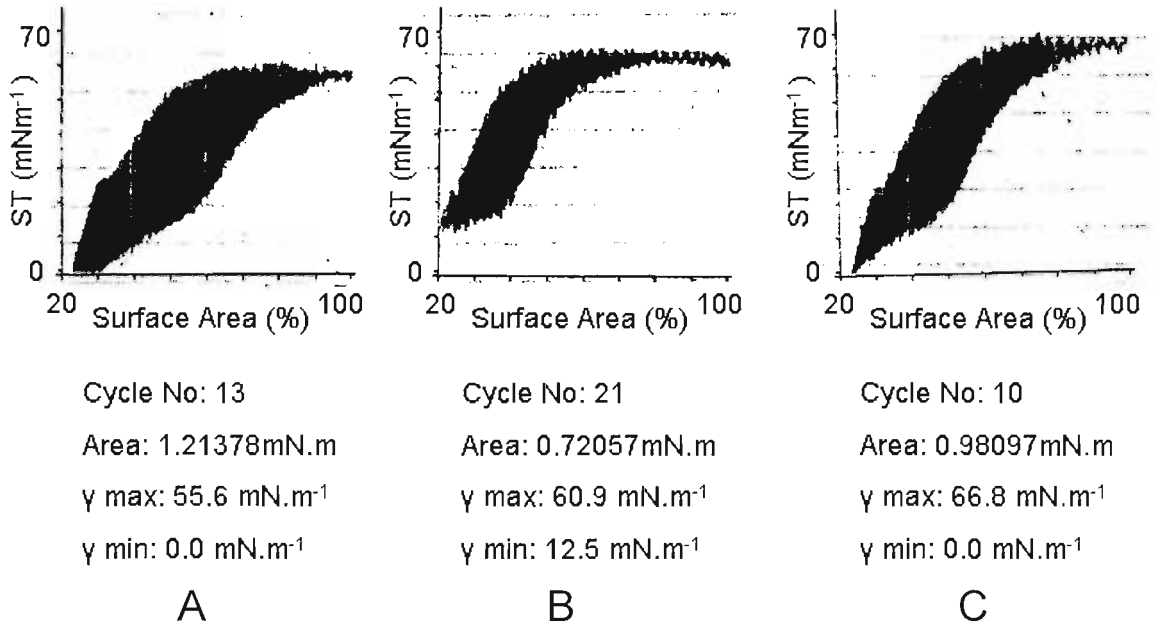

Figure 5.9: ST profiles for a single Pumactant suspension (10.5mg per 80ml) measured at (A) 58% humidity (B) 88% humidity and (C) 45% humidity.

Whether or not the changes in Pumactant ST profile observed at different humidity's were in fact an artefact of the Wilhelmy balance rather than a surface chemistry phenomenon was considered. The platinum dipping plate is very hydrophilic and under saturated aqueous atmospheric conditions, water from the air could condense onto the exposed surfaces of the plate making it heavier. The effect on the force transducer in the Wilhelmy balance would be equivalent to that of increased surface tension at the interface caused by a greater downward force on the plate.

5.3.1.2.2 ST measurements at low and high humidity using a filter paper dipping plate

To determine whether or not the humidity dependant variations in ST were an artefact of the balance, the platinum dipping plate was replaced with a piece of filter paper (the filter paper first being lowered into the trough to absorb liquid before the balance was calibrated, see section 2.6.3). Theoretically, making ST measurements using pre-wetted filter paper should minimise the surface adsorption of water molecules from the atmosphere during measurements. Pumactant was administered using the VPAG and equilibrium ST was measured (section 2.6.3), initially under ambient atmospheric conditions (figure 5.10a). The atmosphere was then saturated with water and a second ST profile was acquired on the same sub phase (figure 5.10b). Humidification of the

atmosphere was then halted and a final ST profile acquired once again under ambient laboratory conditions (figure5.10c).

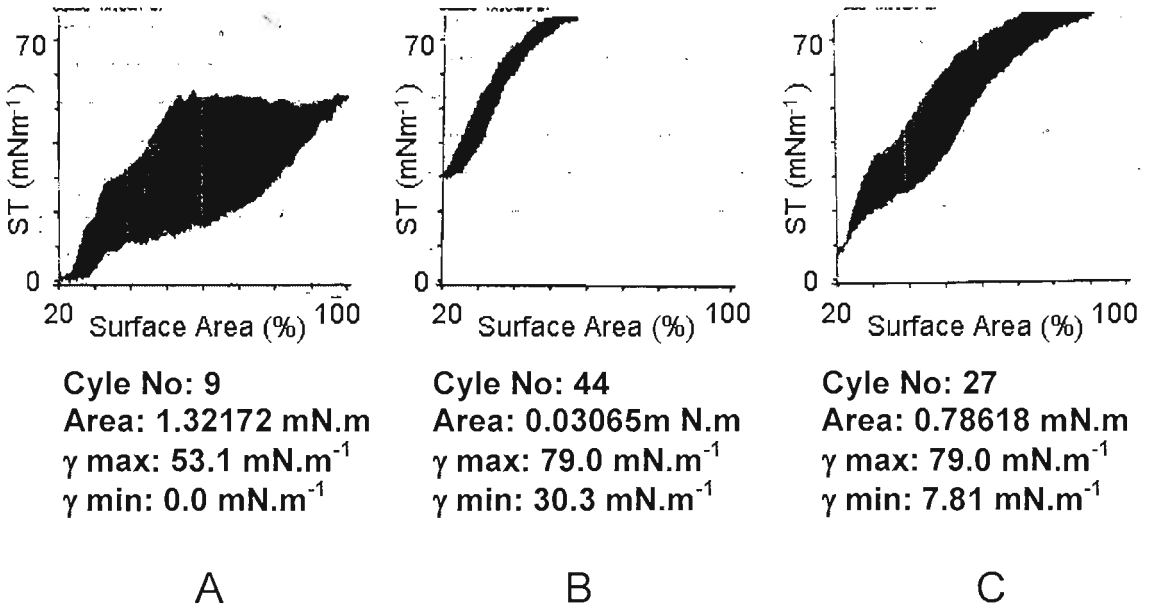

Figure 5.10: Effect of humidity on ST when measured using a filter paper dipping plate. ST measurements carried out for the same dry powder administration at (A) 47% humidity (B) >92% humidity and (C) 52% humidity. Actuations were carried out using the VPAG for 2 seconds using 1 bar actuation pressure and 2 bar vial vibration pressure.

When the humidity was increased, minimum surface tension increased and hysteresis was significantly reduced in accordance with measurements made using the platinum Wilhelmy plate (section 5.3.1.2.). This phenomenon was again reversible, although the surface tension never returns to 0 $mM.m^{-1}$. Although these data are not conclusive, they do strongly implicate the role of humidity in the physical chemistry of surfactant at interfaces.

Similar effects of humidity on apparent ST have been observed on measurements made using a pulsating bubble surfactometer (data unpublished, Wolfgang Bernhard et al). The question still remains whether this phenomenon is an artefact or representative of the surface chemistry occurring in the saturated atmosphere inside the lung. Trying to repeat the experiments described in this section was not trivial because of the time it took to equilibrate atmospheric humidity and hence achieve equilibrium surface tension for each of the respective atmospheric conditions. More often than not, the long term problem of rising baseline through sub phase evaporation made it impossible to record surface tension profiles in more than one atmospheric environment. The humidity experiments detailed in this section need to be investigated in greater detail using

precisely controlled atmospheres and employing other surface chemistry techniques such as pulsating bubble surfactometry or capillary bubble surfactometry (if a method could be devised to both adjust and measure the relative humidity inside the capillary). However this was not within the remit of this project.

5.3.1.3 Characterising interactions between dry powder Pumactant and endogenous surfactant inhibited with plasma proteins

An augmentation in alveolar protein load due to increased endothelial and epithelial permeability is a key consequence of ARDS and asthma. Plasma proteins including albumin [72] and fibrinogen[66] have demonstrated surfactant inhibiting properties *in vitro* and increased concentration of fibrin has been implicated in the severity of the asthmatic response through direct inhibition of the surface tension properties of surfactant[68]. To add further insight into Pumactant function as a surfactant therapy for airways disease, its interaction with surfactant inhibitors clearly warrants investigation. Evaluation of the capacity of Pumactant to regenerate functionally impaired surfactant on the Wilhelmy balance necessitates the use of an impaired surfactant substrate to which Pumactant can be applied. For the experiments described in this section, endogenous surfactant purified from amniotic fluid was used as the endogenous surfactant substrate. This was mixed with protein based inhibitors, to which Pumactant powder was applied. For each of the experiments described, baseline surface tension was measured on a saline sub phase, in order to calibrate the Wilhelmy balance and to ensure that none of its components were contaminated.

5.3.1.3.1 Pumactant applied to amniotic fluid surfactant (AFS) inhibited with bovine serum albumin (BSA)

Following calibration of the balance and recording of baseline surface tension, BSA was added to the sub phase, to a final concentration of 20mg.ml^{-1}. Equilibrium surface tension was then measured to determine any surface active properties of the albumin alone, after which AFS (8.3mg) was added to the BSA (19mgml^{-1}) containing sub phase. Surface area cycling was then recommenced and ST measured. Once equilibrium had been established, dry powder pumactant was applied to the sub phase surface. Equilibrium ST was again measured after which a second Pumactant actuation was

carried out and ST was again measured. Example ST profiles are shown for BSA, BSA/AFS and BSA/AFS plus the first actuation of Pumactant in figure 5.11.

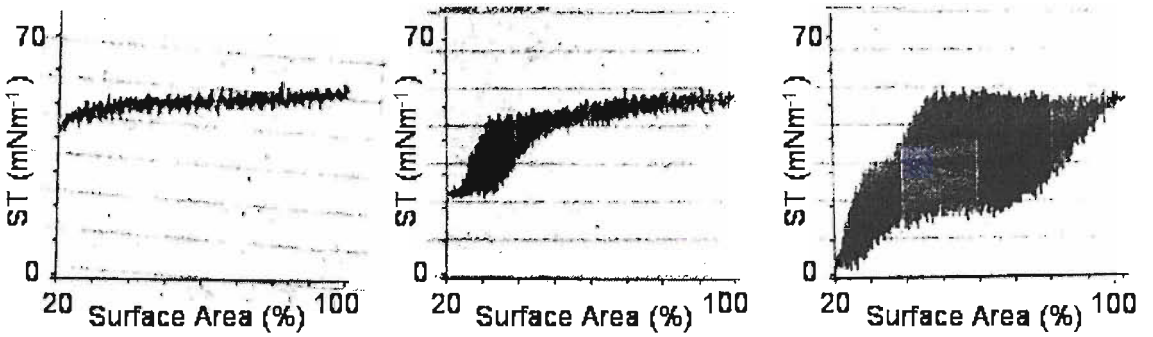

A	B	C
Cycle No: 13	Cycle No: 13	Cycle No: 5
Area: 0.20714mN.m	Area: 0.41708mN.m	Area: 1.36929mN.m
γ max: 55.6 $mN.m^{-1}$	γ max: 51.2 $mN.m^{-1}$	γ max: 48.7 $mN.m^{-1}$
γ min: 42.5 $mN.m^{-1}$	γ min: 22.8 $mN.m^{-1}$	γ min: 3.12 $mN.m^{-1}$

Figure 5.11: ST profile for (A) BSA (20 $mg.ml^{-1}$) (B) BSA (19 $mg.ml^{-1}$) containing AFS (8.3 mg) and (C) following dry powder administration of Pumactant to the sub phase containing BSA (19 $mg.ml^{-1}$) and AFS (8.3 mg). Actuations were carried out using the VPAG for 2 seconds using 1 bar actuation pressure and 2 bar vial vibration pressure. Measurements carried out under physiological conditions (37°C, > 92% RH)

As a control experiment, Pumactant was administered to endogenous surfactant, without BSA. Two pumactant actuations were made and ST measured in between each actuation (see figure 5.12).

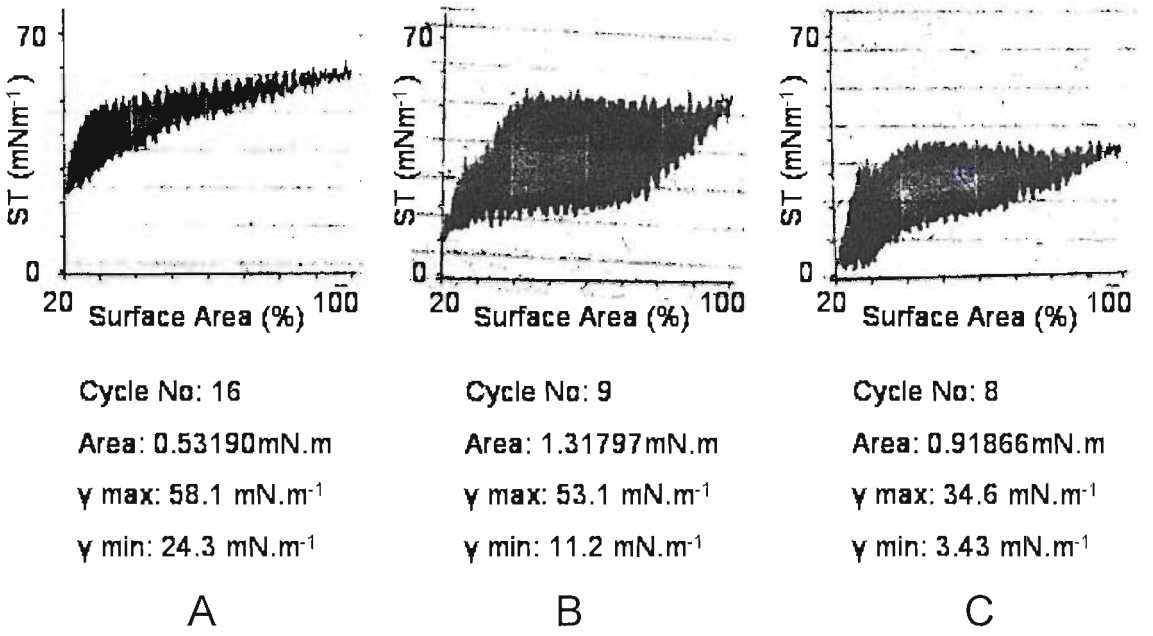

Figure 5.12: ST profiles for (A) AFS (8.3 mg), (B) AFS + 1 dose of dry powder Pumactant (C) AFS + 2 doses of dry powder pumactant applied in the absence of BSA. Pumactant dosing was carried out using the VPAG for 2 seconds, using 1 bar actuation pressure and 2 bar vial vibration pressure. Measurements carried out under physiological conditions (37°C, > 92% RH).

This procedure was carried out in duplicate (triplicate experiments were not possible due to the large quantities of AFS required for each experiment). The surface tension variables for γ min, γ max and hysteresis area for the BSA treated and non BSA treated experiments are given in table 5.2.

Experiment	Mean γ max/ mNm^{-1}	Mean γ min/ mNm^{-1}	Hysteresis area/ mN.m
AFS/BSA	60.1±12.6	28.7±8.3	0.45±0.04
AFS/BSA+Pumactant (1^{st} dose)	60.2±10.4	20.3±9.3	1.31±0.08
AFS/BSA+Pumactant (2^{nd} dose)	69.4±13.2	18.3±6.4	1.16±0.01
AFS	59.1±1.3	25.7±2	0.55±0.02
AFS+Pumactant (1^{st} dose)	57.3±5.9	15±5.3	1.3±0.01
AFS+Pumactant (2^{nd} dose)	49.3±20.8	8.4±7	1.15±0.33

Table 5.2: ST parameters (γ max, γ min and hysteresis area) for two successive dry powder Pumactant actuations onto a sub phase containing either AFS/BSA or AFS alone. Results = mean (N = 2) ± S.D.

Comparison of ST parameters for BSA treated and non BSA AFS revealed no differences for any of the surface tension parameters reported (table 5.2) suggesting that the BSA had no impact on the surface properties of the AFS. Addition of one Pumactant dose to non-treated AFS improved the surface properties of AFS (evidenced by the reduction in γ min and increase in hysteresis area) which was further improved following the second dose. A trend towards lower γ min was also observed following two Pumactant doses to BSA treated AFS although this decrease was not significant. However, hysteresis area was increased after the first Pumactant dose for the BSA treated AFS. For both the BSA treated and non-treated experiments, addition of the second Pumactant dose resulted in a slight reduction in hysteresis area.

5.3.1.3.2 Pumactant applied to AFS inhibited with human plasma

Interactions between Pumactant and AFS treated with plasma were also investigated using the Wilhelmy balance (N=2). Following base line calibration, AFS (3.3 mg) was added to the sub phase and equilibrium ST measured. An 8 ml aliquot of the sub phase was then removed and replaced with plasma acquired from a healthy patient. Dry

powder Pumactant was subsequently actuated onto the sub phase surface under conditions of saturated humidity. ST profiles for AFS alone, AFS plus plasma and AFS plus plasma plus the first dry powder Pumactant dose are given in figure 5.13.

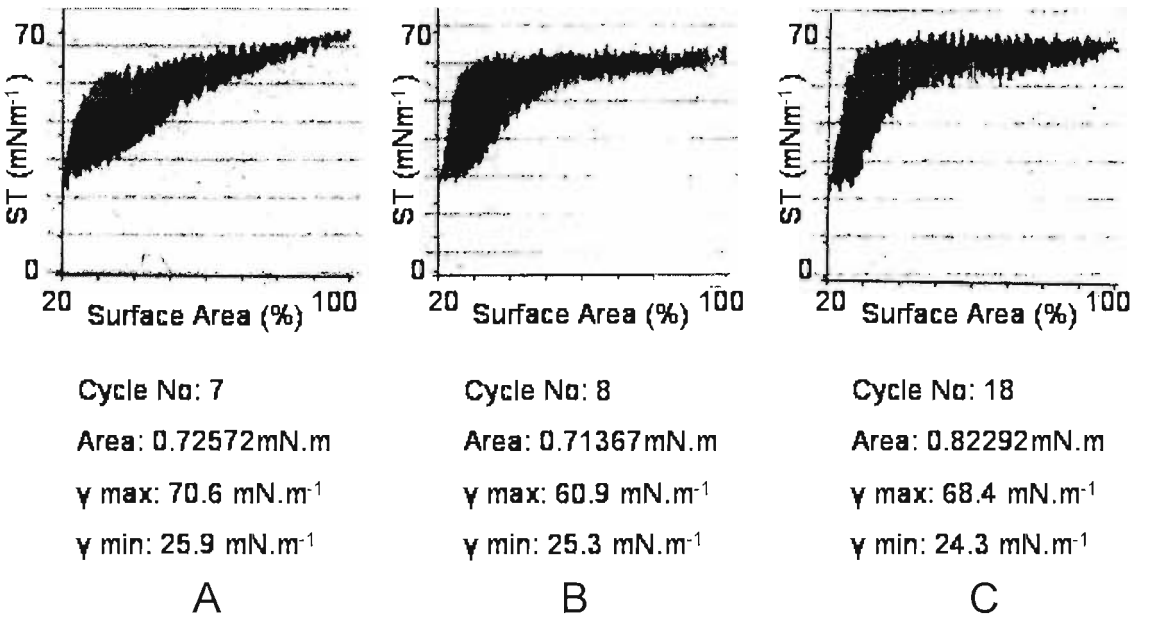

Figure 5.13: ST profiles for (A) AFS (3.3 mg), (B) AFS (3.3 mg) + plasma (8ml) and (C) AFS (3.3 mg) + plasma (8ml) + 1 dose of dry powder pumactant applied using the VPAG. Actuations were carried out for 2 seconds, using 1 bar actuation pressure and 2 bar vial vibration pressure. Measurements carried out under physiological conditions (37°C, > 92% RH).

For comparative purposes, Pumactant was dosed onto AFS in the absence of plasma. To account for the dilution effect on the AFS attributed to removing sub phase in order to add the serum, 8ml of the sub phase was removed and replaced with 8ml saline (see figure 5.14)

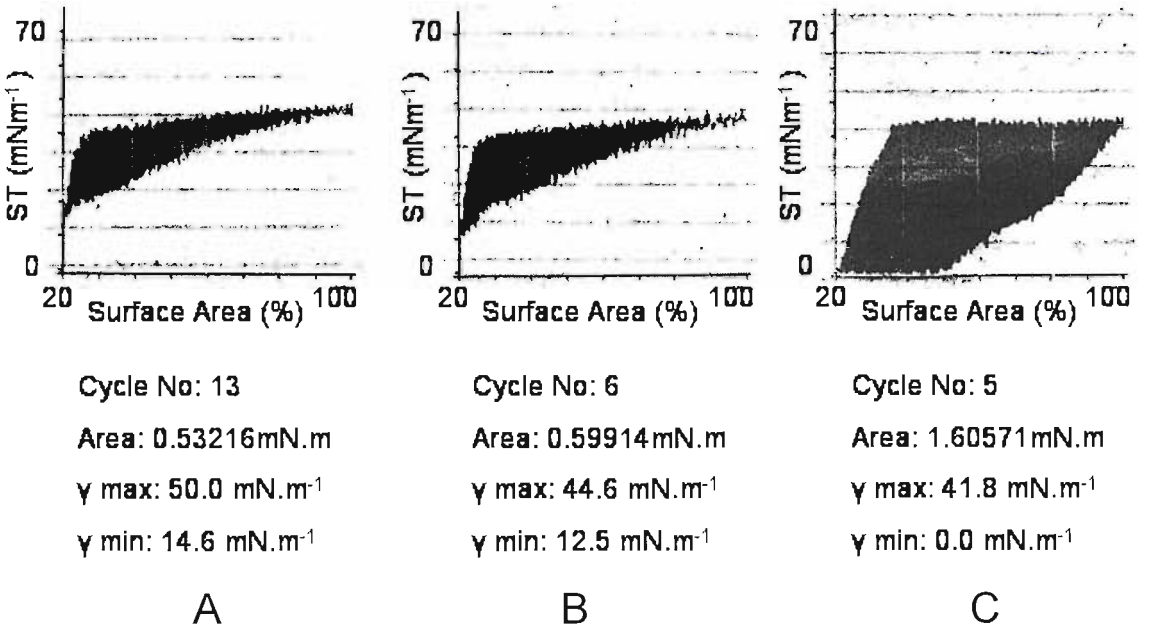

Figure 5.14: ST profiles for (A) AFS (3.3 mg), (B) AFS (3.3 mg) + saline (8ml) and (C) AFS (3.3 mg) + saline (8ml) + 1 dose of dry powder pumactant applied using the VPAG. Actuations were carried out for 2 seconds, using 1 bar actuation pressure and 2 bar vial vibration pressure. Measurements carried out under physiological conditions (37°C, > 92% RH).

The ST parameters γ max, γ min, and hysteresis area for both the plasma treated AFS and the control (saline treated) AFS experiments are summarised in table 5.3.

Experiment	Mean γ max/ mNm^{-1}	Mean γ min/ mNm^{-1}	Hysteresis area/mN.m
AFS/PLASMA	51.2±13.7	20.0±7.6	0.61±1.5
AFS/PLASMA + PUMACTANT(1^{st} dose)	53.1±21.6	19±7.5	0.67±0.21
AFS/PLASMA + PUMACTANT(2^{nd} dose)	55.4±19.7	17.5±8.8	0.73±0.25
AFS/SALINE	44.6	12.5	0.6
AFS/SALINE + PUMACTANT(1^{st} dose)	41.8	0	1.61
AFS/SALINE + PUMACTANT(2^{nd} dose)	41.8	0	1.62

Table 5.3: ST parameters (γ max, γ min and hysteresis area) for two successive dry powder Pumactant actuations onto a sub phase containing either, AFS (3.3 mg) and plasma (8ml) or AFS (3.3 mg) and saline (8 ml). Results = mean (N = 2) ± S.D for plasma treated AFS and N = 1 for AFS diluted with saline (control).

There were no differences between the ST parameters for AFS treated with plasma and AFS/ saline control making it possible to distinguish any surface inhibitory properties of the plasma. Moreover, addition of dry powder pumactant to the plasma treated AFS had no impact on ST parameters suggesting it made no impact on the ST properties of the AFS/plasma mix. In contrast, addition of dry powder pumactant to AFS alone resulted in a reduction in γ min and an increase in hysteresis area. In summary, the results from this series of experiments involving plasma treatment of AFS revealed no inhibitory effects of the plasma, nor any regenerative properties of pumactant.

5.3.1.4 Limitations of the Wilhelmy Surface tension balance

5.3.1.4.1 Problems associated with the technique

There were several difficulties encountered when making Surface tension measurements on the Wilhelmy balance. Firstly, before any surface tension measurements could be attempted, the trough, barrier and platinum plate had to be scrupulously cleaned with chloroform, methanol and water. The plate also had to be heated intensely with a blow torch to ensure decontamination and all glassware used for preparing the sub phase had to be acid washed. Once the balance was set up, baseline surface tension measurements had to be acquired and despite all the precautions taken in setting up the balance, the system was frequently subject to contamination and therefore had to be dismantled and cleaned again, making experiments very time consuming. Even without any complications, measurements would regularly take 1 to 2 hours to acquire.

There were also significant problems experienced in, attempting to administer reproducible quantities of aerosolised phospholipid onto the large surface area of the saline sub phase. Despite all the precautions taken, being airborne, the powder was difficult to contain and it is hard to envisage how this method of application imitates what happens in the lung *in vivo*. For example actuating the powder onto the surface resulted in a lot of particle bounce. It is unclear whether this artefact would occur *in vivo* where particle propulsion through actuation would occur in combination with inhalation by the patient and where the architecture of the bronchial tree is in no way reminiscent of the saline sub phase surface of the Wilhelmy trough.

Further complications include the fact that it is impossible to quantify the amount of lipid at the air-liquid interface using this experimental setup. Although sub phase concentration was easily determined by total lipid extraction and mass spectrometry assay, how the quantity or composition of material in the bulk phase reflects that at the interface is unclear. Moreover, given that the material in the sub phase is composed of material which has been squeezed out of the interface, the relevance of the subphase concentration of lipid to surface activity is entirely questionable.

These problems were compounded by the fact that the Wilhelmy balance is not designed to operate in a humid environment. As a result various components of the machine were starting to corrode due to prolonged exposure to excessive moisture. The

limitations described in this section, combined with those outlined in section 1.5.4.1 made it necessary to research alternative techniques for measuring the surface physical properties of Pumactant.

5.3.1.4.2 Choosing an alternative to the Wilhelmy surface tension balance

There were two serious contenders for the replacement technique, namely pulsating bubble surfactometry and capillary surfactometry. The pulsating bubble surfactometer is designed to mimic the first breath and breathing dynamics. The sample suspension to be evaluated is placed in a small chamber with a piston at one end and a capillary at the other, which is open to the atmosphere. As the piston is drawn downwards, air is sucked down the capillary until a bubble is formed. This emulates the neonates first breath. Moving the piston up and down causes the bubble to expand and contract, thus simulating expansion and contraction of the alveoli during the breathing cycle. As the radius of the bubble is determined by the position of the piston and the pressure around the bubble is recorded, surface tension can be calculated according to Laplace's law, $\Delta P = 2\gamma/R$ [202]. Although this technique is ideal for monitoring surface tension in the alveolus, it is not easily applied to the aerosol delivery setup. Attempting to administer dry powder phospholipid through a capillary onto the inside surface of the bubble would be extremely difficult. Also, even if it were possible to apply Pumactant powder to the bubble interface, it would not help address the problems of isolating and quantifying the surface active interfacial phospholipid material.

The second technique proposed, capillary surfactometry (for a detailed description of the principles and compoments see section 1.5.4.2) is designed to mimic how pulmonary surfactant maintains terminal airway as a posed to alveolar patency. Because the capillary is open at both ends, it means its design is more suitable for aerosol delivery because the powder can be blown through from one end of the capillary to the other. The functional capacity of any lipid deposited in the narrow section of the capillary can then be assessed following introduction of 0.5µl of saline. Crucially, once patency measurements have been obtained, the narrow section of the capillary can be extracted and phospholipid concentration determined which should, in theory, be far more representative of the interfacial lipid. Coupled with the fact that all components of the device which come into contact with lipid are disposed of after use combined with

the speed at which measurements can be made (2 minutes) make this the method of choice.

5.3.2 Pumactant characterisation by capillary surfactometry and Mass spectrometry

5.3.2.1 Pumactant actuation into a capillary

Before any Pumactant measurements involving capillary surfactometry could be attempted, it was necessary to establish whether the amorphous Pumactant powder could physically be actuated into the CS capillaries. Also, given that the assessment of dry powder surfactants by capillary surfactometry is entirely unique, no protocols existed for routine actuation of Pumactant powder into the capillaries, nor for their routine extraction. Hence, once administration of Pumactant into the capillaries could be demonstrated, routine administration and extraction techniques for Pumactant and the capillaries needed to be devised.

Amorphous Pumactant was actuated into four separate CS capillaries from a single Pumactant vial, using a piece of neonatal tubing to interface the VPAG with the capillaries (see section 2.8.2). Subsequently, saline (0.5μl) was added to each capillary and percentage open values recorded on the capillary surfactometer. Mean % open value = 99.3 ± 1.3%.

5.3.2.2 Interactions between Surfactant and low density lipoprotein (LDL) by capillary surfactometry

The molecular species distribution of the altered PtdCho composition in BALF following allergen challenge has been shown to be characteristic of the infiltration of plasma lipoprotein[2]. These observations suggest that surfactant dysfunction in acute exacerbations of asthma may be due, at least in part to interactions between aggregates of surfactant and infiltrating plasma lipoproteins. Consequently, the interactions between LDL and exogenous surfactant were investigated.

5.3.2.2.1 LDL fractionation and separation

In order to study the interaction between LDL and surfactant, it was first necessary to isolate LDL from plasma. LDL was extracted and purified from whole blood and protein concentration of the samples determined (see section 2.7.1.).

5.3.2.2.2 Sample isolation from capillaries and subsequent phospholipid extraction following capillary patency measurements

5.3.2.2.2.1 Isolation of evaluated samples from capillaries

There were a number of options considered for the isolation of the 'active' surfactant component from the capillaries. The main concern when devising a strategy was to isolate material specifically from the narrow section of the capillary, as this was the material that the liquid meniscus had come into contact with, and as such was deemed to be the component facilitating capillary patency. This consideration ruled out the possibility of submersing and sonicating whole capillaries, not only because of the surfactant present in the wide ends of the capillary, but also because of external lipid contamination on the outer surface arising from capillary handling for example. Attempts were made to break off the wide ends of the capillaries leaving the narrow middle section for extraction, however this was proven impractical because the weakest point of each capillary was the narrow middle which was consequently the most prone to breakage. Also, the few successful attempts at breaking off the wider capillary sections resulted in the formation of sharp glass splinters, which were deemed an unacceptable safety hazard.

The final option considered was to use the micropipette supplied with the capillary surfactometer to draw out the liquid meniscus from the capillary once the patency measurement had been made. This method was attractive both because the micropipette was designed to administer material specifically to the narrow capillary and also because the micropipette tips to which samples were exposed, were disposable thus negating the need for laborious cleansing of the capillaries after each use.

Attempts were made at drawing out liquid meniscus from the capillary narrow section once patency measurements had been recorded. However, the amorphous Pumactant was so effective at expelling the liquid meniscus from the capillary, that the meniscus

was irretrievably lost to the wider part of the capillary post patency measurement. Because of this, the surfactant present in the narrow capillary was isolated by instilling and withdrawing 3 separate 0.5µl aliquots of fresh saline using the micropipette before adding the next. The lipid extract from each capillary was transferred directly to mass spectrometry vials, to which DMPC standard (1 nmol) was added. Samples were dried under liquid nitrogen and stored frozen for quantification by mass spectrometry.

Pumactant was quantified by comparing Pumactant DPPC (m/z 734) with DMPC internal standard (m/z 678). Pumactant quantities were 3, 0.18, 0.26 and 0.14 µg for the four actuations respectively.

In designing experiments to explore the interactions between surfactant and LDL, a number of procedures were explored and modified to suit specific requirements. The rationale for experimental design and any further alterations required are described in this section.

5.3.2.2.2.2 Standard vs. 'micro' total lipid extraction

As the sample quantities being handled were very small (3µl), the standard bligh and dyer protocol (section 2.2.4) which is applied to the extraction of larger volumes (typically 800µl) was scaled down accordingly. The scaled down procedure was then used to perform total lipid extracts of LDL samples isolated from the narrow section of the capillaries (see figure 5.15 D). For comparison, LDL samples removed from capillaries following patency measurements were also lipid extracted using the original Bligh and Dyer protocol to check that extraction efficiency had not been compromised (see figure 5.15 C).

As a control experiment LDL was also lipid extracted (using both the standard and micro extraction procedure without adding it to CS capillaries so that sample losses through manipulation/ adherence to the capillary wall etc could be assessed (see figures 5.15 A and B respectively). Each of the LDL lipid extracts were subsequently analysed by ESI-MS/MS for PtdCho composition. An example mass spectrum for each permutation is shown in figure 5.15.

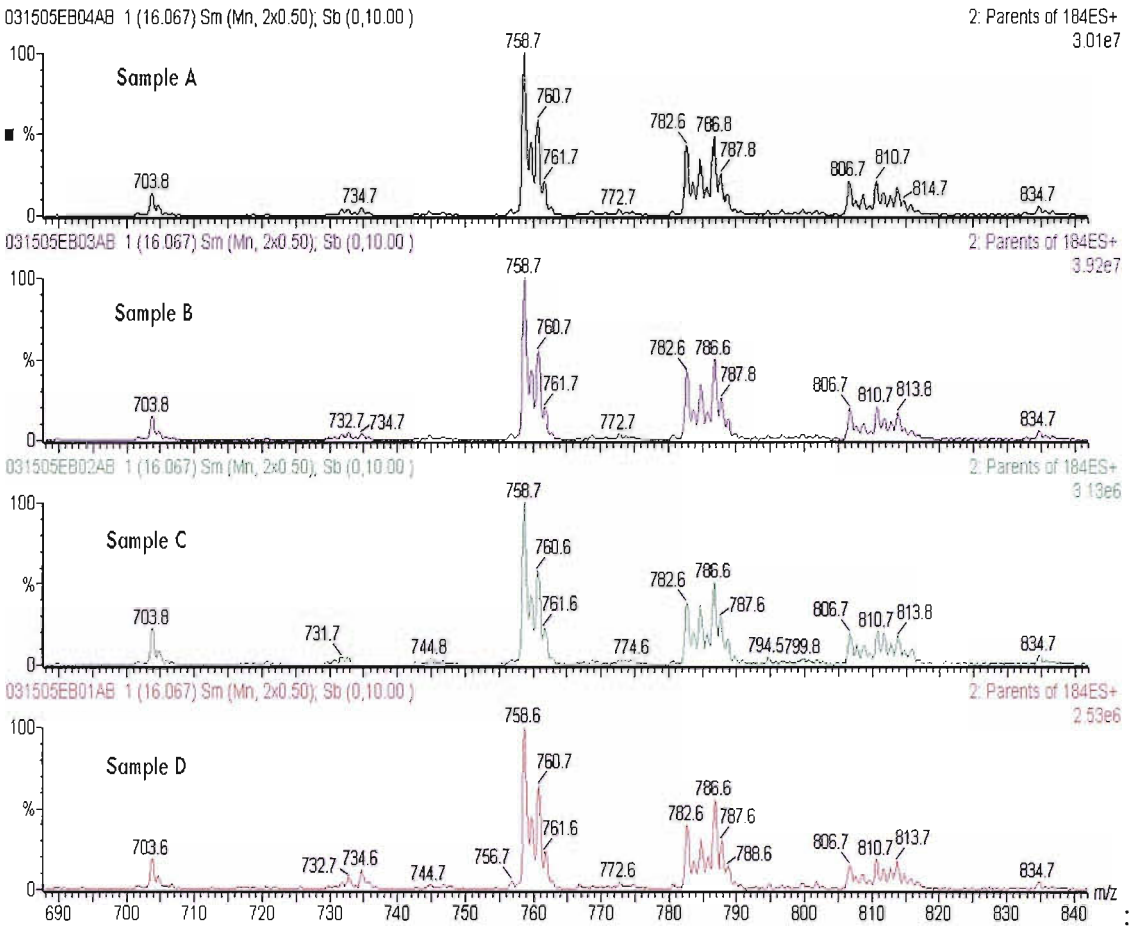

Figure 5.15: PtdCho molecular species composition of purified LDL isolated: (A) using a standard total lipid extraction; (B) using the 'micro' lipid extraction; (C) from a CS capillary using 3 x 0.5µl saline, followed by lipid extraction using the standard extraction and (D) from a CS capillary using 3 x 0.5µl saline, followed by lipid extraction using the 'micro' extraction.

The ion count (top right hand corner of each spectrum) is a direct measure of the quantity of lipid present in each sample and refers to the most abundant peak in the spectrum. The major LDL PtdCho species is PC16:0/18:2 (m/z 758). The relative proportions of each of the molecular species components, is equivalent for all four samples, showing that LDL lipids have been successfully extracted using all four methods. There is a 10 fold drop in ion intensity for samples extracted from CS capillaries (traces C & D) compared to directly extracted samples (traces A & B) (i.e a 10% recovery). Nevertheless, the molecular species profiles are consistent with those obtained for the direct extractions, indicating that there is enough material present to generate quantifiable mass spectrometry data.

Both the direct (figure 5.15 A and B) and capillary based extractions (figure 5.15 C & D) generated the same equivalent phospholipid yield as indicated by their comparative ion counts. In the light of these findings, micro capillary extractions were deemed suitable for experimental use.

5.3.2.2.3 Titrating Pumactant against LDL on the CS

As the concentration of LDL that would inhibit surfactant was not known, initial experiments characterizing interactions between LDL and Pumactant involved titrating Pumactant at a range of concentrations against LDL and vice versa, by capillary surfactometry. All capillary patency measurements were carried out in triplicate. To ensure consistent dosing of Pumactant in titration experiments, Pumactant was prepared as a suspension. Serial dilutions were prepared, from 30 $mgml^{-1}$ to 0.9375 $mgml^{-1}$. The top and bottom concentrations were assessed by capillary surfactometry to ensure that both were able to maintain a patent capillary. LDL was incubated with Pumactant at a ratio of 3:1 with three concentrations of Pumactant (30, 7.5 and 0.9375$mg.ml^{-1}$ respectively). Capillary patency was measured immediately after LDL and Pumactant were mixed together and again after a 1 hour incubation at 37°C (see table 5.4).

Time	Pumactant conc^{-n}/ mg.ml^{-1}	LDL conc^{-n}/ mg.ml^{-1}	% open reading 1	% open reading 2	% open reading 3	Mean % open
0	6	0	90.3	97.1	94.2	93.9
0	0.1875	0	91.8	88.8	90.3	90.3
0	0	2.2	0	0.1	0.2	0.1
0	6	2.2	37.8	0	1.7	13.5
0	1.5	2.2	0	32.1	0	10.7
0	0.1875	2.2	1.9	0	0.1	0.7
1 hour	6	2.2	28.3	0	0	9.4
1 hour	1.5	2.2	29.5	0.2	0	9.9
1 hour	0.1875	2.2	40.6	35.1	28.8	34.8

Table 5.4: Capillary surfactometry percentage open readings (N=3) for Pumactant titration against LDL at t = 0 and t = 1 hours. Individual % open values and means are reported.

Both the upper and lower Pumactant suspension concentrations are capable of maintaining a patent capillary in the absence of LDL, whereas LDL alone exhibited no

surface tension lowering properties. The addition of Pumactant to LDL resulted in a reduction in Pumactants ability to maintain patency at all three concentrations tested immediately after mixing. Although the results are variable, there appears to be a trend towards reduced patency at lower concentrations of Pumactant.

A considerable degree of variation was again observed when the measurements were repeated an hour later (table 5.4 and figure 5.16). Surprisingly, the results on this occasion seemed to suggest the opposite. The lowest concentration of Pumactant appeared to result in a more patent capillary then a higher one. However, due to the huge variability in the results, there does not appear to be any relationship between capillary patency and Pumactant concentration.

5.3.2.2.4 Titrating LDL against Pumactant on the CS

For this series of experiments, the concentration of Pumactant was maintained at 30 $mg.ml^{-1}$. An LDL stock solution ($2.75mgml^{-1}$) was diluted with PBS and mixed with Pumactant. Samples were assessed by capillary surfactometry immediately after mixing and following a two hour incubation at 37°C (see table 5.5.).

Time/ hours	Pumactant conc^{-n}/ mg.ml^{-1}	LDL conc^{-n}/ mg.ml^{-1}	Reading 1 (%)	Reading 2 (%)	Reading 3 (%)	Mean (%)
0	6	0	97.7	98.6	75.5	90.6
0	0	2.2	0.1	0.3	0.2	0.2
0	6	2.2	3.3	0.2	15.6	6.4
0	6	0.275	91.8	19.1	10.8	40.6
0	6	0.1375	20.5	7.3	0	9.3
0	6	0.069	75.7	79.2	90.1	81.7
2	6	2.2	0	3	0	1
2	6	0.275	5.8	24.3	99.7	43.3
2	6	0.1375	88.7	12.8	73.4	58.3
2	6	0.069	0	96.1	90.3	62.1

Table 5.5: Capillary surfactometry percentage open readings (N=3) for LDL titration against Pumactant at t = 0 and t = 2 hours.

Once again, Pumactant alone was found capable of maintaining capillary patency whilst LDL was not, in agreement with the experiments outlined in section 5.3.2.2.3. In the titration experiments carried out immediately after mixing a wide range of patency measurements were once again observed, although for the lowest LDL concentration of $0.086mgml^{-1}$ capillary patency was consistently maintained. For the measurements carried out following a two hour incubation, the variability between triplicate measurements was also very apparent and the broad spectrum of results obtained for Pumactant with $0.86mgml^{-1}$ LDL, means that the ability of Pumactant to combat LDL at this concentration much less conclusive.

5.3.2.2.5 Investigating the interaction between Pumactant and LDL treated surfactant by Capillary surfactometry

5.3.2.2.5.1 Efficacy of AFS as healthy endogenous surfactant

To investigate interactions between Pumactant and endogenous surfactant impaired with LDL on the CS required a source of endogenous surfactant. Although surfactant can be isolated from patient sputa and lavage samples, justifying their collection from healthy patients is difficult, particularly in the case of lavage which is an invasive procedure. The only other reliable source of healthy surfactant is from amniotic fluid collected at full term from caesarean sections. In the last few weeks of pregnancy, the foetus produces surfactant which it breaths out into amniotic fluid. During elective caesarean sections amniotic fluid is normally suctioned off and discarded. However the amniotic fluid can be collected and pooled instead and surfactant isolated form it by ultracentrifugation. Because the ethical approval required to collect these samples had not been obtained amniotic fluid derived surfactant samples which had been in long term freezer storage (5 years) were used. Amniotic fluid surfactant (AFS) from three separate batches collected from 2000 – 2001 were quantified for phospholipid phosphorus and tested for surface activity using the CS (see Table 5.6).

Concentration of Amniotic Fluid Surfactant	Reading 1 (%)	Reading 2 (%)	Reading 3 (%)	Mean (%)
2.43mg/ml	2.4	2.1	0.5	1.7
6mg/ml	85.5	95.1	24.4	68.3
7mg/ml	33.4	73.9	16.5	41.3

Table 5.6: Capillary surfactometry percentage open readings for three separate batches of AFS (N=3).

The first batch of AFS tested (2.43mgml^{-1}) showed very little surface activity. For the remaining two batches there was huge variability in the patency measurements obtained. Although the AFS had been in freezer storage (-20°C) it was five years old. The variable CS results suggested that the surface activity of the AFS had become compromised over this time. These batches of AFS could therefore not be included in experiments in which they were treated with LDL and Pumactant because it would be impossible to evaluate the results.

5.3.2.2.6 LDL and Survanta (a surfactant extract)

The lack of a reliable source of endogenous surfactant made it impossible to evaluate Pumactants capacity to rejuvenate inhibited endogenous surfactant in vitro. The only alternative, given the available resources and time constraints, was to compare Pumactant LDL interactions with a non synthetic surfactant preparation. Survanta® (beractant), a bovine lung extract, was chosen because it contains the two hydrophobic surfactant proteins SP-B and SP-C, both which have proven beneficial surface chemical properties. Survanta is a liquid suspension designed to be administered intratracheally.

Survanta was diluted from the stock (25mgml^{-1}) to the working concentrations shown in table 5.7 using saline and characterised either alone or in combination with LDL as summarised below. 0.5µl aliquots were introduced in the capillaries as previously described.

Concentration of Survanta ®	Concentration of LDL	Survanta: LDL ratio	Reading 1 (%)	Reading 2 (%)	Reading 3 (%)	Mean (%)
None	1.76mg/ml	N/A	8.1	10.6	6	8.3
5mg/ml	None	N/A	93.7	99.9	99.9	97.8
1.76mg/ml	None	N/A	95.8	99.9	97.8	97.8
0.586mg/ml	None	N/A	96.4	99.9	98.1	98.2
5mg/ml	1.76mg/ml	3:1	72	64.1	59.3	65.1
1.76mg/ml	1.76mg/ml	1:1	69.3	87.8	80.5	79.2
0.586mg/ml	1.76mg/ml	1:3	93.7	18.1	19.2	43.6

Table 5.7: Characterisation of LDL and Survanta alone and in combination by CS. Results shown are individual readings (N=3) plus the mean.

LDL alone was not capable of maintaining capillary patency, whereas Survanta consistently maintained patency at all three given concentrations. When LDL was added to Survanta, capillary patency clearly became compromised for all Survanta concentrations. Consistent with previous observations (sections 5.2.2.3 and 5.2.2.4) the variability in patency was much greater for combined LDL/Survanta though there does seem to a trend towards higher patency with a higher Survanta/LDL ratio.

5.4 Discussion

The experiments detailed in this chapter were devised and carried out in an attempt to understand some of the surface chemistry of Pumactant, both as a dry powder and a saline suspension in isolation, in combination with surfactant inhibitors and when applied to endogenous surfactant whose surface properties have been compromised by the presence of surfactant inhibitors. As discussed in chapter 4, dry powders for inhalation are required to be below 5μm in diameter in order to pass into the airways. Pumactant of this particle size (micronised) was not available for *in vitro* experiments, therefore all the experiments using dry powder material were carried out with amorphous dry powder. It is entirely feasible that the micronised Pumactant powder would not behave in the same way, a consideration which needs to be made when evaluating these results.

Results described in the first half of the chapter employed the use of a Wilhelmy surface tension balance, through which a number of interesting observations were made despite the inherent problems associated with the device. It should also be noted that the technique is largely qualitative and only able to report large changes in the surface chemistry between systems.

When dry powder was compared to Pumactant suspension, it was impossible to draw conclusions between the two systems, despite their comparative surface tension profiles because the relationship between lipid sub phase concentration and what is available on the surface is not known. For pre-prepared suspensions, the lipid is in micellar form even before it is added to the sub phase. Adding it to the trough merely dilutes what lipid is present. Nevertheless, some of this material is able to rapidly make itself available to exert surface chemical effects at the interface as was made apparent by the reduced γ min (relative to saline) even upon the first surface area cycle of the balance. On the other hand, lipid dispensed as a dry powder is immediately available to exert surface chemical effects without needing to 'break out' onto the surface [199]. The fact that equilibrium surface tension profiles were established for both dry powder and lipid suspensions shows that surface active lipid reservoirs must have been available to replenish the interface upon surface expansion. To further understand what is occurring at the air-liquid interface at the molecular level under the two conditions, high resolution imaging processes are required, for example atomic force microscopy or X-ray diffraction.

High humidity significantly reduced the surface activity of Pumactant, both when measured as a dry powder and a saline suspension (figures 5.8 and 5.9) an effect that was reversed when the humidity was lowered. Surface tension measurements made with Pumactant powder using a filter paper dipping plate gave the same results suggesting that this phenomenon was not an artefact associated with the Wilhelmy balance (figure 5.10). These observations are supported by experiments carried out by Colacicco et al [203], who measured the surface tension characteristics of DPPC at low and high humidity using a surface tension balance. However, they also discovered that the addition of cholesteryl palmitate permanently produced low minimum surface tension irrespective of humidity. Furthermore, long chain PtdCho (PC18:0/18:0) was able to produce low minimum surface tension at high humidity. These results call into question the widely assumed significance of DPPC in maintaining alveolar patency in the lung. The impact

of humidity is clearly important, given the highly humid environment inside the lung and is in need of further investigation using surface imaging techniques. It may be that adjusting the composition of Pumactant to include a greater proportion of longer chain PtdCho species may greatly improve surface activity of Pumactant both *in vitro* and *in vivo*. A further consideration is the impact of humidity on delivery of the material. How quickly will the material become hydrated and is the form of the hydrated state take is also important? If micelles are formed prior to deposition this is likely to impact on the spreading ability of the lipid in the light of Bangham and Morleys [199] obsevations that dry particulate surfactant spreads better than hydrated material.

Characterisation of the effects of two well known surfactant inhibitors (BSA and plasma) was attempted using the Wilhelmy balance. The results showed no improvement in surface activity in the presence of either inhibitor. Measurements were carried out at high humidity which probably further impeded improvement in surface tension properties. Nevertheless these conditions probably best mimicked those experienced *in vivo*.

Making surface tension measurements on the Wilhemy balance was both complex and time consuming. Limitations of probing interfacial effects on the Wilhelmy balance became apparent when characterising the effects of plasma and BSA on Pumactant using this technique. Problems with sample dilution in a large sub phase means subtle changes are lost. Also, the volumes involved are on a much larger scale than the volumes in the lung. Therefore the procedure required large quantities of precious amniotic fluid surfactant samples. Moreover, the technique was easily prone to contamination. As a result, an alternative procedure was sought for the high throughput screening of sample surface activity requiring only small sample volumes. The technique also had to be compatible with characterising dry powders. Capillary surfactometry fulfilled these criteria. First, amorphous pumactant was characterised in the absence of endogenous surfactant and inhibitors. The high patency results obtained demonstrated the capacity of the amorphous material to access the narrow portion of the capillary. The capillary surfactometer was then used to probe interactions between surfactant and LDL. Heeley et al[2] demonstrated the presence of lipoproteins in surfactant of asthmatics following allergen challenge. LDL was shown to inhibit the surface tension reducing capacity of Pumactant by capillary surfactometry.

Capillary patency measurements carried out on AFS revealed a loss of surface activity whilst in storage. This prevented repeat experiments of those carried out on the Wilhelmy balance determining the ability of Pumactant to counter the effects of protein inhibitors on endogenous surfactant. Instead, the ability of Survanta, an artificial surfactant derived from bovine lung extract to maintain capillary patency was assessed. It was thought that survanta would supersede Pumactant in countering the affects of LDL because it contains the surfactant proteins B and C. Unfortunately capillary patency measurements were again variable and therefore largely inconclusive although a trend towards improved patency with a higher Survanta to LDL ratio was observed. The causes for the variability in CS measurements remain unknown.

Chapter 6
Pumactant and its impact on inflammatory cell responses

6.1 Introduction

6.1.1 Allergy and asthma

An immune response evokes a battery of effector molecules that act to remove antigen from the body. These effector molecules usually induce a sub-clinical localised inflammatory response that eliminates antigen without extensively damaging the host's tissue. Under certain circumstances, the immune system can mount an inappropriate or heightened inflammatory response resulting in significant tissue damage or even death. This inappropriate response is termed hypersensitivity or allergy.[204]

Several forms of hypersensitive reaction can be distinguished, reflecting differences in the effector molecules generated in the course of the reaction, each involving distinct mechanisms, cells and mediator molecules.[204] Allergic reactions are induced by certain types of antigens referred to as allergens and are distinguished from normal humoral responses by the recruitment of immunoglobulin E (IgE) antibodies which facilitate the release of potent pharmacologically active mediators. Most humans only exhibit significant IgE responses as a defence against parasitic infections. People who mount inappropriate IgE responses against common environmental antigens are said to be atopic. The clinical manifestations of hypersensitive reactions are related to the biological effects of the mediators released. These mediators act on local tissues as well as on populations of secondary effector cells, including eosinophils, neutrophils and T lymphocytes. When generated in response to parasitic infections, these mediators initiate a beneficial defence process. Vasodilation and increased vascular permeability result from the release of mediators and bring an influx of plasma and inflammatory cells to attack the pathogen. Conversely, mediator release induced by inappropriate antigens (allergens), results in an unnecessary increase in vascular permeability and inflammation whose detrimental effects far outweigh any beneficial effect. The clinical manifestations of hypersensitive reactions can range from serious life-threatening conditions, such as systemic anaphylaxis and asthma, to hay fever and eczema.[204]

The asthmatic response comprises an early followed by a late response. The early response occurs within minutes of allergen exposure, mainly involving the mediators histamine, leukotriene C_4 (LTC_4) and prostaglandin D_2 (PGD_2) and results in bronchoconstriction, vasodilation and an accumulation of mucus in the airways. The

late asthmatic response occurs hours later and involves additional mediators including IL-4, IL-5, IL-16, and TNF_{α} which result in an increase in endothelial cell adhesion and the recruitment of inflammatory cells including eosinophils and neutrophils into the bronchial tissue. The neutrophils are capable of causing significant tissue injury through the release of toxic enzymes, oxygen radicals and cytokines.

6.1.2 The role of T lymphocytes in the pathogenesis of asthma

The T cell hypothesis of asthma developed from studies of late asthmatic reactions (LARs)[205] and acute severe asthma (status asthmaticus)[206] and was supported by the observation that there was a T_H2-type T-cell cytokine profile in this disease.[207] Since these initial observations, the emphasis of research has shifted from mast cells and eosinophils playing a central role in driving inflammation associated with asthma to T cells, particularly of the T_H2 subset.[208] It is well known that allergen specific IgE synthesis is T cell dependent through cognate activation of B lymphocytes and T cell-derived cytokines such as IL-4 and IL-13.[209] Growing interest in the role of T cells in asthma arose from the concept that, in addition to participating in IgE synthesis, T-cell products might also have direct effects on the airways through IL-5 mediated recruitment of inflammatory cells, particularly eosinophils. T cells are now considered to play an essential role in the orchestration of airway inflammation characteristic of asthma[210,211]. The relentless increase in the prevalence of asthma and allergic diseases highlights the need for devising preventative strategies. Allergic diseases are polygenic with several genes on different chromosomes involved in the genesis of these disorders [212]. As genetic manipulation to prevent these disorders is not yet in sight, it may be that manipulation/suppression of inflammatory cell responses in the lung could represent a potentially useful adjunct therapy.

6.1.3 Cellular phospholipids and T cell signalling

Phospholipids, the building blocks of cellular membranes separate the intracellular compartment from the extracellular environment and compartmentalise specialised intracellular organelles. Cellular phospholipids were considered as relatively inert structural components for many years, but recent discoveries have shown them to be crucial to many cellular functions[213]. Besides providing structural and compartmental

frameworks, the many roles of cellular phospholipids include acting as substrate molecules for phospholipase enzymes involved in signalling mechanisms, providing the necessary physicochemical environment for the various membrane associated receptors, enzymes and proteins and providing sites for the binding of proteins involved in cellular signalling processes.

All cells require signalling mechanisms to communicate and function. These signal-transduction pathways begin with receptors that detect the arrival of a signal. T-cell signalling is initiated by the binding of antigen to a membrane receptor. The antigen receptor on T-lymphocytes (TCR) has a highly complex structure and is subject to very tight multi-component regulation. Successful proliferation is then dependant upon activity of various intracellular signalling cascades, producing second messengers (some of which are phospholipids) which ultimately lead to the activation of the molecule protein kinase C (PKC). Activation of tyrosine kinases Fyn and Lck by phosphorylation are two of the earliest known events following occupancy of the TCR. One of the other targets for protein phosphorylation is phospholipase Cγ1 (PLC- γ1). PLC-γ1 hydrolyses the lipid signalling molecule phosphatidylinositol 4,5-*bis*phosphate (PIP_2) to generate the lipid second messengers 1,4,5-*tris*phosphate (IP_3) and 1,2-diacylglycerol (DAG). Release of DAG and calcium ions result in recruitment and activation of a protein kinase C (PKCθ), which ultimately activates NF-AT a potent T cells specific nuclear factor. The collective effect of the several activated transcription factors generated by these signal transduction pathways is to increase the expression of several genes and to induce the expression of others, including the gene that encodes the T-cell, growth promoting cytokine interleukin 2 (IL-2).[204]

6.1.3.1 The role of Phosphatidylinositol (PtdIns) and Phosphatidylinositol-4,5-bis-phosphoate (PIP_2) in intracellular signalling in T-cells

The metabolism of phosphoinositides is coupled to the action of numerous hormones, transmitter substances and growth factors as part of signal transducing mechanisms across the plasma membrane. PtdIns may undergo enzymatic phosphorylation in the 3- or 4- position of the inositol ring. The resulting PtdIns phosphates (PIP) may then be further phosphorylated. PtdIns-4-phosphate can be phosphorylated in the 5-position to phosphatidylinositol 4,5-bisphosphate (PIP_2), which is crucial for hormone and

transmitter signalling across the plasma membrane, including T-cell signalling (see section 1.6.1.4.2 and 6.1.3). Mammalian cells *in vivo* maintain a remarkably consistent and simple molecular species composition of membrane PtdIns dominated by 18:1/20:4 PtdIns.[214] In contrast the dominant membrane phospholipids in PtdCho and PtdEtn are much more complex, comprising in excess of 30-50 molecular species[121]. PIP_2 is synthesised from PtdIns and hydrolysed by PtdIns-specific PLC to generate the second messengers DAG and IP_3.[215] The precise molecular species composition of DAG mobilised appears to be critical for activation of DAG-sensitive isoforms of PKC.[216]

6.1.4 Surfactant and T cell function

T-Lymphocytes obtained from lung lavage have long been known to be less responsive to mitogens than peripheral lymphocytes [37], and the purified phospholipids seemed to cause more inhibition than whole surfactant [217]. There are several possibilities for the mechanism of action of surfactant/ exogenous phospholipid on T-lymphocyte function. Firstly, surfactant may exert its immunosuppressive effects by adhering to the extracellular surface of the cell thus masking the TCR/CD3 complex and inhibiting the initiation of TCR/CD3 mediated signalling. The second possibility is that surfactant phospholipid alters the T-lymphocyte plasma membrane phospholipid composition which in turn could influence cell membrane fluidity and/or the substrates available to phospholipases (e.g. PLC-γ). A change in membrane fluidity could disrupt the formation of detergent resistant microdomains at the immune synapse (lipid rafts) which are thought to be vital in the initiation and propagation of TCR-mediated cell signalling [218]. Changes in the phospholipid substrates available for T-lymphocyte signalling, e.g. PIP_2, could result in subsequent production of DAG molecular species that are less efficient at activating PKC, impairing signal transduction and thus altering the overall cellular response. The possible sites of action of surfactant lipids on T cell activation are summarised in figure 6.1.

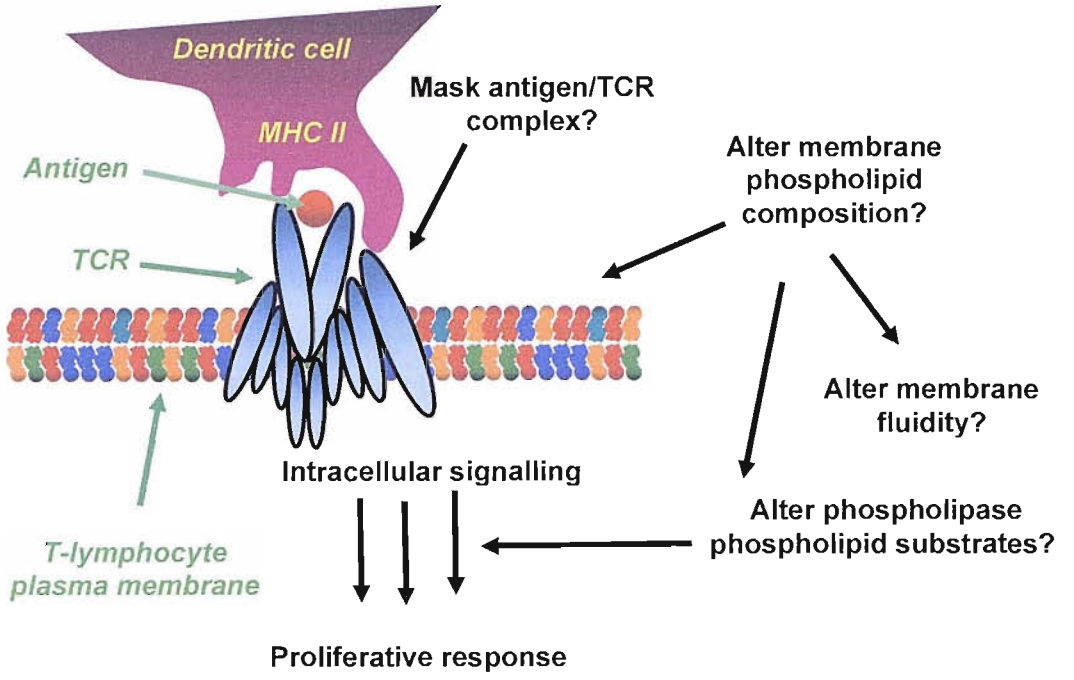

Figure 6.1: Schematic representation of the initiation and propagation of the T-lymphocyte signal and the possible sites at which surfactant phospholipid may exert its immunosuppressive effects

The possible contribution of Pumactant phospholipids to each of the proposed mechanisms discussed above were investigated and are discussed in this chapter.

6.2 Methods

6.2.1 Effects of Pumactant PtdCho on T-cell responses

The impact of Pumactant on T-cell responses was assessed using a mouse/T-cell hybridoma (B3Z cells) specific for OVA peptide. The B3Z cell line incorporates a reporter gene (lacZ) which expresses a β-galactosidase in response to cell activation and proliferation. Cells were incubated with Pumactant and stimulated with peptide. Following over night incubation, the extent of cell activation was gauged by lysing cells with detergent and incubating cells with β-galactoside substrate (chromophore conjugated to β-galactoside). Optical densities were then measured on a plate reader and differences between active and control cells calculated as a percentage (section 2.9.5.2).

6.2.2 Quantifying exogenous PtdCho incorporation in T-cell membranes and assessment of cellular distribution

Jurkat cells were incubated with Pumactant labelled with [*methyl*-d_9]DPPC and BODIPY PtdCho fluorophore. Cellular phospholipids isolated by total lipid extraction and the extent of exogenous DPPC incorporation into cells was measured by ESI-MS/MS implementing precursor ion scanning to diagnostic product ions m/z = +184 for endogenous PtdCho and m/z = + 193 for [*methyl*-d_9] containing species (section 2.11).

Cellular distribution of exogenous Pumactant was assessed by confocal microscopy. Following overnight incubation with BODIPY PtdCho labelled Pumactant, cells were fixed, incubated with a nuclear counterstain and examined by confocal microscopy (section 2.12).

6.2.3 Composition of cellular phosphoinositides (PtdIns and PIP_2) by ESI-MS/MS

Cellular phosphoinositides were isolated using acid lipid extractions and characterised by ESI-MS/MS using diagnostic pre-cursor ion scanning (PtdIns = precursors of m/z = -241, PIP_2 = precursors of m/z = 401 and NL of m/z = 98).

PtdIns synthesis and metabolism was studied by incubating cells with [*myo*-d_6]inositol, followed by acidified lipid extraction. PtdIns characterisation was performed using ESI-MS/MS using diagnostic pre-cursor ion scanning m/z = -241 (endogenous PtdIns) and m/z = -247 (newly synthesised PtdIns) (see section 2.13).

6.3 Results

6.3.1 Exogenous surfactant and T cell reponses

In order to evaluate the effects of Pumactant action on inflammatory cells, it was first necessary to develop a model T-lymphocyte system which would generate a reproducible and quantifiable response to stimulation. Using T lymphocytes from whole blood was ruled out because of the heterogeneity inherent in primary lymphoid cultures

and the fact that the cells can only be propagated for a limited time. B3Z cells are an OVA specific mouse/T cell hybridoma which incorporate a reporter construct consisting of the bacterial β-galactosidase gene (lacZ) under the transcriptional control of the nuclear factor of activated T cells (NF-AT) element of the human IL-2 enhancer.[219] The lacZ assay was developed for the detection of ligand induced activation of single T cells. In this assay, B3Z cells are stimulated with a specific OVA peptide (sequence SIINFEKL) and then incubated with chlorophenol red beta-galactoside (CPRG) a conjugated substrate with a reporter chromophore. Cleavage of the galactoside causes a colour change from yellow to red. A schematic of the B3Z cell reporter construct is shown in figure 6.2

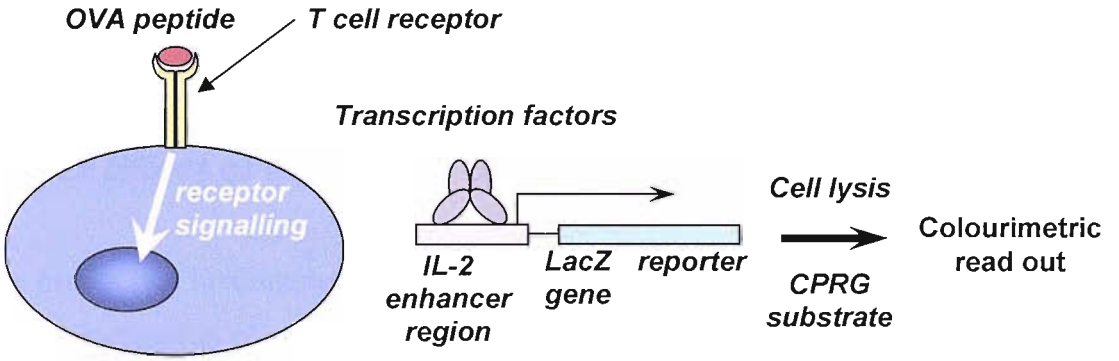

Figure 6.2: The B3Z T-cell hybridoma. Stimulation of the cell upon binding of the T cell receptor with peptide antigen results in both the production and intracellular accumulation of lacZ as well as the production of IL-2. LacZ expression is visualised following cell lysis and the addition of CPRG chromophore substrate

6.3.1.1 OVA titration on B3Z cells

OVA peptide was titrated to establish a working concentration with which to stimulate the cells. B3Z cells were stimulated with either 1nM, 10nM, 1μM or 10 μM OVA peptide in triplicate overnight on a 96 well round bottomed plate ($1x10e^5$ per well). Cells were then washed and incubated with CPRG until a red colour developed. Absorbance was measured at 570nm (table 6.1).

OVA concentration/ μM	$O.D_{570nm}$ - blank / a.u.
10	0.73 ± 0.015
1	0.16 ± 0.018
0.1	0.13 ± 0.006
0.01	0.11 ± 0.012

Table 6.1: OVA peptide titration on B3Z cells. Cells were incubated in triplicate. Optical density was measured following a 3 hour incubation with CPRG. Results = mean (N=3) ± S.D.

A strong cellular response was required so that subtle changes in cellular activation evoked by the presence of exogenous surfactant could be detected. Stimulating the cells with less than 10 μM OVA did not elicit a great enough response from the cells, therefore this was chosen to stimulate the cells.

6.3.1.2 Effect of Pumactant on B3Z cell stimulation

The events that link antigen recognition by the T-cell receptor to cellular proliferation involve instigation of a large number of accessory signalling molecules (section 6.1.3). Whilst commitment of T cells to proliferation requires long term signalling through the TCR and costimulatory receptors (approximately 20 hours)[220] the consequences of initial signalling events such as a sharp rise in cytosolic Ca^{2+} concentration are evident within seconds of stimulation.[221]

To distinguish between the possible effects of Pumactant on antigen/TCR binding and subsequent signal transduction B3Z cells were either pre-incubated for two hours with pumactant and stimulated with OVA peptide or incubated with Pumactant and immediately stimulated with peptide (section 2.9.5.2) over night. Cells were then washed to remove excess Pumactant and Ova agonist and incubated with CPRG substrate (see figure 6.3).

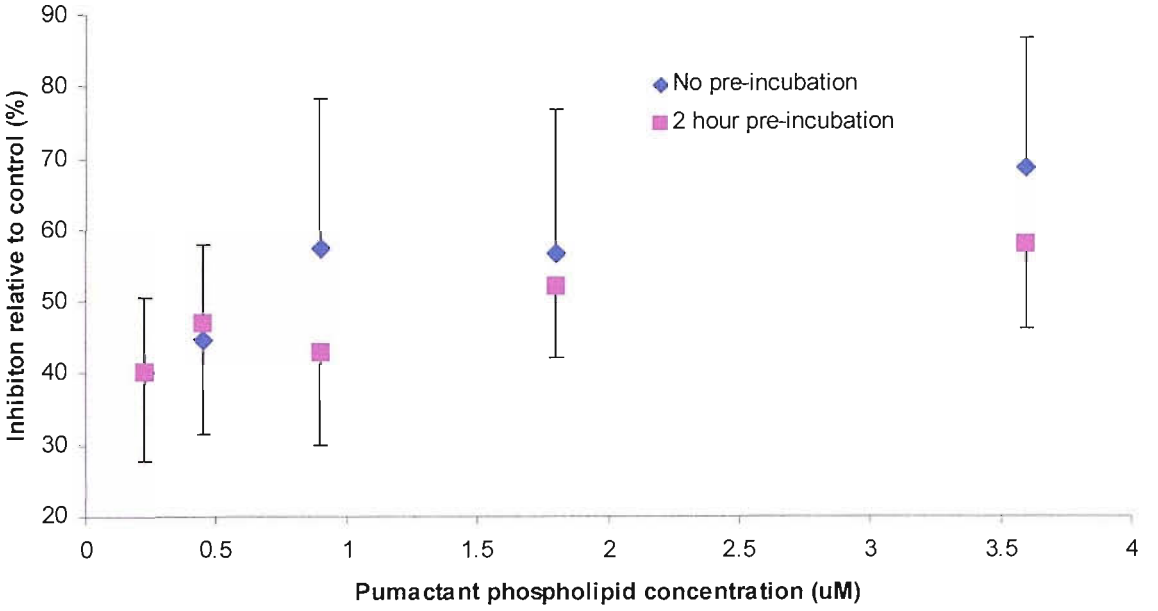

Figure 6.3: B3Z cell response following pre-incubation with Pumactant (0.225μM-3.6μM) for two hours followed by stimulation with OVA peptide or incubation with Pumactant followed by immediate stimulation. Results = Mean (N=3) ± S.D.

A concentration dependant inhibition of cell activation with increasing Pumactant phospholipid was observed for both pre-incubated cells and cells stimulated upon incubation. Pumactant had an immediate effect on the extent of cell stimulation at all the concentrations. This effect was also maintained when cells were pre-incubated for two hours. These results demonstrate the successful development of a model reporter system for T cell activation in the presence of Pumactant and reveal a direct effect of Pumactant phospholipid on T-cell activation. The immediacy of the effect implicates either Pumactant impairing antigen/TCR ligation or affecting the initial events in signal transduction.

6.3.1.3 Agonist stimulation of Jurkat cells

Results in section 6.3.1.2 clearly demonstrate a direct and immediate effect of Pumactant phospholipids on the B3Z cell reporter assay. Because B3Z cells are a mouse/human T-cell hybridoma, an alternative cell line was sought which was more representative of human T-lymphocytes in order to investigate mechanisms of action of Pumactant phospholipids. The human leukaemia T cell line Jurkat was derived from a patient with T lymphoblastic lymphoma.[222] Jurkat cells resemble resting T-cells in both morphology and activation requirements[222] and cells were chosen because they

represent a well characterised model system with reported proliferative responses to a range of agonists and, being an immortal cell line, are also available in large quantities necessary for laboratory experiments.

In order to validate the Jurkat cells as an appropriate T-lymphocyte model and verify an appropriate response to stimulation the cells were subjected to a range of agonists known to evoke proliferative responses in T-lymphocytes. Previous work by one of the department's PhD students investigated agonist stimulated proliferation of T cells using either OKT3, PMA and calcium ionophore alone and in combination to stimulate the cells. However, none of the agonists produced a positive Jurkat cell proliferative response that was consistent between experiments largely because of the high basal rate of cell division generated by this immortal cell line.[223] Therefore agonist stimulated production of IL-2 was explored as a marker of Jurkat cell activation. Jurkat cells, at a concentration of 1 x 10^6 cellsml^{-1}, were stimulated with 20 $ngml^{-1}$ PMA, 100 μgml^{-1} OKT3, 10 μgml^{-1} PHA[224] and OKT3 + PMA (100μgml^{-1} and 20$ngml^{-1}$ respectively), for 24 hours. Supernatants isolated, and quantified for Human IL-2 content by ELISA (figure 6.4):

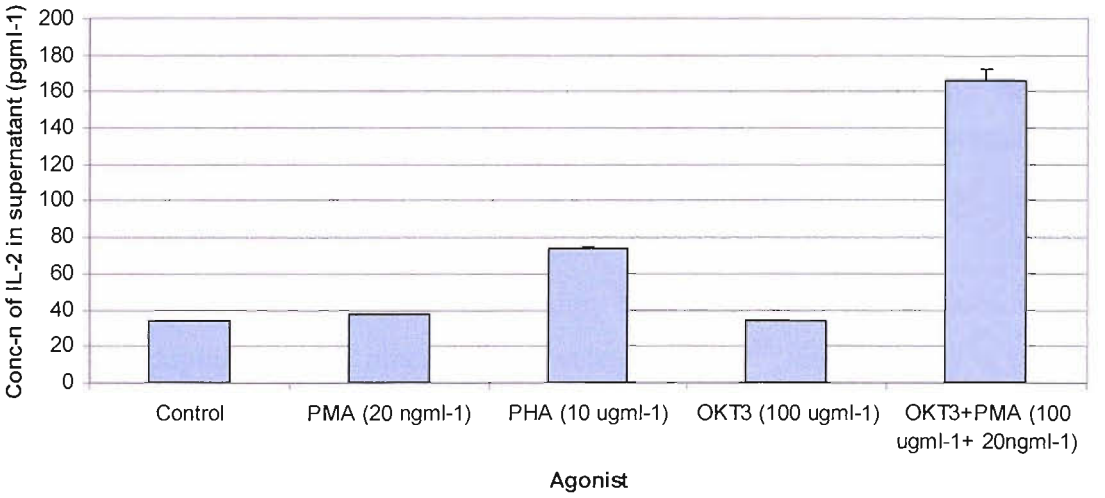

Figure 6.4: IL-2 concentration of Jurkat cell supernatant following agonist stimulation for 24 hours. Results = Mean (N=3) ± S.D.

Stimulation with PHA gave a 2.18-fold increase in IL-2 production relative to controls ($P < 0.001$). Stimulation with PMA or OKT3 did not significantly stimulate IL-2 production but co-stimulation of Jurkat cells with PMA and OKT3 gave a 4.91-fold ($P < 0.001$) and 4.4-fold ($P < 0.001$) increase relative to controls and PMA stimulated cells

respectively. The positive response of the cells to agonists successfully validated Jurkat cells as a model T-lymphocyte system for the purpose of these experiments.

6.3.2 Incorporation and distribution of exogenous surfactant in Jurkat cells

Alteration in the composition of cell membrane phospholipid due to the incorporation of specific exogenous phospholipid molecular species is one possible mechanistic explanation for the suppressive effect of Pumactant on cell response. The impact of exogenous Pumactant phospholipid on cell phospholipid composition was therefore investigated.

6.3.2.1 Pumactant PtdCho incorporation into whole cells using ESI-MS/MS

6.3.2.1.1 Labelling Pumactant

In order to measure Pumactant DPPC incorporation into cells it needs to be labelled so as to distinguish it from the endogenous material. Deuterium labelling provides a means to quantify exogenous PtdCho by mass spectrometry (discussed in detail in chapter 3), whilst the use of fluorescent label makes it possible to visualise exogenous lipid distribution. It was decided that two PtdCho labels would be combined so that any changes in membrane composition detected by mass spectrometry could be supplemented with distribution data. The bodipy fluorophore was chosen because it is intrinsically lipophilic unlike other long wavelength dyes[225], consequently a PtdCho molecule incorporating this fluorophore into the fatty acid side chain is more likely to mimic the properties of the natural phospholipids.

Pumactant enriched with [*methyl*-D_9]DPPC was combined with bodipy PtdCho (β-bodipy500/510 C_{12}-HPC) prior to sterilisation with 70% EtOH (section 2.11.1). An aliquot of the sample was characterised for endogenous and deuterated PtdCho content using diagnostic precursor ion scanning (Pre-cursors of 184 and 193 respectively) (figure 6.5)

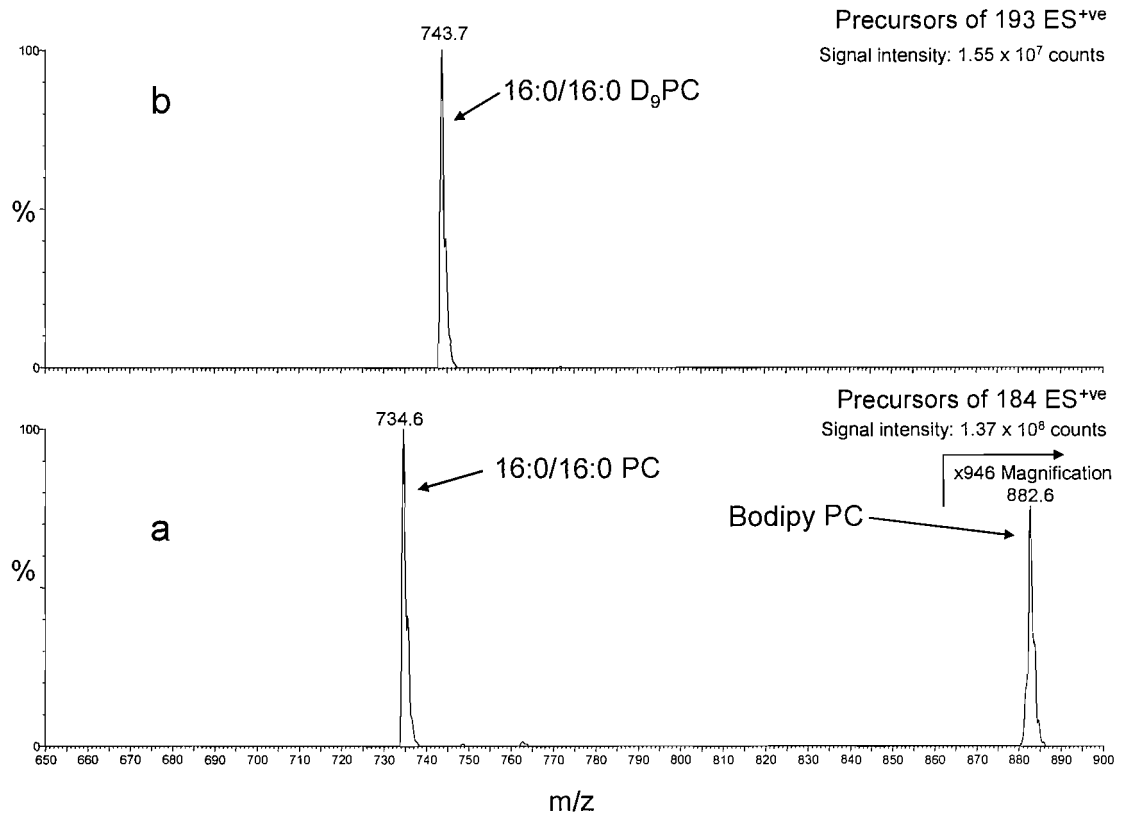

Figure 6.5: Mass spectra of Pumactant PtdCho showing (a) endogenous DPPC and bodipy PtdCho (precursors of +184) and (b) deuterated DPPC (precursors of +193). The peak corresponding to bodipy PtdCho (m/z 882.6) was magnified 946 fold so that it was visible on the same scale as the DPPC

The enrichment of [*methyl*-D_9]DPPC was calculated from the relative intensities of the endogenous and deuterated DPPC peaks (m/z 734 and 743 respectively) following intensity corrections for the ^{13}C isotope effect and loss of signal with increasing mass. Bodipy PtdCho enrichment was calculated as a fraction of total Pumactant PtdCho in the same way. Bodipy enrichment was 0.19 ± 0.04 % of the total PtdCho in the sample. The [*methyl*-D_9]DPPC labelled pumactant containing bodipy PtdCho will be referred to as labelled Pumactant throughout this chapter.

6.3.2.1.2 Incubating Jurkat cells with deuterium labelled Pumactant

In order to investigate Pumactant incorporation into whole cell PtdCho, Jurkat cells were incubated with labelled Pumactant (section 6.3.2.1.1 above) for 2, 24 and 48 hours in triplicate vs. control. Cells were washed with PBS at each time point, lipid extracted and characterised by ESI-MS/MS (see sections 2.11.2 – 2.11.4). Precursor ion scans for

endogenous PtdCho (m/z 184) and [*methyl*-D_9] labelled PtdCho (m/z 193) were collected as sequential scans for each sample. Comparative mass spectra showing endogenous Jurkat cell PtdCho for non treated control cells and cells treated with Pumactant for two hours are given in figure 6.6.

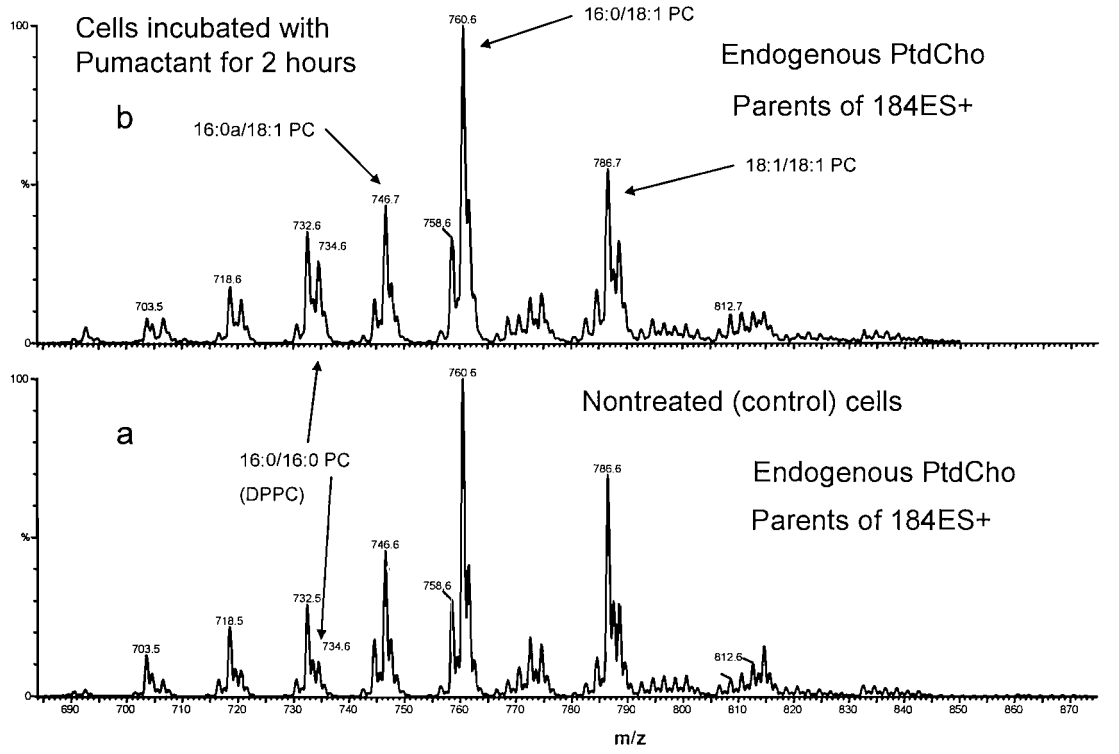

Figure 6.6: Endogenous Jurkat cell PtdCho for (a) non-treated cells and (b) cells treated with Pumactant for two hours

Jurkat cell PtdCho consisted predominantly of monounsaturated species (PC16:0/18:1, PC18:1/18:1 and PC16:0a/18:1) with PC16:0/18:1 as the dominant species (figure 6.6a). Following a 2 hour incubation, Jurkat cell DPPC has increased whilst the remaining PtdCho species remain unchanged (figure 6.6b). The peak corresponding to bodipy PtdCho (m/z 882) was not detectable above background noise in the spectrum.

Jurkat cell PtdCho molecular species data were transformed using the macro developed in the laboratory (section 2.2.2) and the ion intensities for the major PtdCho molecular species selected (given in table 2.3 section 2.11.4). These were then used to determine PtdCho composition at each of the time points (figure 6.7).

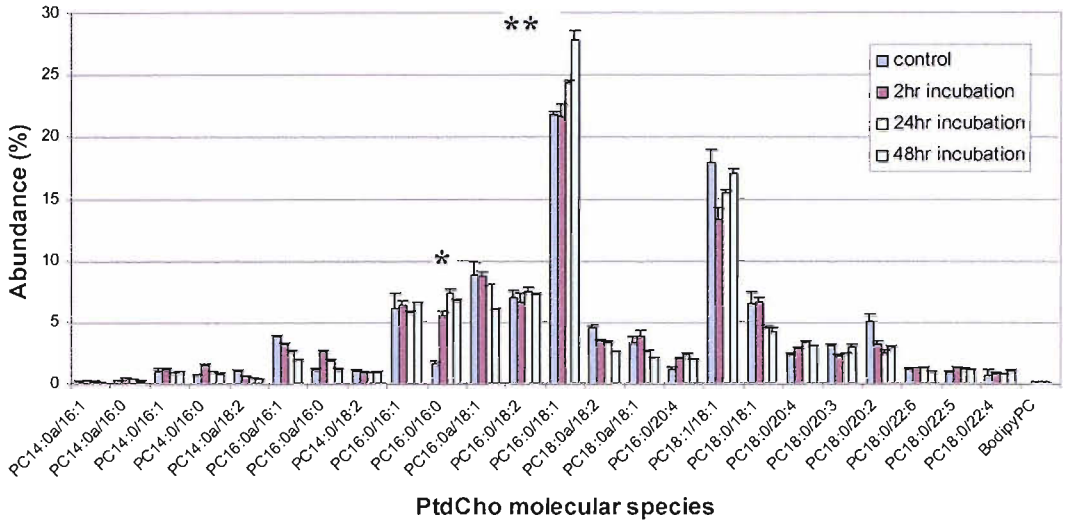

Figure 6.7: Endogenous PtdCho molecular species composition of Jurkat cells following 2, 24 and 48 hour incubations with labelled Pumactant. Result = mean (N=3) ± S.D. *PC16:0/16:0; P < 0.001 Control vs 2, 24 and 48 hours, **PC16:0/18:1; P < 0.001 Control vs 24 and 48 hours.

Incubation with exogenous Pumactant resulted in an increase in DPPC by two hours relative to control (from 1.5 ± 0.25 to 5.5 ± 0.33%). This increase was maintained for 48 hours but not increased. Between 2 and 48 hours, the proportion of PC16:0/18:1 had increased from 22 ± 0.94 to 28 ± 0.76. This presumably occurred to counter the effects of inserting a short chain disaturated species into the membrane and the consequences on membrane fluidity. Bodipy PtdCho was not detectable in the cellular PtdCho pool at any of the time points. However, given that the bodipy was present in very small quantities in the labelled Pumactant it may either be present but below the threshold of detection or have been metabolised or alternatively not taken up into the cell membrane.

Comparison of mass spectra showing endogenous and deuterated PtdCho at 24 hours revealed significant metabolism of the labelled DPPC predominantly to PC16:0/18:1 (figure 6.8).

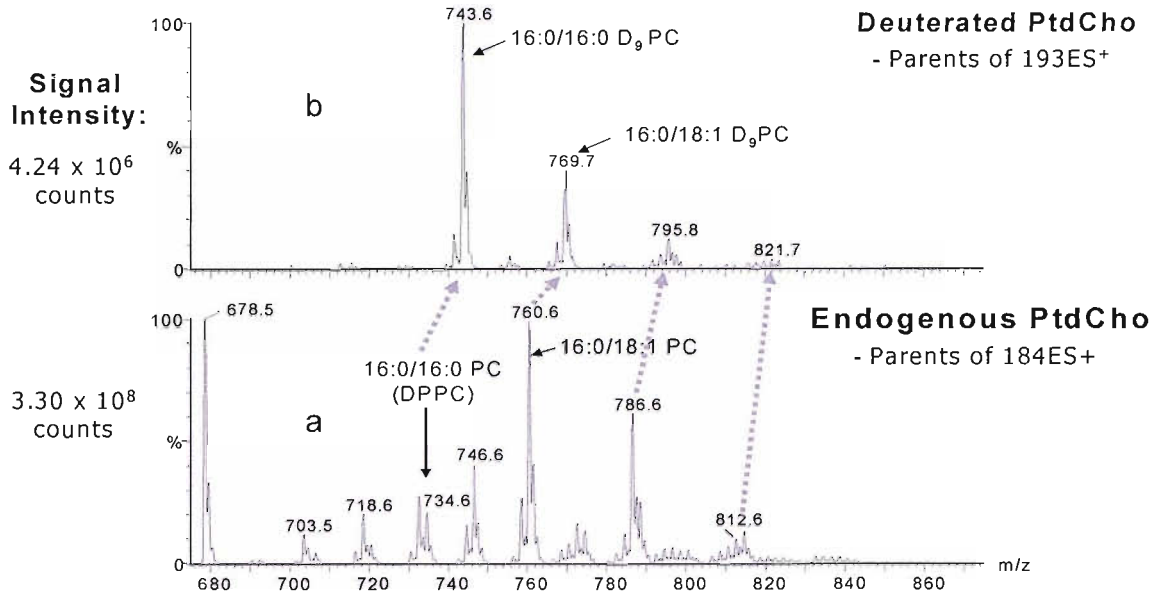

Figure 6.8: Mass spectra showing Jurkat cell (a) endogenous PtdCho and (b) deuterated PtdCho molecular species following 24 hour incubation with labelled Pumactant

Molecular species composition data for deuterated PtdCho (precursors of m/z + 193) was also calculated for 2, 24 and 48 hour time points (figure 6.9) using the macro developed in the laboratory (figure 6.9).

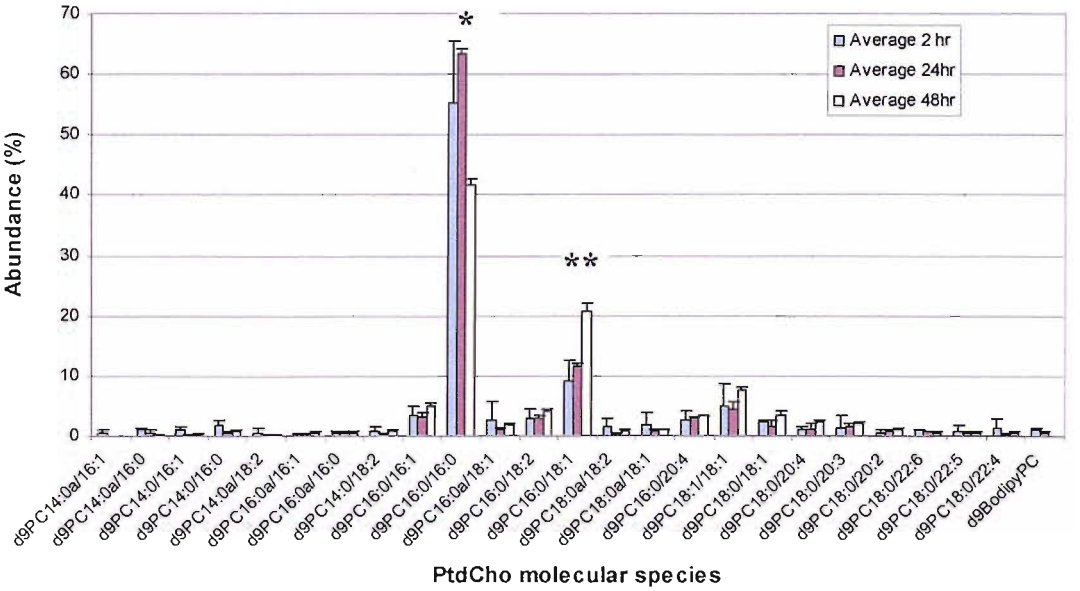

Figure 6.9: [*methyl-d*$_9$]PtdCho composition of Jurkat cells follow 2,24 and 48 hour incubations with labelled Pumactant. Results = mean (N=3) ± S.D. *d9PC16:0/16:0; P < 0.001 24 vs 48 hours, **d9PC16:0/18:1; P < 0.001 48 vs 2 and 24 hours.

Pumactant DPPC metabolism was determined at each time point by ratio of the sum of the ion intensities of the non-DPPC molecular species containing deuterium label (see figure 6.8b) to the sum of all the deuteriated PtdCho species (including DPPC). By 24 hours, 36.5 ± 0.8% of D_9 labelled DPPC had been metabolised predominantly to PC16:0/18:1. This increased to 58.3 ± 1.1% by 48 hours. A poor signal response following 2 hour incubations resulted in the greater variation observed between replicates.

The changes in cell PtdCho composition following Pumactant incubation appeared relatively minor. What was not clear was whether this small change was due to limited availability of exogenous DPPC or to tight regulation of membrane composition by the cells. The availability of exogenous DPPC relative to the quantity of Jurkat cell PtdCho was therefore calculated. The quantity of membrane PtdCho in the non-treated cells was determined by comparing the sum of the ion intensities for cellular PtdCho to the ion intensity corresponding to a known quantity of DMPC internal standard (a non-physiologic molecular species (present at m/z 678)) which had been added to the cells prior to total lipid extraction. Cellular PtdCho was 3.2 ± 0.7 nmol per $1x10^6$ cells.

Pumactant is 70% DPPC by weight, therefore 70g in every 100g is DPPC. Hence, in 300nmol Pumactant phospholipid (the amount added to $1x10^6$ cells) 210nmol is DPPC. The ratio of exogenous DPPC to Jurkat cell PtdCho was therefore 66 to 1. Given this 65 fold excess in available exogenous DPPC, it can be concluded that the small change in cell composition must be due to tight regulation of cellular PtdCho composition rather than a lack of available substrate given such a vast excess of extracellular DPPC. This observation is further supported by the fact that between time = 0 and 48 hours, total cellular PtdCho increased almost six fold from 3.2 ± 0.7 nmol to 19 ± 2.5 nmol. Despite the synthesis of large quantities of membrane PtdCho in the presence of a vast excess of exogenous DPPC, cellular composition remains tightly controlled.

6.3.2.2 Exogenous lipid distribution in Jurkat and B3Z cells by fluorescence detection

Cellular distribution of bodipy labelled PtdCho was determined by fluorescence confocal microscopy. Both Jurkat cells and B3Z cells were incubated with bodipy labelled Pumactant for 24 hours. Cells were fixed, incubated with either TO-PRO-3 or propidium iodide (PI) nuclear counter stain and mounted on APES coated slides (section 2.12). Representative cross sectional images for both cell types using x40 are x100 magnification respectively (see figure 6.10a and b).

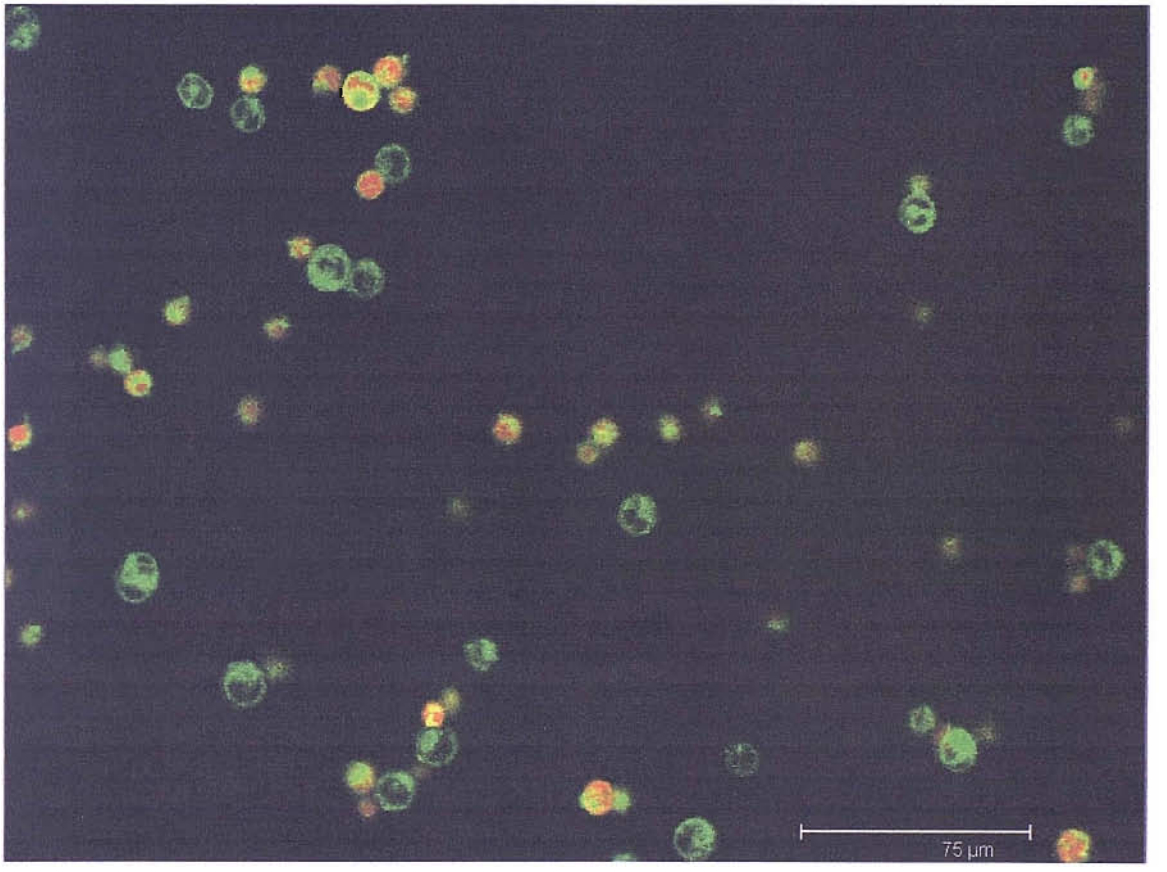

Figure 6.10a: Cross section of Jurkat cells showing incorporation of bodipy labelled PtdCho (green) and Propidium Iodide nuclear counter stain. (x 40 magnification)

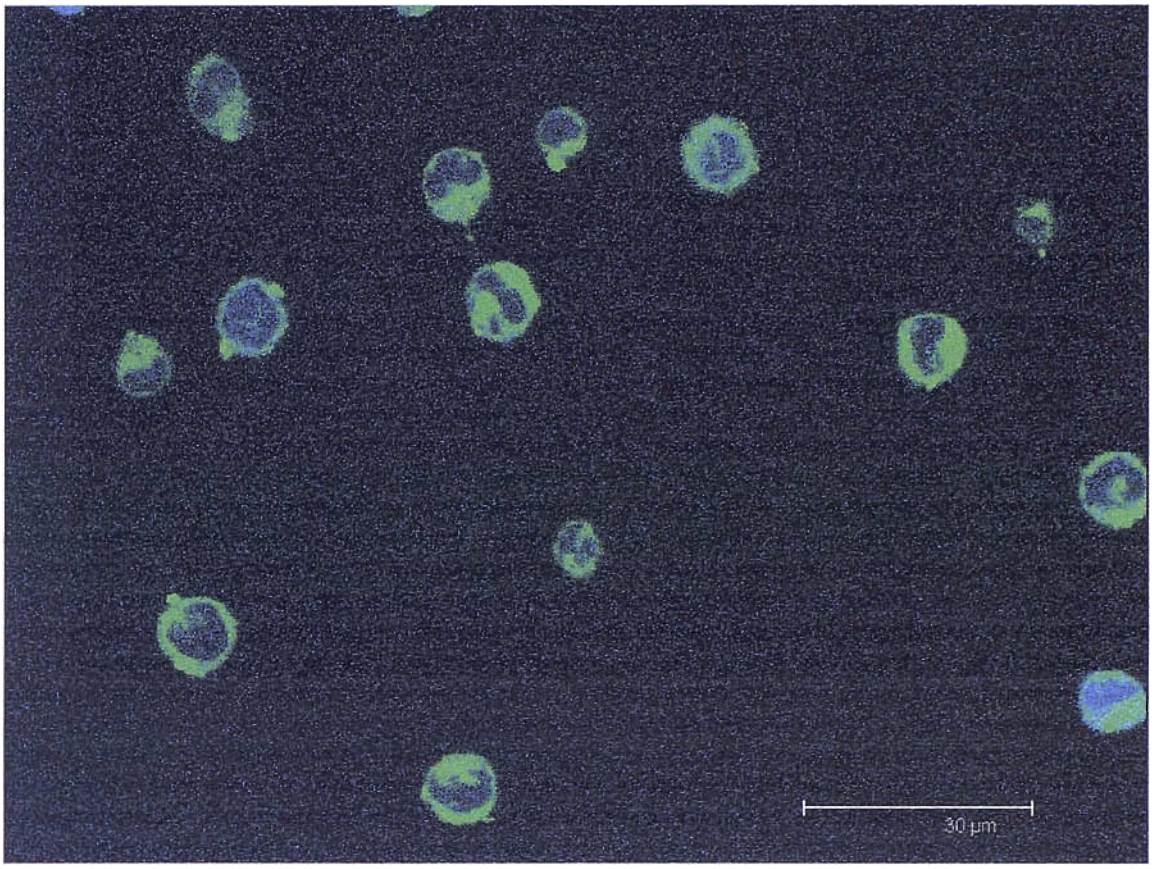

Figure 6.10b: Cross section of B3Z cells showing incorporation of bodipy labelled PtdCho (green) and TO-PRO-3 nuclear counter stain (blue). 100 x magnification

Jurkat cells reflected a typical T-lymphocyte morphology with a very large nucleus (figure 6.10a). Fluorescence microscopy of a cross section of the cell revealed bodipy present both within proximity of the plasma membrane at the periphery and in the cytosol (figure 6.10a). PI nuclear staining was not as successful as TO-PRO-3 staining, having not penetrated all the cell nuclei (figure 6.10a vs 6.10b) nevertheless, bodipy (green) fluorescence is clearly visible in the cytosol as well as at the membrane of all the cells. Like Jurkat cells, B3Z cells also have a large nucleus (figure 6.10b) and BODIPY is again clearly visible in the cell cytosol as well as towards the (plasma membrane) periphery.

The confocal data following incubation of Jurkat and B3Z cells with BODIPY labelled PtdCho highlight the well documented excellent fluorescent properties of the BODIPY fluorophore. Bodipy is present abundantly within the cells despite its absence in PtdCho mass spectra of whole cell lipid extracts (see section 6.3.2.1). The reasons for BODIPY internalisation into the cells is unclear but could reflect metabolism of the BODIPY

labelled PtdCho as observed through [*methyl*-d_9] labelling of Pumactant. The tight control of Jurkat cell membrane PtdCho composition, despite the abundance of exogenous DPPC suggests that alteration of bulk membrane PtdCho is unlikely to be responsible for Pumactant induced T-cell suppression upon stimulation. Consequently the effect of Pumactant on specific cell signalling substrates was investigated.

6.3.3 The impact of Pumactant on Phosphatidylinositol (PtdIns), Phosphatidylinositol-4,5-bis-phosphate (PIP_2) composition in Jurkat cells

Hydrolysis of inositol containing phospholipids is an integrated membrane dependant signalling response and occurs down stream of the initial antigen receptor-driven tyrosine phosphorylation events resulting from antigen-T cell ligation (see section 6.1.3.1). As such it is a potential target system for modulation following cellular exposure to exogenous surfactant phospholipid. The specificity of DAG composition has been shown to be selective for particular PKC isoforms, hence alteration of PIP_2 molecular species composition through incubation with exogenous lipid added to cells offers a plausible mechanism by which Pumactant could alter cellular activation.

6.3.3.1 Evaluation of methods for the isolation of PIP_2

Methods in use for detecting phosphoinositides in cell extracts include receptor displacement assays and radiometric measurements of chromatographically separated de-acylated products following cell labelling with radioisotope precursors[226,227,228]. These techniques are very demanding, and in some cases practically infeasible as when it comes to the labelling of organs and tissues of animals. Perhaps even more significantly, they also do not provide molecular species data.

ESI-MS is now used routinely for the analysis of phospholipids in total cell extracts, however, possibly due to their unique chemical properties, and low abundance phosphoinositides have proven very difficult to detect. A recent publication by Wenk et al[229] described the isolation and analysis of phosphoinositides (PtdIns, PIP and PIP_2) from total lipid extracts by ESI-MS. In their method, phosphoinositides were isolated by acidified total lipid extractions and resuspended in $CHCl_3$/MeOH (1:1) containing 300 mM piperidine. One of the characteristics of PIP_2 which makes it so difficult to isolate

and detect is it's highly amphiphilic nature, combining a very polar headgroup with a hydrophobic tail. The use of piperidine base in the mass spectrometry solvent seems counter intuitive, because this would render the acidic headgroup even less soluble in hydrophobic $CHCl_3$ solvents unless the piperidine is behaving as a phase modifier. More recently Brown et al[230] published an ESI-MS method which included isolation and quantification of phosphatidylinositol trisphosphate (PIP_3). To minimise interference from other phospholipids an initial extraction of bulk lipid using neutral solvents was followed by an acidic extraction in which PIP_2 and PIP_3 was isolated.

The initial aim for this part of the work was therefore to validate and develop a method for the routine extraction and quantification of polyphosphoinositides from cells by ESI-MS/MS. Mass spectrometry parameters were optimised using combined DPPI and $DPPIP_2$ standards prepared at a ratio of 9:1 in $CHCl_3$/MeOH/H_2O (1:2:0.8) solvent. All analyses were conducted by direct injection on a micromass Quattro Ultima with a solvent of $CHCl_3$/MeOH/H_2O (9:9:2 v/v), 30 mM piperidine. An example spectrum is given in figure 6.11:

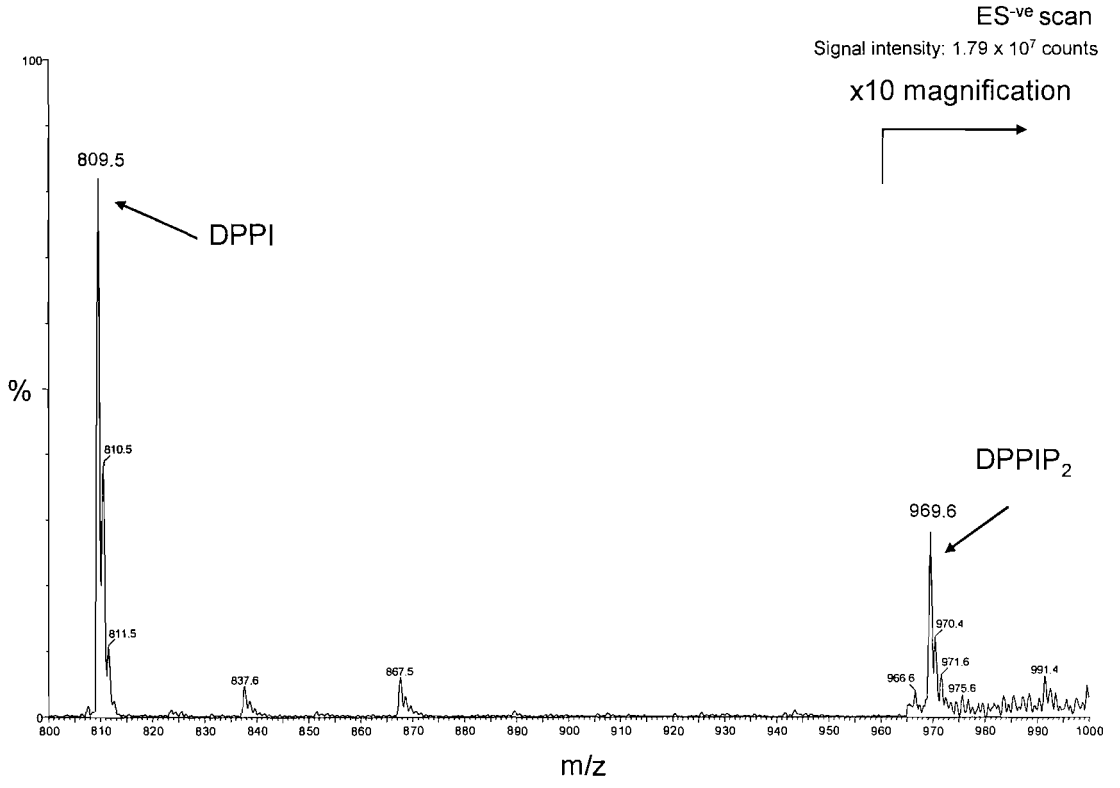

Figure 6.11: Negative ionisation mass spectrum of DPPI (m/z = 809) and $DPPIP_2$ (m/z = 969) standards mixed in a ratio of 9:1

The molecular ion response for standard $DPPIP_2$ was consistently less than 50% that of DPPI for the pure standards. $DPPIP_2$ is theoretically capable of generating a doubly charged ion through loss of a proton from both phosphates on the inositol head group, however the m/2 ion was only ever present as a minor ion in PIP_2 spectra (data not shown).

Following successful detection of pure PtdIns and PIP_2 standards by mass spectrometry, a reliable extraction method was sought. A number of extractions were investigated using the phase transfer catalysts tetrabutylammonium hydroxide (TBAH) and tetrabutylammonium sulphate (TBAS) using both DPPI and $DPPIP_2$ standards as well as B3Z and Jurkat cells (section 2.13.3). In order to compare extraction methods, standards and cells were also extracted using a more conventional acid extraction as described by Wenk et al[229] (section 2.13.2).

Following extraction, product ion spectra for PIP_2 molecular species were investigated for diagnostic ions specific to PtdIns and PIP_2 respectively. An example fragment ion spectrum for the major PIP_2 species in Jurkat cells (18:0/20:4 PIP_2 (m/z 1045 a.m.u.) is given in figure 6.12.

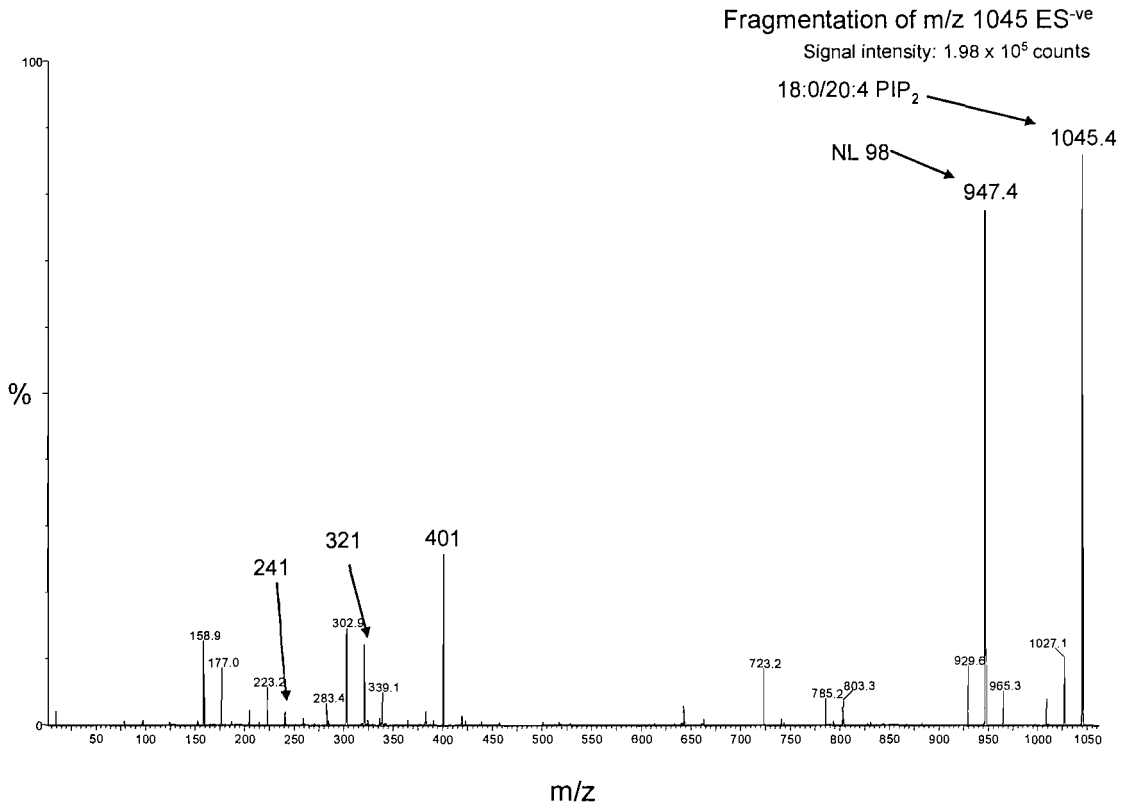

Figure 6.12: Representative fragmentation ion spectrum of m/z 1045 (18:0/20:4 PIP_2) under negative ionisation conditions. NL 98 = phosphate loss (NL = neutral loss), m/z 401 = IP_3-H_2O, m/z 321 = IP_2-H_2O, m/z 241 = IP-H_2O

Diagnostic ion scans used to trace PIP_2 were neutral loss of m/z 98 a.m.u., (which although not specific for PIP_2 was the most readily detectable transition), precursors of m/z 401 a.m.u. (IP_3-H_2O). Precursor ion scanning of m/z 241 a.m.u. (IP-H_2O) was used to determine PtdIns composition.

The task of successfully isolating PIP_2 was considerably more taxing than expected. Whereas pure standards were relatively easy to detect, isolating either standard or endogenous PIP_2 from cell extracts was non-trivial. One explanation for the poor recovery of PIP_2 is through binding of the very polar headgroup attaches itself to polar surfaces such as the hydroxyl groups on the sides of glass tubes used during lipid extraction and binding to metal surfaces such as the capillary of the mass spectrometer. To minimise PIP_2 losses in this way, all glassware was deactivated through silination (section 2.13.1). However, subsequent test extractions using silinated glassware did not improve PIP_2 recovery.

Besides the very polar head group, the other problem that has to be dealt with is the highly amphiphilic nature of the PIP_2 molecule. This property, which makes PIP_2 ideally suited to hydrophilic/ hydrophobic interfaces (such as the membrane bi-layer) complicates partitioning from the aqueous to the organic phase during extractions.

Despite these difficulties, PIP_2 was successfully characterised on a few occasions from acidified lipid extracts of cells following thorough cleansing of the ESI-MS/MS source. Examples of PtdIns and PIP_2 extracted from both B3Z cells and Jurkat cells are shown in figures 6.13 and 6.14:

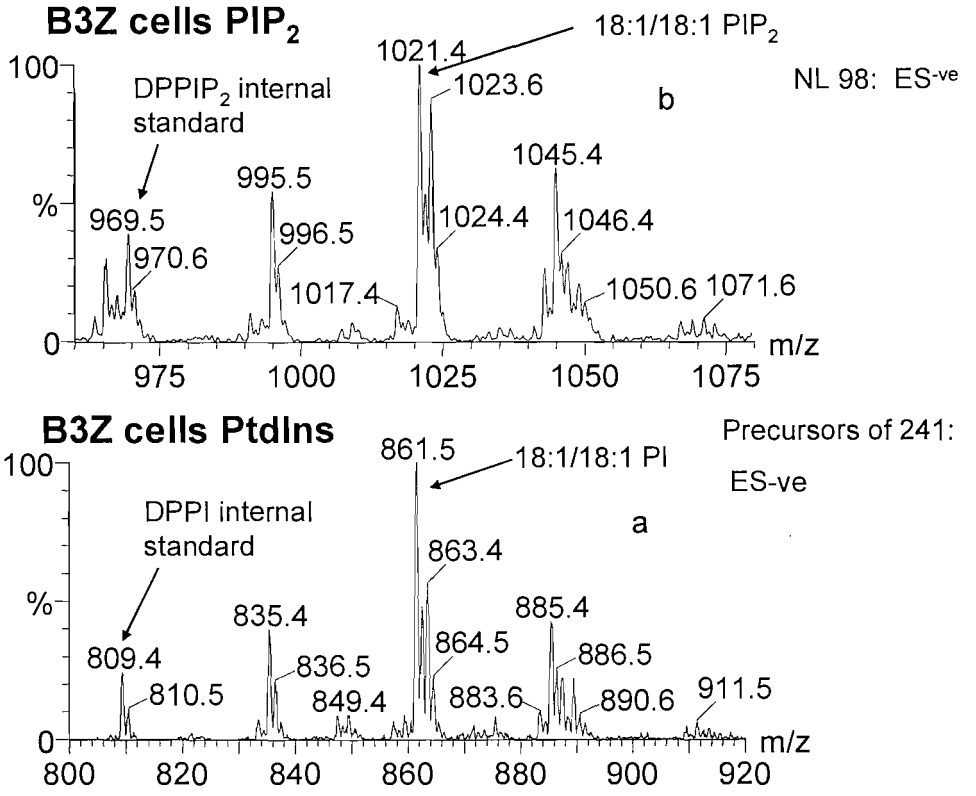

Figure 6.13: Negative ionisation mass spectra of (a) PtdIns and (b) PIP_2 molecular species composition of B3Z cells

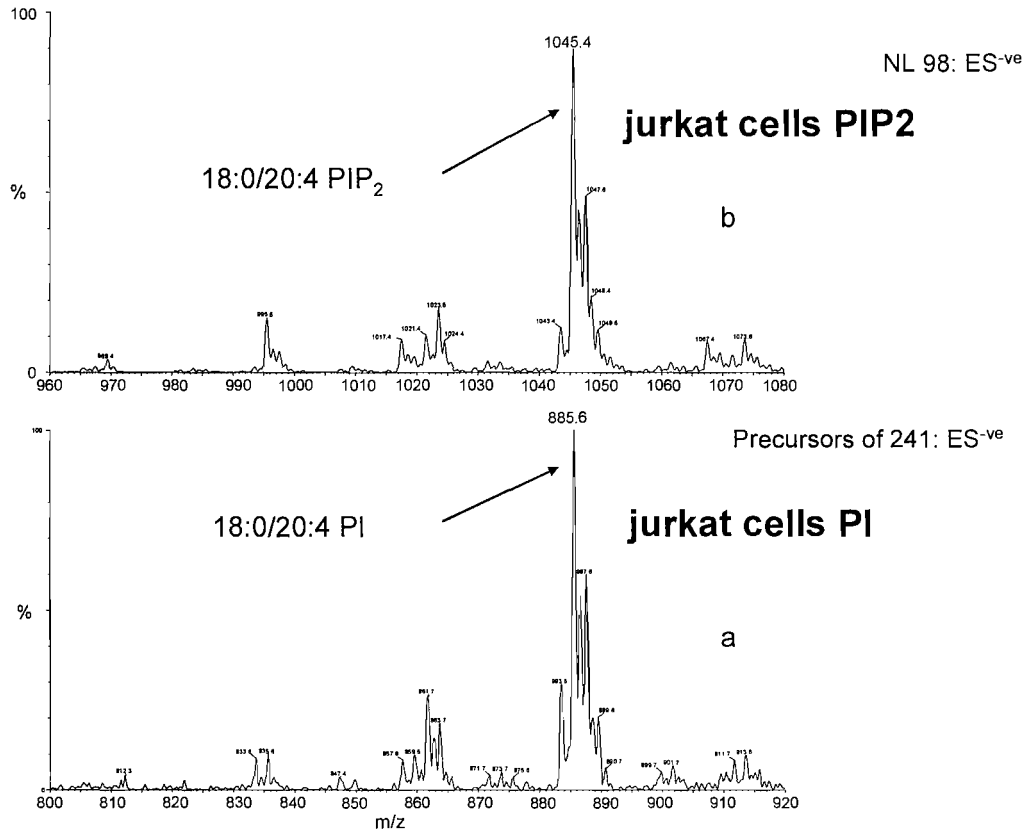

Figure 6.14: Negative ionisation mass spectra showing (a) PtdIns and (b) PIP_2 molecular species composition for Jurkat cells having undergone few (< 10) passages.

PtdIns composition varied considerably not only between cell types (figure 6.13a cf figure 6.14a) but also for the same cell type following several passages (i.e. > 20) (figure 6.14a vs figure 6.15a) ranging from essentially polyunsaturated (18:0/20:4, m/z 885) typically seen *in vivo*[231] to mono-unsaturated 18:0/18:2 (m/z 861). The corresponding PIP_2 molecular species compositions from these initial analyses directly reflected that of PtdIns at all times, with no apparent selectivity for the physiological 18:0/20:4 species suggesting little molecular specificity in PIP_2 synthesis nor hydrolysis to DAG.

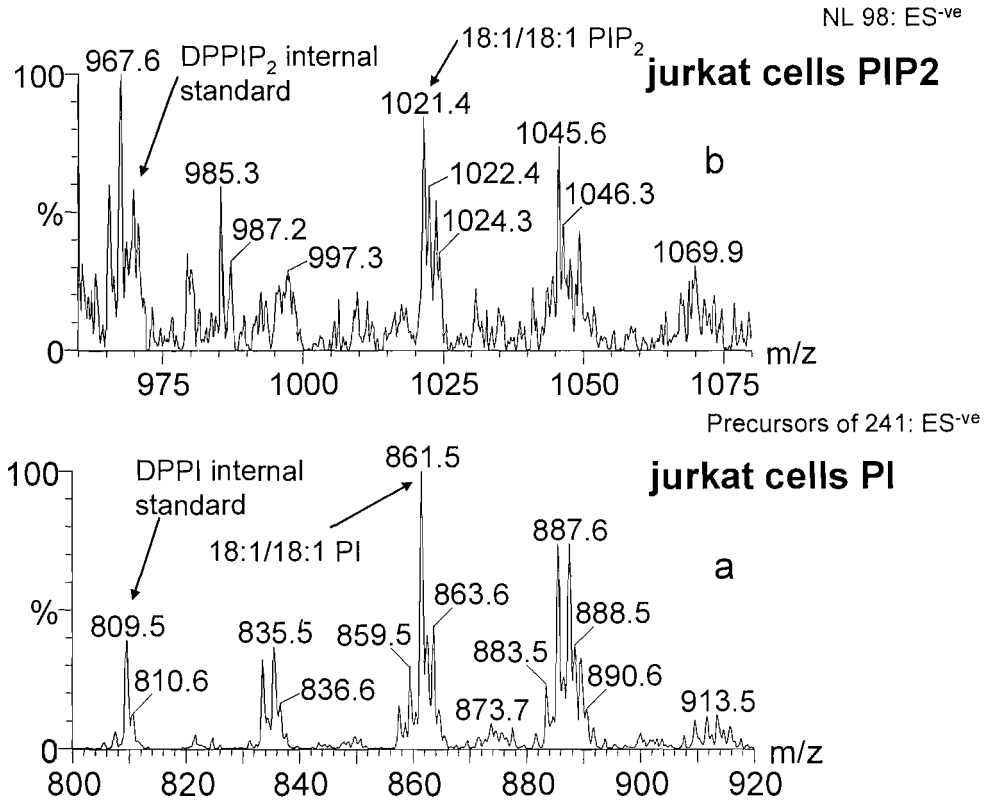

Figure 6.15: Negative ionisation mass spectra showing (a) PtdIns and (b) PIP_2 molecular species composition for Jurkat cells having undergone multiple passages (> 20).

On top of the problems experienced with extracting PIP_2 molecular species, was the added problem of species detection by mass spectrometry. Following successful extraction, repeat analysis of the same sample revealed a progressive decline in PIP_2 signal response following repeat sample infusions (figure 6.16) despite responses to other classes of phospholipid remaining unchanged. Eventually, the PIP_2 signal response was completely lost, even to newly added PIP_2 standard.

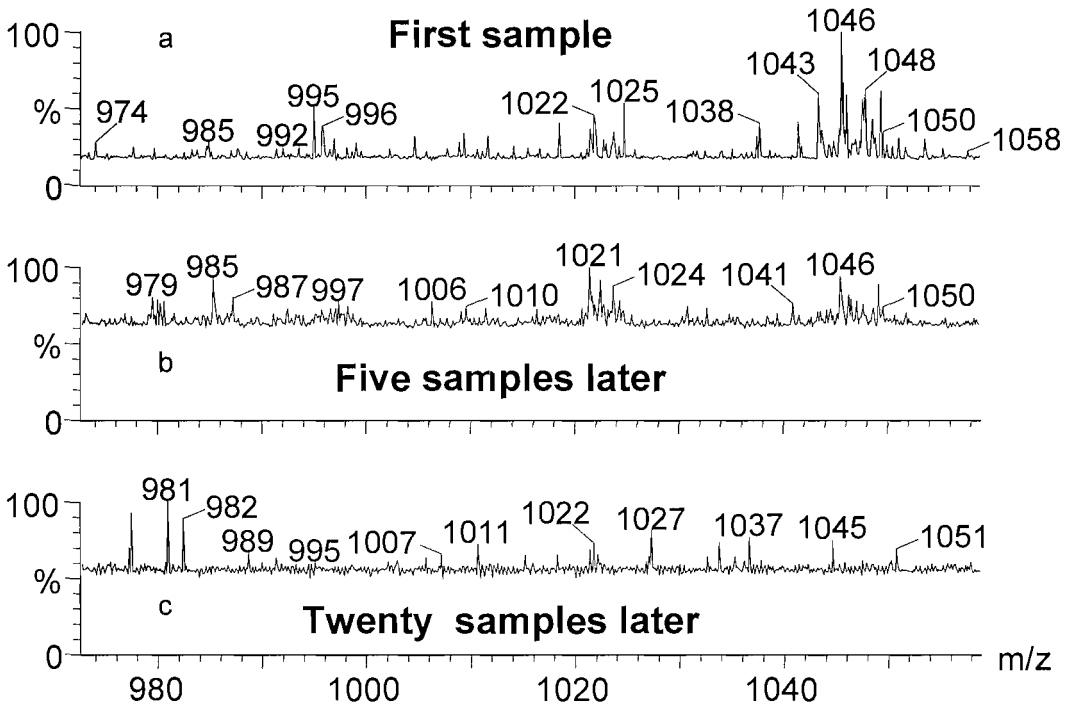

Figure 6.16: Negative ionisation mass spectra showing the ion response to Jurkat cell PIP_2 molecular species (a) for the initial sample following rigorous cleansing of the ESI source and capillary tubing, (b) following 5 previous sample infusions and (c) following 20 previous sample infusions. Loss of signal intensity is denoted by the rising baseline

The most plausible explanation for this time dependent effect is avid binding of PIP_2 to proteolipid deposits within the capillary tubing.

6.3.3.2 Probing the synthesis and metabolism of PtdIns for cells in culture

Further attempts at reliably extracting and quantifying PIP_2 molecular species from whole cells were abandoned because of the numerous complications associated with this highly amphiphilic molecule (section 6.3.3.1). However, because PIP_2 composition always reflected PtdIns for cells in culture and importantly, PtdIns can be reproducibly and quantifiably extracted from cultured cells, it can be reasonably assumed that its composition could be used as a surrogate marker for PIP_2 composition. A method was therefore devised to determine the synthesis and composition of PtdIns molecular species composition in cultured cells as a marker for PIP_2.

Jurkat cell PtdIns synthesis and metabolism was studied by ESI-MS to determine incorporation patterns of deuteriated *myo*-d_6-inositol into molecular species of PtdIns in a protocol directly analogous to the analysis of PtdCho synthesis using d_9 labelled choline (chapter 3).

Cells were incubated with *myo*-d_6-inositol for 1.5, 3, 4.5, 6 and 24 hours (section 2.12.5). Cell pellets were then isolated, washed with PBS, acid extracted and analysed by ESI-MS/MS (sections 2.13.5.2 and 2.13.5.3). Comparison of newly synthesised (precursors of m/z 247) and endogenous (m/z 241) PtdIns molecular species composition permitted calculation of the relative incorporation rates of the deuteriated label. Relative enrichments in turn allowed assessment of whether obligatory remodelling of all newly synthesised PtdIns via lysoPtdIns determined the pattern of PtdIns synthesis.

Endogenous PtdIns composition did not vary significantly with time over the first 6 hours (figure 6.17); the reasons underlying the increased content of PI18:0/20:4 at 24 hours are not clear but could reflect either adaptation to the stage of cell growth or an effect of altered inositol supply.

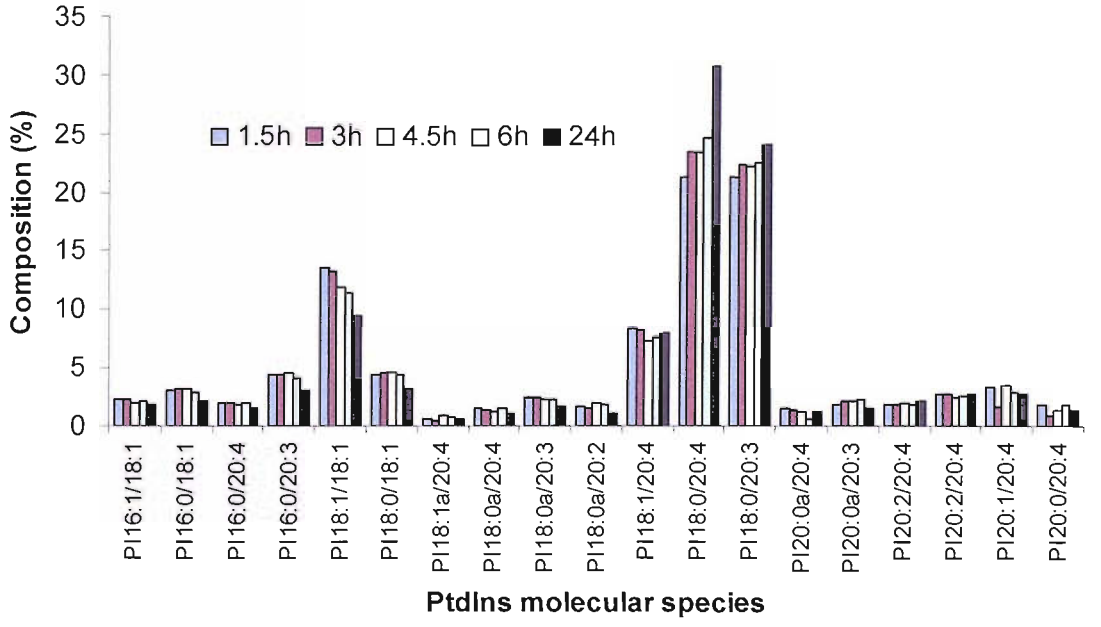

Figure 6.17: Endogenous Jurkat PtdIns molecular species composition following incubation with *myo*-d_6-inositol for 1.5,3,4,5,6 and 24 hours. Results = mean (N=2).

Analysis of the newly synthesised PtdIns molecular species incorporating deuteriated inositol mirrored the endogenous PtdIns composition (figure 6.18).

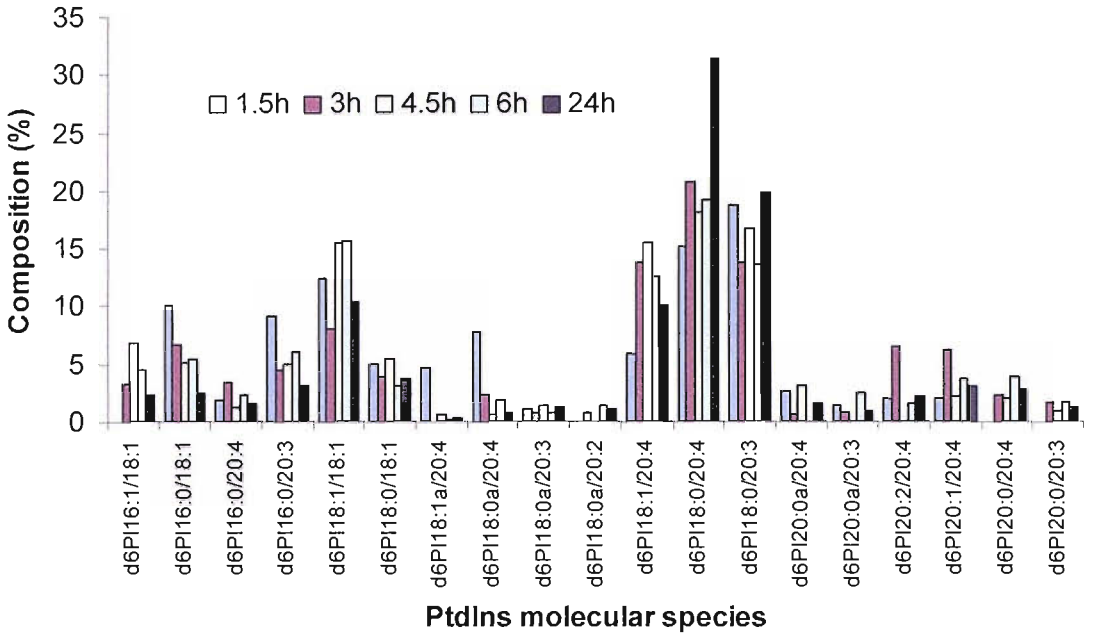

Figure 6.18: Molecular species composition of newly synthesised Jurkat cell PtdIns following incubation with *myo*-d_6 inositol for 1.5,3,4,5 and 6 hours. Results = mean (N=2).

6.3.3.3 Evaluation of Jurkat cell PtdIns molecular species profile following incubation with Pumactant

The PtdIns composition for Jurkat cells incubated for 2, 24 and 48 hours with 300μM Pumactant labelled with [*methyl*-d_9]DPPC and bodipyPtdCho was characterised to determine whether the exogenous surfactant had had any effect on cell membrane PtdIns composition. Samples already prepared in MS solvent following determination of Jurkat cell PtdCho composition (see section 6.3.2.1.2) were used to determine PtdIns composition using diagnostic pre-cursor ion scanning (for product ion m/z 241) in negative ionisation mode (see figure 6.19).

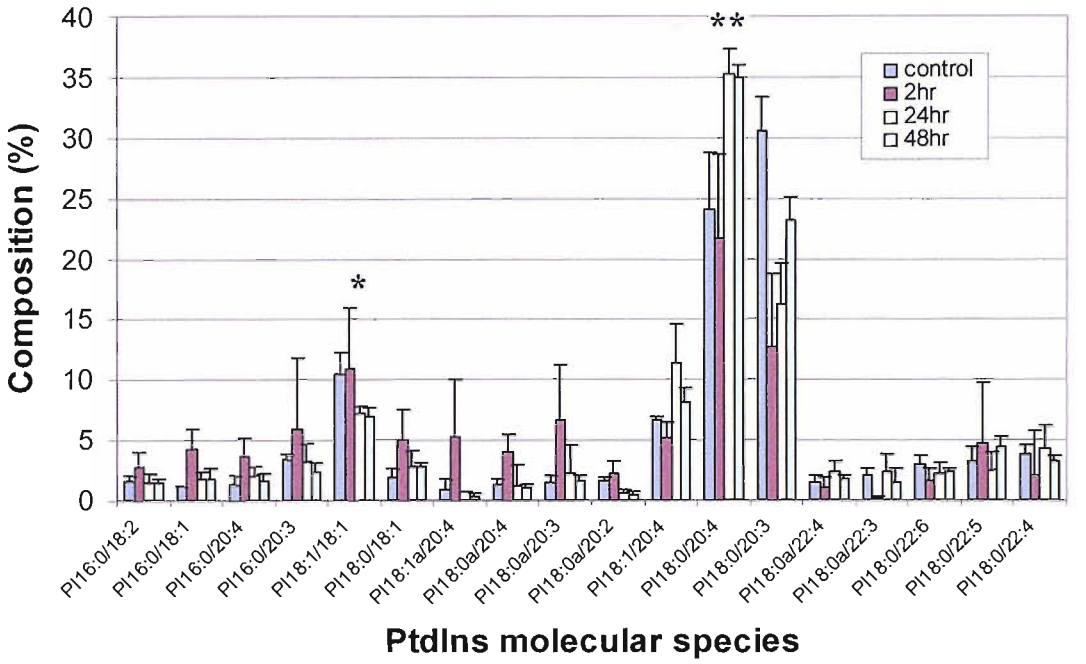

Figure 6.19: Jurkat cell PtdIns molecular species composition following 2, 24 and 48 hr incubations with 300μM Pumactant containing [*methyl-d_9*]DPPC and bodipy PtdCho. Result = mean (N=3) ± S.D. *PI18:1/18:1; P < 0.05 Control vs 24 and 48 hours, **PI18:0/20:4; P < 0.05 Control and 2 hours vs 24 and 48 hours respectively.

PtdIns composition was significantly different for control and 2 hour incubations compared to 24 and 48 hours, being relatively enriched in PI18:1/18:1 where-as by 24 and 48 hours PtdIns composition shifted to become relatively enriched in PI18:0/20:4. Reasons for these changes are unclear but reflect the changes observed in PtdIns composition described above (section 6.3.3.1) for B3Z and Jurkat cultured cells as well as IMR-32 cultured cells.[232]

6.4 Discussion

The pathology associated with lung surfactant was initially recognised in infant respiratory distress syndrome as a quantitative surfactant deficiency.[1] Today, biochemical and biophysical abnormalities have been reported in various lung diseases including ARDS, pneumonia and cardiogenic lung oedema.[45] Whilst surfactant was initially thought to play a role solely in the biophysical behaviour of the lung, its more recently discovered immunomodulatory properties make surfactant a key player in innate and adaptive immunity in the lung. The central event in the generation of both humoral and cell mediated immune responses is the activation and clonal expansion of

T_H cells. T lymphocyte proliferation and cytokine release is an important step in the activation of the adapative immune system in asthma. The T-cell response can induce B lymphocyte differentiation into specific IgE antibody secreting plasma cells. In addition, IL-5 release by T-lymphocytes attracts and activates eosinophils and prolongs their survival. Cell membrane phospholipids play a vital role in determining the sequence of intracellular events, as they are substrates for hydrolysis by phospholipase enzymes[233]. Alterations in intracellular signalling will produce a modification in physiology and ultimate function[234]. Previous studies have shown that the functional capacity of T cells may be modulated by the composition of fatty acids within and the release of membrane phospholipids.

Wilsher et al[38] demonstrated that purified phospholipids inhibited lymphocyte proliferation stimulated by PHA to a greater extent than whole surfactant. Coonrod et al[32] described lysophospholipids and free fatty acids present in surfactant as facilitating enhanced killing by alveolar macrophages. The major component of surfactant, DPPC has long been considered crucial to maintaining alveolar patency during the respiratory cycle however, recent mass spectrometry analysis of sputum samples derived from a number of marsupials[235] revealed a number of unsaturated phospholipid species present at higher concentrations than DPPC, suggesting that the very high concentration of DPPC normally present in mammalian lung surfactant is not necessary for the lungs to maintain patency. In contrast, large surfactant aggregates (LSA) and BALF from patients suffering from ARDS and Pneumonia were found to be depleted in DPPC relative to controls, implicating diminished quantities of the disaturated species in airways disease[6]. In combination, these observations clearly identify the need for assessment of individual phospholipid molecular species on the inflammatory cell response, in particular DPPC.

The B3Z-T cell assay offers distinct advantages over conventional methods for measuring cell activation. Firstly, the clonal B3Z-T cell receptor is activated by direct addition of antigen (OVA peptide) to the cell culture without requiring antigen presentation by an APC. This interaction is cognate as would occur between antigen and T-cells *in vivo*, thus negating the need to activate the receptor with anti-TCR antibodies furthermore, the expression of the lacZ gene upon TCR-activation gives a quick and reliable readout of T-cell activation, thus abolishing the need for time consuming assays to detect markers of cell proliferation (e.g. IL-2.).

Suppression of B3Z cell activation was observed irrespective of whether the cells had been pre-incubated with Pumactant or not (figure 6.3) implying a direct and immediate effect of surfactant phospholipid on cellular activation with little time for altering cell membrane composition. This hypothesis was strengthened by evidence of very tight control in PtdCho cell membrane composition exercised by Jurkat cells in culture (figure 6.7) despite the wide availability of exogenous lipid substrate.

In contrast, visualisation of exogenous lipid distribution using a BODIPY labelled PtdCho fluorophore suggested wide spread coverage both of the cell cytosol and plasma membrane periphery (figures 6.10a and 6.10b). These observations question the validity of BODIPY PtdCho as a reliable marker of DPPC particularly as the two have very different physical characteristics. Nevertheless, the widely cytosolic distribution of bodipy in both B3Z and Jurkat cells was unexpected. Bodipy is hydrophobic, unlike the majority of fluorescent dyes emitting in the visible light region such as the polar fluorescent dye NBD and has been used in a number of studies of the structure and function of membranes and individual lipids.[225] Studies of bodipy insertion into artificial membranes revealed that although BODIPY had a clear tendency to locate in the polar head group region of the bilayer, it was less prevalent than the polar fluorophores NBD and dansyl.[236] Moreover, membrane depth analysis of BODIPY PtdCho when BODIPY was attached to the end of a C_{12} acyl chain, revealed two locations for the BODIPY moiety, one of which showed the fluorescent group deeply buried in the membrane bi-layer.[236] Analysis of the deuteriated cell PtdCho molecular species revealed substantial metabolism of incorporated [*methyl-*d_9]DPPC following 24 hour incubation, it is therefore possible that BODIPY PtdCho could have been catabolised during the 24 hour incubation period thus accounting for the widespread distribution of the fluorophore.

If changes in bulk membrane composition do not explain the changes in cellular activation, it is possible that direct impairment of TCR-antigen ligation or specific changes to cell signalling substrates could be implicated or even perhaps local specific perturbations of plasma membrane composition. Various attempts were made at isolating pure plasma membrane fractions from whole cells to try to answer this question without success. The lengthy complex procedures required for isolating and purifying plasma membranes make it impossible to guarantee retention of any

selectively incorporated exogenous lipid, nor to prevent its selective degradation during processing.

As a membrane signalling molecule, PIP_2 is potential target for molecular species modification brought about through localised changes in plasma membrane composition and recent publications have demonstrated the feasibility of measuring phosphoinositides by ESI-MS/MS[229,237]. PIP_2 molecular species composition is very tightly regulated by mammalian cells *in vivo*[232] a finding which is not altogether unsurprising given that DAG acyl chain molecular species composition has been found to determine the PKC isoform activated.[216] Although reliable and reproducible quantification of PIP_2 was never achieved, successful extraction and determination of PIP_2 and PtdIns for cells in culture revealed both a lack of control of PIP_2 molecular species regulation but nevertheless a close agreement between PtdIns and PIP_2 composition (figures 6.13 – 6.15). Moreover, newly synthesised PtdIns composition was found to reflect newly synthesised PtdIns over a 24 hour period (figures 6.17 and 6.18) with little evidence of a requirement for acyl remodelling to generate equilibrium PtdIns composition from newly synthesised material.

In contrast, endogenous PtdIns composition was found to alter significantly between 2 and 24 hours following incubation with Pumactant reducing in PI18:1/18:1 and increasing in PI18:0/20:4 and PI18:0/20:3. However, results from a repeat experiment in which PtdIns composition was measured at 24 hours following Pumactant incubation vs control showed no alteration in PtdIns composition (data not shown) suggesting that the altered PtdIns composition is more likely to be dependant on factors including the batch of cells used,, the difference in passage number, the fatty acid composition of a particular batch of fetal calf serum used or the state of cell nourishment. Taken together these results demonstrate the significant differences between cell lines and primary cells and the problems encountered when trying to extrapolate the results from one to the other. Clearly very tight control will be required over the origins of cell lines, the number of passages used, even the nutritional status, including the level of confluence in order to validate the results obtained from cells in culture in future.

Chapter 7
General Discussion

7.1 General discussion

Asthma is the most common chronic disease affecting children. Together with the atopic disorders of eczema and allergic rhinitis, they constituted a third of all chronic disorders 30 years ago[238]. The consequences on health, career attainment and health economic burden on communities is escalating at an alarming rate and must be a cause for major concern. The increased diversity of genes influencing allergen presentation, combined with the enormous increase in the range of allergens to which individuals have been exposed over the past few decades, means that there is a far higher probability that an allergic reaction will be induced. If genetic and environmental diversity is the explanation for the remarkably wide variations in prevalence of atopy throughout the world, then it will become increasingly more difficult to identify intervention strategies that will have any impact on this phenomenon. In the end, the future of atopy prevention may well rest with immune modulation and control of the environment. In the case of airways diseases (including asthma), the impact of surfactant abnormalities are becoming more and more apparent along with the need to develop fast acting therapies which are non-invasive and easy to administer. One of the major draw backs to developing surfactant therapy has been its extortionate cost. For instance, Survanta® (a bovine lung surfactant extract (section 1.9.1.1)) used to treat NRDS which is instilled by endobronchial tube at a dose of $100mgkg^{-1}$ body weight, costs £300 per 200 mg of phospholipid[239]. This would amount to over £10,000 per treatment for an adult (assuming a body mass of 70 kg). In the case of animal surfactant extracts, this problem is compounded by the potential deleterious health effects associated with using an animal derived product. In this respect, the discovery that prophylactic administration of Pumactant as a novel dry powder could obliterate the early phase asthmatic response[9] heralded a potential breakthrough for surfactant therapy as an adjunct therapy for airways disease. Pumactant, being purely lipid based is considerably cheaper to manufacture than surfactant containing recombinant proteins and animal based surfactants. The large clinical improvement witnessed in the asthma trial provided the basis for the experimental work described in this thesis and the possible sites of action of Pumactant in the lung directed the areas of research investigated.

Determination of the physical characteristics of Pumactant interactions required the ability to generate large reproducible doses of material consistent with the doses found

to elicit a clinical effect[9]. The increased efficacy in the administration of larger doses of surfactant was demonstrated when guinea pigs suffering asthma like symptoms following treatment with sulphur Mustard aerosol showed greater improvement with increasing bolus doses of Curosurf[240]. The target dose for Pumactant dry powder was outside the scope of any of the dry powder inhalers currently available. Whilst custom built devices had been constructed for the asthma clinical trial[9], these required active inhalation by the patient from a spacer device (a chamber positioned between the actuation device and the patient from which the patient inhales). A device was therefore developed (the VPAG), capable of actively delivering metered doses of both respirable and amorphous Pumactant (chapter 4) under a variety of actuation conditions. This device is now being patented[177].

Pumactant is more likely to be administered as a rescue therapy following the onset of an asthma attack rather than prophylactically. Once inhaled, it will adsorb to the surface of the airways which are lined with surfactant which have been compromised by plasma exudates including proteins[241] with well characterised surfactant inhibitory properties[66]. Physical interactions between Pumactant and endogenous surfactant were modelled using a Wilhelmy balance (chapter 5) using physiological conditions and surface tension measurements were carried out at body temperature and saturated humidity. High humidity significantly reduced surface activity, an effect which was reversible. This was supported by surface activity measurements reported for pure DPPC at low and high humidity by Colacicco et al[203] which showed that the addition of cholesteryl esters (also found in lung lavage)[242] or longer chain PtdCho could improve surface activity *in* vitro. The capacity of pumactant to counter the effects of inhibitory proteins was also assessed *in vitro* using the Wilhelmy balance. Whilst Pumactant was shown to counter the effects of BSA, the impact of Pumactant on the inhibition caused by plasma proteins was less clear.

Pumactant, as a natural product, does not exhibit any of the side effects associated with steroids, nevertheless, the long term effects of persistent exposure of the lungs to exogenous lipid are not known. Using a combination of ESI-MS/MS and stable isotope labels, methods were developed for the determination of phospholipid synthesis in metabolism in liver and lung in humans *in vivo* for the first time.[243] Using this now well established methodology, it would be possible to monitor the metabolism of exogenous

phospholipid labelled with non toxic deuterium isotope as part of a larger scale clinical trial to determine the efficacy of Pumactant as a long term asthma therapy.

The ability of surfactant components to modulate immune cell function is well known, however, the tools and techniques required to elucidate mechanisms of action of specific surfactant components are only now coming to light. The combination of powerful ESI-MS/MS techniques combined with stable isotope labelling of whole cells has made it possible to determine the extent of exogenous lipid incorporation into whole cell membranes PtdCho molecular species along with interrogation of potential knock on effects on PtdIns cell signalling lipids.

7.2 Future work

Preliminary experiments showed that the VPAG device is capable of actuating respirable Pumactant using freshly prepared micronised material. Particle size distribution measurements can now be carried out to determine whether the device is capable of de-aggregating the powder to generate a respirable dose. With the development of ESI-MS/MS methodology, the effects of long term persistent exposure to Pumactant on surfactant synthesis and metabolism in humans can be explored. Hopefully these measurements could be interfaced with MRI imaging techniques which are able to visualise deuterium thus negating the need for radio labels.

Pumactant is unlikely to be the ideal therapy for the treatment of adult airways disease because it does not contain the associated surfactant specific proteins which have been shown to be crucial for both the organisation of surfactant at the air-liquid interface (SP-B and SP-C) as well as in modulation of the immune response (SP-A and SP-D). More work on screening Pumactant against plasma inhibitors to test efficacy is required, with particular attention being paid to both the surfactant specific PtdCho molecular species as well as the longer chain PtdCho species.

The impact of DPPC on the B3Z cell response clearly highlights the requirement for further investigation into the impact of individual phospholipid molecular species on inflammatory cell properties and the B3Z assay provides a tool for rapid screening of these species. The effect of the two other significant phospholipid molecular species

specific to lung surfactant 16:0/14:0 and 16:0/16:1 PtdCho particularly warrant further investigation.

As exogenous DPPC has not been found to alter bulk membrane phospholipid composition, the other possible target sites warrant investigation. Of particular interest is the possibility of selective incorporation of exogenous lipid into plasma membranes. A novel two phase aqueous method[244] for the isolation of plasma membranes has recently been exploited in our laboratory. This method enabled the characterisation of plasma membranes by ESI-MS/MS. Combining this method with deuterium labelling of exogenous lipid would enable determination of any selective enrichment.

Other possible targets for exogenous phospholipid include direct impedance of antigen T-cell receptor signalling. Phosphorylation of Zap 70 is one of the initial signalling events following antigen T-cell receptor ligation. The phosphorylation state of Zap70 following activation of T cells could be determined using PhosphoZap70 antibodies. Depending on the outcome, the interaction between the T-cell receptor and antigen can be directly probed by Fluorescence Resonance Energy Transfer (FRET) analysis using the B3Z cell assay with fluorescently labelled OVA and accompanying FRET partner on the TCR B chain. Initially co-localisation between, two fluorophores could be assed before checking for close proximity interactions required for FRET to occur.

In summary, the mechanisms of action which enabled the novel synthetic dry powder lipid based surfactant Pumactant to obliterate the early phase asthmatic response when prophylactically administered to mild asthmatics prior to bronchial provocation remains unknown. However, the various methods developed to probe the Pumactant-endogenous surfactant interaction pave the way for future research in this area and should ideally be implemented to compliment future Pumactant based clinical trials, particularly when the efficacy of Pumactant as a rescue therapy is assessed. Moreover, the delivery device developed for the administration of dry powder Pumactant could also be employed in future clinical trials.

List of References

(1) Avery, M. E.; Mead, J. Surface Properties in Relation to Atelectasis and Hyaline Membrane Disease. *AMA. J. Dis. Child* **1959,** *97,* 517-523.

(2) Heeley, E. L.; Hohlfeld, J. M.; Krug, N.; Postle, A. D. Phospholipid Molecular Species of Bronchoalveolar Lavage Fluid After Local Allergen Challenge in Asthma. *American Journal of Physiology-Lung Cellular and Molecular Physiology* **2000,** *278,* L305-L311.

(3) Dargaville, P. A.; South, M.; McDougall, P. N. Surfactant Abnormalities in Infants With Severe Viral Bronchiolitis. *Arch. Dis. Child* **1996,** *75,* 133-136.

(4) Lusuardi, M.; Capelli, A.; Carli, S.; Tacconi, M. T.; Salmona, M.; Donner, C. F. Role of Surfactant in Chronic Obstructive Pulmonary Disease: Therapeutic Implications. *Respiration* **1992,** *59 Suppl 1,* 28-32.

(5) Griese, M.; Birrer, P.; Demirsoy, A. Pulmonary Surfactant in Cystic Fibrosis. *Eur. Respir. J.* **1997,** *10,* 1983-1988.

(6) Schmidt, R.; Meier, U.; Yabut-Perez, M.; Walmrath, D.; Grimminger, F.; Seeger, W.; Gunther, A. Alteration of Fatty Acid Profiles in Different Pulmonary Surfactant Phospholipids in Acute Respiratory Distress Syndrome and Severe Pneumonia. *Am. J. Respir. Crit Care Med.* **2001,** *163,* 95-100.

(7) Gunther, A.; Ruppert, C.; Schmidt, R.; Markart, P.; Grimminger, F.; Walmrath, D.; Seeger, W. Surfactant Alteration and Replacement in Acute Respiratory Distress Syndrome. *Respir. Res.* **2001,** *2,* 353-364.

(8) Nakos, G.; Pneumatikos, J.; Tsangaris, I.; Tellis, C.; Lekka, M. Proteins and Phospholipids in BAL From Patients With Hydrostatic Pulmonary Edema. *Am. J. Respir. Crit Care Med.* **1997,** *155,* 945-951.

(9) Babu, K. S.; Woodcock, D. A.; Smith, S. E.; Staniforth, J. N.; Holgate, S. T.; Conway, J. H. Inhaled Synthetic Surfactant Abolishes the Early Allergen-Induced Response in Asthma. *Eur. Respir. J.* **2003,** *21,* 1046-1049.

(10) Siuzdak, G. *Mass Spectrometry for Biotechnology*; Academic Press: 1996.

(11) Harwood, J. L. Lung Surfactant. *Prog. Lipid Res.* **1987,** *26,* 211-256.

(12) Hamm, H.; Fabel, H.; Bartsch, W. The Surfactant System of the Adult Lung: Physiology and Clinical Perspectives. *Clin. Investig.* **1992,** *70,* 637-657.

(13) Schlame, M.; Casals, C.; Rustow, B.; Rabe, H.; Kunze, D. Molecular Species of Phosphatidylcholine and Phosphatidylglycerol in Rat Lung Surfactant and Different Pools of Pneumocytes Type II. *Biochem. J.* **1988,** *253,* 209-215.

(14) von Neergard, K. Neue Auffassungen Uber Einen Grundbegriff Der Atemmechanik. *Z Ges Exp Med* **1929,** *66,* 373-383.

(15) answers.com. Surface tension. http://www.answers.com/topic/surface-tension . 2006.
Ref Type: Internet Communication

(16) Clements, J. A. Surface Tension of Lung Extracts. *Proc. Soc. Exp. Biol. Med.* **1957,** *95,* 170-172.

(17) Frerking, I.; Gunther, A.; Seeger, W.; Pison, U. Pulmonary Surfactant: Functions, Abnormalities and Therapeutic Options. *Intensive Care Med* **2001,** *27,* 1699-1717.

(18) Perez-Gil, J.; Keough, K. M. Interfacial Properties of Surfactant Proteins. *Biochim. Biophys. Acta* **1998,** *1408,* 203-217.

(19) Takahashi, A.; Fujiwara, T. Proteolipid in Bovine Lung Surfactant: Its Role in Surfactant Function. *Biochem. Biophys. Res. Commun.* **1986,** *135,* 527-532.

(20) Yu, S. H.; Possmayer, F. Reconstitution of Surfactant Activity by Using the 6 KDa Apoprotein Associated With Pulmonary Surfactant. *Biochem. J.* **1986,** *236,* 85-89.

(21) Sen, A.; Hui, S. W.; Mosgroberanthony, M.; Holm, B. A.; Egan, E. A. Localization of Lipid Exchange Sites Between Bulk Lung Surfactants and Surface Monolayer - Freeze-Fracture Study. *Journal of Colloid and Interface Science* **1988,** *126,* 355-360.

(22) Palaniyar, N.; Zhang, L.; Kuzmenko, A.; Ikegami, M.; Wan, S.; Wu, H.; Korfhagen, T. R.; Whitsett, J. A.; McCormack, F. X. The Role of Pulmonary Collectin N-Terminal Domains in Surfactant Structure, Function, and Homeostasis in Vivo. *J. Biol. Chem.* **2002,** *277,* 26971-26979.

(23) Bangham, A. D. Lung Surfactant: How It Does and Does Not Work. *Lung* **1987,** *165,* 17-25.

(24) Schurch, S. Surface Tension Properties of Surfactant. *Clin. Perinatol.* **1993,** *20,* 669-682.

(25) Macklem, P. T.; Proctor, D. F.; Hogg, J. C. The Stability of Peripheral Airways. *Respir. Physiol* **1970,** *8,* 191-203.

(26) Enhorning, G.; Holm, B. A. Disruption of Pulmonary Surfactants Ability to Maintain Openness of A Narrow Tube. *Journal of Applied Physiology* **1993,** *74,* 2922-2927.

(27) Jarjour, N. N.; Enhorning, G. Antigen-Induced Airway Inflammation in Atopic Subjects Generates Dysfunction of Pulmonary Surfactant. *American Journal of Respiratory and Critical Care Medicine* **1999,** *160,* 336-341.

(28) Braun, A.; Steinecker, M.; Schumacher, S.; Griese, M. Surfactant Function in Children With Chronic Airway Inflammation. *J. Appl. Physiol* **2004,** *97,* 2160-2165.

(29) Coonrod, J. D.; Jarrells, M. C.; Yoneda, K. Effect of Rat Surfactant Lipids on Complement and Fc-Receptors of Macrophages. *Infection and Immunity* **1986,** *54,* 371-378.

(30) Lyons, C. R.; Ball, E. J.; Toews, G. B.; Weissler, J. C.; Stastny, P.; Lipscomb, M. F. Inability of Human Alveolar Macrophages to Stimulate Resting T- Cells Correlates With Decreased Antigen-Specific T-Cell- Macrophage Binding. *Journal of Immunology* **1986,** *137,* 1173-1180.

(31) Hunninghake, G. W. Immunoregulatory Functions of Human Alveolar Macrophages. *American Review of Respiratory Disease* **1987,** *136,* 253-254.

(32) Coonrod, J. D.; Yoneda, K. Detection and Partial Characterization of Anti-Bacterial Factor(S) in Alveolar Lining Material of Rats. *Journal of Clinical Investigation* **1983,** *71,* 129-141.

(33) Chao, W.; Spragg, R. G.; Smith, R. M. Inhibitory Effect of Porcine Surfactant on the Respiratory Burst Oxidase in Human Neutrophils. Attenuation of P47phox and P67phox Membrane Translocation As the Mechanism. *J. Clin. Invest* **1995,** *96,* 2654-2660.

(34) Cheng, G.; Ueda, T.; Nakajima, H.; Nakajima, A.; Kinjyo, S.; Motojima, S.; Fukuda, T. Suppressive Effects of SP-A on Ionomycin-Induced IL-8 Production and Release by Eosinophils. *Int. Arch. Allergy Immunol.* **1998,** *117 Suppl 1,* 59-62.

(35) Hohlfeld, J.; Knoss, S.; Schael, M.; Fabel, H.; Krug, N. Pulmonary Surfactant Inhibits Expression of HLA-DR and CD69 on Human Eosinophils (Abstract). *Am. J. Respir. Crit Care Med.* **2000,** *161,* A662.

(36) Okumura, M.; Tsuruoka, M.; Isohama, Y.; Kai, H.; Takahama, K.; Miyata, T. Activated Eosinophils Stimulate Phosphatidylcholine Secretion in Primary Culture of Rat Type II Pneumocytes. *Biochem. Mol. Biol. Int.* **1996,** *38,* 569-575.

(37) Ansfield, M. J.; Kaltreider, H. B.; Benson, B. J.; Caldwell, J. L. Immunosuppressive Activity of Canine Pulmonary Surface Active Material. *J. Immunol.* **1979,** *122,* 1062-1066.

(38) Wilsher, M. L.; Hughes, D. A.; Haslam, P. L. Immunoregulatory Properties of Pulmonary Surfactant: Effect of Lung Lining Fluid on Proliferation of Human Blood Lymphocytes. *Thorax* **1988,** *43,* 354-359.

(39) Kremlev, S. G.; Umstead, T. M.; Phelps, D. S. Effects of Surfactant Protein-A and Surfactant Lipids on Lymphocyte-Proliferation In-Vitro. *American Journal of Physiology-Lung Cellular and Molecular Physiology* **1994,** *11,* L357-L364.

(40) Lesur, O.; Mancini, N. M.; Janot, C.; Chabot, F.; Boitout, A.; Polu, J. M.; Gerard, H. Loss of Lymphocyte Modulatory Control by Surfactant Lipid Extracts From Acute Hypersensitivity Pneumonitis - Comparison With Sarcoidosis and Idiopathic Pulmonary Fibrosis. *European Respiratory Journal* **1994,** *7,* 1944-1949.

(41) Fujiwara, T.; Maeta, H.; Chida, S.; Morita, T.; Watabe, Y.; Abe, T. Artificial Surfactant Therapy in Hyaline-Membrane Disease. *Lancet* **1980,** *1,* 55-59.

(42) Ashbaugh, D. G.; Bigelow, D. B.; Petty, T. L.; Levine, B. E. Acute Respiratory Distress in Adults. *Lancet* **1967,** *2,* 319-323.

(43) Bernard, G. R.; Artigas, A.; Brigham, K. L.; Carlet, J.; Falke, K.; Hudson, L.; Lamy, M.; Legall, J. R.; Morris, A.; Spragg, R.; Cochin, B.; Lanken, P. N.; Leeper, K. V.; Marini, J.; Murray, J. F.; Oppenheimer, L.; Pesenti, A.; Reid, L.; Rinaldo, J.; Villar, J.; Vanasbeck, B. S.; Dhainaut, J. F.; Mancebo, J.; Matthay, M.; Meyrick, B.; Payen, D.; Perret, C.; Fowler, A. A.; Schaller, M. D.; Hudson, L. D.; Hyers, T.; Knaus, W.; Matthay, R.; Pinsky, M.; Bone, R. C.; Bosken, C.; Johanson, W. G.; Lewandowski, K.; Repine, J.; Rodriguezroisin, R.; Roussos, C.; Antonelli, M. A.; Beloucif, S.; Bihari, D.; Burchardi, H.; Lemaire, F.; Montravers, P.; Petty, T. L.; Robotham, J.; Zapol, W. The American-European Consensus Conference on Ards - Definitions, Mechanisms, Relevant Outcomes, and Clinical-Trial Coordination. *American Journal of Respiratory and Critical Care Medicine* **1994,** *149,* 818-824.

(44) Clements, J. A. Lung Surfactant: A Personal Perspective. *Annual Review of Physiology* **1997,** *59,* 1-21.

(45) Gunther, A.; Siebert, C.; Schmidt, R.; Ziegler, S.; Grimminger, F.; Yabut, M.; Temmesfeld, B.; Walmrath, D.; Morr, H.; Seeger, W. Surfactant Alterations in Severe Pneumonia, Acute Respiratory Distress Syndrome, and Cardiogenic Lung Edema. *Am. J. Respir. Crit Care Med.* **1996,** *153,* 176-184.

(46) Gregory, T. J.; Longmore, W. J.; Moxley, M. A.; Whitsett, J. A.; Reed, C. R.; Fowler, A. A., III; Hudson, L. D.; Maunder, R. J.; Crim, C.; Hyers, T. M. Surfactant Chemical Composition and Biophysical Activity in Acute Respiratory Distress Syndrome. *J. Clin. Invest* **1991,** *88,* 1976-1981.

(47) Hallman, M.; Spragg, R.; Harrell, J. H.; Moser, K. M.; Gluck, L. Evidence of Lung Surfactant Abnormality in Respiratory Failure. Study of Bronchoalveolar Lavage Phospholipids, Surface Activity, Phospholipase Activity, and Plasma Myoinositol. *J. Clin. Invest* **1982,** *70,* 673-683.

(48) Pison, U.; Seeger, W.; Buchhorn, R.; Joka, T.; Brand, M.; Obertacke, U.; Neuhof, H.; Schmit-Neuerburg, K. P. Surfactant Abnormalities in Patients With Respiratory Failure After Multiple Trauma. *Am. Rev. Respir. Dis.* **1989,** *140,* 1033-1039.

(49) Gunther, A.; Schmidt, R.; Feustel, A.; Meier, U.; Pucker, C.; Ermert, M.; Seeger, W. Surfactant Subtype Conversion Is Related to Loss of Surfactant Apoprotein B and Surface Activity in Large Surfactant Aggregates. Experimental and Clinical Studies. *Am. J. Respir. Crit Care Med.* **1999,** *159,* 244-251.

(50) Veldhuizen, R. A.; McCaig, L. A.; Akino, T.; Lewis, J. F. Pulmonary Surfactant Subfractions in Patients With the Acute Respiratory Distress Syndrome. *Am. J. Respir. Crit Care Med.* **1995,** *152,* 1867-1871.

(51) Gunther, A.; Mosavi, P.; Heinemann, S.; Ruppert, C.; Muth, H.; Markart, P.; Grimminger, F.; Walmrath, D.; Temmesfeld-Wollbruck, B.; Seeger, W.

Alveolar Fibrin Formation Caused by Enhanced Procoagulant and Depressed Fibrinolytic Capacities in Severe Pneumonia. Comparison With the Acute Respiratory Distress Syndrome. *Am. J. Respir. Crit Care Med.* **2000,** *161,* 454-462.

(52) Pison, U.; Tam, E. K.; Caughey, G. H.; Hawgood, S. Proteolytic Inactivation of Dog Lung Surfactant-Associated Proteins by Neutrophil Elastase. *Biochim. Biophys. Acta* **1989,** *992,* 251-257.

(53) Baker, C. S.; Evans, T. W.; Randle, B. J.; Haslam, P. L. Damage to Surfactant-Specific Protein in Acute Respiratory Distress Syndrome. *Lancet* **1999,** *353,* 1232-1237.

(54) Ratjen, F.; Doring, G. Cystic Fibrosis. *Lancet* **2003,** *361,* 681-689.

(55) Djukanovic, R.; Roche, W. R.; Wilson, J. W.; Beasley, C. R. W.; Twentyman, O. P.; Howarth, P. H.; Holgate, S. T. Mucosal Inflammation in Asthma. *American Review of Respiratory Disease* **1990,** *142,* 434-457.

(56) Holgate, S. T. The Rising Trends in Asthma - Introduction. *Rising Trends in Asthma* **1997,** *206,* 1-4.

(57) Gordon, J. R.; Burd, P. R.; Galli, S. J. Mast Cells As a Source of Multifunctional Cytokines. *Immunol. Today* **1990,** *11,* 458-464.

(58) Evans, T. W.; Rogers, D. F.; Aursudkij, B.; Chung, K. F.; Barnes, P. J. Inflammatory Mediators Involved in Antigen-Induced Airway Microvascular Leakage in Guinea Pigs. *Am. Rev. Respir. Dis.* **1988,** *138,* 395-399.

(59) Liu, M.; Wang, L.; Enhorning, G. Surfactant Dysfunction Develops When the Immunized Guinea-Pig Is Challenged With Ovalbumin Aerosol. *Clin. Exp. Allergy* **1995,** *25,* 1053-1060.

(60) Wang, J. Y.; Shieh, C. C.; Yu, C. K.; Lei, H. Y. Allergen-Induced Bronchial Inflammation Is Associated With Decreased Levels of Surfactant Proteins A and D in a Murine Model of Asthma. *Clin. Exp. Allergy* **2001,** *31,* 652-662.

(61) Haley, K. J.; Ciota, A.; Contreras, J. P.; Boothby, M. R.; Perkins, D. L.; Finn, P. W. Alterations in Lung Collectins in an Adaptive Allergic Immune Response. *Am. J. Physiol Lung Cell Mol. Physiol* **2002,** *282,* L573-L584.

(62) Kurashima, K.; Fujimura, M.; Matsuda, T.; Kobayashi, T. Surface Activity of Sputum From Acute Asthmatic Patients. *Am. J. Respir. Crit Care Med.* **1997,** *155,* 1254-1259.

(63) Wright, S. M.; Hockey, P. M.; Enhorning, G.; Strong, P.; Reid, K. B.; Holgate, S. T.; Djukanovic, R.; Postle, A. D. Altered Airway Surfactant Phospholipid Composition and Reduced Lung Function in Asthma. *J. Appl. Physiol* **2000,** *89,* 1283-1292.

(64) Hohlfeld, J. M.; Ahlf, K.; Enhorning, G.; Balke, K.; Erpenbeck, V. J.; Petschallies, J.; Hoymann, H. G.; Fabel, H.; Krug, N. Dysfunction of Pulmonary Surfactant in Asthmatics After Segmental Allergen Challenge. *Am. J. Respir. Crit Care Med.* **1999,** *159,* 1803-1809.

(65) Fuchimukai, T.; Fujiwara, T.; Takahashi, A.; Enhorning, G. Artificial Pulmonary Surfactant Inhibited by Proteins. *J. Appl. Physiol* **1987,** *62,* 429-437.

(66) Seeger, W.; Grube, C.; Gunther, A.; Schmidt, R. Surfactant Inhibition by Plasma Proteins: Differential Sensitivity of Various Surfactant Preparations. *Eur. Respir. J.* **1993,** *6,* 971-977.

(67) Durmowicz, A. G.; Stenmark, K. R. Acute Respiratory Failure. In *Disorders of the Respiratory Tract in Children*; Chernick, V., Boat, T. F., Kendig, E. L., Eds.; WB Saunders Co: Philadelphia, 1998.

(68) Seeger, W.; Stohr, G.; Wolf, H. R.; Neuhof, H. Alteration of Surfactant Function Due to Protein Leakage: Special Interaction With Fibrin Monomer. *J. Appl. Physiol* **1985,** *58,* 326-338.

(69) Andersson, S.; Kheiter, A.; Merritt, T. A. Oxidative Inactivation of Surfactants. *Lung* **1999,** *177,* 179-189.

(70) Amirkhanian, J. D.; Merritt, T. A. Inhibitory Effects of Oxyradicals on Surfactant Function: Utilizing in Vitro Fenton Reaction. *Lung* **1998,** *176,* 63-72.

(71) Seeger, W.; Thede, C.; Gunther, A.; Grube, C. Surface Properties and Sensitivity to Protein-Inhibition of a Recombinant Apoprotein C-Based Phospholipid Mixture in Vitro--Comparison to Natural Surfactant. *Biochim. Biophys. Acta* **1991,** *1081,* 45-52.

(72) Holm, B. A.; Notter, R. H. Effects of Hemoglobin and Cell Membrane Lipids on Pulmonary Surfactant Activity. *J. Appl. Physiol* **1987,** *63,* 1434-1442.

(73) Ganong, W. F. Energy Balance, Metabolism and Nutrition. In *Review of Medical Physiology*; Appleton and Lange: 1999; Chapter 17.

(74) Takahashi, A.; Nemoto, T.; Fujiwara, T. Biophysical Properties of Protein-Free, Totally Synthetic Pulmonary Surfactants, ALEC and Exosurf, in Comparison With Surfactant TA. *Acta Paediatr. Jpn.* **1994,** *36,* 613-618.

(75) Corcoran, J. D.; Berggren, P.; Sun, B.; Halliday, H. L.; Robertson, B.; Curstedt, T. Comparison of Surface Properties and Physiological Effects of a Synthetic and a Natural Surfactant in Preterm Rabbits. *Arch. Dis. Child Fetal Neonatal Ed* **1994,** *71,* F165-F169.

(76) Rauprich, P.; Stichtenoth, G.; Walter, G.; Johansson, J.; Robertson, B.; Herting, E. Resistance of New Recombinant Surfactant Preparations to Inhibition by Meconium. *Biol. Neonate* **1999,** *76,* 42-43.

(77) Stenson, B. J.; Glover, R. M.; Parry, G. J.; Wilkie, R. A.; Laing, I. A.; Tarnow-Mordi, W. O. Static Respiratory Compliance in the Newborn. III: Early Changes After Exogenous Surfactant Treatment. *Arch. Dis. Child Fetal Neonatal Ed* **1994,** *70,* F19-F24.

(78) Sinclair, J. C.; Haughton, D. E.; Bracken, M. B.; Horbar, J. D.; Soll, R. F. Cochrane Neonatal Systematic Reviews: a Survey of the Evidence for Neonatal Therapies. *Clin. Perinatol.* **2003,** *30,* 285-304.

(79) Murdoch, E.; Kempley, S. T. Randomized Trial Examining Cerebral Haemodynamics Following Artificial or Animal Surfactant. *Acta Paediatr.* **1998,** *87,* 411-415.

(80) Ainsworth, S. B.; Beresford, M. W.; Milligan, D. W.; Shaw, N. J.; Matthews, J. N.; Fenton, A. C.; Ward Platt, M. P. Pumactant and Poractant Alfa for Treatment of Respiratory Distress Syndrome in Neonates Born at 25-29 Weeks' Gestation: a Randomised Trial. *Lancet* **2000,** *355,* 1387-1392.

(81) Kukkonen, A. K.; Virtanen, M.; Jarvenpaa, A. L.; Pokela, M. L.; Ikonen, S.; Fellman, V. Randomized Trial Comparing Natural and Synthetic Surfactant: Increased Infection Rate After Natural Surfactant? *Acta Paediatrica* **2000,** *89,* 556-561.

(82) Spragg, R. G.; Gilliard, N.; Richman, P.; Smith, R. M.; Hite, D.; Pappert, D.; Robertson, B.; Curstedt, T.; Strayer, D. Acute Effects of A Single-Dose of Porcine Surfactant on Patients With the Adult-Respiratory-Distress-Syndrome. *Chest* **1994,** *105,* 195-202.

(83) Weg, J. G.; Balk, R. A.; Tharratt, R. S.; Jenkinson, S. G.; Shah, J. B.; Zaccardelli, D.; Horton, J.; Pattishall, E. N. Safety and Potential Efficacy of An Aerosolized Surfactant in Human Sepsis-Induced Adult-Respiratory-Distress-Syndrome. *Jama-Journal of the American Medical Association* **1994,** *272,* 1433-1438.

(84) Gregory, T. J.; Steinberg, K. P.; Spragg, R.; Gadek, J. E.; Hyers, T. M.; Longmore, W. J.; Moxley, M. A.; Cai, G. Z.; Hite, R. D.; Smith, R. M.; Hudson, L. D.; Crim, C.; Newton, P.; Mitchell, B. R.; Gold, A. J. Bovine Surfactant Therapy for Patients With Acute Respiratory Distress Syndrome. *Am. J. Respir. Crit Care Med.* **1997,** *155,* 1309-1315.

(85) Spragg, R. G.; Smith, R. M.; Harris, K.; Lewis, J.; Hafner, D.; Germann, P. Effect of Recombinant SP-C Surfactant in a Porcine Lavage Model of Acute Lung Injury. *J. Appl. Physiol* **2000,** *88,* 674-681.

(86) Spragg, R. G.; Lewis, J. F.; Wurst, W.; Hafner, D.; Baughman, R. P.; Wewers, M. D.; Marsh, J. J. Treatment of Acute Respiratory Distress Syndrome With Recombinant Surfactant Protein C Surfactant. *Am. J. Respir. Crit Care Med.* **2003,** *167,* 1562-1566.

(87) Spragg, R. G.; Lewis, J. F.; Walmrath, H. D.; Johannigman, J.; Bellingan, G.; Laterre, P. F.; Witte, M. C.; Richards, G. A.; Rippin, G.; Rathgeb, F.; Hafner, D.; Taut, F. J.; Seeger, W. Effect of Recombinant Surfactant Protein C-Based Surfactant on the Acute Respiratory Distress Syndrome. *N. Engl. J. Med.* **2004,** *351,* 884-892.

(88) Ekelund, L.; Burgoyne, R.; Brymer, D.; Enhorning, G. Pulmonary Surfactant Release in Fetal Rabbits As Affected by Terbutaline and Aminophyllin. *Scand. J. Clin. Lab Invest* **1981,** *41,* 237-245.

(89) Dobbs, L. G.; Mason, R. J. Pulmonary Alveolar Type II Cells Isolated From Rats. Release of Phosphatidylcholine in Response to Beta-Adrenergic Stimulation. *J. Clin. Invest* **1979,** *63,* 378-387.

(90) Van Golde, L. M. Synthesis of Surfactant Lipids in the Adult Lung. *Annu. Rev. Physiol.* **1985,** *47,* 765-774.

(91) Liu, M.; Wang, L.; Li, E.; Enhorning, G. Pulmonary Surfactant Given Prophylactically Alleviates an Asthma Attack in Guinea-Pigs. *Clin. Exp. Allergy* **1996,** *26,* 270-275.

(92) Kurashima, K.; Fujimura, M.; Tsujiura, M.; Matsuda, T. Effect of Surfactant Inhalation on Allergic Bronchoconstriction in Guinea Pigs. *Clin. Exp. Allergy* **1997,** *27,* 337-342.

(93) Madan, T.; Kishore, U.; Singh, M.; Strong, P.; Clark, H.; Hussain, E. M.; Reid, K. B.; Sarma, P. U. Surfactant Proteins A and D Protect Mice Against Pulmonary Hypersensitivity Induced by Aspergillus Fumigatus Antigens and Allergens. *J. Clin. Invest* **2001,** *107,* 467-475.

(94) Strong, P.; Reid, K. B.; Clark, H. Intranasal Delivery of a Truncated Recombinant Human SP-D Is Effective at Down-Regulating Allergic Hypersensitivity in Mice Sensitized to Allergens of Aspergillus Fumigatus. *Clin. Exp. Immunol.* **2002,** *130,* 19-24.

(95) Kurashima, K.; Ogawa, H.; Ohka, T.; Fujimura, M.; Matsuda, T.; Kobayashi, T. A Pilot Study of Surfactant Inhalation in the Treatment of Asthmatic Attack. *Arerugi* **1991,** *40,* 160-163.

(96) Oetomo, S. B.; Dorrepaal, C.; Bos, H.; Gerritsen, J.; van der Mark, T. W.; Koeter, G. H.; van Aalderen, W. M. Surfactant Nebulization Does Not Alter Airflow Obstruction and Bronchial Responsiveness to Histamine in Asthmatic Children. *Am. J. Respir. Crit Care Med.* **1996,** *153,* 1148-1152.

(97) Anzueto, A.; Jubran, A.; Ohar, J. A.; Piquette, C. A.; Rennard, S. I.; Colice, G.; Pattishall, E. N.; Barrett, J.; Engle, M.; Perret, K. A.; Rubin, B. K. Effects of Aerosolized Surfactant in Patients With Stable Chronic Bronchitis: a Prospective Randomized Controlled Trial. *JAMA* **1997,** *278,* 1426-1431.

(98) Tibby, S. M.; Hatherill, M.; Wright, S. M.; Wilson, P.; Postle, A. D.; Murdoch, I. A. Exogenous Surfactant Supplementation in Infants With Respiratory Syncytial Virus Bronchiolitis. *Am. J. Respir. Crit Care Med.* **2000,** *162,* 1251-1256.

(99) Bangham, A. D.; Miller, N. G. A.; Davies, R. J.; Greenough, A.; Morley, C. J. Introductory-Remarks About Artificial Lung Expanding Compounds (Alec). *Colloids and Surfaces* **1984,** *10,* 337-341.

(100) Fuell, T. The history of ALEC and Britannia Pharmaceuticals. 2005. Ref Type: Personal Communication

(101) Morley, C. J.; Bangham, A. D.; Miller, N.; Davis, J. A. Dry Artificial Lung Surfactant and Its Effect on Very Premature Babies. *Lancet* **1981,** *1,* 64-68.

(102) Morley, C. J.; Banhham, A. D.; Johnson, P.; Thorburn, G. D.; Jenkin, G. Physical and Physiological Properties of Dry Lung Surfactant. *Nature* **1978,** *271,* 162-163.

(103) Young, P. M.; Thompson, J.; Woodcock, D.; Aydin, M.; Price, R. The Development of a Novel High-Dose Pressurized Aerosol Dry-Powder Device (PADD) for the Delivery of Pumactant for Inhalation Therapy. *J. Aerosol Med.* **2004,** *17,* 123-128.

(104) Bligh, E. G.; Dyer, W. J. A Rapid Method of Total Lipid Extraction and Purification. *Can. J. Med. Sci.* **1959,** *37,* 911-917.

(105) Hunt, A. N.; Clark, G. T.; Attard, G. S.; Postle, A. D. Highly Saturated Endonuclear Phosphatidylcholine Is Synthesized in Situ and Colocated With CDP-Choline Pathway Enzymes. *J. Biol. Chem.* **2001,** *276,* 8492-8499.

(106) DeLong, C. J.; Hicks, A. M.; Cui, Z. Disruption of Choline Methyl Group Donation for Phosphatidylethanolamine Methylation in Hepatocarcinoma Cells. *J. Biol. Chem.* **2002,** *277,* 17217-17225.

(107) Haslem, P. L.; Postle, A. D.; Raymonos, K.; Baker, C. S. Measurement of Pulmonary Sufactant Components and Function in Bronchoalveolar Lavage Fluid. *European Respiratory Review* **1999,** *9,* 43-69.

(108) Merritt, T. A.; Hallman, M.; Bloom, B. T.; Berry, C.; Benirschke, K.; Sahn, D.; Key, T.; Edwards, D.; Jarvenpaa, A. L.; Pohjavuori, M.; . Prophylactic Treatment of Very Premature Infants With Human Surfactant. *N. Engl. J. Med.* **1986,** *315,* 785-790.

(109) Hallman, M.; Merritt, T. A.; Schneider, H.; Epstein, B. L.; Mannino, F.; Edwards, D. K.; Gluck, L. Isolation of Human Surfactant From Amniotic Fluid and a Pilot Study of Its Efficacy in Respiratory Distress Syndrome. *Pediatrics* **1983,** *71,* 473-482.

(110) BARTLETT, G. R. Phosphorus Assay in Column Chromatography. *J. Biol. Chem.* **1959,** *234,* 466-468.

(111) Bernhard, W.; Haagsman, H. P.; Tschernig, T.; Poets, C. F.; Postle, A. D.; van Eijk, M. E.; von der, H. H. Conductive Airway Surfactant: Surface-Tension Function, Biochemical Composition, and Possible Alveolar Origin. *Am. J. Respir. Cell Mol. Biol.* **1997,** *17,* 41-50.

(112) Gobley, M. Examen comparatif du jaune d'ouefe et de la materiere cerebrale. J.Pharm.Chim. 11, 409. 1847.

(113) Vitiello, F.; Zanetta, J. P. Thin-Layer Chromatography of Phospholipids. *J. Chromatogr.* **1978,** *166,* 637-640.

(114) Gilfillan, A. M.; Chu, A. J.; Smart, D. A.; Rooney, S. A. Single Plate Separation of Lung Phospholipids Including Disaturated Phosphatidylcholine. *J. Lipid Res.* **1983,** *24,* 1651-1656.

(115) Bernhard, W.; Linck, M.; Creutzburg, H.; Postle, A. D.; Arning, A.; Martin-Carrera, I.; Sewing, K. F. High-Performance Liquid Chromatographic Analysis of Phospholipids From Different Sources With Combined Fluorescence and Ultraviolet Detection. *Anal. Biochem.* **1994,** *220,* 172-180.

(116) Huang, Z. H.; Gage, D. A.; Sweeley, C. C. Characterization of Diacylglycerolphosphocholine molecular species by FAB-CAD-MS/MS. Journal American Society Mass Spectrometry 3, 71-78. 1992.

(117) Clay, K. L.; Wahlin, L.; Murphy, R. C. Interlaboratory Reproducibility of Relative Abundances of Ion Currents in Fast Atom Bombardment Mass-Spectral Data. *Biomedical Mass Spectrometry* **1983,** *10,* 489-494.

(118) Cheng, C.; Gross, M. L. Applications and Mechanisms of Charge-Remote Fragmentation. *Mass Spectrom. Rev* **2000,** *19,* 398-420.

(119) Han, X.; Gross, R. W. Electrospray Ionization Mass Spectroscopic Analysis of Human Erythrocyte Plasma Membrane Phospholipids. *Proc. Natl. Acad. Sci. U. S. A* **1994,** *91,* 10635-10639.

(120) Kayganich, K.; Murphy, R. C. Molecular-Species Analysis of Arachidonate Containing Glycerophosphocholines by Tandem Mass-Spectrometry. *Journal of the American Society for Mass Spectrometry* **1991,** *2,* 45-54.

(121) Brugger, B.; Erben, G.; Sandhoff, R.; Wieland, F. T.; Lehmann, W. D. Quantitative Analysis of Biological Membrane Lipids at the Low Picomole Level by Nano-Electrospray Ionization Tandem Mass Spectrometry. *Proc. Natl. Acad. Sci. U. S. A* **1997,** *94,* 2339-2344.

(122) Han, X.; Gubitosi-Klug, R. A.; Collins, B. J.; Gross, R. W. Alterations in Individual Molecular Species of Human Platelet Phospholipids During Thrombin Stimulation: Electrospray Ionization Mass Spectrometry-Facilitated Identification of the Boundary Conditions for the Magnitude and Selectivity of Thrombin-Induced Platelet Phospholipid Hydrolysis. *Biochemistry* **1996,** *35,* 5822-5832.

(123) Smith, P. B.; Snyder, A. P.; Harden, C. S. Characterization of Bacterial Phospholipids by Electrospray Ionization Tandem Mass Spectrometry. *Anal. Chem.* **1995,** *67,* 1824-1830.

(124) Li, C.; McClory, A.; Wong, E.; Yergey, J. A. Mass Spectrometric Analysis of Arachidonyl-Containing Phospholipids in Human U937 Cells. *J. Mass Spectrom.* **1999,** *34,* 521-536.

(125) Burdge, G. C.; Hunt, A. N.; Postle, A. D. Mechanisms of Hepatic Phosphatidylcholine Synthesis in Adult Rat: Effects of Pregnancy. *Biochem. J.* **1994,** *303 (Pt 3),* 941-947.

(126) Burdge, G. C.; Kelly, F. J.; Postle, A. D. Synthesis of Phosphatidylcholine in Guinea-Pig Fetal Lung Involves Acyl Remodelling and Differential Turnover of Individual Molecular Species. *Biochim. Biophys. Acta* **1993,** *1166,* 251-257.

(127) Bunt, J. E.; Carnielli, V. P.; rcos Wattimena, J. L.; Hop, W. C.; Sauer, P. J.; Zimmermann, L. J. The Effect in Premature Infants of Prenatal Corticosteroids on Endogenous Surfactant Synthesis As Measured With Stable Isotopes. *Am. J. Respir. Crit Care Med.* **2000,** *162,* 844-849.

(128) Torresin, M.; Zimmermann, L. J. I.; Cogo, P. E.; Cavicchioli, P.; Badon, T.; Giordano, G.; Zacchello, F.; Sauer, P. J. J.; Carnielli, V. P. Exogenous Surfactant Kinetics in Infant Respiratory Distress Syndrome: A Novel Method With Stable Isotopes. *American Journal of Respiratory and Critical Care Medicine* **2000,** *161,* 1584-1589.

(129) Cavicchioli, P.; Zimmermann, L. J. I.; Cogo, P. E.; Badon, T.; Giordano, G.; Torresin, M.; Zacchello, F.; Carnielli, V. P. Endogenous Surfactant Turnover in Preterm Infants With Respiratory Distress Syndrome Studied With Stable Isotope Lipids. *American Journal of Respiratory and Critical Care Medicine* **2001,** *163,* 55-60.

(130) Hunt, A. N.; Clark, G. T.; Neale, J. R.; Postle, A. D. A Comparison of the Molecular Specificities of Whole Cell and Endonuclear Phosphatidylcholine Synthesis. *FEBS Lett.* **2002,** *530,* 89-93.

(131) DeLong, C. J.; Shen, Y. J.; Thomas, M. J.; Cui, Z. Molecular Distinction of Phosphatidylcholine Synthesis Between the CDP-Choline Pathway and Phosphatidylethanolamine Methylation Pathway. *J. Biol. Chem.* **1999,** *274,* 29683-29688.

(132) Ashton, M. R.; Postle, A. D.; Hall, M. A.; Smith, S. L.; Kelly, F. J.; Normand, I. C. Phosphatidylcholine Composition of Endotracheal Tube Aspirates of Neonates and Subsequent Respiratory Disease. *Arch. Dis. Child* **1992,** *67,* 378-382.

(133) Pin, I.; Gibson, P. G.; Kolendowicz, R.; Girgis-Gabardo, A.; Denburg, J. A.; Hargreave, F. E.; Dolovich, J. Use of Induced Sputum Cell Counts to Investigate Airway Inflammation in Asthma. *Thorax* **1992,** *47,* 25-29.

(134) Vance, D. E. Boehringer Mannheim Award Lecture. Phosphatidylcholine Metabolism: Masochistic Enzymology, Metabolic Regulation, and Lipoprotein Assembly. *Biochem. Cell Biol.* **1990,** *68,* 1151-1165.

(135) Vance, D. E.; Ridgway, N. D. The Methylation of Phosphatidylethanolamine. *Prog. Lipid Res.* **1988,** *27,* 61-79.

(136) Walkey, C. J.; Yu, L.; Agellon, L. B.; Vance, D. E. Biochemical and Evolutionary Significance of Phospholipid Methylation. *J. Biol. Chem.* **1998,** *273,* 27043-27046.

(137) Kramar, R.; Kremser, K.; Raab, R. Enhancement of Choline Dehydrogenase Activity in Rat Liver Mitochondria by Clofibrate Feeding. *Hoppe Seylers. Z. Physiol Chem.* **1984,** *365,* 1207-1210.

(138) Chern, M. K.; Pietruszko, R. Evidence for Mitochondrial Localization of Betaine Aldehyde Dehydrogenase in Rat Liver: Purification, Characterization, and Comparison With Human Cytoplasmic E3 Isozyme. *Biochem. Cell Biol.* **1999,** *77,* 179-187.

(139) Cui, Z.; Vance, D. E. Expression of Phosphatidylethanolamine N-Methyltransferase-2 Is Markedly Enhanced in Long Term Choline-Deficient Rats. *J. Biol. Chem.* **1996,** *271,* 2839-2843.

(140) Watkins, S. M.; Zhu, X.; Zeisel, S. H. Phosphatidylethanolamine-N-Methyltransferase Activity and Dietary Choline Regulate Liver-Plasma Lipid Flux and Essential Fatty Acid Metabolism in Mice. *J. Nutr.* **2003,** *133,* 3386-3391.

(141) Koc, H.; Mar, M. H.; Ranasinghe, A.; Swenberg, J. A.; Zeisel, S. H. Quantitation of Choline and Its Metabolites in Tissues and Foods by Liquid Chromatography/Electrospray Ionization-Isotope Dilution Mass Spectrometry. *Anal. Chem.* **2002,** *74,* 4734-4740.

(142) Hunt, A. N.; Postle, A. D. Dynamic Lipidomic Insights into Phosphatidylcholine Synthesis From Organelle to Organism. *Spectroscopy-An International Journal* **2005,** *19,* 127-135.

(143) Postle, A. D. Method for the Sensitive Analysis of Individual Molecular Species of Phosphatidylcholine by High-Performance Liquid Chromatography Using Post-Column Fluorescence Detection. *J. Chromatogr.* **1987,** *415,* 241-251.

(144) Postle, A. D.; Mander, A.; Reid, K. B.; Wang, J. Y.; Wright, S. M.; Moustaki, M.; Warner, J. O. Deficient Hydrophilic Lung Surfactant Proteins A and D With Normal Surfactant Phospholipid Molecular Species in Cystic Fibrosis. *Am. J. Respir. Cell Mol. Biol.* **1999,** *20,* 90-98.

(145) Burdge, G. C.; Postle, A. D. Phospholipid Molecular Species Composition of Developing Fetal Guinea Pig Brain. *Lipids* **1995,** *30,* 719-724.

(146) Cui, Z.; Shen, Y. J.; Vance, D. E. Inverse Correlation Between Expression of Phosphatidylethanolamine N-Methyltransferase-2 and Growth Rate of Perinatal Rat Livers. *Biochim. Biophys. Acta* **1997,** *1346,* 10-16.

(147) Tessitore, L.; Dianzani, I.; Cui, Z.; Vance, D. E. Diminished Expression of Phosphatidylethanolamine N-Methyltransferase 2 During Hepatocarcinogenesis. *Biochem. J.* **1999,** *337 (Pt 1),* 23-27.

(148) Grundy, S. M. Approach to Lipoprotein Management in 2001 National Cholesterol Guidelines. *Am. J. Cardiol.* **2002,** *90,* 11i-21i.

(149) Brehm, B. J.; Seeley, R. J.; Daniels, S. R.; D'Alessio, D. A. A Randomized Trial Comparing a Very Low Carbohydrate Diet and a Calorie-Restricted Low Fat Diet on Body Weight and Cardiovascular Risk Factors in Healthy Women. *J. Clin. Endocrinol. Metab* **2003,** *88,* 1617-1623.

(150) Samaha, F. F.; Iqbal, N.; Seshadri, P.; Chicano, K. L.; Daily, D. A.; McGrory, J.; Williams, T.; Williams, M.; Gracely, E. J.; Stern, L. A Low-Carbohydrate As Compared With a Low-Fat Diet in Severe Obesity. *N. Engl. J. Med.* **2003,** *348,* 2074-2081.

(151) Amato, M.; Petit, K.; Fiore, H. H.; Doyle, C. A.; Frantz, I. D., III; Nielsen, H. C. Effect of Exogenous Surfactant on the Development of Surfactant Synthesis in Premature Rabbit Lung. *Pediatr. Res.* **2003,** *53,* 671-678.

(152) Patton, J. S. Mechanisms of Macromolecule Absorption by the Lungs. *Advanced Drug Delivery Reviews* **1996,** *19,* 3-36.

(153) Weibel, E. R. Functional Morphology of the Growing Lung. *Respiration* **1970,** *27,* Suppl-35.

(154) Weibel, E. R. Morphometric Estimation of Pulmonary Diffusion Capacity. V. Comparative Morphometry of Alveolar Lungs. *Respir. Physiol* **1972,** *14,* 26-43.

(155) Klingele, T. G.; Staub, N. C. Alveolar Shape Changes With Volume in Isolated, Air-Filled Lobes of Cat Lung. *J. Appl. Physiol* **1970,** *28,* 411-414.

(156) Gil, J.; Weibel, E. R. Morphological Study of Pressure-Volume Hysteresis in Rat Lungs Fixed by Vascular Perfusion. *Respir. Physiol* **1972,** *15,* 190-213.

(157) Wang, N. S.; Thurlbeck, W. M. Scanning Electron Microscopy of the Lung. *Hum. Pathol.* **1970,** *1,* 227-231.

(158) Ganderton, D.; Jones, T. M. *Drug Delivery to the Respiratory Tract*; 1987.

(159) Theil, C. G. From Susie's Question to CFC Free: an Inventors Perspective on Forty Years of MDI Development and Regulation. *Respir. Drug Delivery* **1996,** *5,* 115-123.

(160) O'callaghan, C.; wright, P. The Metered-Dose Inhaler. In *Drug Delivery to the Lung*; Bisgaard, H., O'callaghan, C., Smaldone, G. C., Eds.; Marcel Dekker, Inc.: New York, 2002; Chapter 10.

(161) Pauwels, R.; Newman, S.; Borgstrom, L. Airway Deposition and Airway Effects of Antiasthma Drugs Delivered From Metered-Dose Inhalers. *Eur. Respir. J.* **1997,** *10,* 2127-2138.

(162) Smith, I. J.; Parry-Billings, M. The Inhalers of the Future? A Review of Dry Powder Devices on the Market Today. *Pulm. Pharmacol. Ther.* **2003,** *16,* 79-95.

(163) Smith, I. J. The Challenge of Reformulation. *J. Aerosol Med.* **1995,** *8 Suppl 1,* S19-S27.

(164) Bell, J. International Development of Portable Inhalers. *J. Investig. Allergol. Clin. Immunol.* **1997,** *7,* 417-419.

(165) Bell, J. H.; Hartley, P. S.; Cox, J. S. Dry Powder Aerosols. I. A New Powder Inhalation Device. *J. Pharm. Sci.* **1971,** *60,* 1559-1564.

(166) Hetzel, M. R.; Clark, T. J. Comparison of Salbutamol Rotahaler With Conventional Pressurized Aerosol. *Clin. Allergy* **1977,** *7,* 563-568.

(167) Pakes, G. E.; Brogden, R. N.; Heel, R. C.; Speight, T. M.; Avery, G. S. Ipratropium Bromide: a Review of Its Pharmacological Properties and Therapeutic Efficacy in Asthma and Chronic Bronchitis. *Drugs* **1980,** *20,* 237-266.

(168) Pedersen, S. Aerosols and Other Devices. In *Childhood Asthma and Other Wheezing Disorders*; Silverman, M., Ed.; Chapman and Hall: 1995.

(169) Auty, R. M.; Brown, K.; Neale, M. G.; Snashall, P. D. Respiratory Tract Deposition of Sodium Cromoglycate Is Highly Dependent Upon Technique of Inhalation Using the Spinhaler. *Br. J. Dis. Chest* **1987,** *81,* 371-380.

(170) Pitcairn, G. R.; Hunt, H. M. A.; Dewberry, H.; Pavia, D.; Newman, S. P. A Comparison of In-Vitro Drug-Delivery From 2 Dry Powder Inhalers, the Aerohaler(R) and the Rotahaler(R). *Stp Pharma Sciences* **1994,** *4,* 33-37.

(171) Wetterlin, K. Turbuhaler: a New Powder Inhaler for Administration of Drugs to the Airways. *Pharm. Res.* **1988,** *5,* 506-508.

(172) Hickey, A. J.; Dunbar, C. A. A New Millenium for Inhaler Technology. *Pharm. Technol.* **1997,** *21,* 116-125.

(173) Developments in inhaler technology. PA consulting group . 2005.
Ref Type: Internet Communication

(174) Dennis, J. H.; Nerbrink, O. New Nebulizer Technology. In *Drug Deliver to the Lung*; Bisgaard, H., O'callaghan, C., Smaldone, G. C., Eds.; Marcel Dekker Inc.: New York, 2002; Chapter 9.

(175) Osier, M.; Oberdorster, G. Intratracheal Inhalation Vs Intratracheal Instillation: Differences in Particle Effects. *Fundam. Appl. Toxicol.* **1997,** *40,* 220-227.

(176) de Boer, A. H.; Le Brun, P. P.; van der Woude, H. G.; Hagedoorn, P.; Heijerman, H. G.; Frijlink, H. W. Dry Powder Inhalation of Antibiotics in Cystic Fibrosis Therapy, Part 1: Development of a Powder Formulation With Colistin Sulfate for a Special Test Inhaler With an Air Classifier As De-Agglomeration Principle. *Eur. J. Pharm. Biopharm.* **2002,** *54,* 17-24.

(177) VPAG Inhaler System. 0500677.0. 2005. UK. 14-1-2005.

(178) Thite, A. Vibration characterisation of the VPAG vibration table. 2004. Personal Communication

(179) Vibratechniques Ltd. Model GT pneumatic turbine vibrators. 2002.

(180) Chan, H. K.; Eberl, S.; Daviskas, E.; Constable, C.; Young, I. Changes in Lung Deposition of Aerosols Due to Hygroscopic Growth: a Fast SPECT Study. *J. Aerosol Med.* **2002,** *15,* 307-311.

(181) Preparations for inhalation. [5.1], 2843-2847. 2005. European Pharmacopoeia.
Ref Type: Serial (Book,Monograph)

(182) Seale, J. P.; Harrison, L. I. Effect of Changing the Fine Particle Mass of Inhaled Beclomethasone Dipropionate on Intrapulmonary Deposition and Pharmacokinetics. *Respir. Med.* **1998,** *92 Suppl A,* 9-15.

(183) Leach, C. L. Improved Delivery of Inhaled Steroids to the Large and Small Airways. *Respir. Med.* **1998,** *92 Suppl A,* 3-8.

(184) Melchor, R.; Biddiscombe, M. F.; Mak, V. H.; Short, M. D.; Spiro, S. G. Lung Deposition Patterns of Directly Labelled Salbutamol in Normal Subjects and in Patients With Reversible Airflow Obstruction. *Thorax* **1993,** *48,* 506-511.

(185) Fishwick, D.; Bradshaw, L.; Macdonald, C.; Beasley, R.; Gash, D.; Bengtsson, T.; Bondesson, E.; Borgstrom, L. Cumulative and Single-Dose Design to Assess the Bronchodilator Effects of Beta2-Agonists in Individuals With Asthma. *Am. J. Respir. Crit Care Med.* **2001,** *163,* 474-477.

(186) Weda, M.; Zanen, P.; de Boer, A. H.; Gjaltema, D.; Ajaoud, A.; Barends, D. M.; Frijlink, H. W. Equivalence Testing of Salbutamol Dry Powder Inhalers: in Vitro Impaction Results Versus in Vivo Efficacy. *Int. J. Pharm.* **2002,** *249,* 247-255.

(187) O'Riordan, T. G.; Greco, M. J.; Perry, R. J.; Smaldone, G. C. Nebulizer Function During Mechanical Ventilation. *Am. Rev Respir. Dis.* **1992,** *145,* 1117-1122.

(188) Diot, P.; Morra, L.; Smaldone, G. C. Albuterol Delivery in a Model of Mechanical Ventilation. Comparison of Metered-Dose Inhaler and Nebulizer Efficiency. *Am. J. Respir. Crit Care Med.* **1995,** *152,* 1391-1394.

(189) Fink, J. B.; Dhand, R.; Duarte, A. G.; Jenne, J. W.; Tobin, M. J. Aerosol Delivery From a Metered-Dose Inhaler During Mechanical Ventilation. An in Vitro Model. *Am. J. Respir. Crit Care Med.* **1996,** *154,* 382-387.

(190) Fink, J. B.; Dhand, R.; Grychowski, J.; Fahey, P. J.; Tobin, M. J. Reconciling in Vitro and in Vivo Measurements of Aerosol Delivery From a Metered-Dose Inhaler During Mechanical Ventilation and Defining Efficiency-Enhancing Factors. *Am. J. Respir. Crit Care Med.* **1999,** *159,* 63-68.

(191) Wildhaber, J. H.; Hayden, M. J.; Dore, N. D.; Devadason, S. G.; LeSouef, P. N. Salbutamol Delivery From a Hydrofluoroalkane Pressurized Metered-Dose Inhaler in Pediatric Ventilator Circuits: an in Vitro Study. *Chest* **1998,** *113,* 186-191.

(192) Garner, S. S.; Wiest, D. B.; Bradley, J. W. Albuterol Delivery by Metered-Dose Inhaler With a Pediatric Mechanical Ventilatory Circuit Model. *Pharmacotherapy* **1994,** *14,* 210-214.

(193) Fuller, H. D.; Dolovich, M. B.; Chambers, C.; Newhouse, M. T. Aerosol Delivery During Mechanical Ventilation - A Predictive Invitro Lung Model. *Journal of Aerosol Medicine-Deposition Clearance and Effects in the Lung* **1992,** *5,* 251-259.

(194) Cochrane, C. G.; Revak, S. D. Pulmonary Surfactant Protein B (SP-B): Structure-Function Relationships. *Science* **1991,** *254,* 566-568.

(195) Merritt, T. A.; Kheiter, A.; Cochrane, C. G. Positive End-Expiratory Pressure During KL4 Surfactant Instillation Enhances Intrapulmonary Distribution in a Simian Model of Respiratory Distress Syndrome. *Pediatr. Res.* **1995,** *38,* 211-217.

(196) Wang, Y.; Griffiths, W. J.; Curstedt, T.; Johansson, J. Porcine Pulmonary Surfactant Preparations Contain the Antibacterial Peptide Prophenin and a C-Terminal 18-Residue Fragment Thereof. *FEBS Lett.* **1999,** *460,* 257-262.

(197) Ikegami, M.; Hesterberg, T.; Nozaki, M.; Adams, F. H. Restoration of Lung Pressure-Volume Characteristics With Surfactant: Comparison of Nebulization Versus Instillation and Natural Versus Synthetic Surfactant. *Pediatr. Res.* **1977,** *11,* 178-182.

(198) Grathwohl, C.; Newman, G. E.; Phizackerley, P. J.; Town, M. H. Structural Studies on Lamellated Osmiophilic Bodies Isolated From Pig Lung. 31P NMR Results and Water Content. *Biochim. Biophys. Acta* **1979,** *552,* 509-518.

(199) Bangham, A. D.; Morley, C. J.; Phillips, M. C. The Physical Properties of an Effective Lung Surfactant. *Biochim. Biophys. Acta* **1979,** *573,* 552-556.

(200) Smith, R.; Tanford, C. Critical Micelle Concentration of L-Alpha-Dipalmitoylphosphatidylcholine in Water and Water/Methanol Solutions. *Journal of Molecular Biology* **1972,** *67,* 75-&.

(201) Bangham, A. D. Membrane Models With Phospholipids. *Prog. Biophys. Mol. Biol.* **1968,** *18,* 29-95.

(202) Enhorning, G. Pulmonary Surfactant Function Studied With the Pulsating Bubble Surfactometer (PBS) and the Capillary Surfactometer (CS). *Comp Biochem. Physiol A Mol. Integr. Physiol* **2001,** *129,* 221-226.

(203) Colacicco, G.; Basu, M. K.; Scarpelli, E. M. PH, Temperature, Humidity and the Dynamic Force-Area Curve of Dipalmitoyl Lecithin. *Respir. Physiol* **1976,** *27,* 169-186.

(204) Goldsby, R. A.; Kindt, T. J.; Osborne, B. A. *Kuby Immunology*; W.H. Freeman and Company/New York: 2000.

(205) Gonzalez, M. C.; Diaz, P.; Galleguillos, F. R.; Ancic, P.; Cromwell, O.; Kay, A. B. Allergen-Induced Recruitment of Bronchoalveolar Helper (OKT4) and Suppressor (OKT8) T-Cells in Asthma. Relative Increases in OKT8 Cells in Single Early Responders Compared With Those in Late-Phase Responders. *Am. Rev Respir. Dis.* **1987,** *136,* 600-604.

(206) Corrigan, C. J.; Hartnell, A.; Kay, A. B. T Lymphocyte Activation in Acute Severe Asthma. *Lancet* **1988,** *1,* 1129-1132.

(207) Robinson, D. S.; Hamid, Q.; Ying, S.; Tsicopoulos, A.; Barkans, J.; Bentley, A. M.; Corrigan, C.; Durham, S. R.; Kay, A. B. Predominant TH2-Like Bronchoalveolar T-Lymphocyte Population in Atopic Asthma. *N. Engl. J. Med.* **1992,** *326,* 298-304.

(208) Castro, M.; Chaplin, D. D.; Walter, M. J.; Holtzman, M. J. Could Asthma Be Worsened by Stimulating the T-Helper Type 1 Immune Response? *Am. J. Respir. Cell Mol. Biol.* **2000,** *22,* 143-146.

(209) Vercelli, D. Immunoglobulin E and Its Regulators. *Curr. Opin. Allergy Clin. Immunol.* **2001,** *1,* 61-65.

(210) Ray, A.; Cohn, L. Th2 Cells and GATA-3 in Asthma: New Insights into the Regulation of Airway Inflammation. *J. Clin. Invest* **1999,** *104,* 985-993.

(211) Corrigan, C. J. The Role of the T Cell in the Immunopathogenesis of Asthma. *Chem. Immunol.* **2000,** *78,* 39-49.

(212) Arshad, S. H. Primary Prevention of Asthma and Allergy. *J. Allergy Clin. Immunol.* **2005,** *116,* 3-14.

(213) Postle, A. D. Composition and Role of Phospholipids in the Body. In *Encyclopedia of Human Nutrition, 2nd Edition*; Caballero, B., Allen, L., Prentice, A., Eds.; Elsevier Science London: 2005.

(214) Augert, G.; Blackmore, P. F.; Exton, J. H. Changes in the Concentration and Fatty Acid Composition of Phosphoinositides Induced by Hormones in Hepatocytes. *J. Biol. Chem.* **1989,** *264,* 2574-2580.

(215) Lee, S. B.; Rhee, S. G. Significance of PIP2 Hydrolysis and Regulation of Phospholipase C Isozymes. *Curr. Opin. Cell Biol.* **1995,** *7,* 183-189.

(216) Madani, S.; Hichami, A.; Legrand, A.; Belleville, J.; Khan, N. A. Implication of Acyl Chain of Diacylglycerols in Activation of Different Isoforms of Protein Kinase C. *FASEB J.* **2001,** *15,* 2595-2601.

(217) Wilsher, M. L.; Hughes, D. A.; Haslam, P. L. Immunoregulatory Properties of Pulmonary Surfactants - Influence of Variations in the Phospholipid Profile. *Clinical and Experimental Immunology* **1988,** *73,* 117-122.

(218) Anderson, R. G.; Jacobson, K. A Role for Lipid Shells in Targeting Proteins to Caveolae, Rafts, and Other Lipid Domains. *Science* **2002,** *296,* 1821-1825.

(219) Sanderson, S.; Shastri, N. LacZ Inducible, Antigen/MHC-Specific T Cell Hybrids. *Int. Immunol.* **1994,** *6,* 369-376.

(220) Lezzi, G.; Karjalainen, K.; Lanzavecchia, A. The Duration of Antigenic Stimulation Determines the Fate of Naive and Effector T Cells. *Immunity* **1998,** *8,* 89-95.

(221) Weiss, A. T-Cell Activation. In *Fundamental Immunology*; Raven,New York: 1993.

(222) Manger, B.; Weiss, A.; Weyand, C.; Goronzy, J.; Stobo, J. D. T Cell Activation: Differences in the Signals Required for IL 2 Production by Nonactivated and Activated T Cells. *J. Immunol.* **1985,** *135,* 3669-3673.

(223) Williams, S. J. Immunoregulatory Properties of Lung Surfactant. 2001. Ref Type: Personal Communication

(224) Carmo, A. M.; Castro, M. A.; Arosa, F. A. CD2 and CD3 Associate Independently With CD5 and Differentially Regulate Signaling Through CD5 in Jurkat T Cells. *J. Immunol.* **1999,** *163,* 4238-4245.

(225) Maier, O.; Oberle, V.; Hoekstra, D. Fluorescent Lipid Probes: Some Properties and Applications (a Review). *Chem. Phys. Lipids* **2002,** *116,* 3-18.

(226) Gray, A.; Van Der, K. J.; Downes, C. P. The Pleckstrin Homology Domains of Protein Kinase B and GRP1 (General Receptor for Phosphoinositides-1) Are Sensitive and Selective Probes for the Cellular Detection of Phosphatidylinositol 3,4-Bisphosphate and/or Phosphatidylinositol 3,4,5-Trisphosphate in Vivo. *Biochem. J.* **1999,** *344 Pt 3,* 929-936.

(227) Alter, C. A.; Wolf, B. A. Identification of Phosphatidylinositol 3,4,5-Trisphosphate in Pancreatic Islets and Insulin-Secreting Beta-Cells. *Biochem. Biophys. Res. Commun.* **1995,** *208,* 190-197.

(228) Nasuhoglu, C.; Feng, S.; Mao, J.; Yamamoto, M.; Yin, H. L.; Earnest, S.; Barylko, B.; Albanesi, J. P.; Hilgemann, D. W. Nonradioactive Analysis of Phosphatidylinositides and Other Anionic Phospholipids by Anion-Exchange High-Performance Liquid Chromatography With Suppressed Conductivity Detection. *Anal. Biochem.* **2002,** *301,* 243-254.

(229) Wenk, M. R.; Lucast, L.; Di Paolo, G.; Romanelli, A. J.; Suchy, S. F.; Nussbaum, R. L.; Cline, G. W.; Shulman, G. I.; McMurray, W.; De Camilli, P. Phosphoinositide Profiling in Complex Lipid Mixtures Using Electrospray Ionization Mass Spectrometry. *Nat. Biotechnol.* **2003,** *21,* 813-817.

(230) Milne, S. B.; Ivanova, P. T.; DeCamp, D.; Hsueh, R. C.; Brown, H. A. A Targeted Mass Spectrometric Analysis of Phosphatidylinositol Phosphate Species. *J. Lipid Res.* **2005,** *46,* 1796-1802.

(231) Holub, B. J.; Kuksis, A.; Thompson, W. Molecular Species of Mono-, Di-, and Triphosphoinositides of Bovine Brain. *J. Lipid Res.* **1970,** *11,* 558-564.

(232) Postle, A. D.; Dombrowsky, H.; Clarke, H.; Pynn, C. J.; Koster, G.; Hunt, A. N. Mass Spectroscopic Analysis of Phosphatidylinositol Synthesis Using 6-Deuteriated-Myo-Inositol: Comparison of the Molecular Specificities and Acyl Remodelling Mechanisms in Mouse Tissues and Cultured Cells. *Biochem. Soc. Trans.* **2004,** *32,* 1057-1059.

(233) Galdiero, F.; Carratelli, C. R.; Bentivoglio, C.; Capasso, C.; Cioffi, S.; Folgore, A.; Gorga, F.; Ianniello, R.; Mattera, S.; Nuzzo, I.; . Correlation Between Modification of Membrane Phospholipids and Some Biological Activity of Lymphocytes, Neutrophils and Macrophages. *Immunopharmacol. Immunotoxicol.* **1991,** *13,* 623-642.

(234) Mander, A.; Keenleyside, G.; Postle, A. D. Membrane Phosphatidylcholine Composition of Human Lymphocytes in Neonates. *Biochem. Soc. Trans.* **1997,** *25,* 346S.

(235) Lang, C. J.; Postle, A. D.; Orgeig, S.; Possmayer, F.; Bernhard, W.; Panda, A. K.; Jurgens, K. D.; Milsom, W. K.; Nag, K.; Daniels, C. B. Dipalmitoylphosphatidylcholine Is Not the Major Surfactant Phospholipid Species in All Mammals. *Am. J. Physiol. Regul. Integr. Comp. Physiol* **2006,** *289,* 1426-1439.

(236) Kaiser, R. D.; London, E. Determination of the Depth of BODIPY Probes in Model Membranes by Parallax Analysis of Fluorescence Quenching. *Biochim. Biophys. Acta* **1998,** *1375,* 13-22.

(237) Arnold, C.; Adams, E.; Vollman, J.; Giebner, D.; Maurer, M.; Dreyer, G.; Bailey, L.; Anderson, M.; Mefford, L.; Beaumont, E.; Sutton, D.; Puppala, B.; Mangurten, H. H.; Secrest, J.; Lewis, W. J.; Carteaux, P.; Bednarek, F.; Welsberger, S.; Gosselin, R.; Pantoja, A. F.; Belenky, A.; Campbell, P.; Patole, S.; Duenas, M.; Kelly, M.; Alejo, W.; Lewallen, P.; DeanLieber, S.; Hanft, M.; Ferlauto, J.; Newell, R. W.; Bagwell, J.; Levine, D.; Lipp, R. W.; Harkavy, K.; Vasa, R.; Birenbaum, H.; Broderick, K. A.; Santos, A. Q.; Long, B. A.; Gulrajani, M.; Stern, M.; Hopgood, G.; Hegyi, T.; Alba, J.; Christmas, L.; McQueen, M.; Nichols, N.; Brown, M.; Quissell, B. J.; Rusk, C.; Marks, K.; Gifford, K.; Hoehn, G.; Pathak, A.; Wong, S.; Marino, B.; Hunt, P.; Fox, V.; Sharpstein, C.; Feldman, B.; Johnson, N.; Beecham, J.; Balcom, R.; Helmuth, W.; Boylan, D.; Frakes, C.; Magoon, M.; Reese, K.; Schwersenski, J.; Schutzman, D.; Soll, R.; Horbar, J. D.; Leahy, K.; Troyer, W.; Juzwicki, C.; Anderson, P.; Dworsky, M.; Reynolds, L.; Urrutia, J.; Gupta, U.; Adray, C. A Multicenter, Randomized Trial Comparing Synthetic Surfactant With Modified Bovine Surfactant Extract in the Treatment of Neonatal Respiratory Distress Syndrome. *Pediatrics* **1996,** *97,* 1-6.

(238) Warner, J. O. Worldwide Variations in the Prevalence of Atopic Symptoms: What Does It All Mean? *Thorax* **1999,** *54 Suppl 2,* S46-S51.

(239) Duncan, C. Monthly index of medical specialities. 2000. Haymarket Publishing Services Ltd.

(240) van Helden, H. P.; Kuijpers, W. C.; Diemel, R. V. Asthmalike Symptoms Following Intratracheal Exposure of Guinea Pigs to Sulfur Mustard Aerosol: Therapeutic Efficacy of Exogenous Lung Surfactant Curosurf and Salbutamol. *Inhal. Toxicol.* **2004,** *16,* 537-548.

(241) Heeley, E. L.; Hohlfeld, J. M.; Krug, N.; Postle, A. D. Phospholipid Molecular Species of Bronchoalveolar Lavage Fluid After Local Allergen Challenge in Asthma. *Am. J. Physiol Lung Cell Mol. Physiol* **2000,** *278,* L305-L311.

(242) Colacicco, G.; Scarpelli, E. M. Pulmonary Surfactants: Molecular Structure and Biological Activity. In *Biological Horizons in Surface Science*; Prince, L. M., Sears, D. F., Eds.; New York academic press: 1973.

(243) Bernhard, W.; Pynn, C. J.; Jaworski, A.; Rau, G. A.; Hohlfeld, J. M.; Freihorst, J.; Poets, C. F.; Stoll, D.; Postle, A. D. Mass Spectrometric Analysis of Surfactant Metabolism in Human Volunteers Using Deuteriated Choline. *Am. J. Respir. Crit Care Med.* **2004**.

(244) Morre, D. J.; Morre, D. M. Preparation of Mammalian Plasma Membranes by Aqueous Two-Phase Partition. *Biotechniques* **1989,** *7,* 946-4, 956.